UNIVERSITY OF SOUTHAMPTON

Synthesis and Coordination Chemistry of New Distibine and Mixed Phospha-thia Ligands

Melissa Louise Matthews

A Thesis Submitted for the Degree of Doctor of Philosophy

Department of Chemistry

March 2004

UNIVERSITY OF SOUTHAMPTON

ABSTRACT

FACULTY OF SCIENCE

CHEMISTRY

Doctor of Philosophy

"Synthesis and Coordination Chemistry of New Distibine and Mixed Phospha-thia Ligands"

by Melissa Louise Matthews

High yield syntheses of a series of novel distibine ligands are reported, together with detailed investigations into their coordination chemistry with a wide range of transition metals.

The xylyl-distibines 1,2-, 1,3- and 1,4-$C_6H_4(CH_2SbMe_2)_2$ have been prepared by reaction of Me_2SbCl with the appropriate Grignard reagent. The phenylene-distibines 1,3- and 1,4-$C_6H_4(SbMe_2)_2$ have also been prepared following the same synthetic route. All of the novel ligands and their methiodide derivatives have been characterised by ^1H and $^{13}C\{^1H\}$NMR spectroscopy, mass spectrometry and microanalysis. Crystal structures of 1,4-$C_6H_4(CH_2SbMe_2)_2$ and [1,3-$C_6H_4(CH_2SbMe_3)_2]I_2$ are reported. The synthesis of 1,2-$C_6H_4(CH_2SbPh_2)_2$ is also described, together with the attempted synthesis of 1,2-$C_6H_4(SbPh_2)_2$.

Iron, tungsten and nickel carbonyl complexes of the above ligands have been prepared and the crystal structure of [{$Fe(CO)_4$}$_2${μ-1,3-$C_6H_4(CH_2SbMe_2)_2$}] is described. The coordination modes and electronic properties of the novel ligands are investigated in detail and, where appropriate, their spectroscopic properties are compared with other related Group 15 ligands.

Complexes of 1,2-$C_6H_4(CH_2SbMe_2)_2$ with Cu(I), Ag(I), Pt(II), Pd(II), Rh(III), Ni(II) and Co(III) are described. The compounds have been characterised by IR, UV-vis, ^1H, ^{63}Cu, and ^{59}Co NMR spectroscopy, mass spectrometry and microanalysis as appropriate. The crystal structures of [Cu{1,2-$C_6H_4(CH_2SbMe_2)_2$}$_2$][BF_4], [Pt{1,2-$C_6H_4(CH_2SbMe_2)_2$}$_2$][PF_6]$_2$, [Pd{1,2-$C_6H_4(CH_2SbMe_2)_2$}$_2$][PF_6]$_2$, [$PtCl_2${1,2-$C_6H_4(CH_2SbMe_2)_2$}], and [NiI{1,2-$C_6H_4(CH_2SbMe_2)_2$}$_2$][ClO_4] are reported and the ligating behaviour is compared with that of 1,2-$C_6H_4(SbMe_2)_2$ and related aliphatic-backboned distibines.

The coordination chemistry of the mixed donor P/O and P/S ligands $Ph_2P(CH_2)_2O(CH_2)_2O(CH_2)_2PPh_2$ (L^1) and $Ph_2P(CH_2)_2S(CH_2)_2S(CH_2)_2PPh_2$ (L^2) with Ag(I) and Cr(0), Mo(0), W(0), Mn(I) and Re(I) carbonyls is investigated. The coordination modes adopted by the ligands have been probed by $^{31}P\{^1H\}$ NMR spectroscopy. Crystal structures of [Ag(L^1)][CF_3SO_3], [Ag(L^1)][ClO_4], [Ag(L^1)(NO_3)], [$Ag_2(L^1)_3$][CF_3SO_3]$_2$ and [$Mo(CO)_4(L^1)$] are reported

The attempted template synthesis of 1,2-$C_6H_4PH(CH_2)_3S(CH_2)_3PH$ (P_2S) using $Mn(CO)_3$ and $Re(CO)_3$ templates is described. The intermediate species [$M(CO)_3X${1,2-$C_6H_4(PH_2)_2$}], [$M(CO)_3${1,2-$C_6H_4(PH_2)_2CF_3SO_3$}] and [$M(CO)_3${1,2-$C_6H_4(PH_2)_2$}{$S(CH_2CHCH_2)_2$}][CF_3SO_3] have been isolated and characterised by IR, ^1H, ^{31}P and ^{55}Mn NMR spectroscopy and mass spectrometry as appropriate. The crystal structure of [$ReBr(CO)_3${1,2-$C_6H_4(PH_2)_2$}] is also described. Attempted cyclisations are described in detail, together with spectroscopic evidence supporting successful isolation of [$Re(CO)_3${P_2S}][CF_3SO_3].

Table of Contents

List of Figures

List of Tables

List of Schemes

Acknowledgements

I would like to thank my supervisors Dr. Gill Reid and Prof. Bill Levason for all their help and guidance throughout the course of the Ph.D. I would also like to thank Dr. Mike Webster for his kind help with the X-ray crystallography, and my friends in the department.

Finally I would like to thank my family for all their encouragement and give special thanks to Robin for all his support – I couldn't have done it without him.

Abbreviations

Techniques

APCI	atmospheric pressure chemical ionisation
EDX	energy dispersive X-ray
ES^+	positive ion electrospray
EI	electron impact
FAB	fast atom bombardment
IR	infra red
NMR	nuclear magnetic resonance
UV/VIS	ultra violet visible

Solvents

dmf	N,N-dimethyl formamide
dmso	dimethyl sulfoxide
Et_2O	diethyl ether
MeCN	acetonitrile
thf	tetrahydrofuran

Ligands and Complexes

M	metal
L	ligand
L-L	bidentate ligand
E	Group 15 atom (P, As, Sb or Bi)
X	halide (Cl, Br or I)
R	alkyl or aryl substituent
L^1	$Ph_2P(CH_2)_2O(CH_2)_2O(CH_2)_2PPh_2$
L^2	$Ph_2P(CH_2)_2S(CH_2)_2S(CH_2)_2PPh_2$
dpsm	$Ph_2SbCH_2SbPh_2$
dmsm	$Me_2SbCH_2SbMe_2$

P_2S	1,2-$C_6H_4PH(CH_2)_3S(CH_2)_3PH$
cod	1,5-cyclooctadiene
nbd	norbornadiene; [2.2.1] hepta-2,5-diene
tmpa	tetramethyl-1,3-propanediamine
tht	tetrahydrothiophene
cp	cyclopentadienyl

General

AIBN	2,2'-azobis(isobutyronitrile)
acac	acetylacetonate
ppm	parts per million
Kf	formation constant
Kd	dissociation constant
δ	chemical shift
δ(coord)	chemical shift upon coordination
TMS	trimethylsilane
m/z	mass to charge ratio
RT	room temperature
^{i}Pr	iso-Propyl
^{i}Bu	iso-Butyl
w	weak
m	medium
s	strong
vs	very strong
bs	broad and strong
sh	shoulder
tbp	trigonal bipyramidal

Chapter 1

Introduction

1.1 Introduction

The coordination chemistry of phosphine and arsine ligands was first investigated over one hundred years ago. Initially organoarsenic chemistry developed at a faster rate than that of the phosphines due mainly to the lower air sensitivity of arsines and easier preparations. However in the 1960's interest in organophosphorus chemistry began to grow and the transition metal chemistry of tertiary phosphine ligands became, and still remains, one of the most intensely studied areas of coordination chemistry. This interest was driven by the superior coordination ability of phosphines in particular to harder metal centres, and also by the development of NMR spectroscopic techniques which allowed the increased study of the spin ½, ^{31}P nucleus.[1]

Although the coordination chemistry of stibines began in the early twentieth century, this area of chemistry has always received limited attention, in part due to the weaker coordinating ability of stibine ligands. Studies have been largely confined to soft metals in low oxidation states and studies of ditertiary stibines only appeared post 1970.[1]

Very little work has been carried out on the coordination chemistry of bismuthine ligands due to their very poor donor ability and to the very weak C-Bi bonds, which break easily in the presence of metal centres.[2]

In contrast to phosphines, the heavier donor ligands lack an NMR probe. All naturally occurring arsenic, antimony and bismuth nuclei are quadrupolar and in the low symmetry environments in ER_3 ligands (E = As, Sb or Bi), no resonances are observed due to fast quadrupolar relaxation.[1, 2]

The work in this thesis is primarily concerned with the synthesis and coordination chemistry of distibine ligands, mixed donor phosphine containing ligands, and phosphine macrocycles. The chemistry of antimony donor ligands has been the subject of a number of reviews, the most important of which are listed in Table 1.1. The synthesis of stibine ligands is dicussed in the introduction to chapter 2 and the coordination chemistry of distibine ligands with a range of transition metals is described in detail in the introductions to chapters 3 and 4.

Topic	Reference
Arsines, stibines, bismuthines	1
Coordination chemistry of stibine and bismuthine ligands	2
Transition metal complexes containing monotertiary arsines and stibines	3
Phosphine, arsine and stibine complexes of the transition elements	4
Organoantimony compounds	5
Synthesis of organoarsenic, -antimony and –bismuth compounds	6
Organoarsenic and organoantimony compounds	7
Synthesis of organoantimony and organobismuth compounds	8
Coordination chemistry of organostibines	9

Table 1.1 – Recent reviews of stibine chemistry

1.2 Bonding in Group 15 Metal Complexes (M-ER_3 E = P, As, Sb or Bi)

The theoretical background to the bonding of Group 15 ligands to metals has been developed for phosphines. It is assumed that the same bonding models apply to the heavier Group 15 analogues and the literature focuses on trends down the group and any differences from the M-PR_3 model.[1, 2]

1.2.1 Electronic effects

The first description of an M-PR_3 bond was proposed by Chatt in 1950.[10, 11] This bonding model was comprised of two components, firstly σ-donation from the lone pair on phosphorus to an appropriate empty d-orbital on the metal, and secondly π-back-donation from a filled metal dπ-orbital into an empty 3d orbital on phosphorus. However in the 1960's the Chatt bonding model was reconsidered. It was believed that the empty 3d orbitals on phosphorus were too high in energy and too diffuse for the back-bonding process to occur.[12] However it is difficult to explain the stability of zero-valent metal complexes on the grounds of σ-bonding alone.

In 1985 Orpen and Connelly proposed an alternative model in which the P-X σ^* orbital (X = CH_3, H or F) accepts electron density from the metal.[13] The advantage of this

new model is that the new acceptor orbital retains the *e*-symmetry necessary for π-back-donation to occur, but it is lower in energy than the 3d-orbitals proposed by Chatt.

X-ray crystallographic data on several pairs of metal complexes which differ in oxidation state alone e.g. $[Mn(CO)\{Ph_2P(CH_2)_2PPh_2\}\{\eta^5\text{-}C_5H_4Ph\}]^{0/+1}$ have shown that increasing the metal oxidation state lengthens the M-P bond but reduces the P-X bond length (X = CH_3, H or F).[13] These observations are consistent with the presence of a P-X σ^* component within the π-bond. It is therefore widely accepted that σ-bonding provides the main component of M-PR_3 bonding with the π-component becoming more significant with electronegative R-groups.

Detailed calculations for the heavier ligands are unavailable but it is assumed that the same bonding model applies. As Group 15 is descended the ligands become both weaker σ-donors and weaker π-acceptors. Weaker σ-donation is attributed to the larger energy separation between the valence s- and p-orbitals as the donor atom becomes heavier. This results in an increased p-component in the E-C bonds (E = P, As, Sb or Bi) and an increased s-character in the lone pair. As a consequence the lone pair has poorer directional properties which, together with the more diffuse orbitals of the heavier atoms and the weaker bonds formed by these atoms in general, results in poor ligating properties.[1] The decrease in π-acceptance down Group 15 is due to the reduced electronegativity of the acceptor atom and to the more diffuse orbitals.[1]

1.2.1 Steric effects

The steric properties of phosphines are normally expressed in terms of Tolman's cone angles. The cone encloses the van der Waals radii of all ligand atoms over all rotational orientations about the M-P bond (Figure 1.1).[14] In general, the greater the steric bulk of the ligand the greater the value of θ. Ligands with large cone angles tend to favour lower coordination numbers, the formation of less sterically crowded isomers and have increased rates in dissociation reactions.[15]

Since the Tolman model is geometrically based it can be extended to the heavier Group 15 ligands by taking into account the increased size of the donor atom and the corresponding increase in *d*(M-E) (E = As, Sb or Bi). McAuliffe has compared the cone angles of common Group 15 ligands and the results have shown that stibines have smaller

cone angles by ca. 2-5 % than the corresponding phosphines, with bismuthines having smaller cone angles again by a similar amount.[16] However it is important to note that cone angles can only be used as a relative measure as real ligands are not solid cones and allow intermeshing of substituents.

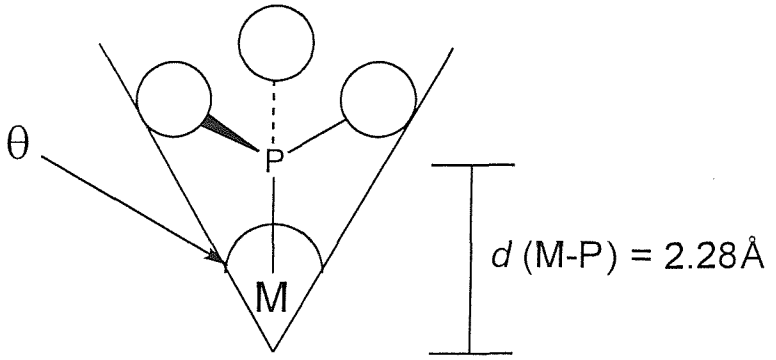

Figure 1.1 – Representation of Tolman's cone angle

The large increase in available X-ray crystallographic data during recent years has allowed more detailed studies of ligand steric effects.

Orpen and co-workers examined a large range of Ph_3P-E fragments (in which E = a wide range of transition metals and main group elements).[17] They found that when E = a light non-metal, the ∠C-P-C increases towards the tetrahedral angle, yet when E = a transition metal the PPh_3 ligands adopt geometries very similar to that of triphenylphosphine itself.[17]

A more recent study on the coordination chemistry of the stibine ligand $Ph_2SbCH_2SbPh_2$ by Levason *et al* found that the coordinated $SbPh_2$ group has ∠C-Sb-C all larger than those in the 'free' ligand.[18] These observations indicated that the trends observed for phosphines by Orpen may not be true for the heavier group 15 donor ligands. A subsequent study of Ph_3Sb-M fragments (in which M = a transition metal) showed that in all complexes the ∠C-Sb-C were larger than that in Ph_3Sb itself (∠C-Sb-C(av.) = 96.27(21))°, ranging up to ca. 104°.[19] A similar study of Ph_3As transition metal complexes showed that ∠C-As-C also increased on coordination from an average of 99.4(4)° in free triphenylarsine to an average of 102.3(13)° upon complexation.[19]

This increase in angle in the heavier Group 15 donor ligands upon coordination can be attributed to changes in the proportion of s/p character in the E-C bond (E = P, As, Sb). In the 'free' ligand the E-C bonds have higher p-character as group 15 is descended. Upon coordination an increase in s/p mixing will increase the ∠C-E-C.[1, 19] A more detailed explanation must await high level MO calculations.

1.2.1 Coordination Modes

ER_3 ligands (E = P, As or Bi, R = alkyl or aryl) typically behave as monodentate ligands towards metal centres. However Werner and co-workers have shown that both PR_3 (R = Me or Et) and SbR_3 (R = ^{i}Pr, Et or Me) can behave as bridging ligands in several Rh(I) carbene complexes e.g. *trans*-$[Rh_2Cl_2(\mu\text{-}CR_2)_2(\mu\text{-}SbR_3)_2]$.[20, 21]

Diphosphinomethanes ($R_2PCH_2PR_2$) can function either as chelating, monodentate or bridging ligands depending on the metal ion and conditions involved. When phosphorus is replaced with one of the heavier Group 15 donor atoms their larger size increases the strain within the 4-membered chelate ring. This, together with an overall poorer donor ability disfavours chelation as a coordination mode. Instead diarsinomethanes ($R_2AsCH_2AsR_2$) and distibinomethanes ($R_2SbCH_2SbR_2$) prefer to bond as monodentate or bridging ligands.[1, 4, 9]

Diphosphines and diarsines with two carbon backbones usually chelate to metal centres to form stable five-membered chelate rings. Three carbon backboned diphosphines, diarsines and distibines also typically behave as chelate ligands.[1]

1.3 Bonding in Metal Carbonyl Complexes (M-CO)

CO is the most studied σ-donor π-acceptor ligand. Bonding to a metal centre involves a synergic mechanism. Overlap of a filled carbon σ-orbital with a metal σ-orbital leads to transfer of electron density from carbon to the metal. This results in an unacceptably high level of electron density on the metal and as a result back-bonding occurs through overlap of a filled metal dπ or hybrid dpπ orbital with the empty $p\pi^*$ orbital on CO.[22]

In a mixed carbonyl complex $ML_x(CO)_{6-x}$ the position of the ν(CO) stretch in the IR spectrum can be used as an indicator of donor strength. A strong σ-donor ligand will

transfer a significant amount of electron density to the metal centre resulting in an increase in the level of π-back-donation to the CO ligand. π-back-donation strengthens the M-C bond but the transfer of electron density into the $p\pi^*$ orbital on CO will weaken the C≡O bond resulting in a low frequency shift in the IR spectrum.

1.4 Synthesis of Phosphine Ligands

1.4.1 Primary and Secondary Phosphines

Primary phosphines RPH_2 are usually prepared by reduction of RPX_2, $RP(S)X_2$, $RP(O)X_2$ etc with $LiAlH_4$,[4, 16] for example phenylphosphine ($PhPH_2$) is obtained by the $LiAlH_4$ reduction of $PhPCl_2$.[23] Similarly, secondary phosphines R_2PH can also be prepared by $LiAlH_4$ reduction as described above. They can also be obtained by hydrolysis of the corresponding phosphide or by alkylation and hydrolysis of MPRH.[4, 16]

1.4.2 Tertiary Phosphines

Tertiary phosphines are easily prepared by the reaction of PX_3, RPX_2 or R_2PX with a Grignard or organolithium reagent to yield PR'_3, RPR'_2, R_2PR' respectively. They can also be prepared by the reaction of alkali phosphides MPR_2 with R'X.[4, 16] Mixed aryl alkyl phosphines are normally prepared by the reaction of Ph_2PCl or $PhPCl_2$ with an organolithium or Grignard reagent.[4, 16]

Unsymmetrical secondary and tertiary phosphines can be obtained in good yield by the addition of a primary or secondary phosphine to an olefinic double bond. This reaction can be catalysed by strong non-oxidising acids, strong bases such as potassium butoxide[24-26] or by free radical initiation.[27] The latter can be achieved by UV irradiation,[24] or more commonly by a free radical initiator such as AIBN.[27] The reaction occurs with both free and coordinated phosphines[28] and has been used as a method of ring closure for the synthesis of phosphine containing macrocycles. For example the macrocyclic complex *fac*-$[Mo(CO)_3\{[12]aneP_3\}]$ is prepared by the free radical initiated cyclooligomerization of the macrocyclic precursor $[Mo(CO)_3\{CH_2{=}CHCH_2PH_2\}_3]$ by AIBN (Scheme 1.1).[28, 29]

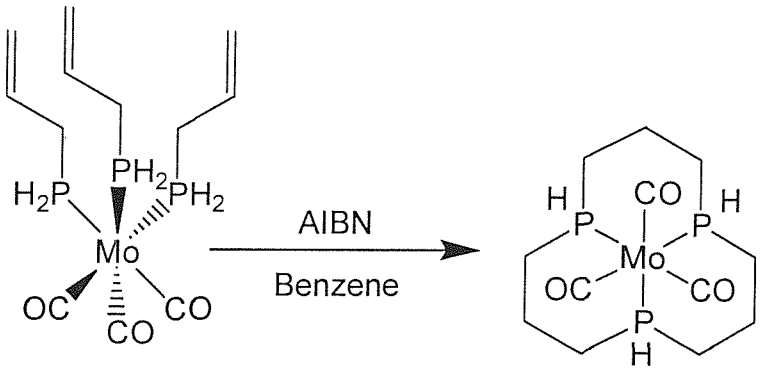

Scheme 1.1 – Free radical initiated cyclisation of *fac*-$[Mo(CO)_3\{CH_2{=}CHCHCH_2PH_2)_3]$[28, 29]

1.4.3 Diphosphines

Diphosphines are usually prepared by the reaction of alkali metal phosphides with a dihalogenoalkane. The reactions must be carried out under an anhydrous, O_2 free atmosphere and the resulting diphosphines can be obtained in high yield and in reasonable purity if excess dihaloalkane is avoided.[16] For example the bis(diphenylphosphino)alkanes $Ph_2P(CH_2)_nPPh_2$ (n = 1-3) can be easily prepared by the reaction of $X(CH_2)_nX$ with $LiPPh_2$ in thf.[30, 31] The analogous alkyl substituted diphosphines $R_2P(CH_2)_2PR_2$ (R = Me or Et) can be isolated as highly air-sensitive and pyrophoric oils by reaction of $LiPR_2$ with the appropriate dihalogenoalkane.[32, 33]

cis- and *trans*-1,2-bis(diphenylphosphino)ethylene $Ph_2PCH{=}CHPPh_2$ can be prepared by the reaction of *cis*- and *trans*-ClCH=CHCl respectively with two equivalents of Ph_2PLi in thf.[34]

As with the corresponding distibines (see chapter 2), phenylene based diphosphines are more difficult to prepare. *p*-$C_6H_4(PPh_2)_2$ can be prepared in high yield by reaction of $LiPPh_2$ with *p*-$C_6H_4Br_2$ or *p*-$C_6H_4ClSO_3Na$.[35, 36] However the *ortho*-isomer can be prepared in good yield from $LiPPh_2$ and *o*-$C_6H_4F_2$ in thf.[37] It can be prepared in higher yields by the reaction shown overleaf in Scheme 1.2 although this is much more time consuming.[38]

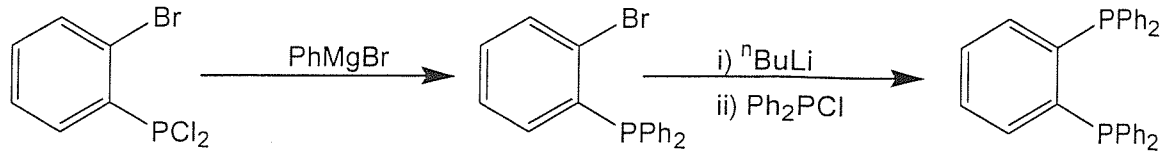

Scheme 1.2 – Synthesis of *o*-$C_6H_4(PPh_2)_2$[38]

The tetrafluorophenyl analogue can be prepared form *o*-$C_6F_4Br_2$.[39] Whilst the methyl analogue *o*-$C_6H_4(PMe_2)_2$ can be prepared in low yield by reaction of *o*-$C_6H_4X_2$ and $NaPMe_2$ in thf.[40] Alternatively it can be prepared by reduction of the corresponding phosphonite by $LiAlH_4$ to give the diprimary phosphine *o*-$C_6H_4(PH_2)_2$ and subsequent deprotonation and reaction with MeI (Scheme 1.3).[41]

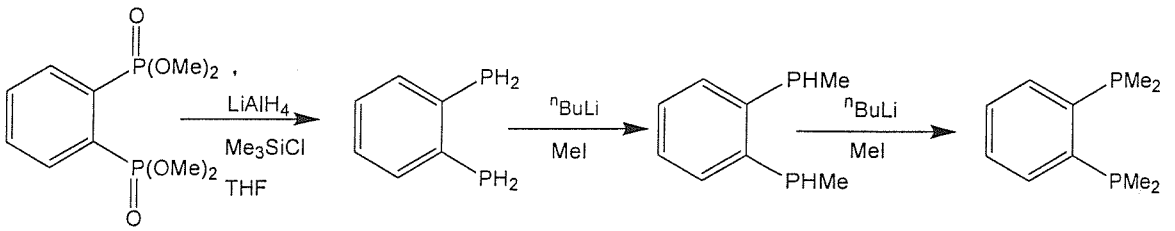

Scheme 1.3 – Synthesis of *o*-$C_6H_4(PMe_2)_2$[41]

The synthesis of phosphine containing macrocycles is discussed in detail in the introduction to chapter 6.

1.5 Applications of Acyclic Phosphine Chemistry

The properties of transition metal phosphine complexes can be tuned or completely altered by varying the substituents on phosphorus. This ability to 'tune' the metal complex has led to the use of transition metal phosphine complexes in a range of catalytic applications, including hydrogenation, hydrosilylation and polymerisation.[4] Both selectivity and specificity can be varied by steric and electronic control, which is achieved by alteration of ligand substituents. For example the homogeneous reduction of alkenes, alkynes and other unsaturated substances can be catalysed using 'Wilkinson's catalyst' $RhCl(PPh_3)_3$ (Scheme 1.4).[42, 43]

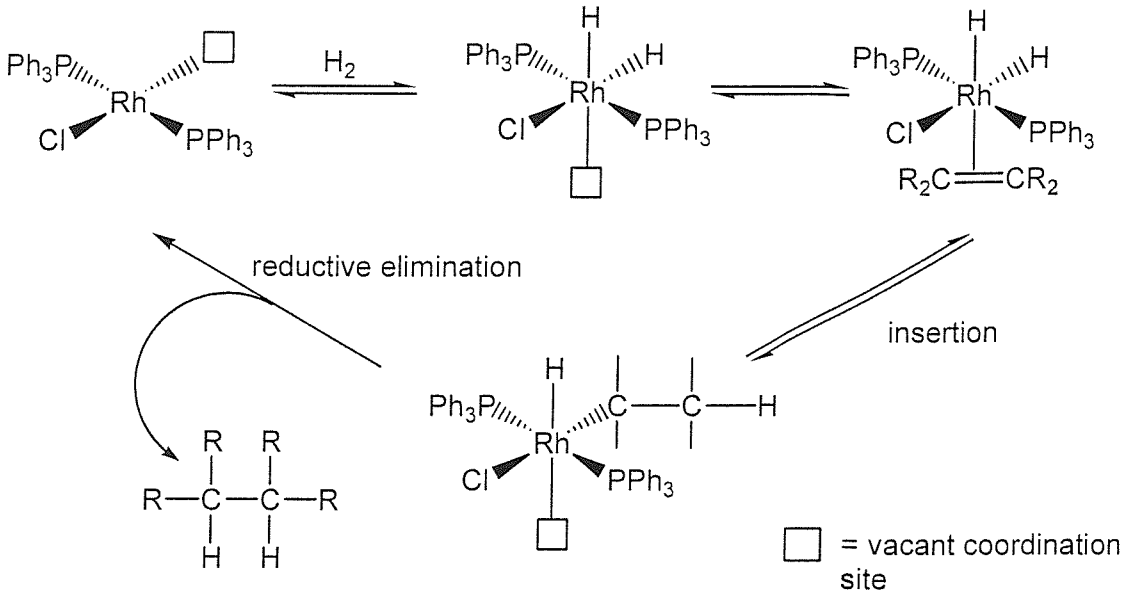

Scheme 1.4 – Catalytic cycle for Wilkinson's Catalyst

The catalytic cycle requires dissociation of one of the triphenylphosphine ligands to leave a vacant coordination site. Rhodium complexes with alkylphosphines, which are more basic and less sterically hindered than aryl complexes, are less catalytically active due to a lower tendency for dissociation. The triphenylphosphine ligands also influence the orientation and complexation of the unsaturated species and also influence the stability of the intermediate species.[42, 43]

For all types of catalysis, separation of the product and catalyst is important to allow recycling of the catalyst. This may be achieved in one of two ways, either by supporting the catalyst on a solid support or by tailoring the solubility of the catalyst so it resides in a different phase to the product. Both of these rely on functionalisation of the ligand.[44] For example water soluble catalysts can be made by attaching water solubilising functionalities to the ligand, and much work has been carried out using water soluble tertiary phosphines such as $P(C_6H_4SO_3^-Na^+)_3$.[43] Similarly solubility in fluorinated solvents can be achieved by the addition of fluorinated chains to the ligands e.g. $P(CH_2CH_2(CF_2)_5CF_3)_3$ which has applications in fluorous phase catalysis.[44]

Interest in multidentate mixed donor phosphine containing ligands, in particular P/O and P/N ligands, stems from their potential to act as hemilabile ligands. Acyclic phosphine ligands are strong σ-donors and form stable complexes with many metal ions.

Phosphine ligation may enhance the binding properties of hard O and N donor atoms. Hemilabile ligands such as these can form complexes with one donor atom strongly bound to the metal centre whilst the other is more weakly bound. This allows the latter to dissociate, forming a vacant coordination site which may be important in homogeneous catalysis.[45]

Rhodium(I) complexes of P/O donor ligands have been used as catalysts in the carbonylation of methyl iodide (Scheme 1.5). The formation and cleavage of the Rh-O bond is an intrinsic part of the mechanism.[44]

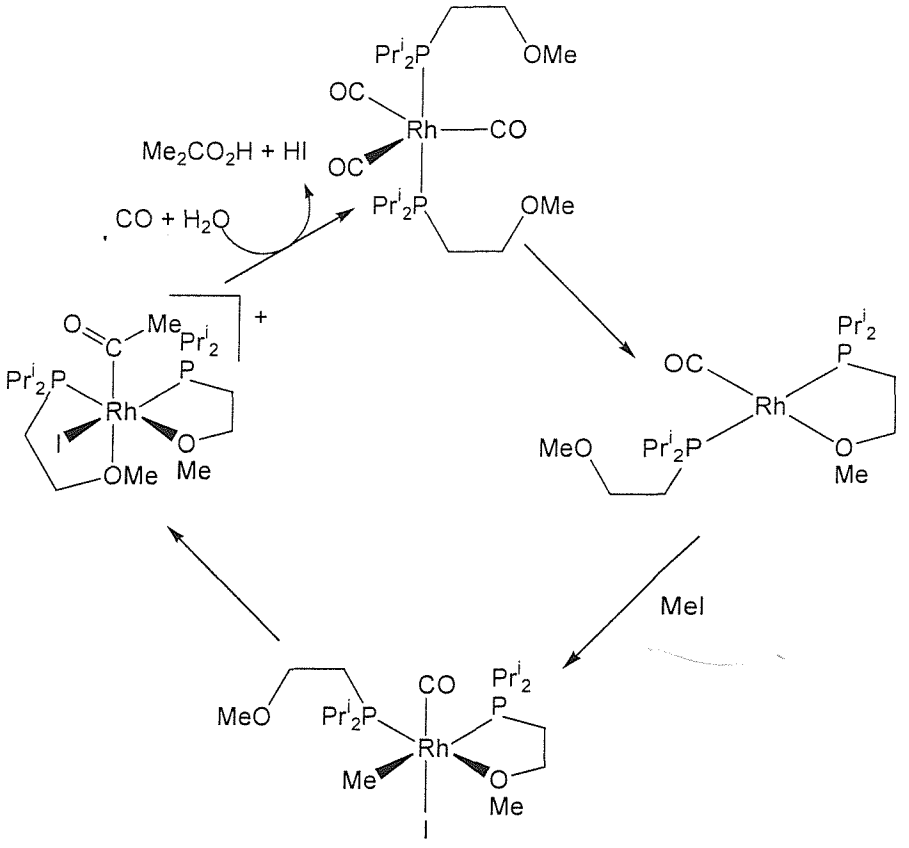

Scheme 1.5 – A simplified catalytic cycle for the carbonylation of methyliodide to give ethanoic acid [44]

1.6 The Chelate Effect

The term chelate effect refers to the enhanced stability of a complex containing chelating ligands when compared to that of a similar system containing monodentate ligands.[15] Consideration of the thermodynamic relationship shown below shows that both enthalpic and entropic factors are influential in complex stability.

$$\Delta G^\circ = \Delta H^\circ - T\Delta S^\circ$$

$$\Delta G^\circ = -RT\ln\beta$$

(G = Gibbs free energy, H = enthalpy, S = entropy, T = temperature, R = gas constant, β = formation / stability constant.)

The formation /stability constant (β) increases as ΔG° decreases. There are two ways in which this can be achieved, making ΔH° more negative or by making ΔS° more positive.[15]

The enthalpy differences arise from electrostatic interactions between the ligands. With monodentate ligands repulsion increases as the ligands are brought together prior to complexation due to electrostatic repulsion between negative charges or dipole moments. With chelating ligands this repulsion is partially built into the ligand framework and hence there is no significant increase in enthalpy upon coordination. The second main factor influencing the enthalpy term is solvation. There is an enthalpic penalty associated with desolvation. In general the solvation of chelating ligands is lower than that of their monodenatate analogues.

The entropy term arises from the increased probability of a multidentate ligand coordinating to a metal centre. Once one end of the ligand has complexed the other end is held in close proximity to the metal centre increasing the likelihood of coordination. This explains the decreasing magnitude of the chelate effect with increasing ring size.[15] With monodentate ligands the binding of one ligand has no influence on the binding of the other.

1.7 Macrocyclic Chemistry

For the purpose of this discussion a macrocycle will be defined as a cyclic molecule consisting of at least nine atoms, of which a minimum of three must be donor atoms, thus allowing the macrocycle to bind a metal centre within the central cavity.

Whilst much research has been directed towards azamacrocycles, crown ethers and thioether macroycles, research into the chemistry of phosphine macrocycles has been much more limited, due mainly to experimental difficulties.[46] However the ability of phosphine macrocycles to easily bind to a wide range of transition metals in varying oxidation states, and the unusual catalytic properties expected from some of these complexes has led to a rise in interest in this field. A number of phosphorus containing macrocycles are now known and the synthetic routes to phosphine macrocycles are reviewed in the introduction to chapter 6.

1.7.1 The Macrocyclic Effect

The stability of macrocyclic complexes is usually much greater than that of their acyclic analogues, a fact that cannot be attributed to the chelate effect alone. This enhanced stability is known as the macrocyclic effect.[47] As with the chelate effect, the magnitude of the macrocyclic effect is determined by both enthalpic and entropic factors, although the thermodynamics are less understood than for the chelate effect.[48, 49]

The magnitude of the enthalpic term can be influenced by a variety of factors including ring size, metal ion and donor type.[50, 51] However solvation is thought to play a major role.[47, 52] In general macrocycle solvation is poorer than that of the analogous open chain ligands and is dependent on ring size, solvents, degree of hydrogen bonding and the metal ion present. Therefore for complexation to occur, less enthalpic energy is required to break hydrogen bonds with the solvent.[52]

Macrocyclic ligands have less rotational and translational freedom than their open chain analogues. As a result of this preorganisation there is a less dramatic ordering effect upon coordination, which gives rise to a favourable entropy term.[48] If we consider the equation below in which $L_{(mac)}$ refers to the macrocyclic ligand and $L_{(oc)}$ refers to an open chain ligand we can see that upon complexation of the macrocycle the open chain ligand is released into solution leading to a rise in disorder and hence an increase in entropy.

$$ML_{(oc)} + L_{(mac)} \rightleftharpoons ML_{(mac)} + L_{(oc)}$$

Generally macrocyclic complexes have very high kinetic stability, greater than that of their open-chain analogues. Both coordination and ligand dissociation reactions with macrocyclic ligands are usually slower than those with their open chain analogues.

$$M^{x+} + L_{(mac)} \underset{k_d}{\overset{k_f}{\rightleftharpoons}} [ML_{(mac)}]^{x+}$$

The formation constant (k_f) is much smaller than with open chain complexes, for example for cyclam $k_f = 10^6$ whilst for the analogous open chain ligand $H_2N(CH_2)_2NH(CH_2)_2NH(CH_2)_2NH_2$ $k_f = 10^8$.[48] This is due to the reduced flexibility of the macrocyclic ligand. Following coordination of one donor atom, the macrocycle is forced into a high energy conformation to enable coordination of the remaining donor atoms, and thus the energy barrier for the reaction is higher. For an open chain ligand which has greater flexibilty, coordination is quicker and requires less energy.[48] The dissociation constant (k_d) is also much smaller for macrocyclic complexes. This arises from the flexibility of the coordinative bonds. For dissociation to occur elongation and cleavage of the M-L bond is required. In a macrocyclic complex this leads to significant ring strain within the structure and hence is disfavoured.[53]

1.7.2 Macrocycle Synthesis

There are a variety of procedures for synthesising macrocycles, however most can be divided into two main categories; template reactions or high dilution synthesis. Any macrocycle synthesis must maximise yields of the desired product by inhibiting polymerisation and other competing reactions. Both methods offer benefits and disadvantages which are discussed below in sections 1.7.2.1 and 1.7.2.2 and are summarised in Table 1.2.

1.7.2.1 High Dilution Synthesis

A high dilution reaction involves the reaction of two functionalised species to form the macrocycle.[53] The reactions are typically performed under high dilution conditions, as a result the concentration of unreacted reagents in solution at any one time is small. This promotes intramolecular cyclisation over intermolecular reactions that may result in polymerisation.

High dilution reactions are typically used in the synthesis of thioether and selenoether macrocycles,[54, 55] although such systems have been employed in the synthesis of some phosphine (Scheme 1.6),[46] arsine[56] and azamacrocycles.[57]

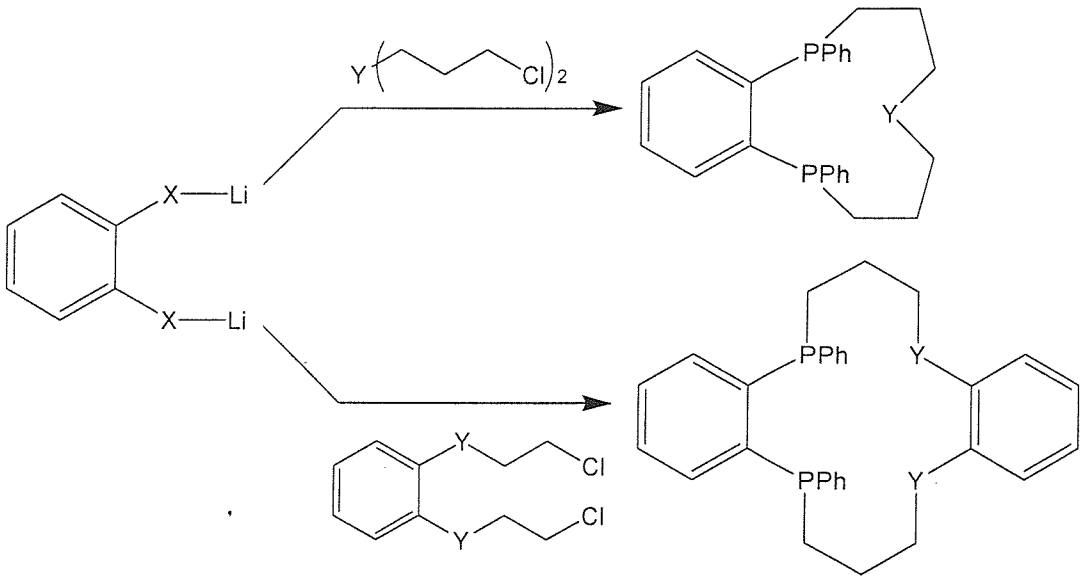

Scheme 1.6 – Kyba high dilution syntheses of phosphine macrocycles (X = PPh, Y = PPh, S, O, NMe, NPh, CH_2 or AsPh).[58, 59]

One particular drawback of the high dilution approach in the synthesis of phosphine macrocycles is the occurrence of mixtures of stereoisomers which are often extremely difficult to separate. It is difficult to convert mixtures of stereoisomers into a single preferred form due to the high energy barrier to inversion at phosphorus (section 1.8).

High dilution syntheses are often very lengthy and if using primary or secondary phosphines substantial oxidation may occur during the reaction. Also many of the reactive precursors are water sensitive necessitating the use of rigorously anhydrous conditions.

1.7.2.2 Template Synthesis

In a template reaction the generation of the cyclic product is influenced by the presence of a metal ion. The metal ion acts as a template for cyclisation to occur.[60] Three

possible roles for the metal ion have been proposed; a thermodynamic, a kinetic and an equilibrium template effect.[61]

A reaction is said to proceed by a kinetic template effect when the metal ion acts by coordinating the reactants and directing the steric course of the reaction to give a product that would not be formed in its absence.[62]

In the case of the thermodynamic template effect, cyclisation can occur in the absence of the metal ion, however macrocycle formation is favoured in its presence as the macrocycle is removed from the equilibrium.[63]

The equilibrium template effect is a combination of the previous two effects. The reactants react reversibly to form an intermediate that can form a stable complex with the metal ion. Hence in its presence all of the reactants proceed to the macrocycle whilst in its absence a mixture of products is obtained.

With the synthesis of phosphine macrocycles the template approach has several disadvantages. Coordination to a metal centre substantially weakens P-H bonds and as a consequence deprotonation can occur. Once deprotonated the metal-coordinated phosphide can undergo further reaction to form phosphido-bridged dimers or clusters thus preventing macrocyclisation. Secondly many phosphines form extremely stable complexes with transition metal ions and as result cyclisation of the phosphine macrocycle precursors can be hindered. Once cyclised the high stability of the complexes can lead to difficulties in demetallation.

The advantages and disadvantages of the two synthetic methods are summarised in Table 1.2.

Template Synthesis		High Dilution Synthesis	
Advantages	Disadvantages	Advantages	Disadvantages
Metal complex formed directly	Not all metals are suitable as templates	Statistically favours cyclisation over polymerisation	Slow reaction times
Some macrocycles cannot be prepared as free ligands	Demetallation can be difficult	Forms the free ligand directly	Large volumes of solvents are often required
Unstable precursors can achieve stabilisation upon complexation to a, metal ion	May obtain bi- or tri- nuclear macrocyclic complexes	Procedure can be used when demetallation is difficult	Can be difficult to separate stereoisomers
Isolate a stable product, usually in high yield		Typically good yields	

Table 1.2 – Advantages and disadvantages of template synthesis vs. high dilution synthesis

1.7.2 Applications of Macrocyclic Chemistry

As described in section 1.7.1 most macrocyclic complexes are both kinetically and thermodynamically more stable than their analogous open-chain ligand complexes. This high stability has led to the use of macrocycles in a wide range of technological applications.

The ability of macrocycles to selectively extract certain metal ions from a mixture has potential use in the mining industry, and may provide an environmentally friendly alternative to pyrometallurgy.[48] Crown ethers show remarkable selectivity for alkali and alkaline earth metals, with the selectivity being dependent on parameters such as cavity size, solvation energies and number of donor atoms.[60] For example 14-crown-4

selectively binds lithium due to the small diameter of the macrocyclic cavity.[64] As well as having potential applications in purification processes, the selectivity of crown ethers is similar to that of many naturally occurring antibiotics and as a result they can be used as models for ion transport in biological systems.[65, 66]

The ability of macrocycles to selectively bind metal ions has led to applications within the medical and electronics industries. Macrocyclic ligands that can bind radioactive metals such as the example shown below in Figure 1.2, or macrocyclic lanthanide complexes can be used as imaging agents and in chemotherapeutic applications.[48]

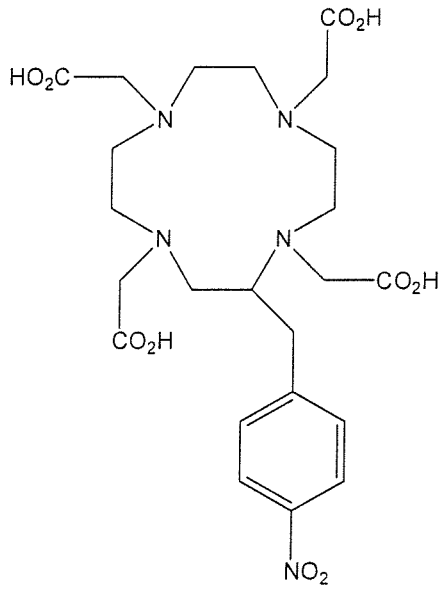

Figure 1.2 – A macrocyclic ligand proposed for the binding of ^{90}Y for use in radiotherapy

Proposals have been made for microelectronic devices that will incorporate macrocyclic ligands which can detect or recognise particular metal ions. It may be possible for the binding of a metal ion to trigger some change within the system such as a change in colour.[48]

Macrocyclic complexes can also exhibit catalytic behaviour. Azamacrocycles and their organometallic and coordination compounds play important catalytic roles in the activation of small molecules such as CO_2.[67] For example the electrocatalytic reduction

of CO_2 can be achieved in the presence of $[Ni\{[14]aneN_4\}]^{2+}$ and a number of water soluble derivatives.[68]

Tridentate macrocycles such as the P_2S donor macrocycle studied in chapter 6 can act as face-capping $6e^-$ donor ligands for transition metals. They are neutral analogues of the Cp^- ligand, complexes of which are important catalyst precursors. For example $[TiCl_2Cp_2]$ catalyses olefin polymerisation in the presence of $AlClEt_2$.[69] These macrocycles are often 'tuneable' through variation of ring size, substituents and donor type, which in turn can alter the electronic properties of the coordinated metal.

Many macrocyclic ligands and complexes occur in nature. Metal complexes of macrocycles based on the porphyrin ring system (Figure 1.6) play major roles in a variety of biological systems.

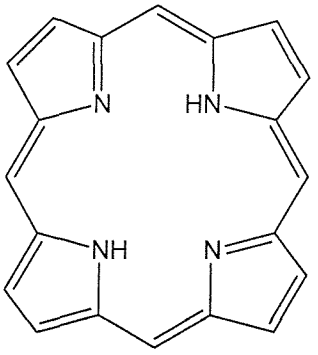

Figure 1.3 – Porphyrin structure

Vitamin B_{12}, chlorophyll, haemoglobin and myoglobin all contain porphyrin derivatives in their molecular framework.[48, 60] Much research has been directed towards the synthesis of model compounds for these natural macrocycles to enable detailed studies into their functions. For example cobalt corrinoid complexes have been investigated as models for vitamin B_{12}.[66]

Macrocyclic coordination chemistry can also be used to model the metal-binding sites in proteins. Although these sites are not formally macrocyclic, the well-defined arrangement of donor atoms at the binding sites can be mimicked by a macrocyclic ligand containing similar donor atoms.[48]

1.8 Inversion at Phosphorus

One common problem with the high dilution synthesis of phosphine macrocycles is the formation of mixtures of stereoisomers. This problem can also arise in the synthesis of acyclic multidentate phosphine ligands. The stereoisomers may not be easily converted to a single preferred form due to the high energy barrier to inversion at phosphorus. For example Ciampolini has prepared the large ring P_4S_2 donor macrocycle $Ph_4[22]aneP_4S_2$ by reaction of bis(3-chloropropyl)sulfide with the dilithium salt of 1,2-bis(phenylphosphino)ethane, the macrocycle is isolated as a mixture of five stereoisomers. (Figure 1.4).[70]

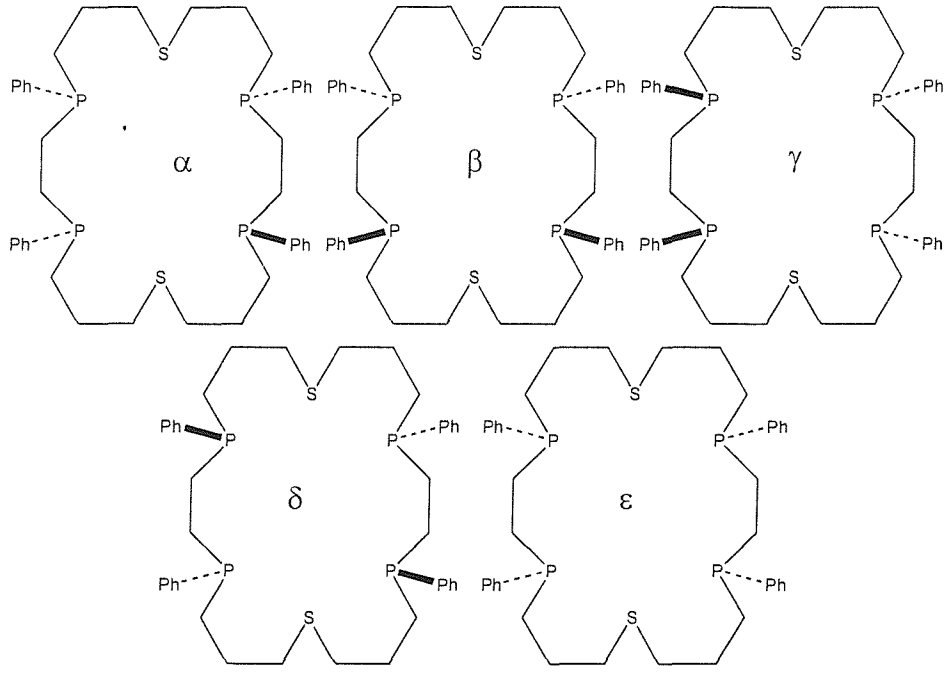

Figure 1.4 – The five stereisomers of $Ph_4[22]aneP_4S_2$ [70]

The separation of the individual stereoisomers is a lengthy process involving fractional crystallisation as well as ion-exchange chromatography of their nickel salts.

A Group 15 atom (E) with three different substituents is chiral and thus stereoisomers are possible and inversion may occur (Figure 1.5). However the inversion barrier is much higher than that for the Group 16 ligands (~150 KJ mol^{-1} for free PR_3).[53] The rate of inversion is further reduced by coordination to a metal centre and by ring

strain in five membered chelate rings. Electronegative substituents on E also lead to an increase in the activation barrier to inversion.[53]

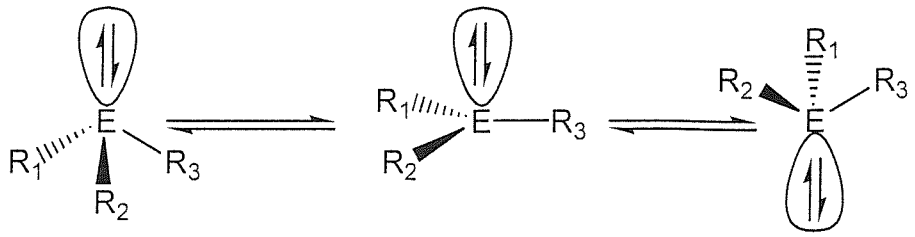

trigonal planar transition state

Figure 1.5 – Inversion at phosphorus

1.9 Aims of Research

- To develop a new synthetic route for the preparation of multidentate stibines in sufficiently high yields to allow a detailed study of their chemistry.

- To investigate the coordination chemistry of the novel distibines with a range of transition metal centres to probe the coordination modes, spectroscopic properties and donor properties, and to compare their chemistry with related Group 15 ligands.

- To explore the coordination chemistry of the mixed donor acyclic ligands $Ph_2P(CH_2)_2O(CH_2)_2O(CH_2)_2PPh_2$ and $Ph_2P(CH_2)_2S(CH_2)_2S(CH_2)_2PPh_2$ with Ag(I) salts and with a variety of transition metal carbonyls, to investigate the effect of combining both phosphine and ether, and phosphine and thioether functions within a single ligand, and to obtain new metallocyclic species.

- To develop a new synthetic route to P_2S donor macrocycles using a template procedure based on the use of $Mn(CO)_3$ and $Re(CO)_3$ fragments.

1.10 References

1. W. Levason and G. Reid, 'Arsines, Stibines, Bismuthines', Vol. 1, Chapter 16, 'Comprehensive Coordination Chemistry II', J. A. McCleverty and T. J. Meyer (Ed.), Elsevier, Oxford, (2003).
2. N. R. Champness and W. Levason, *Coord. Chem. Rev.*, **133**, (1994), 115.
3. J. C. J. Cloyd and C. A. McAuliffe, 'Transition Metal Complexes Containing Monotertiary Arsines and Stibines', Chapter 3, 'Transition Metal Complexes of Phosphorus, Arsenic and Antimony Ligands', C. A. McAuliffe (Ed.), Macmillan, London, (1973).
4. C. A. McAuliffe and W. Levason, 'Studies in Inorganic Chemistry, Vol. 1: Phosphine, Arsine and Stibine Complexes of the Transition Elements', Elsevier, Amsterdam, (1978).
5. 'Gmelin Handbuch der Anorganische Chemie, Organoantimony Compounds, Part 1', (1981).
6. K.-Y. Akiba and Y. Yamamoto, 'Syntheses of Organoantimony and Organobismuth Compounds', 'Chem. Org. Arsenic, Antimony and Bismuth Compd.' S. Patai (Ed.), Wiley, New York, (1994).
7. W. J. Cross, S. M. Godfrey, C. A. McAuliffe, A. G. Mackie and R. B. Pritchard, 'Organoarsenic and Organoantimony Compounds: Synthesis, Properties and Uses in Organic Transformations', Chapter 5, 'The Chemistry of Arsenic, Antimony and Bismuth', N. C. Norman (Ed.), Blackie, London, (1998).
8. S. Samaan, 'Methods in Organic Chemistry (Houben-Weyl) Vol. 13, Pt. 8: Metalloorganic Compounds, Arsenic, Antimony, Bismuth', (1978).
9. W. Levason and C. A. McAuliffe, *Acc. Chem. Res.*, **11**, (1978), 363.
10. J. Chatt, *Nature*, **165**, (1950), 637.
11. J. Chatt and A. A. Williams, *J. Chem. Soc.*, (1951), 3061.
12. W. Levason, 'The Chemistry of Organophosphorus Compounds Vol 1', F. R. Hartley, John Wiley and Sons, Chichester, (1990).
13. A. G. Orpen and N. G. Connelly, *J. Chem. Soc., Chem. Commun.*, (1985), 1310.
14. C. A. Tolman, *Chem. Rev.*, **77**, (1977), 313.

15. F. A. Cotton and G. Wilkinson, 'Introduction to Ligands and Complexes', Chapter 2, 'Advanced Inorganic Chemistry 5th Edition', Wiley Interscience, New York, (1987).
16. C. A. McAuliffe, 'Phosphorus, Arsenic, Antimony and Bismuth Ligands', Chapter 14, Vol. 2, 'Comprehensive Coordination Chemistry I', G. Wilkinson, R. D. Gillard and J. A. McCleverty, Pergamon, (1987).
17. B. J. Dunne, R. B. Morris and A. G. Orpen, *J. Chem. Soc., Dalton Trans.*, (1991), 653.
18. A. M. Hill, N. J. Holmes, A. R. J. Genge, W. Levason, M. Webster and S. Rutschow, *J. Chem. Soc., Dalton Trans.*, (1998), 825.
19. N. J. Holmes, W. Levason and M. Webster, *J. Chem. Soc., Dalton Trans.*, (1998), 3457.
20. P. Schwab, N. Mahr, J. Wolf and H. Werner, *Angew. Chem.*, **106**, (1994), 82.
21. T. Pechmann, C. D. Brandt and H. Werner, *Angew. Chem. Int. Ed.*, **39**, (2000), 3909.
22. F. A. Cotton and G. Wilkinson, 'Introduction to Ligands and Complexes', Chapter 2, 'Advanced Inorganic Chemistry 5th Edition', Wiley Interscience, New York, (1988).
23. W. Kuchen and H. Buchwald, *Chem. Ber.*, **91**, (1955), 2296.
24. A. R. Stiles, F. F. Rust and W. E. Vaughan, *J. Am. Chem. Soc.*, **74**, (1952), 3282.
25. K. Maitra, V. J. Catalano, J. Clark and J. H. Nelson, *Inorg. Chem.*, **37**, (1998), 1105.
26. K. Maitra, V. J. Catalano and J. H. Nelson, *Bull. Soc. Chim. Fr.*, **134**, (1997), 471.
27. M. M. Rauhut, H. A. Currier, H. M. Semsel and V. P. Systrach, *J. Org. Chem.*, **26**, (1961), 5138.
28. B. N. Diel, P. F. Brandt, R. C. Haltiwanger, M. L. J. Hackney and A. D. Norman, *Inorg. Chem.*, **28**, (1989), 2811.
29. B. N. Diel, R. C. Haltiwanger and A. D. Norman, *J. Am. Chem. Soc.*, **104**, (1982), 4700.
30. K. D. Crosbie and G. M. Sheldrick, *J. Inorg. Nucl. Chem.*, **31**, (1969), 3684.
31. L. Horner, *Pure Appl. Chem.*, **9**, (1964), 225.
32. C. E. Wymore and J. C. Bailar, *J. Inorg. Nucl. Chem.*, **14**, (1960), 42.
33. K. Issleib and G. Doll, *Chem. Ber.*, **96**, (1963), 1544.
34. A. M. Aguiar and D. Daigle, *J. Am. Chem. Soc.*, **86**, (1964), 2299.
35. H. Zorn, H. Schindlbauer and H. Hagen, *Monatsch.*, **95**, (1964), 422.

36. H. Schindlbauer, *Monatsch.*, **96**, (1965), 2051.

37. H. C. E. McFarlane and W. McFarlane, *Polyhedron*, **2**, (1983), 303.

38. L. Horner, P. Beck and V. G. Toscano, *Chem. Ber.*, **94**, (1961), 2122.

39. P. G. Eller and D. W. Meek, *J. Organomet. Chem.*, **22**, (1970), 631.

40. W. Levason, K. G. Smith, C. A. McAuliffe, F. P. McCullough, R. D. Sedgwick and S. G. Murray, *J. Chem. Soc., Dalton Trans.*, (1979), 1718.

41. E. P. Kyba, S. T. Liu and R. L. Harris, *Organometallics*, **2**, (1983), 1877.

42. F. A. Cotton and G. Wilkinson, 'Homogeneous Catalytic Synthesis of Organic Chemicals by Transition Metal Complexes', Chapter 28, 'Advanced Inorganic Chemistry Fifth Edition', Wiley Interscience, New York, (1988).

43. B. C. Gates, 'Catalysis', Volume 5, 'Kirk-Othmer Encyclopedia of Chemical Technology Fourth Edition', M. Howe-Grant, Wiley Interscience, New York, (1993).

44. A. D. Burrows, *Sci. Prog.*, **85**, (2002), 199.

45. S. J. Chadwell, S. J. Coles, P. G. Edwards and M. J. Hursthouse, *J. Chem. Soc., Dalton Trans.*, (1996), 1105.

46. A. Caminade and J. Majoral, *Chem. Rev.*, **94**, (1994), 1183.

47. D. K. Cabbiness and D. W. Margerum, *J. Am. Chem. Soc.*, **91**, (1969), 6540.

48. E. C. Constable, 'Coordination Chemistry of Macrocyclic Compounds', Oxford University Press, Oxford, (1999).

49. A. Dei and R. Gori, *Inorg. Chim. Acta.*, **14**, (1975), 157.

50. R. T. Meyers, *Inorg. Chem.*, **17**, (1978), 952.

51. R. D. Hancock and V. J. Thom, *J. Am. Chem. Soc.*, **104**, (1982), 291.

52. F. P. Hinz and D. W. Margerum, *J. Am. Chem. Soc.*, **96**, (1974), 4993.

53. D. J. H. Smith, 'Comprehensive Organic Chemistry Part 10', I. O. Sutherland, (1979).

54. D. G. Booth, W. Levason, J. J. Quirk, G. Reid and S. M. Smith, *J. Chem. Soc., Dalton Trans.*, (1997), 3493.

55. A. J. Barton, A. R. J. Genge, W. Levason and G. Reid, *J. Chem. Soc., Dalton Trans.*, (2000), 2163.

56. E. P. Kyba and S.-S. P. Chou, *J. Org. Chem.*, **46**, (1981), 860.

57. L. F. Lindoy, 'The Chemistry of Macrocyclic Ligand Complexes', Cambridge University Press, Cambridge, (1989).

58. E. P. Kyba, A. M. John, S. B. Brown, C. W. Hudson, M. J. McPhaul, A. Harding, K. Larsen, S. Niedzwiecki and R. E. Davis, *J. Am. Chem. Soc.*, **102**, (1980), 139.

59. E. P. Kyba, R. E. Davis, C. W. Hudson, A. M. John, S. B. Brown, M. J. McPhaul, L.-K. Liu and A. C. Glover, *J. Am. Chem. Soc.*, **103**, (1981), 3868.

60. M. Bochmann, 'Organometallics 1; Complexes With Transition Metal-Carbon σ-Bonds', Oxford University Press, Oxford, (1994).

61. M. C. Thompson and D. H. Busch, *J. Am. Chem. Soc.*, **86**, (1964), 3651.

62. M. D. S. Healy and A. J. Rest, *Adv. Inorg. Chem. Radiochem.*, **21**, (1978), 1.

63. F. Abbà, G. de Sanns, L. Fabbrizzi, M. Licchelli, A. M. M. Lanfredi, P. Pallavinci, A. Poggi and F. Ugozzoli, *Inorg. Chem.*, **33**, (1994), 1366.

64. J. J. Christensen, J. O. Hill and R. M. Izatt, *Science*, **174**, (1971), 459.

65. J. J. Christensen, D. J. Eatough and R. M. Izatt, *Chem. Rev.*, **74**, (1974), 351.

66. Y. Murakamni, Chapter 10, 'Biomimetic Chemistry', D. Dolphin, C. McKerna, Y. Murakamni and I. Tabusm (Eds.), American Chemical Society, Washington, (1980).

67. J. Canales, J. Ramirez, G. Estiu and J. Costamagna, *Polyhedron*, **19**, (2000), 2373.

68. M. Beley, J. P. Collin, R. Ruppert and J. P. Sauvage, *J. Chem. Soc., Chem. Commun.*, (1984), 1315.

69. M. Bochmann, *J. Chem. Soc., Dalton Trans.*, (1996), 255.

70. M. Ciampolini, N. Nardi, P. L. Orioli, S. Mangani and F. Zanobini, *J. Chem. Soc., Dalton Trans.*, (1984), 2265.

Chapter 2

Synthesis of New Ditertiary Stibines With Xylyl- and Phenylene- Backbones

2.1 Introduction

2.1.1 Ligand Synthesis

Although a number of antimony containing ligands are known, their syntheses are often lengthy and low yielding as a result of the weak C-Sb bond. The preparation of novel stibines in moderate to high yield, in particular polydentate ligands, remains a challenging synthetic problem.

2.1.1.1 Tertiary Stibines

Symmetrical tertiary stibines (R_3Sb) are usually prepared by the reaction of $SbCl_3$ with the appropriate Grignard reagent in diethyl ether, although alkyl lithium reagents may also be used.[1]

Reaction of $SbCl_3$ with Ph_3Sb in a 2:1 or 1:2 ratio yields $PhSbCl_2$ or Ph_2SbCl respectively.[2, 3] These can then react with RLi or RMgX to give mixed phenylalkylstibines $Ph_{3-x}R_xSb$.[3, 4] Alternatively cleavage of an R group from a tertiary stibine R_3Sb (where R can be alkyl or aryl) can be achieved with sodium/liquid ammonia or less commonly with Li/thf to give R_2Sb^-, which can then be alkylated by reaction with R'X to give $R'R_2Sb$.[5-7]

Trialkyl- and alkylaryl-stibines are air-sensitive oils and must be handled under nitrogen, whilst triaryl-stibines are air-stable solids.

2.1.1.2 Distibines

In general C-Sb bonds are weak and can easily be broken by nucleophiles such as alkyl-lithium reagents or Grignard reagents. This may be a competing reaction in the stepwise procedure used to synthesis multidentate stibine ligands and therefore reaction conditions must be chosen carefully.

The distibinoalkane ligands $R_2Sb(CH_2)_nSbR_2$ (R = Me or Ph; n = 1,3 or 4) are readily made from $NaSbR_2$ and the appropriate α,ω-dihaloalkane in liquid ammonia.[5, 8-11] All attempts to prepare the dimethylene backboned ligands $R_2Sb(CH_2)_2SbR_2$ with a variety of R groups have failed, instead elimination of ethene occurs to give R_4Sb_2.[12] Similarly reaction of R_2Sb^- (R = Ph or Me) with either *cis*- or *trans* ClCH=CHCl results

in elimination of ethyne to again give R_4Sb_2 as the product.[6, 13] However the acetylenic stibines $R_2SbC{\equiv}CSbR_2$ can be prepared by reaction of R_2SbX with either $NaC{\equiv}CH$ or $XMgC{\equiv}CMgX$.[14]

Recent coordination studies of the distibinoalkane ligands have revealed significant differences from the much-studied phosphine and arsine ligands.[1] They are soft, moderate σ-donor ligands and in certain cases may act as weak π-acceptors. They have a tendency to promote higher coordination numbers which is due in part to their donor properties but also due to smaller cone angles.[1] Distibines have a tendency to adopt a *cis*-stereochemistry and in the presence of certain metal centres the weak C-Sb bond is broken resulting in ligand fragmentation.

The syntheses of distibines with aromatic backbones are much more difficult. Low yields of *p*-$C_6H_4(SbPh_2)_2$ can be obtained by the reaction of the corresponding lithium species *p*-$C_6H_4Li_2$ with Ph_2SbCl.[15]

2.1.1.3 *o*-Phenylene Distibine Ligands

The ligand *o*-$C_6H_4(SbMe_2)_2$, the antimony analogue of the famous "diars" ligand *o*-$C_6H_4(AsMe_2)_2$ has by far the strongest coordinating properties of all the distibines[1] but its synthesis is extremely difficult and yields are very low.

Reaction of *o*-dichlorobenzene with $NaSbMe_2$ in liquid ammonia yields only trace amounts of *o*-$C_6H_4(SbMe_2)_2$ [13] and attempts to prepare the phenyl analogue by this route are unsuccessful. Yields of only 5 % are obtained using *o*-dibromobenzene[16] and even with *o*-bromoiodobenzene the yield is only 9 %.[16]

Better yields (ca. 20-30 %) may be obtained using the route developed by Levason and co-workers which is shown in Scheme 1.1.[17] This procedure highlights many of the problems associated with the synthesis of multidentate stibine ligands. The procedure is lengthy, gives poor overall yields and involves handling the highly hazardous intermediate Me_3Sb on a relatively large scale. Trimethylantimony is extremely volatile and pyrophoric and as a consequence is very difficult to store. It is normally stored as Me_3SbX_2 (X = Cl or Br) and then decomposed by pyrolysis when required to Me_2SbX.

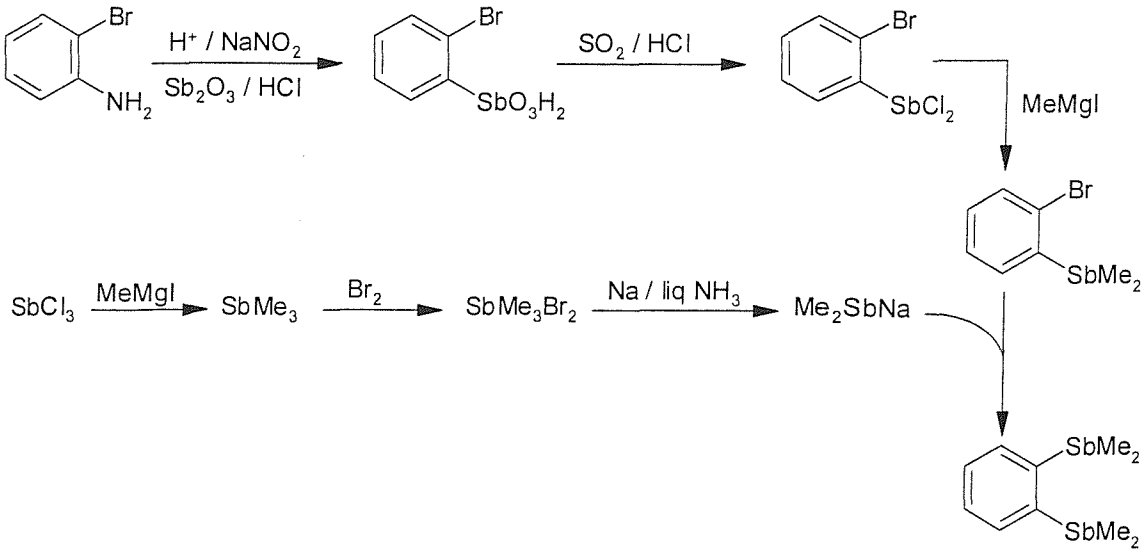

Scheme 2.1 – Synthesis of *o*-$C_6H_4(SbMe_2)_2$[17]

The phenyl analogue *o*-$C_6H_4(SbPh_2)_2$ can be prepared in 25 % yield using a similar route from *o*-$C_6H_4Br(SbPh_2)$ and $NaSbPh_2$ in liquid ammonia.[13]

Only one tritertiary stibine, $MeC(CH_2SbPh_2)_3$, has been prepared by reaction of $MeC(CH_2Br)_3$ with $NaSbPh_2$ in liquid ammonia.[18]

The following work was initiated with the aim of developing new routes to distibine ligands with non-alkane backbones, which would avoid the problems associated with traditional syntheses. These problems include low overall yields, long multi-step reactions and the use of hazardous intermediates. In particular it was important to avoid the use of $SbMe_3$, a highly air-sensitive, volatile and pyrophoric liquid. A xylyl backbone was initially selected as the CH_2 groups provide a useful signature in both ^1H and $^{13}C\{^1H\}$ NMR with which to monitor the reactions.

2.2 Results and Disussion

2.2.1 Synthesis of 1,2-$C_6H_4(CH_2SbMe_2)_2$, 1,3-$C_6H_4(CH_2SbMe_2)_2$ and 1,4-$C_6H_4(CH_2SbMe_2)_2$

Reaction of Ph_3Sb with two equivalents of $SbCl_3$ in the absence of solvent results in the formation of crude $PhSbCl_2$.[2] This can easily be converted to $PhMe_2Sb$ by reaction with MeMgI. The reaction also yields smaller quantities of Ph_2MeSb which arise either from a Ph_2SbCl impurity in the crude $PhSbCl_2$ or via substituent scrambling during reaction with the Grignard reagent. However the two products can easily be separated by distillation under vacuum. $PhMe_2Sb$ can be prepared in large quantities, and although mildly air-sensitive can be stored for long periods of time under N_2 with no evidence of decomposition. It therefore provides a viable alternative to the use of $SbMe_3$ as described below.

The $PhMe_2Sb$ is easily converted to Me_2SbCl by cleavage of the phenyl group. This is achieved by saturating a toluene solution of the ligand with hydrogen chloride gas.[19] The Me_2SbCl can be isolated by removal of the solvent *in vacuo* but for the following reactions it was easier to remove excess HCl by purging the reaction mixture with N_2 and then use the toluene solution directly.

Reaction of Me_2SbCl with Na in liquid NH_3 gave $NaSbMe_2$, which then reacted with 0.5 equivalents of α,α'-dibromo-*o*-xylene to afford 1,2-$C_6H_4(CH_2SbMe_2)_2$. The ^1H NMR spectrum of the crude product revealed three broad multiplets, one in the aromatic region, a second at 4.8 ppm and a third very large, complex multiplet in the region δ 0.8-2.0 ppm, clearly indicating a mixture of products and some decomposition. Purification was achieved by Kugelröhr distillation, however the ligand was only obtained in a 6 % yield. Large amounts of Me_4Sb_2 were generated during the reaction and subsequent work-up but no other by-products could be identified.

Much higher yields of 1,2-$C_6H_4(CH_2SbMe_2)_2$ were obtained by the reaction of Me_2SbCl in toluene with the di-Grignard reagent 1,2-bis(chloromagnesiomethyl)benzene, prepared following the literature procedure,[20] from magnesium powder and α,α'-dichloro-*o*-xylene in dry thf (Scheme 2.2). The ^1H NMR spectrum of the crude oil shows a single methyl resonance at δ 0.99 ppm, a single methylene resonance at δ 3.07

ppm and a multiplet at 7.33-7.77 ppm corresponding to the aromatic protons, integrating correctly for the desired ligand. The $^{13}C\{^{1}H\}$ NMR spectrum is also consistent with the formation of 1,2-$C_6H_4(CH_2SbMe_2)_2$, with no evidence of decomposition or aromatic impurities as observed with the previous route. Therefore no further purification was necessary and the ligand was isolated in 88 % yield.

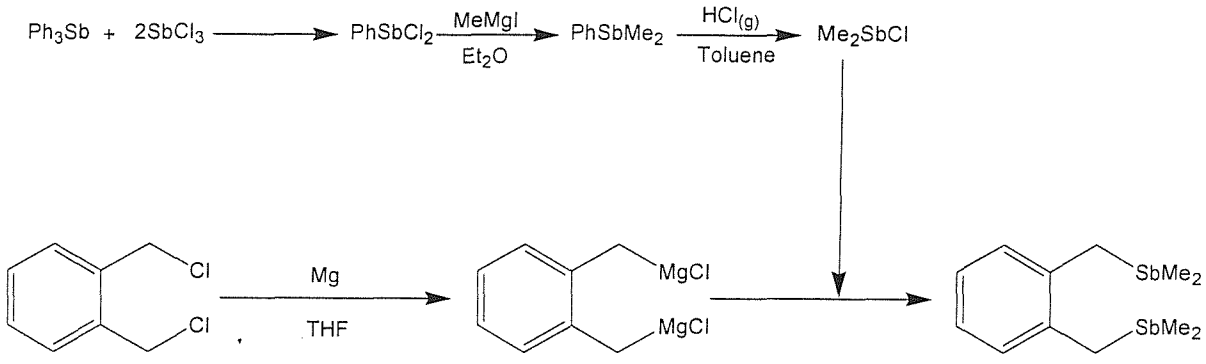

Scheme 2.2 – Synthesis of 1,2-$C_6H_4(CH_2SbMe_2)_2$

The contrast in yields of 1,2-$C_6H_4(CH_2SbMe_2)_2$ using the two different routes is striking. The extremely low yield of distibine obtained using the first route in which the antimony nucleophile ($SbMe_2^-$) attacks the α,α'-dichloro-*o*-xylene is consistent with reports that antimony nucleophiles have a tendency to break existing C-Sb bonds as well as substituting C-X bonds.[1, 17, 21, 22] However it is interesting to note that in the second route, when the nucleophilic Grignard reagent attacks the antimony electrophile (Me_2SbCl) no such problems are observed. The Grignard route has provided a clean and extremely high yielding route to the novel distibine 1,2-$C_6H_4(CH_2SbMe_2)_2$. The relative simplicity of the procedure, combined with the high yield contrasts sharply with reported distibine ligand syntheses.[1] We were therefore keen to apply this route to the preparation of other distibine ligands.

The analogous *meta*- and *para*-substituted distibines, 1,3-$C_6H_4(CH_2SbMe_2)_2$ and 1,4-$C_6H_4(CH_2SbMe_2)_2$ were prepared from the corresponding di-Grignard reagent and Me_2SbCl in 56 and 50 % yield respectively. 1,3-$C_6H_4(CH_2SbMe_2)_2$ is an air sensitive oil

whilst 1,4-$C_6H_4(CH_2SbMe_2)_2$ is an air-sensitive crystalline solid. All the distibine ligands must therefore be handled and stored under N_2.

The ^1H NMR spectra of the *meta*- and *para*-distibines are consistent with the formulations but unexceptional. The $^{13}C\{^1H\}$ NMR spectra of all three ligands show the methyl resonance to low frequency of TMS at ~-3 ppm. A similar effect is observed with methyl groups on other heavy atoms such as I, Pb or Te and can be attributed to spin-orbit effects of the heavy atom.[23]

All three distibines have also been characterised by EI^+ mass spectrometry and all spectra show characteristic antimony isotope patterns (^{121}Sb 57.3 %, ^{123}Sb 42.7 %, for simplicity only the values corresponding to the ^{121}Sb isotope are quoted). The EI^+ mass spectrum of 1,2-$C_6H_4(CH_2SbMe_2)_2$ shows no evidence of a parent ion, however there are two major clusters of peaks which have the correct isotopic distribution for the fragment ions $[P\text{-}Me]^+$ *m/z* 391, and $[P\text{-}SbMe_2]^+$ *m/z* 255. However the EI^+ mass spectra of 1,3-$C_6H_4(CH_2SbMe_2)_2$ and 1,4-$C_6H_4(CH_2SbMe_2)_2$ both show strong $[P]^+$ ions at *m/z* 406.

2.2.2 Synthesis of 1,2-$C_6H_4(CH_2SbMe_3)_2I_2$, 1,3-$C_6H_4(CH_2SbMe_3)_2I_2$ and 1,4-$C_6H_4(CH_2SbMe_3)_2I_2$

All three distibine ligands were further characterised by reaction with excess iodomethane in acetone to form the corresponding dimethiodides $C_6H_4(CH_2SbMe_3)_2I_2$. Both ^1H and $^{13}C\{^1H\}$ NMR spectra show single resonances for the methyl and methylene groups, shifted significantly to high frequency from those in the free ligand. The presence of only single methyl and methylene resonances indicates quarternisation has occurred at both antimony centres.

Further evidence for the formation of the dimethiodides can be found in the electrospray mass spectra. The ES^+ spectra of 1,2-$C_6H_4(CH_2SbMe_3)_2I_2$ and 1,3-$C_6H_4(CH_2SbMe_3)_2I_2$ (Figure 2.1) both show peaks with the correct isotopic distribution for $[C_6H_4(CH_2SbMe_3)_2]^{2+}$ *m/z* 218. Whilst the ES^+ mass spectrum of 1,4-$C_6H_4(CH_2SbMe_2)_2I_2$ shows a major species at *m/z* 563 corresponding to $[1,4\text{-}C_6H_4(CH_2SbMe_3)_2I]^+$.

The ready formation of the dimethiodides is in contrast with work carried out on the related phenylene based ligands [*o*-$C_6H_4(EMe_2)_2$] (E = P, As or Sb) which undergo

only monoquarternisation to give [*o*-$C_6H_4(EMe_2)(EMe_3)I$] due to deactivation of the second EMe_2 centre by inductive effects from the EMe_3^+. The presence of the xylyl backbone appears to prevent the transmission of these electronic effects through the ring, thus allowing diquarternisation.

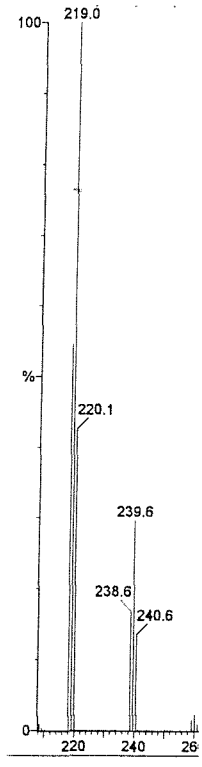

Figure 2.1 – ES^+ Mass spectrum of 1,3-$C_6H_4(CH_2SbMe_3)_2I_2$ in MeCN

2.2.3 Synthesis of 1,2-$C_6H_4(CH_2SbPh_2)_2$

Attempts were made to prepare the analogous diphenyl-distibine ligand 1,2-$C_6H_4(CH_2SbPh_2)_2$ by reaction of Ph_2SbNa (prepared by reaction of Ph_2SbCl with sodium in liquid ammonia[6]) with α,α'-dibromo-*o*-xylene. A large amount of decomposition occured during the reaction and much unidentifiable black solid was isolated. The EI^+ mass spectrum of the crude reaction mixture showed no evidence for the formation of the ligand, instead the major species present were Ph_3Sb and $Ph_2SbSbPh_2$.

However reaction of a toluene solution of Ph_2SbCl [2, 3] with the di-Grignard reagent 1,2-bis(chloromagnesiomethyl)benzene,[20] prepared from magnesium powder and

α,α'-dichloro-*o*-xylene in thf, afforded 1,2-$C_6H_4(CH_2SbPh_2)_2$ as a waxy solid in 14 % yield. Again substantial decomposition was observed during the reaction, but any decomposition products were removed from the final ligand by filtering a solution of the crude reaction mixture through Celite. The ^1H NMR spectrum shows a single methylene resonance at δ 2.82 ppm, and a multiplet corresponding to the aromatic protons at δ 7.09-7.48 ppm. The $^{13}C\{^1H\}$ NMR spectrum is also consistent with the formation of 1,2-$C_6H_4(CH_2SbPh_2)_2$.

Diarylalkylstibines do not quarternise with MeI,[24] so instead the ligand was further characterised as the tetraiodo derivative 1,2-$C_6H_4(CH_2SbPh_2I_2)_2$ prepared by reaction with diiodine. Unfortunately the product is extremely insoluble, dissolving only in d_6-DMSO, and the residual solvent and water signals in d_6-DMSO mask the methylene region in NMR, and thus no useful NMR data was obtained. However satisfactory microanalytical data was obtained, confirming the formation of 1,2-$C_6H_4(CH_2SbPh_2I_2)_2$.

2.2.4 Crystallographic Analysis of 1,4-$C_6H_4(CH_2SbMe_2)_2$ and 1,3-$C_6H_4(CH_2SbMe_3)_2I_2$

Single crystals of 1,4-$C_6H_4(CH_2SbMe_2)_2$ suitable for X-ray diffraction were obtained directly from the reaction, and the structure (Figure 2.2 and Tables 2.1 & 2.2) shows a centrosymmetric molecule. The values of d(C-Sb) and ∠C-Sb-C are unexceptional, falling within the expected range,[1] but the structure provides unequivocal proof of the identity of the novel distibine ligand.

Crystals of the dimethiodide 1,3-$C_6H_4(CH_2SbMe_3)_2I_2$ were obtained by slow evaporation of an acetone solution. The structure (Figure 2.3 and Tables 2.3 & 2.4) shows each antimony atom in an extremely distorted tetrahedral environment. The C-Sb bond lengths are, on average, only slightly shorter than those observed in 1,4-$C_6H_4(CH_2SbMe_2)_2$.

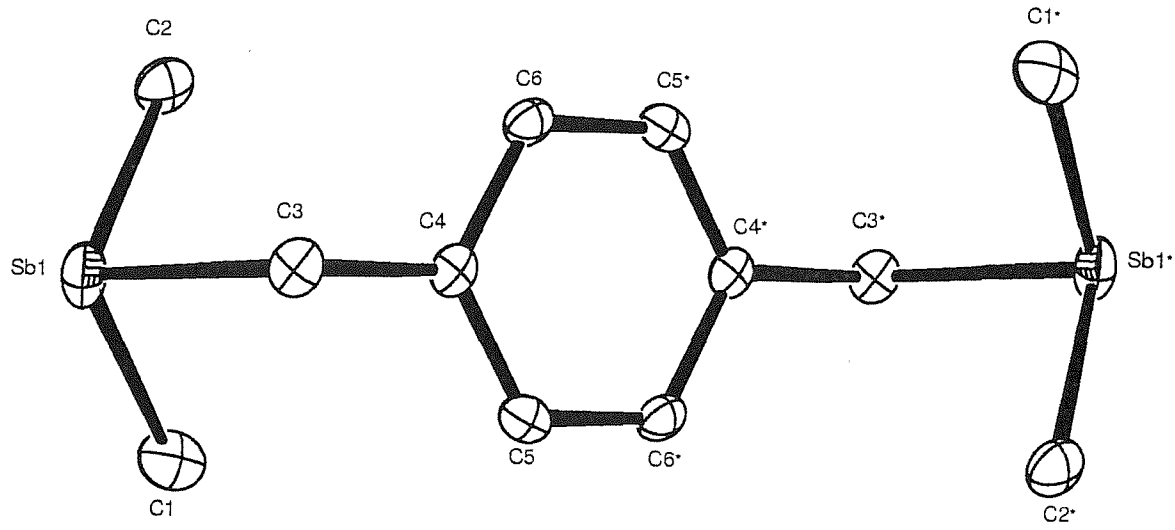

Figure 2.2- View of the structure of 1,4-$C_6H_4(CH_2SbMe_2)_2$ with numbering scheme adopted. Ellipsoids are drawn at 40 % probability. H atoms are omitted for clarity.

Bond Lengths (Å)	
Sb-C(1)	2.153(4)
Sb-C(2)	2.148(4)
Sb-C(3)	2.192(3)
Bond Angles (°)	
C(1)-Sb-C(2)	93.79(15)
C(1)-Sb-C(3)	96.84(14)
C(2)-Sb-C(3)	97.12(14)

Table 2.1 - Selected Bond Lengths (Å) and Angles (°) for 1,4-$C_6H_4(CH_2SbMe_2)_2$

Table 2.2 – Crystal Data and Structure Refinement Details for 1,4-$C_6H_4(CH_2SbMe_2)_2$

Compound	1,4-$C_6H_4(CH_2SbMe_2)_2$
empirical formula	$C_{12}H_{20}Sb_2$
Fw	407.78
cryst. System	Monoclinic
space group	$P2_1/n$ (no. 14)
a (Å)	6.1174 (12)
b (Å)	17.749 (4)
c (Å)	6.7048 (16)
β (°)	100.766 (8)
volume ($Å^3$)	715.2 (3)
Z	2
density (calc.) (mg / m^3)	1.894
abs coef (mm^{-1})	3.745
F(000)	388
total no. of obsns	5538 (R_{int} = 0.078)
no. of unique obsns	1621
min, max transmission	0.303, 0.418
no. of parameters, restraints	66, 0
goodness-of-fit on F^2	1.04
R1, wR2 ($I > 2\sigma(I)$)[b]	0.034, 0.083
R1, wR2 (all data)	0.040, 0.087

Temperature = 120 K; wavelength (Mo-Kα) = 0.71073 Å; θ (max) = 27.5 deg.

[b] $R1 = \Sigma \, || F_o| - |F_c|| / \Sigma |F_o|$ $\quad wR2 = [\Sigma w(F_o^2 - F_c^2)^2 / \Sigma w F_o^4]^{1/2}$

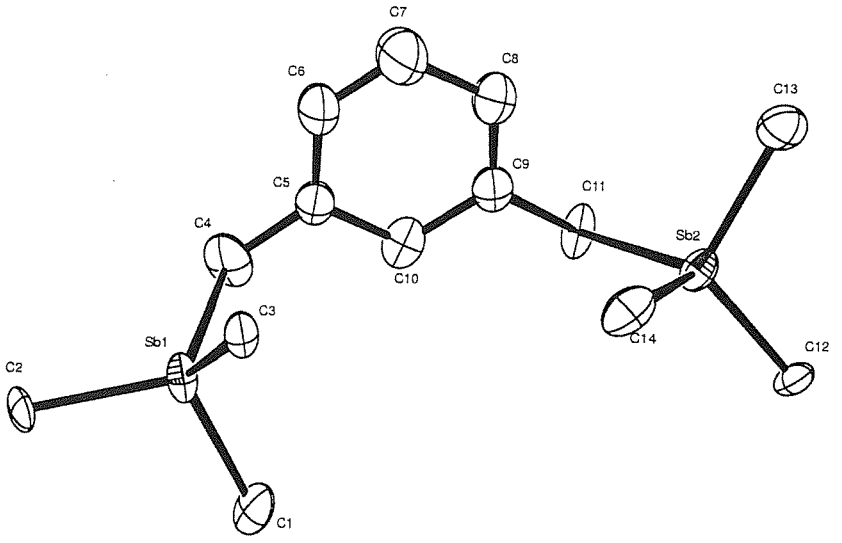

Figure 2.3 – View of the structure of the cation in 1,3-$C_6H_4(CH_2SbMe_3)_2I_2$ with numbering scheme adopted. Ellipsoids are drawn at 40 % probability. H atoms are omitted for clarity.

Bond Lengths (Å)		*Bond Angles* (°)	
Sb(1)-C(1)	2.096(9)	C(1)-Sb(1)-C(2)	106.7(4)
Sb(1)-C(2)	2.110(8)	C(1)-Sb(1)-C(3)	110.8(9)
Sb(1)-C(3)	2.130(19)	C(1)-Sb(1)-C(4)	103.2(10)
Sb(1)-C(4)	2.12(2)	C(2)-Sb(1)-C(3)	115.3(9)
Sb(2)-C(11)	2.174(15)	C(2)-Sb(1)-C(4)	112.6(10)
Sb(2)-C(12)	2.099(6)	C(3)-Sb(1)-C(4)	107.5(4)
Sb(2)-C(13)	2.121(9)	C(11)-Sb(2)-C(12)	112.3(9)
Sb(2)-C(14)	2.025(19)	C(11)-Sb(2)-C(13)	104.1(11)
		C(11)-Sb(2)-C(14)	107.3(5)
		C(12)-Sb(2)-C(13)	108.4(3)
		C(12)-Sb(2)-C(14)	115.0(8)
		C(13)-Sb(2)-C(14)	109.2(11)

Table 2.3 – Selected Bond Lengths (Å) and Angles (°) for 1,3-$C_6H_4(CH_2SbMe_3)_2I_2$

Table 2.4 – Crystal Data and Structure Refinement Details for $1,3\text{-}C_6H_4(CH_2SbMe_3)_2I_2$

compound	$[1,3\text{-}C_6H_4(CH_2SbMe_3)_2]I_2$
empirical formula	$C_{14}H_{26}I_2Sb_2$
fw	691.65
cryst. System	monoclinic
space group	C2 (no. 5)
a (Å)	22.721(4)
b (Å)	7.0975(15)
c (Å)	16.478(3)
β (°)	121.006(7)
volume ($Å^3$)	2277.5 (7)
Z	4
density (calc.) (mg / m^3)	2.017
abs coef (mm^{-1})	5.072
F(000)	1272
total no. of obsns	9172 (R_{int} = 0.065)
no. of unique obsns	5048
min, max transmission	0.681, 0.992
no. of parameters, restraints	164, 1
goodness-of-fit on F^2	1.05
R1, wR2 ($I > 2\sigma(I)$)[b]	0.046, 0.119
R1, wR2 (all data)	0.063, 0.129

Temperature = 120 K; wavelength (Mo-Kα) = 0.71073 Å; θ (max) = 27.5 deg.

[b] $R1 = \sum || F_0| - |F_c|| / \sum |F_0|$ $\quad wR2 = [\sum w(F_0^2 - F_c^2)^2 / \sum wF_0^4]^{1/2}$

2.2.5 Attempted Synthesis of 1,3-$C_6H_4(SbMe_2)_2$ – Method 1

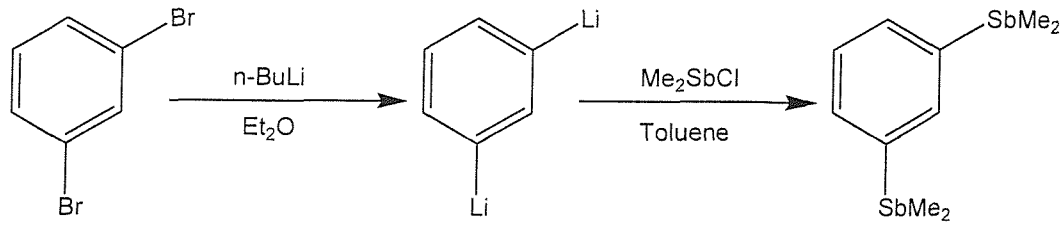

Scheme 2.3 – Attempted synthesis of 1,3-$C_6H_4(SbMe_2)_2$

Attempts were made to synthesise 1,3-$C_6H_4(SbMe_2)_2$ using the route developed by Matano *et* al for the preparation of the analogous bismuth ligands [25] (Scheme 2.3). Reaction of α,α'-dibromo-*m*-benzene with four equivalents of ^{n}BuLi yields the corresponding dilithium species. Four equivalents of ^{n}BuLi are needed in order to convert the ^{n}BuBr produced into LiBr and octane, thus preventing any side-reactions. Addition of two equivalents of Me_2SbCl, prepared as detailed above, followed by work-up gave a white oily residue.

The ^{1}H NMR spectrum of the crude product showed one major methyl resonance at δ 1.02 with a smaller second peak at δ 1.01 ppm. The $^{13}C\{^{1}H\}$ NMR spectrum also shows two methyl resonances at δ -0.9 and -1.3 ppm as well as a large number of peaks in the aromatic region, clearly indicating a mixture of species. The crude oil was purified by Kugelröhr distillation and a product was collected as a colourless oil at 100°C, 0.3 mm Hg. NMR data on the residue remaining after distillation shows no evidence of the desired ligand and appears to be mainly decomposition products. The ^{1}H NMR spectrum of the oil shows a single methyl resonance at δ 1.00 ppm and a multiplet at 7.18 – 7.65 ppm corresponding to the aromatic protons. The $^{13}C\{^{1}H\}$ NMR spectrum also shows a single methyl resonance at δ -0.9 ppm, with six peaks in the aromatic region at δ 123.3, 128.3, 130.1, 131.3. 133.4 and 137.3 ppm. The $^{13}C\{^{1}H\}$ NMR spectrum of 1,3-$C_6H_4(SbMe_2)_2$ should show only four aromatic resonances, therefore the product collected cannot be the desired ligand. The aromatic resonance at 123.4 is clearly

indicative of an *ipso*-C-Br atom[26] indicating that the oil isolated is in fact 1,3-$C_6H_4Br(SbMe_2)$.

The product was further characterised as the methiodide species 1,3-$C_6H_4Br(SbMe_3)I$ prepared by reaction with excess iodomethane in acetone. The ^1H and $^{13}C\{^1H\}$ NMR spectra show single methyl resonances shifted significantly from those in the free ligand, as well as peaks corresponding to the aromatic ring. The ES^+ mass spectrum shows two major ions with the correct isotopic distribution for $[C_6H_4Br(SbMe_3)]^+$ *m/z* 321, and $[C_6H_5(SbMe_3)]^+$ *m/z* 243, again confirming the identity of the product as 1,3-$C_6H_4Br(SbMe_2)$.

The failure of this route was unexpected, but the reaction was not further investigated since the route discussed in 2.2.6 was successful

2.2.6 Synthesis of 1,3-$C_6H_4(SbMe_2)_2$ and 1,4-$C_6H_4(SbMe_2)_2$

Following the success of the Grignard route in the synthesis of the xylyl-based distibines, attempts were made to prepare the phenylene ligands from the appropriate Grignard reagents. Due to the known difficulties involved in the synthesis of phenylene di-Grignards the addition of a small amount of anthracene is required. The reaction of magnesium and anthracene in dry thf is reversible and forms a magnesium anthracene.3thf complex. Highly reactive magnesium is formed via the reverse reaction of this equilibrium which can then react with the appropriate dihalobenzene to form the corresponding di-Grignard in good yield.[27]

The Grignard reagent 1,3-bis(bromomagnesio)benzene was prepared following the literature procedure,[27] from magnesium powder, anthracene and α,α'-dibromo-*m*-benzene in dry thf at 60°C. Addition of a toluene solution of Me_2SbCl yields the ligand 1,3-$C_6H_4(SbMe_2)_2$ as a yellow oil. The ^1H and $^{13}C\{^1H\}$ NMR spectra of the crude oil are consistent with the formation of the ligand but show several minor impurities in both the methyl and aromatic regions, therefore purification was attempted by Kugelröhr distillation. A small amount of $PhSbMe_2$ was collected but the bulk of the crude mixture did not distil even at 200°C, 0.3 mm Hg. Both the ^1H and $^{13}C\{^1H\}$ NMR spectra of the involatile fraction are consistent with the formation of 1,3-$C_6H_4(SbMe_2)_2$ with single methyl resonances at δ 1.00 and δ -1.3 ppm respectively. Importantly the

aromatic region of the $^{13}C\{^1H\}$ NMR spectrum shows four resonances with no evidence of 1,3-$C_6H_4Br(SbMe_2)$. A small amount of anthracene is carried through from the Grignard and is evident in the NMR spectra. The EI^+ mass spectrum of the ligand shows peaks at *m/z* 380, 365, 350 and 335 corresponding to the parent ion *m/z* 378 $[1,3\text{-}C_6H_4(^{121}SbMe_2)_2]^+$ and successive loss of the methyl groups.

The dimethiodide 1,3-$C_6H_4(SbMe_3)_2I_2$ was prepared by reaction with excess iodomethane in acetone. The ^1H NMR spectrum shows the methyl resonance shifted significantly by 1.2 ppm to δ 2.19 ppm with no evidence of a second peak to lower frequency. Similarly the $^{13}C\{^1H\}$ NMR spectrum shows a single methyl resonance at δ 4.6 ppm, indicating that quarternisation has occurred at both antimony centres.

The ES^+ mass spectrum of the dimethiodide (Figure 2.5) provides clear evidence for the formation of 1,3-$C_6H_4(SbMe_3)_2I_2$ with peaks at *m/z* 535, 393, 243 and 204, corresponding to $[1,3\text{-}C_6H_4(^{121}SbMe_3)_2I]^+$, $[1,3\text{-}C_6H_4(^{121}SbMe_3)(^{121}SbMe_2)]^+$, $[PhSbMe_3]^+$ and $[1,3\text{-}C_6H_4(^{121}SbMe_3)_2]^{2+}$. Interestingly the mass spectrum also shows peaks with the correct isotopic distributions for the tristibine dimethiodide $[\{1,3\text{-}C_6H_4(SbMe_3)\}_2(SbMe)I]^+$ *m/z* 747 and $[\{1,3\text{-}C_6H_4(SbMe_3)\}_2(SbMe)]^{2+}$ *m/z* 310 (Figure 2.4). Feltham *et al* report a similar arsenic containing species as a by-product in the synthesis of diars (1,2-$C_6H_4(AsMe_2)_2$).[28] It is probable that the tristibine is formed as a result of scrambling at high temperatures during the attempted Kugelröhr distillation, however it must be present only as a minor product as there is no evidence for the tristibine in either the ^1H or $^{13}C\{^1H\}$ NMR spectra.

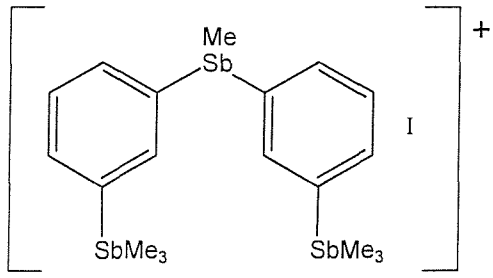

m/z 747

Figure 2.4- Representation of $[\{1,3\text{-}C_6H_4(SbMe_3)_2\}_2(SbMe)I]^+$

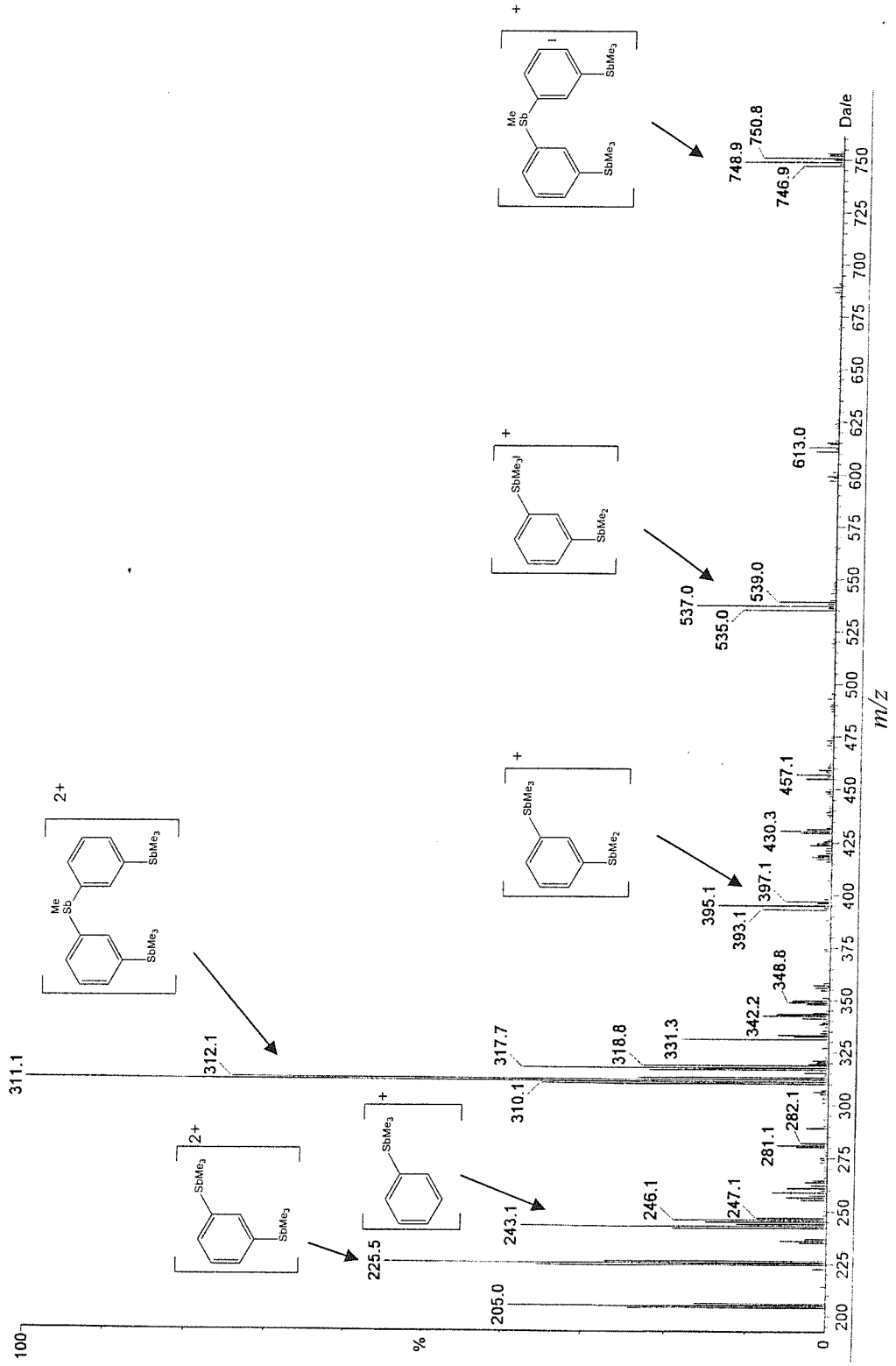

Figure 2.5- ES$^+$ Mass Spectrum of 1,3-$C_6H_4(SbMe_3)_2I_2$ in MeCN

The analogous *para*-substituted ligand 1,4-$C_6H_4(SbMe_2)_2$ was similarly prepared from the corresponding Grignard reagent, and was isolated in 58 % yield. Other than small amounts of anthracene carried through from the Grignard the ligand was spectroscopically pure, obviating the need for distillation. A dimethiodide was prepared by reaction with excess iodomethane in acetone. The ^1H NMR spectrum shows a single aromatic resonance at δ 7.89 ppm and interestingly two peaks at δ 1.82 and 1.86 ppm. Integration of the spectrum suggests that the singlet at δ 1.86 ppm corresponds to the methyl protons of the diquarternised species. There is no resonance corresponding to unquarternised $SbMe_2$ in the NMR spectrum and therefore the second methyl signal at δ 1.82 ppm cannot be due to monoquarternisation. The $^{13}C\{^1H\}$ NMR spectrum is consistent with the formation of the dimethiodide but again shows a second methyl resonance at 3.56 ppm. The ES^+ mass spectrum is consistent with the formation of 1,4-$C_6H_4(SbMe_3)_2I_2$ with peaks at *m/z* 535, 225 and 204 corresponding to [1,4-$C_6H_4(SbMe_3)_2I$], [1,4-$C_6H_4(SbMe_3)_2MeCN]^{2+}$ and [1,4-$C_6H_4(SbMe_3)_2]^{2+}$. The mass spectrum also shows a cluster of peaks at *m/z* 243 corresponding to $[PhSbMe_3]^+$, however comparison of the NMR spectra with those of $PhSbMe_3I$ shows that the second methyl resonance is not due to the formation of $PhSbMe_3I$. The reaction was repeated in refluxing propanol in an attempt to obtain a pure sample of the dimethiodide, but again the ^1H and $^{13}C\{^1H\}$NMR spectra show two methyl resonances at δ 1.84, 1.81, 4.26 and 3.39 ppm respectively. The ^1H and $^{13}C\{^1H\}$ NMR spectra of the free ligand show no impurities in the methyl region and therefore this second species must be generated during the subsequent reactions possibly through ligand decomposition.

2.2.7 Attempted Synthesis of 1,2-$C_6H_4(SbPh_2)_2$

Attempts have been made to prepare the diphenyl distibine ligand 1,2-$C_6H_4(SbPh_2)_2$ by two new routes. The phenyl derivative was chosen over the methyl analogue as the ligand and its precursors are air-stable allowing an easier investigation of the two synthetic routes. If successful it was hoped that the procedure could be extended to the synthesis of the much more reactive ligand 1,2-$C_6H_4(SbMe_2)_2$.

Unfortunately the procedure used in the synthesis of 1,3-$C_6H_4(SbMe_2)_2$ and 1,4-$C_6H_4(SbMe_2)_2$ cannot be extended to the *ortho*-ligand as the appropriate Grignard reagent cannot be prepared.[29]

The ligand *o*-$C_6H_4(SbPh_2)_2$ has been prepared previously in 26 % yield by reaction of $NaSbPh_2$ with *o*-$C_6H_4Br(SbPh_2)$ in liquid ammonia.[13] However the synthesis of the starting material *o*-$C_6H_4Br(SbCl_2)$ is difficult and low yielding.[30] The introduction of antimony onto the benzene ring is achieved by the formation of the stibonic acid *o*-$C_6H_4Br(SbO_3H_2)$ which is a low-yielding reaction, and the product obtained is of uncertain purity. The first attempted synthesis outlined below in Scheme 2.4 uses the alternative starting material *o*-$C_6H_4Cl(SbPh_2)$ which is easily prepared from the appropriate Grignard reagent. The mono-Grignard reagent 1-(bromomagnesio)-2-chlorobenzene was prepared by reaction of 1-bromo-2-chlorobenzene with magnesium turnings, activated with 1,2-dibromoethane, in dry diethyl ether.[29] A solution of Ph_2SbCl in dry thf, prepared by reaction of $SbCl_3$ with 2 equivalents of Ph_3Sb[3], was added to the Grignard reagent to yield 1,2-$C_6H_4Cl(SbPh_2)$ as a yellow oil. The ^1H NMR of the oil is uninformative showing a broad multiplet in the aromatic region. However the EI^+ mass spectrum shows peaks with the correct isotopic distribution for 1,2-$C_6H_4Cl(SbPh_2)$ *m/z* 386 as well as several fragment ions.

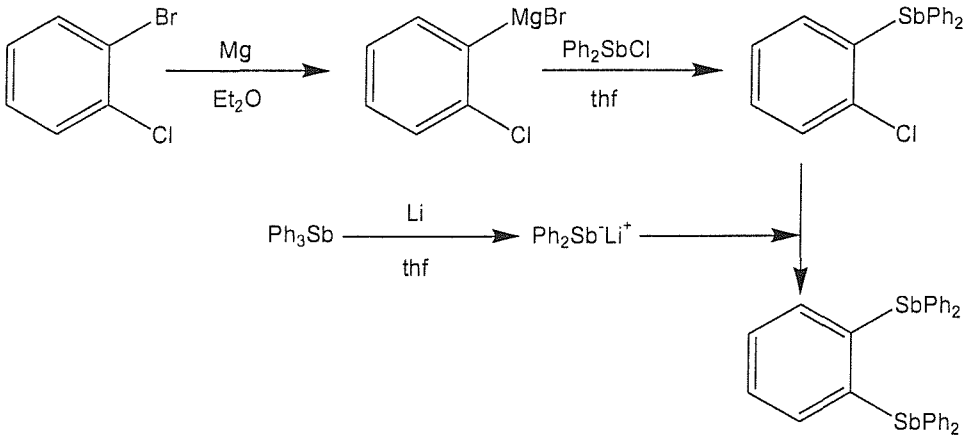

Scheme 2.4- Attempted Synthesis of 1,2-$C_6H_4(SbPh_2)_2$

A solution of $Ph_2Sb^-Li^+$ was prepared by reaction of Ph_3Sb with freshly crushed Li in dry thf, followed by addition of ^tBuCl to remove PhLi. The deep red solution was added dropwise to a solution of 1,2-$C_6H_4Cl(SbPh_2)$ in dry thf until the red coloration was no longer discharged. Standard work-up gave a yellow oil. The EI^+ mass spectrum shows evidence of unreacted 1,2-$C_6H_4Cl(SbPh_2)$ and Ph_3Sb. Comparison of the mass spectrum with that of the ligand obtained by the original procedure[13] shows no evidence of 1,2-$C_6H_4(SbPh_2)_2$. Although *o*-$C_6H_4Cl(SbPh_2)$ is much easier to prepare than the bromo analogue, Cl is much more difficult to substitute than Br. Therefore the failure of this reaction can be attributed to the difficulty of substituting Cl for $^-SbPh_2$.

The related diphosphine ligand *o*-$C_6H_4(PPh_2)_2$ cannot be prepared by the reaction of $LiPPh_2$ or $NaPPh_2$ with *o*-dichloro- or *o*-dibromobenzene (yields < 1%).[31, 32] The ligand can be prepared in low yield (ca. 18 %) by reaction of *o*-$C_6H_4Cl(PPh_2)_2$, prepared by reaction of Ph_2PCl with the Grignard reagent *o*-$C_6H_4Cl(MgBr)$, and $NaPPh_2$ in liquid NH_3.[33] Much better yields of ca. 35 % are achieved by the direct reaction of $NaPPh_2$ with *o*-difluorobenzene.[34] Reaction of $LiPPh_2$ in thf with *o*-difluorobenzene is also successful.[35]

A second attempt was made to prepare the analogous distibine ligand *o*-$C_6H_4(SbPh_2)_2$ using a similar procedure to that outlined above. A solution of $Ph_2Sb^-Li^+$ in thf, prepared as detailed above, was added dropwise to a solution of 1,2-difluorobenzene in dry thf, however the EI^+ mass spectrum of the isolated product again shows no evidence for the formation of 1,2-$C_6H_4(SbPh_2)_2$ instead the major species present are Ph_3Sb and fragments thereof.

2.3 Conclusions

New high yield syntheses from convenient starting materials have been developed for three xylyl and two phenylene-backboned distibine ligands. The Grignard route used has proved highly successful and has shown many advantages over the more traditional Na/liquid NH_3 route used in other distibine syntheses, including high yields, ease of procedure, little evidence of decomposition and high spectroscopic purity of crude products. The ligands and their dimethiodide derivatives have been fully characterised, and the crystal structures of 1,4-$C_6H_4(CH_2SbMe_2)_2$ and 1,3-$C_6H_4(CH_2SbMe_3)_2I_2$ have

been obtained. These structures represent two of only three distibines or their derivatives with non-alkane backbones to have been structurally characterised, the third being $[CoCl_2\{o\text{-}C_6H_4(SbMe_2)_2\}_2]_2[CoCl_4]$.[36]

Metal carbonyl complexes of the five ligands will be described in chapter 3, and complexes of the xylyl-backboned ligands with late transition metal halides will be described in chapter 4.

2.4 Experimental

Synthesis of $PhMe_2Sb$: Methylmagnesiumiodide was prepared from iodomethane (42.6 g, 0.30 mmol) and magnesium turnings (7.7 g, 0.32 mmol) in diethyl ether (1 L), and stirred for 45 mins. to ensure complete reaction. Dichlorophenylstibine (40 g, 0.15 mmol) in diethyl ether (250 mL) was added dropwise with stirring, and the yellow suspension stirred at RT for 3 h. The reaction was hydrolysed with aqueous NH_4Cl (~1 mol dm^{-3}, 300 mL) and the organic layer separated. The aqueous was washed with diethyl ether (3 x 100 mL) and the combined organics dried over anhydrous $MgSO_4$. The solvent was removed at atmospheric pressure and the residual oil fractionated *in vacuo*. The $PhMe_2Sb$ was obtained at 40-42°C (0.3 mm Hg). Yield 15.4 g (49 %). Ph_2SbMe was obtained at 80°C (0.3 mm Hg). Yield 8.4 g (24 %).

$PhMe_2Sb$: ^1H NMR ($CDCl_3$): δ 1.15 (s, 6H, $C\underline{H}_3$), 7.46 (m, 3H, *m*, *p*-C<u>H</u>), 7.72 (m, 2H, *o*-C<u>H</u>). ^{13}C {^1H} NMR ($CDCl_3$): δ -0.9 ($\underline{C}H_3$), 128.4 (*p*-<u>C</u>H), 128.8 (*m*-<u>C</u>H), 135.2 (*o*-<u>C</u>H), 137.7 (*i*-<u>C</u>).

Ph_2SbMe: ^1H NMR ($CDCl_3$): δ 1.27 (s, 3H, $C\underline{H}_3$), 7.38-7.45 (m, 6H, *m,p*-C<u>H</u>), 7.59-7.68 (m, 4H, *o*-C<u>H</u>). $^{13}C\{^1H\}$ NMR ($CDCl_3$): 0.71 ($\underline{C}H_3$), 128.7 (*p*-<u>C</u>H), 128.9 (*m*-<u>C</u>H), 135.7 (*o*-<u>C</u>H), 138.2 (*i*-<u>C</u>).

A dimethiodide $PhSbMe_3I$ was prepared by quarternisation with excess iodomethane in acetone and recrystallisation from acetone/diethyl ether. Required for $[C_9H_{14}ISb]$ C = 29.15, H = 3.81 %; found C =29.23, H = 3.51 %. ^1H NMR (d_6-DMSO): δ 1.83 (s, 9H, $C\underline{H}_3$), 7.52 – 7.80 (m, 5H, Ar-C<u>H</u>). ^{13}C {^1H} NMR (d_6-DMSO): δ 3.64 ($\underline{C}H_3$), 129.3, 131.3, 134.2 (Ar-<u>C</u>H). Electrospray mass spectrum (MeCN): found *m/z* = 243. Calc. for $[Ph^{121}SbMe_3]^+$ 243.

Synthesis of 1,2-$C_6H_4(CH_2SbMe_2)_2$ Method 1: Hydrogen chloride gas was bubbled through a solution of $PhSbMe_2$ (7.0 g, 31.0 mmol) in dry toluene (50 mL) for ca. 15 mins. and then the solution was purged with N_2 to remove any excess hydrogen chloride. This solution was added dropwise to a solution of sodium (1.4 g, 62.0 mmol) in liquid ammonia (250 mL) at -78°C. The reaction was stirred for 2 h. and a solution of α,α'-dibromo-*o*-xylene (4.1 g, 15.5 mmol) in dry diethyl ether (150 mL) was added dropwise. When addition was complete the reaction was allowed to warm to RT, and then hydrolysed with aqueous NH_4Cl (~1 mol dm^{-3}, 200 mL). The organic layer was separated and the aqueous washed with diethyl ether (2 x 100 mL). The combined organics were dried over anhydrous $MgSO_4$. The solvent was removed *in vacuo*, and the residual oil purified by Kugelröhr distillation. The ligand was obtained at 200°C (0.5 mm Hg). Yield 400 mg (6 %).

Method 2: 1,2-Bis(chloromagnesiomethyl)benzene was prepared following the literature procedure, from magnesium powder (1.7 g, 70 mmol) which was activated with 1,2-dibromoethane (0.2 mL) in thf (5 mL). Thf (15 mL) was added followed by the dropwise addition over 3.5 h of α,α'-dichloro-*o*-xylene (3.1 g, 17.7 mmol) in thf (175 mL). After 15 h. this solution was treated dropwise with a toluene solution of Me_2SbCl, prepared as above from $PhMe_2Sb$ (8.0 g, 35.0 mmol), and stirred overnight. The reaction was hydrolysed with aqueous NH_4Cl (~1 mol dm^{-3}, 50 mL), the organic layer was separated and the aqueous washed with diethyl ether (2 x 100 mL). The combined organics were dried over anhydrous $MgSO_4$, and the solvent removed *in vacuo* to give the ligand as a fawn coloured oil. Yield 6.3 g (88 %). ^1H NMR ($CDCl_3$): δ 0.99 (s, 12H $C\underline{H}_3$), 3.07 (s, 4H, $C\underline{H}_2$), 7.33-7.77 (m, 4H, Ar-C<u>H</u>). $^{13}C\{^1H\}$ NMR ($CDCl_3$): -3.1 ($\underline{C}H_3$), 21.3 ($\underline{C}H_2$), 124.5 (4,5-<u>C</u>H), 128.5 (3,6-<u>C</u>H), 127.6 (*i*-<u>C</u>). Electron impact mass spectrum (CH_2Cl_2): found *m/z* = 393, 255. Calc. for [1,2-$C_6H_4(CH_2{}^{121}SbMe_2)(CH_2{}^{121}SbMe)$] 391, [1,2-$C_6H_4(CH_2)(CH_2{}^{121}SbMe_2)$] 255.

A dimethiodide 1,2-$C_6H_4(CH_2SbMe_3)_2I_2$ was prepared by quarternisation with excess iodomethane in acetone and recrystallisation from acetone/diethyl ether. Required for [$C_{14}H_{26}I_2Sb_2$] C = 24.31, H = 3.79 %; found C = 24.18, H = 3.92 %.

^{1}H NMR (d_6-DMSO): δ 1.61 (s, 18H, C$\underline{H}_3$), 3.80 (s, 4H, C$\underline{H}_2$), 7.33-7.42 (m, 4H, Ar-C$\underline{H}$). ^{13}C {^{1}H} NMR (d_6-DMSO): δ 6.21 (C$\underline{H}_3$), 28.2 (C$\underline{H}_2$), 131.3 (4,5-C$\underline{H}$), 134.4 (3,6-C$\underline{H}$), 136.7 (*I*-C$\underline{H}$) Electrospray mass spectrum (MeCN): found *m/z* = 551, 219. Calc. for [1,2-$C_6H_4(CH_2{}^{121}SbMe_3)(CH_2{}^{121}SbMe_2)I]^+$ 548, [1,2-$C_6H_4(CH_2{}^{121}SbMe_3)_2]^{2+}$ 218.

Synthesis of 1,3-$C_6H_4(CH_2SbMe_2)_2$: The reaction was carried out as above using magnesium (0.85 g, 35.0 mmol), α,α'-dichloro-*m*-xylene (1.53 g, 8.7 mmol) and $PhMe_2Sb$ (4.0 g, 17.5 mmol), to give the ligand as a yellow oil. Yield 2.0 g (56 %). ^{1}H NMR ($CDCl_3$): δ 0.67 (s, 12H, C$\underline{H}_3$), 2.77 (s, 4H, C$\underline{H}_2$), 6.84-7.41 (4H, m, Ar-C$\underline{H}$). ^{13}C {^{1}H} NMR ($CDCl_3$): -3.3 (C$\underline{H}_3$), 22.3 (C$\underline{H}_2$), 123.7 (4,6-C$\underline{H}$), 126.8, 128.3 (2,5-C$\underline{H}$), 141.0 (*i*-C$\underline{H}$). Electron impact mass spectrum (CH_2Cl_2): found *m/z* 408. Calc. for [1,3-$C_6H_4(CH_2{}^{121}SbMe_2)_2$] 406.

A dimethiodide was prepared by quarternisation with excess iodomethane in acetone and recrystallisation from acetone/diethyl ether. Required for $[C_{14}H_{26}I_2Sb_2].1/2Me_2CO$ C = 25.83, H = 4.05 %; found C = 25.49, H = 3.73 %. ^{1}H NMR (d_6-DMSO): δ 1.58 (s, 18H, C$\underline{H}_3$), 3.74 (s, 4H, C$\underline{H}_2$), 7.24-7.43 (m, 4H, Ar-C$\underline{H}$). ^{13}C{^{1}H} NMR (d_6-DMSO): δ 2.1 (C$\underline{H}_3$), 26.8 (C$\underline{H}_2$), 127.2, 128.7, 129.6 (Ar-C$\underline{H}$), 135.6 (*i*-C$\underline{H}$). Electrospray mass spectrum (MeCN): found *m/z* 219. Calc. for $[1,3\text{-}C_6H_4(CH_2{}^{121}SbMe_2)_2]^{2+}$ = 218.

Synthesis of 1,4-$C_6H_4(CH_2SbMe_2)_2$: The reaction was carried out as above using α,α'-dichloro-*p*-xylene (1.53 g, 8.7 mmol). The ligand was purified by Kugelröhr distillation to give a white crystalline solid (temp 125°C, 0.5 mm Hg). Yield = 1.8 g (50 %). ^{1}H NMR ($CDCl_3$): δ 0.5 (s, 12H, C$\underline{H}_3$), 2.7 (s, 4H, C$\underline{H}_2$), 6.7, 7.2 (m, 4H, Ar-C$\underline{H}$). ^{13}C{^{1}H} NMR ($CDCl_3$): δ -3.3 (C$\underline{H}_3$), 21.8 (C$\underline{H}_2$), 127.6 (Ar-C$\underline{H}$), 136.7 (*i*-C$\underline{H}$). Electron impact mass spectrum (CH_2Cl_2): found *m/z* 408, 255. Calc. for [1,4-$C_6H_4(CH_2{}^{121}SbMe_2)_2$] 406, [1,4-$C_6H_4(CH_2)(CH_2{}^{121}SbMe_2)$] 255.

A dimethiodide was prepared by quarternisation with excess iodomethane in acetone and recrystallisation from acetone/diethyl ether. Required for $[C_{14}H_{26}I_2Sb_2]$ C = 24.31, H = 3.79 %; found C = 24.06, H = 3.61 %. ^{1}H NMR (d_6-DMSO): δ 1.4 (s, 18H, C$\underline{H}_3$), 3.6 (s, 4H, C$\underline{H}_2$), 7.2 (s, 4H, Ar-C$\underline{H}$). $^{13}C\{^1H\}$ NMR (d_6-DMSO): δ 1.9 (C$\underline{H}_3$), 26.7 (C$\underline{H}_2$), 129.3 Ar-C$\underline{H}$), 133.2 (*i*-C). Electrospray mass spectrum (MeCN): found *m/z* 565. Calc. for $[1,4\text{-}C_6H_4(CH_2{}^{121}SbMe_3)_2I]^+$ 563.

Synthesis of 1,2-$C_6H_4(CH_2SbPh_2)_2$: A solution of α,α'-dichloro-*o*-xylene (1.53 g, 8.7 mmol) in dry thf (175 mL) was added dropwise over 3.5 h to a suspension of magnesium powder (0.85 g, 35.0 mmol) which was activated by 1,2-dibromoethane (0.2 mL) in dry thf (10 mL), and the resulting mixture was stirred at RT for 15 h. To this was added a solution of Ph_2SbCl (prepared from Ph_3Sb (4.1 g, 11.6 mmol) and $SbCl_3$ (1.33 g, 5.8 mmol)) in dry toluene (50 mL), and the reaction was stirred at RT for 15 h. The reaction was hydrolysed with aqueous NH_4Cl (~1 mol dm^{-3}, 150 mL) and the organic layer was separated. The aqueous was washed with diethyl ether (2 x 100 mL) and the combined organics were filtered through celite and dried over anhydrous $MgSO_4$. The solvent was removed *in vacuo* to give the ligand as a waxy brown solid. Yield 0.78 g (13 %). ^{1}H NMR ($CDCl_3$): δ 2.82 (s, 4H, C$\underline{H}_2$), 7.09-7.48 (m, 24H, Ar-C$\underline{H}$). $^{13}C\{^1H\}$ NMR ($CDCl_3$): δ 34.3 (C$\underline{H}_2$), 126.5, 128.8, 129.0, 129.3, 134.6 136.4 (Ar-C$\underline{H}$).

The tetra-iodo derivative was prepared by dissolving a sample of the ligand in CH_2Cl_2 and adding a solution of I_2 in CH_2Cl_2 dropwise at 0°C until the colour was no longer discharged. The mixture was stirred for 1 h and then refrigerated. The resulting orange-yellow solid was filtered, washed with ice-cold diethyl ether and dried *in vacuo*. Required for $[C_{32}H_{86}I_4Sb_2]$ C = 33.03, H = 2.50 %; found C = 32.99, H = 2.60 %.

Synthesis of 1,3-$C_6H_4Br(SbMe_2)$: A solution of *m*-dibromobenzene (1.29 g, 5.46 mmol) in dry diethyl ether (50 mL) was added dropwise to ^nBuLi (2.5 M hexanes, 8.7 mL, 21.8 mmol), and the reaction was refluxed for 3 h. A solution of Me_2SbCl, prepared as above from $PhMe_2Sb$ (2.5 g, 10.92 mmol), in toluene was added dropwise and the reaction was stirred at RT for 15 h. The reaction was hydrolysed with aqueous NH_4Cl (~1 mol dm^{-3}, 100 mL) and the organic layer separated. The aqueous was washed with diethyl ether (2 x 100 mL) and the combined organics were dried over anhydrous $MgSO_4$. The solvent was removed *in vacuo* to give the product as an off-white oil. Yield 0.83 g (49 %). ^1H NMR ($CDCl_3$): δ 1.00 (s, 6H, $C\underline{H}_3$), 7.18-7.66 (m, 4H, Ar-C<u>H</u>). $^{13}C\{^1H\}$ NMR ($CDCl_3$): δ -0.89 ($\underline{C}H_3$), 123.4 (*i*-<u>C</u>Br), 128.3, 130.1, 131.3, 133.4 (Ar-<u>C</u>H), 137.3 (*i*-<u>C</u>Sb).

A methiodide derivative was prepared by quarternisation with excess iodomethane in acetone, followed by recrystallisation from acetone/diethyl ether. ^1H NMR (d_6-DMSO): δ 1.85 (s, 9H, $C\underline{H}_3$), 7.5-8.0 (m, 4H, Ar-C<u>H</u>). $^{13}C\{^1H\}$ NMR (d_6-DMSO): δ 4.4 ($\underline{C}H_3$), 122.6 (*i*-<u>C</u>Br), 129.2, 131.1, 132,7, 132.9 (Ar-<u>C</u>H), 133.8 (*i*-<u>C</u>Sb). Electrospray mass spectrum (MeCN): found *m/z* 323, 243. Calc. for $[1,3\text{-}C_6H_4Br(^{121}SbMe_3)]^+$ 323, $[C_6H_5(^{121}SbMe_3)]^+$ 243.

Synthesis of 1,3-$C_6H_4(SbMe_2)_2$: 1,3-Bis(bromomagnesio)benzene was prepared following the literature procedure,[27] from magnesium powder (0.85 g, 35.0 mmol) which was activated with 1,2-dibromoethane (0.2 mL) in thf (5 mL), and anthracene (0.62 g, 3.5 mmol). Thf (40 mL) was added, followed by the dropwise addition of *m*-dibromobenzene (2.0g , 8.75 mmol) in thf (150 mL). After complete addition the reaction was refluxed for 3 h, allowed to cool, and then treated dropwise with a toluene solution of Me_2SbCl, prepared from $PhMe_2Sb$ (4.0 g, 17.5 mmol). The reaction was stirred at RT for 15 h and then hydrolysed with aqueous NH_4Cl (~1 mol dm^{-3}, 100 mL). The organic layer was separated and the aqueous washed with diethyl ether (2 x 100 mL). The combined organics were dried over anhydrous $MgSO_4$ and the solvent removed *in vacuo*. The residue was dissolved in the minimum amount of diethyl ether, filtered to remove anthracene, and the solvent removed *in vacuo* to give the ligand as a yellow oil. Yield 2.0 g (60 %). ^1H NMR ($CDCl_3$): δ 0.97 (s, 12H, $C\underline{H}_3$), 7.20-7.33 (m, 4H, Ar-C<u>H</u>) with

anthracene impurities at δ 7.4, 7.9, 8.3. $^{13}C\{^1H\}$ NMR ($CDCl_3$): δ -1.3 ($\underline{C}H_3$), 127.5, 128.7, 134.6 (Ar-$\underline{C}$H), 137.7 (*i*-$\underline{C}$) with anthracene inpurities at δ 125.3, 126.2, 128.1, 131.8. Electron impact mass spectrum (CH_2Cl_2): found *m/z* 380, 365, 350, 335. Calc. for $[1,3\text{-}C_6H_4(^{121}SbMe_2)_2]^+$ 378, $[1,3\text{-}C_6H_4(^{121}SbMe_2)(^{121}SbMe)]^+$ 363, $[1,3\text{-}C_6H_4(^{121}SbMe)_2]^+$ 348, $[1,3\text{-}C_6H_4(^{121}SbMe)(^{121}Sb)]^+$ 333.

A dimethiodide derivative was prepared by quarternisation with excess iodomethane in acetone, followed by recrystallisation from acetone/diethyl ether. Required for $[C_{12}H_{22}I_2Sb_2]$ C = 21.72, H = 3.34 %; found C = 23.08, H = 3.52 %. ^1H NMR (d_6-DMSO): δ 2.19 (s, 18H, C$\underline{H}_3$), 7.95-8.43 (m, 4H, Ar-C$\underline{H}$). $^{13}C\{^1H\}$ NMR (d_6-DMSO): δ 4.6 ($\underline{C}H_3$), 129.6, 131.0, 136.6 (Ar-$\underline{C}$H), 139.0 (*i*-$\underline{C}$). Electrospray mass spectrum (MeCN): found *m/z* 749, 537, 395, 311, 243, 205. Calc. for $[\{1,3\text{-}C_6H_4(^{121}SbMe_3)\}_2(^{121}SbMe)I]^+$ 747, $[1,3\text{-}C_6H_4(^{121}SbMe_3)_2I]^+$ 535, $[1,3\text{-}C_6H_4(^{121}SbMe_3)(^{121}SbMe_2)]^+$ 393, $[\{1,3\text{-}C_6H_4(^{121}SbMe_3)\}_2(^{121}SbMe)]^{2+}$ 310, $[C_6H_5(^{121}SbMe_3)]^+$ 243, $[1,3\text{-}C_6H_4(^{121}SbMe_3)_2]^{2+}$ 204.

Synthesis of $1,4\text{-}C_6H_4(SbMe_2)_2$: Reaction was carried out as above using magnesium powder (0.42 g, 17.3 mmol), anthracene (0.31 g, 1.73 mmol), *p*-dibromobenzene (1.03 g, 4.37 mmol) and $PhMe_2Sb$ (2 g, 8.74 mmol). Yield 0.97 g (58 %). ^1H NMR ($CDCl_3$): δ 1.01 (s, 12H, C$\underline{H}_3$), 7.53 (s, Ar-C$\underline{H}$) with anthracene impurities at δ 7.4, 7.9, 8.3. $^{13}C\{^1H\}$ NMR ($CDCl_3$): δ -1.31 ($\underline{C}H_3$), 135.0 (Ar-$\underline{C}$H), 137.5 (*i*-$\underline{C}$), with anthracene inpurities at δ 125.3, 126.2, 128.1, 131.8. Electron impact mass spectrum (CH_2Cl_2): found *m/z* 380, 365, 350, 335, 320. Calc. for $[1,4\text{-}C_6H_4(^{121}SbMe_2)_2]^+$ 378, $[1,4\text{-}C_6H_4(^{121}SbMe_2)(^{121}SbMe)]^+$ 363, $[1,4\text{-}C_6H_4(^{121}SbMe)_2]^+$ 350, $[1,4\text{-}C_6H_4(^{121}SbMe)(^{121}Sb)]^+$ 335, $[1,4\text{-}C_6H_4(^{121}Sb)_2]^+$ 320.

A dimethiodide derivative was prepared by quarternisation with excess iodomethane in acetone, followed by recrystallisation from acetone/diethyl ether. ^1H NMR (d_6-DMSO): δ 1.86 (s, 18H, C$\underline{H}_3$), 7.89 (s, 4H, Ar-C$\underline{H}$). $^{13}C\{^1H\}$ NMR (d_6-DMSO): δ 4.65 ($\underline{C}H_3$), 134.2 (Ar-$\underline{C}$H), 136.0 (*i*-$\underline{C}$). Electrospray mass spectrum (MeCN): found *m/z* 537, 523, 243, 226, 205. Calc. for $[1,4\text{-}C_6H_4(^{121}SbMe_3)_2\ I]^+$ 535, $[1,4\text{-}C_6H_4(^{121}SbMe_3)(^{121}SbMe_2)I]^+$ 520,

$[C_6H_5(^{121}SbMe_3)]^+$ 243, $[1,4\text{-}C_6H_4(^{121}SbMe_3)_2MeCN]^{2+}$ 225, $[1,4\text{-}C_6H_4(^{121}SbMe_3)_2]^{2+}$ 204.

Synthesis of 1,2-$C_6H_4Cl(SbPh_2)$: 1-Chloro,2-(bromomagnesio)benzene was prepared from magnesium turnings (1.90 g, 78.4 mmol) activated with 1,2-dibromoethane (0.5 mL) and 1-chloro,2-bromobenzene (13.65 g, 71.3 mmol) in dry diethyl ether (200 mL) and stirred for 1 h to ensure complete reaction. The Grignard was added dropwise to a suspension of Ph_2SbCl (20 g, 64.2 mmol) in dry thf (150 mL) and the reaction stirred at RT for 2h. Reaction was hydrolysed with aqueous NH_4Cl (~1 mol dm^{-3}, 200 mL) and the organic layer separated. The aqueous was washed with dichloromethane (3 x 100 mL) and the combined organics were dried over anhydrous $MgSO_4$. Removal of solvent *in vacuo* gave the ligand as a yellow oil. Yield 17.2 g (62 %). ^1H NMR ($CDCl_3$): δ 7.05-7.67 (m, 10H, Ar-C<u>H</u>). Electron impact mass spectrum (CH_2Cl_2): found *m/z* 388, 311, 234, 198. Calc. for $[1,2\text{-}C_6H_4{}^{35}Cl(^{121}SbPh_2)]^+$ 386, $[1,2\text{-}C_6H_4{}^{35}Cl(^{121}SbPh)]^+$ 309, $[1,2\text{-}C_6H_4{}^{35}Cl(^{121}Sb)]^+$ 232, $[C_6H_5{}^{121}Sb]^+$ 198.

2.5 References

1. N. R. Champness and W. Levason, *Coord. Chem. Rev.*, **133**, (1994), 115.
2. M. Nunn, D. B. Sowerby and D. M. Wesolek, *J. Organomet. Chem.*, **251**, (1983), C45.
3. S. P. Bone and D. B. Sowerby, *J. Chem. Soc., Dalton Trans.*, (1979), 715.
4. C. A. McAuliffe, I. E. Niven and R. V. Parish, *Inorg. Chim. Acta*, **15**, (1975), 67.
5. K. Issleib and B. Hamann, *Z. Anorg. Allgem. Chem*, **343**, (1966), 196.
6. K. K. Chow, W. Levason and C. A. McAuliffe, *J. Chem. Soc., Dalton Trans.*, (1976), 1429.
7. R. A. Bartlett, H. V. R. Dias, H. Hope, B. D. Murray, M. M. Olmstead and P. P. Power, *J. Am. Chem. Soc.*, **108**, (1986), 6921.
8. Y. Matsumura and R. Okawara, *J. Organomet. Chem.*, **25**, (1970), 439.
9. S. Sato, Y. Matsumura and R. Okawara, *Inorg. Nucl. Chem. Let.*, **8**, (1972), 837.
10. S. Sato, Y. Matsumura and R. Okawara, *J. Organomet. Chem.*, **43**, (1972), 333.
11. K. Issleib and B. Hamann, *Z. Anorg. Allgem. Chem.*, **339**, (1965), 289.
12. K. Issleib and B. Hamann, *Z. Anorg. Allgem. Chem.*, **332**, (1964), 179.
13. W. Levason, C. A. McAuliffe and S. G. Murray, *J. Organomet. Chem.*, **88**, (1975), 171.
14. H. Hartmann and G. Kuhl, *Z. Anorg. Allgem. Chem.*, **312**, (1961), 186.
15. H. Zorn, H. Schindlbauer and D. Hammer, *Monatsch. Chem.*, **98**, (1967), 731.
16. E. Shewchuk and S. B. Wild, *J. Organomet. Chem.*, **128**, (1977), 115.
17. W. Levason, K. G. Smith, C. A. McAuliffe, F. P. McCullough, R. D. Sedgwick and S. G. Murray, *J. Chem. Soc., Dalton Trans.*, (1979), 1718.
18. J. Ellermann and A. Veit, *J. Organomet. Chem.*, **290**, (1985), 307.
19. H. Althaus, H. J. Breunig and E. Lork, *Organometallics*, **20**, (2001), 586.
20. M. F. Lappert, T. R. Martin and C. L. Raston, *Inorg. Synth.*, **26**, (1989), 144.
21. W. Levason and C. A. McAuliffe, 'Phosphine, Arsine and Stibine Complexes of the Transition Elements', Elsevier, New York, (1979).

22. W. Levason and G. Reid, 'Arsines, Stibines, Bismuthines', Vol. 1, Chapter 16, 'Comprehensive Coordination Chemistry II', J. A. McCleverty and T. J. Meyer (Ed.), Elsevier, Oxford, (2003).

23. A. A. Cheremisin and P. V. Schastnev, *J. Magn. Res.*, **40**, (1980), 459.

24. G. O. Doak and L. D. Freedman, 'Organometallic Compounds of Arsenic, Antimony and Bismuth', Wiley, New York, (1970).

25. Y. Matano, H. Kurata, T. Murafuji, N. Azuma and H. Suzuki, *Organometallics*, **17**, (1998), 4049.

26. D. H. Williams and I. Fleming, 'Spectroscopic Methods in Organic Chemistry Fifth Edition', The McGraw-Hill Companies, London, (1995).

27. L. Zhang, S. Liao, Y. X. M. Wang, Y. Zhang and D. Yu, *Synth. React. Inorg. Met. Org. Chem.*, **26**, (1996), 809.

28. R. D. Feltham, A. Kasenally and R. S. Nyholm, *J. Organomet. Chem.*, **7**, (1966), 285.

29. B. J. Wakefield, 'Organomagnesium Methods in Organic Synthesis', Academic Press, London.

30. B. R. Cook, C. A. McAuliffe and D. W. Meek, *Inorg. Chem.*, **10**, (1971), 2696.

31. F. A. Hart, *J. Chem. Soc.*, (1960), 3324.

32. W. Levason, Ph.D. Thesis, UMIST, Manchester, (1975).

33. R. Talay and D. Rehder, *Z. Naturforsch.*, **36b**, (1981), 451.

34. H. C. E. McFarlane and W. McFarlane, *Polyhedron*, **2**, (1983), 303.

35. S. J. Higgins and W. Levason, *Inorg. Chem.*, **24**, (1985), 1105.

36. H. C. Jewiss, W. Levason, M. D. Spicer and M. Webster, *Inorg. Chem.*, **26**, (1987), 2102.

Chapter 3

Transition Metal Carbonyl Complexes of Novel Distibine Ligands

3.1 Introduction

The coordination chemistry of distibines has received limited investigation and has generally been confined to soft metals in low oxidation states, for example low valent metal carbonyls and the platinum group metals. The ligands used are of three types: distibinomethanes $R_2SbCH_2SbR_2$, 1,3-distibinopropanes $R_2SbCH_2CH_2CH_2SbR_2$ and 1,2-distibinobenzenes *o*-$C_6H_4(SbR_2)_2$ (where R = Me or Ph).

The distibinomethanes generally act as monodentate or bridging ligands. Their reluctance to chelate can be attributed to strain in the resulting four-membered chelate ring.[1] The distibinopropanes and 1,2-distibinobenzenes usually act as chelate ligands like their phosphine and arsine analogues.

In this introduction the coordination chemistry of distibine ligands with metal carbonyls will be discussed. Coordination with other metal species will be covered in the introduction to chapter 4.

3.1.1 Group 6 Metal Carbonyl Derivatives

The ligands $Ph_2Sb(CH_2)_3SbPh_2$ and *o*-$C_6H_4(SbMe_2)_2$ react with $M(CO)_6$ (M = Cr, Mo or W) to form complexes of the type *cis*-$[M(CO)_4L]$ with the distibines acting as chelating ligands.[2-4] In contrast the distibinomethane ligands $Me_2SbCH_2SbMe_2$ (dmsm) and $Ph_2SbCH_2SbPh_2$ (dpsm) react with Group 6 metal carbonyls to give a variety of different complexes largely dependent on the reactions conditions used.

3.1.1.1 $[M(CO)_5\{\eta^1\text{-L}\}]$

Complexes of the type $[M(CO)_5\{\eta^1\text{-dpsm}\}]$ (M = Cr, Mo or W, dpsm = $Ph_2SbCH_2SbPh_2$) can be prepared either by photolysis of $M(CO)_6$ in thf to give $[M(CO)_5\{thf\}]$, followed by addition of the ligand,[5] or by reaction of $[NEt_4][M(CO)_5Br]$ with the ligand in a 1:1 ratio.[5] The tungsten complex has been structurally characterised and shows one Sb atom bound to a square pyramidal $W(CO)_5$ residue.[5]

In contrast η^1-complexes of the analogous bis(dimethyldistibino)methane (dmsm) are much more difficult to prepare due to the increased sensitivity of the stibine group. Reaction of dmsm with $[M(CO)_5\{thf\}]$ (M = Mo or W) gives air-sensitive oils. The carbonyl region of the $^{13}C\{^1H\}$ NMR spectra show peaks consistent with the formation of

both $[M(CO)_5\{\eta^1\text{-dmsm}\}]$ and $[M_2(CO)_{10}\{\mu\text{-dmsm}\}]$.[5] However upon exposure to air the non-coordinated $SbMe_2$ group oxidises and no samples have been isolated.

3.1.1.2 $[M_2(CO)_{10}\{\mu\text{-L}\}]$

$[M_2(CO)_{10}\{\mu\text{-dmsm}\}]$ (M = Cr, Mo or W) are readily made by reaction of $[M(CO)_6]$ with the ligand in a 2:1 ratio in high boiling solvents.[5]

Reaction of $[M(CO)_5Br]^-$ (M = Cr, Mo or W) with dpsm in a 2:1 ratio gives $[M(CO)_5(\eta^1\text{-dpsm})]$ when M = Mo or W, and a mixture of $[Cr(CO)_5\{\eta^1\text{-dpsm}\}]$ and $[Cr_2(CO)_{10}\{\mu\text{-dpsm}\}]$ when M = Cr.[5] This suggests that coordination of one stibine group reduces the reactivity of the second, but steric effects may also play an important role. The complexes are best prepared by reaction of $[M(CO)_5\{\eta^1\text{-dpsm}\}]$ with $[M(CO)_5\{thf\}]$ (M = Cr or W) , however curiously the Mo complex cannot be made.[5]

3.1.1.3 *cis*-$[\{M(CO)_4L\}_2]$

Displacement of the neutral ligands from $[M(CO)_4\{nbd\}]$ (nbd = norbornadiene, bicyclo[2.2.1]hepta-2,5-diene) or $[W(CO)_4\{Me_2N(CH_2)_3NMe_2\}]$ with either dmsm or dpsm gives poor yields of the *cis*-tetracarbonyl complexes *cis*-$[\{M(CO)_4(L\text{-}L)\}_2]$.[5] The formulation as dimer complexes is based upon the FAB mass spectra which show dimetal fragments. Both tungsten complexes have been structurally characterised and are centrosymmetric dimeric species with the Sb atoms bonded to different W atoms (Figure 3.1)[5]

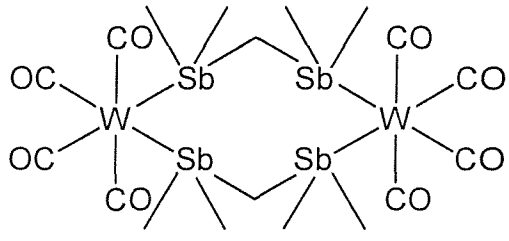

Figure 3.1 – Structure of *cis*-$[\{W(CO)_4(dmsm)_2\}_2]$

3.1.1.4 *fac*-[M(CO)$_3${η^1-dpsm}$_3$]

Reaction of $Mo(CO)_6$ with dpsm in ethanol with $NaBH_4$ as a catalyst yields *fac*-[Mo(CO)$_3${η^1-dpsm}$_3$].[5] The chromium and tungsten analogues cannot be prepared using the same procedure, but can be made in low yield by heating the ligand with either [Cr(CO)$_4${nbd}] or [W(CO)$_3${MeCN}$_3$] in ethanol.[5]

3.1.2 Manganese, Rhenium and Iron Carbonyl Complexes

Dpsm and dmsm react slowly with $Mn_2(CO)_{10}$ in the presence of a [{(Cp)Fe(CO)$_2$}$_2$] catalyst to give [$Mn_2(CO)_8$L].[6] Alternatively, photolysis of $Mn_2(CO)_{10}$ with dpsm yields [$Mn_2(CO)_6${dpsm}$_2$].[7] The crystal structure consists of discrete molecules based on $Mn_2(CO)_{10}$ with the substitution of two distibine ligands for four carbonyl groups.[7] Photolysis of dpsm and dmsm with $Re_2(CO)_{10}$ yields axially substituted [$Re_2(CO)_9$(η^1-L)].[7] No manganese or rhenium carbonyl complexes have been reported for either $R_2Sb(CH_2)_3SbR_2$ or *cis*-$C_6H_4(SbMe_2)_2$.

[Fe(CO)$_4$(η^1-dpsm)] can be obtained in low yield by refluxing $Fe(CO)_5$ with the ligand in n-heptane.[8] Better yields can be obtained using catalysts such as $NaBH_4$/EtOH [9] or [{(Cp)Fe(CO)$_2$}$_2$][10], but the complex is best made from [$Fe_2(CO)_9$] in thf.[6] The X-ray structure of [Fe(CO)$_4${dpsm}] shows the iron centre in a tbp geometry with the Sb atom occupying an axial site.[6]

In contrast reaction of dmsm with $Fe(CO)_5$ or $Fe_2(CO)_9$ yields the ligand bridged dimer complex [$Fe_2(CO)_8${μ-dmsm}].[6]

3.1.3 Cobalt and Rhodium Carbonyl Complexes

Dicobalt octacarbonyl reacts with $R_2SbCH_2SbR_2$ (R = Me, Et, Ph, *p*-MeC_6H_4) to form complexes of the type [$Co_2(CO)_4${μ-CO}$_2${μ-L-L}].[6, 11] Treatment of the complexes with RC≡CR replaces the bridging carbonyl groups to give [$Co_2(CO)_4${RC≡CR}{μ-L-L}][11]

There is only one known rhodium carbonyl complex of a distibine which is the stibine bridged complex [{Rh(CO)Cl{dpsm}}$_2$] which is prepared by reaction of dpsm with rhodium carbonyl chloride.[12]

3.1.4 Nickel Carbonyl Complexes

Reaction of dpsm with $Ni(CO)_4$ in a 1:1 ratio yields $[Ni(CO)_3\{dpsm\}]$ whilst reaction with excess $Ni(CO)_4$ yields the ligand bridged dimer complex $[Ni_2(CO)_6\{dpsm\}]$. Reaction of dmsm with excess $Ni(CO)_4$ also yields the ligand bridged dimer complex $[Ni_2(CO)_6\{dmsm\}]$. The reaction mixture decomposes to give a mixture of $[Ni_2(CO)_6\{dmsm\}]$ and $[Ni(CO)_3\{\eta^1\text{-dmsm}\}]$, interestingly the latter complex cannot be made directly.

The aim of this chapter was to examine the coordination properties of the novel xylyl- and phenylene-distibine ligands previously described in chapter 2. Metal carbonyl complexes can provide useful information on the ligand donor properties by study of the spectator carbonyl ligands through IR and $^{13}C\{^1H\}$ NMR spectroscopy. Useful comparisons can also be made with the existing literature data available on related metal carbonyl complexes. We have chosen to study three metal carbonyl systems; iron, nickel and tungsten carbonyl. Nickel carbonyl is very easy to substitute and Tolman has studied a wide range of phosphine nickel carbonyl complexes and correlated the position of the A_1 $\nu(CO)$ stretch in the IR spectra with relative donor strength. Iron pentacarbonyl usually only monosubstitutes and allows the facile isolation of stable metal carbonyl complexes. In contrast recent studies of distibinomethanes with tungsten carbonyl have shown that a range of different complexes are possible [5] with substitution of one, two or even three carbonyl groups. The type of complex isolated reflects both the bonding and steric properties of the ligands. Therefore the data obtained on the three metal carbonyl systems will provide information on the preferred ligand coordination modes and also details of their electronic properties.

3.2 Results and Discussion

3.2.1 Iron Carbonyl Complexes

The reaction of $[Fe_2(CO)_9]$ in thf at room temperature[13] with each of the three xylyl-backboned distibines in an $[Fe_2(CO)_9]$: ligand ratio of 2:1 (half the contained iron is lost as $Fe(CO)_5$)[13] gave complexes with the stoichiometry $[\{Fe(CO)_4\}_2\{C_6H_4(CH_2SbMe_2)_2\}]$. All three complexes are very soluble in organic solvents, and the solution IR spectra in CH_2Cl_2 show three IR active ν(CO) bands at ca. 2040, 1965 and 1933 cm^{-1} (Figure 3.2 and Table 3.4) consistent with axially substituted tbp iron centres (C_{3v}) (theory $2A_1 + E$).[14] These bands closely resemble those observed in $[Fe(CO)_4(Ph_3Sb)]$ (2048, 1975 and 1942 cm^{-1}, spectra recorded in CCl_4)[15] and in the related distibinomethane complex $[\{Fe(CO)_4\}_2(Me_2SbCH_2SbMe_2)]$ (2040, 1963 and 1931, spectra recorded in $CHCl_3$).[6]

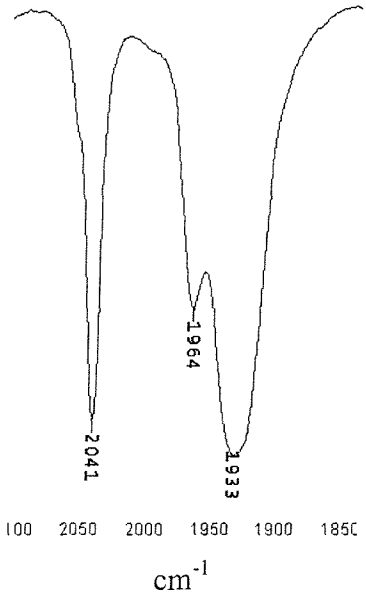

Figure 3.2- Solution IR spectrum (CH_2Cl_2) of $[\{Fe(CO)_4\}_2\{1,3\text{-}C_6H_4(CH_2SbMe_2)_2\}]$

The ^1H and $^{13}C\{^1H\}$ NMR spectra of all three complexes show single methyl and methylene resonances indicating that the ligands are symmetrically bridging two axially substituted $Fe(CO)_4$ units. As usual with iron carbonyl derivatives the $^{13}C\{^1H\}$ NMR spectra show a single carbonyl resonance at ca. δ 213 ppm indicating fluxionality.[6, 13]

The APCI mass spectra of the three complexes show two major features at *m/z* 745 and 577 (based upon ^{121}Sb) corresponding to $[\{Fe(CO)_4\}_2\{ligand\}]^+$ and $[\{Fe(CO)_4\}\{ligand\}]^+$ which provides further support for the formation of ligand bridged dimer complexes.

We have seen no evidence for the formation of the iron tricarbonyl species $[Fe(CO)_3\{1,2\text{-}C_6H_4(CH_2SbMe_2)_2\}]$ which may arise by chelation of the *ortho*-xylyl distibine. A number of chelating diphosphine and diarsine ligands form complexes of the type $[Fe(CO)_3L]$[16] but they are made either under forcing conditions (high temperatures, sealed tubes etc) or by displacement of an organic group (L) from a preformed complex $[Fe(CO)_3L]$. It is unlikely that the distibine ligand would remain intact under such harsh conditions and under the more mild reaction conditions used here diphosphines also form ligand bridged dimer complexes.[17]

Reaction of $1,3\text{-}C_6H_4(SbMe_2)_2$ with two equivalents of $[Fe_2(CO)_9]$ in dry thf yields $[\{Fe(CO)_4\}_2\{1,3\text{-}C_6H_4(SbMe_2)_2\}]$ as a yellow oil. The solution IR spectrum in CH_2Cl_2 is very similar to those observed for the xylyl ligands, showing three ν(CO) bands at 2043, 1966 and 1932 cm^{-1}. The ^1H and $^{13}C\{^1H\}$ NMR spectra show single methyl resonances at δ 1.57 and 0.83 ppm respectively consistent with the formation of a ligand bridged dimer complex. The $^{13}C\{^1H\}$ NMR spectrum also shows a single δ (CO) resonance at 211.4 ppm, again indicating fluxional carbonyl groups. Unfortunately microanalytical data could not be obtained due to the complex being isolated as an oil, however the APCI mass spectrum provides conclusive evidence for the formation of $[\{Fe(CO)_4\}_2\{1,3\text{-}C_6H_4(SbMe_2)_2\}]$, with peaks corresponding to *m/z* 714 $[\{^{56}Fe(CO)_4\}_2\{1,3\text{-}C_6H_4(^{121}SbMe_2)_2\}]$ and *m/z* 546 $[^{56}Fe(CO)_4\{1,3\text{-}C_6H_4(^{121}SbMe_2)_2\}]$.

In contrast reaction of $1,4\text{-}C_6H_4(SbMe_2)_2$ with $[Fe_2(CO)_9]$ in a 1:2 ratio gives the mono-substituted complex $[Fe(CO)_4\{\eta^1\text{-}1,4\text{-}C_6H_4(SbMe_2)_2\}]$. The ^1H NMR shows two methyl resonances at δ 1.52 and 0.98 ppm of approximately equal intensity, corresponding to the coordinated and uncoordinated $SbMe_2$ groups respectively. Similarly the $^{13}C\{^1H\}$ NMR spectrum also shows two methyl resonances at δ -1.4 and 0.9 ppm. The solution IR spectrum (CH_2Cl_2) shows no appreciable difference to that observed for the ligand bridged dimer complexes, exhibiting three ν(CO) bands at 2043, 1966 and 1933 cm^{-1}. With the *para*-substituted distibine it is possible that the second –

$SbMe_2$ group is deactivated by inductive effects from the coordinated end of the ligand, preventing complexation. Inductive effects do not deactivate the *meta*-position which would explain the ready formation of the ligand bridged dimer complex with 1,3-$C_6H_4(SbMe_2)_2$. The APCI mass spectrum provides further evidence for the formation of the η^1-ligand complex with the major species present corresponding to *m/z* 546 [$^{56}Fe(CO)_4\{1,4\text{-}C_6H_4(CH_2{}^{121}SbMe_2)_2\}$].

3.2.2 Crystallographic Analysis of [{Fe(CO)$_4$}$_2${1,3-C$_6$H$_4$(CH$_2$SbMe$_2$)$_2$}]

Crystals of [{Fe(CO)$_4$}$_2${1,3-C$_6$H$_4$(CH$_2$SbMe$_2$)$_2$}] were grown from a CH_2Cl_2 solution of the complex by slow evaporation in the freezer. The structure (Figure 3.3, Tables 3.1 and 3.2) shows a bridging distibine ligand with each antimony atom bonded axially to an $Fe(CO)_4$ residue. The discrete molecule has 2-fold crystallographic symmetry passing through C(10) and C(11). The Fe-Sb bond length (2.4901(11) Å) is very similar to that observed in the related complex [Fe(CO)$_4${Ph$_2$Sb(CH$_2$)SbPh$_2$}] (Fe-Sb = 2.491(2) Å).[6] An increase in the average ∠C-Sb-C of triphenylstibine is observed upon complexation.[5, 18, 19] Although no crystallographic data has been obtained on 1,3-$C_6H_4(CH_2SbMe_2)_2$, the *para*-xylyl ligand has been structurally characterised. It is unlikely that the position of the $SbMe_2$ groups on the benzene ring will affect the angles at Sb, thus useful comparisons can be made between the free ligand and the iron complex. Comparison of 1,4-$C_6H_4(CH_2SbMe_2)_2$ (∠ C-Sb-C = 96° av.) with [{Fe(CO)$_4$}$_2${1,3-C$_6$H$_4$(CH$_2$SbMe$_2$)$_2$}] (∠ C-Sb-C = 103° av.) also shows an increase in the average values of ∠ C-Sb-C upon complexation.

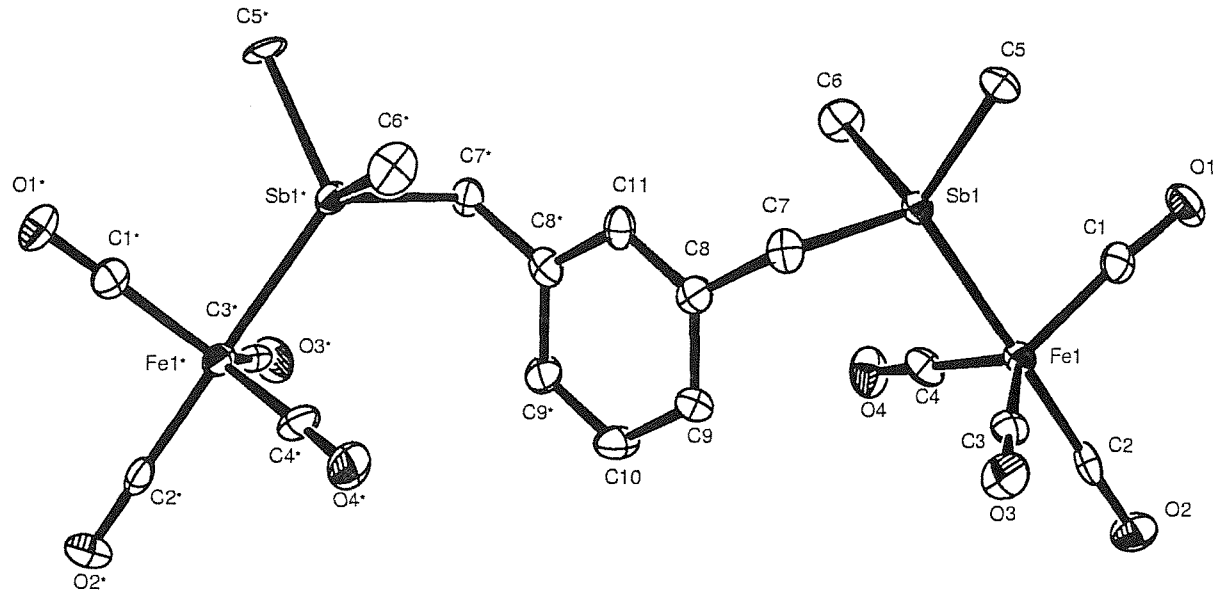

Figure 3.3 – View of the structure of $[\{Fe(CO)_4\}_2\{1,3\text{-}C_6H_4(CH_2SbMe_2)_2\}]$ with numbering scheme adopted. Ellipsoids are drawn at 40 % probability. H atoms are omitted for clarity.

Bond Lengths (Å)		*Bond Lengths* (Å)	
Sb(1)-Fe(1)	2.4901(11)	Fe(1)-C(1)	1.797(8)
Sb(1)-C(5)	2.120(7)	Fe(1)-C(2)	1.784(8)
Sb(1)-C(6)	2.129(6)	Fe(1)-C(3)	1.794(8)
Sb(1)-C(7)	2.146(7)	Fe(1)-C(4)	1.783(8)
C(7)-C(8)	1.505(9)	C(n)-O(n)	1.129(8)-1.152(8)
Bond Angles (°)		*Bond Angles* (°)	
Fe(1)-Sb(1)-C(5)	116.1(2)	Sb(1)-Fe(1)-C(1)	86.6(3)
Fe(1)-Sb(1)-C(6)	114.9(2)	Sb(1)-Fe(1)-C(2)	179.3(2)
Fe(1)-Sb(1)-C(7)	115.9(2)	Sb(1)-Fe(1)-C(3)	88.8(2)
Sb(1)-C(7)-C(8)	110.6(4)	Sb(1)-Fe(1)-C(4)	85.7(2)
C(1)-Fe(1)-C(2)	94.0(3)	C(2)-Fe(1)-C(3)	91.3(3)
C(1)-Fe(1)-C(3)	118.1(3)	C(2)-Fe(1)-C(4)	93.7(3)
C(1)-Fe(1)-C(4)	118.7(3)	C(3)-Fe(1)-C(4)	122.4(3)
C(5)-Sb(1)-C(6)	104.6(3)	C(5)-Sb(1)-C(7)	102.1(3)
C(6)-Sb(1)-C(7)	101.4(3)	Fe(1)-C(n)-O(n)	177.7(7)-178.6(7)

Table 3.1 – Selected bond lengths (Å) and angles (°) for $[\{Fe(CO)_4\}_2\{1,3\text{-}C_6H_4(CH_2SbMe_2)_2\}]$

Table 3.2 – Crystal data and structure refinement details for $[\{Fe(CO)_4\}_2\{1,3\text{-}C_6H_4(CH_2SbMe_2)_2\}]$

compound	$[\{Fe(CO)_4\}_2\{1,3\text{-}C_6H_4(CH_2SbMe_2)_2\}]$
empirical formula	$C_{20}H_{20}Fe_2O_8Sb_2$
fw	743.56
cryst. system	Tetragonal
space group	$P4_12_12$ (No. 92)
a (Å)	10.5264(16)
b (Å)	10.5264(16)
c (Å)	22.924(4)
volume ($Å^3$)	2540.1(7)
Z	4
density (calc) (mg/m^3)	1.944
abs coef (mm^{-1})	3.263
*F*000	1432
total no. of obsns	8902 (R_{int} = 0.071)
no. of unique obsns	2902
min, max transmission	0.851, 0.915
no. of parameters, restraints	148, 0
goodness-of-fit on F^2	1.03
R1, wR2 ($I > 2\sigma(I)$)[b]	0.047, 0.090
R1, wR2 (all data)	0.075, 0.099

Temperature = 120 K; wavelength (Mo-Kα) = 0.71073 Å; θ (max) = 27.5 deg.

[b] $R1 = \sum || F_0| - |F_c|| / \sum |F_0|$ $\quad wR2 = [\sum w(F_0^2 - F_c^2)^2 / \sum wF_0^4]^{1/2}$

3.2.3 Tungsten Carbonyl Complexes

The reaction of 1,4-$C_6H_4(CH_2SbMe_2)_2$ with 2.2 equivalents of $[W(CO)_5(thf)]$, generated *in situ* by the photolysis of $[W(CO)_6]$ in thf, gave $[\{W(CO)_5\}_2\{1,4\text{-}C_6H_4(CH_2SbMe_2)_2\}]$ as a brown solid in good yield. The solution IR spectrum in CH_2Cl_2 shows three ν(CO) bands at ca. 2069, 1995 and 1937 cm^{-1} which is consistent with square pyramidal $W(CO)_5$ residues (C_{4v}) (theory $2A_1 + E$). The position of the three ν(CO) bands are very similar to those found for $[\{W(CO)_5\}_2\{Me_2SbCH_2SbMe_2\}]$ (2070, 1985, 1946 cm^{-1}, spectra recorded in CH_2Cl_2).[5] The ^1H and $^{13}C\{^1H\}$ NMR spectra show single methyl and methylene resonances consistent with the formation of a ligand bridged dimer as observed with the iron carbonyl complexes. Two carbonyl resonances are observed at δ 197.0 and 199.7 ppm in a approximate 4:1 ratio corresponding to carbonyl *trans* carbonyl and carbonyl *trans* antimony respectively. Tungsten satellites were observed on each of the carbonyl resonances (Figure 3.4) and the $^1J(^{183}W\text{-}^{13}C)$ coupling constants are in good agreement with those reported for other tungsten stibine complexes.[5, 20] Some decomposition is observed during the long accumulations required to obtain the $^{13}C\{^1H\}$ NMR data as shown by the appearance of a third carbonyl resonance at δ 193 ppm associated with the formation of $W(CO)_6$. This effect has been observed in other tungsten stibine complexes[5] and the isolated solid is stable if stored under N_2. The APCI mass spectrum shows a parent ion at *m/z* 1055 and a second fragment ion at 1027 corresponding to loss of CO.

Reaction of 1,3-$C_6H_4(CH_2SbMe_2)_2$ with $[W(CO)_5(thf)]$ repeatedly gave $[W(CO)_5\{\eta^1\text{-}1,3\text{-}C_6H_4(CH_2SbMe_2)_2]$ as the product. Addition of excess $[W(CO)_5(thf)]$ to the isolated complex failed to attach a second tungsten and simply led to decomposition. Both ^1H and $^{13}C\{^1H\}$ NMR spectra provide evidence for the ligand coordinating as a monodentate, exhibiting two methyl and two methylene resonances corresponding to the free and coordinated $-CH_2SbMe_2$ groups. The APCI mass spectrum supports the spectroscopic data and shows two peaks at *m/z* 702 and 674 with the correct isotopic distribution for $[W(CO)_4\{1,3\text{-}C_6H_4(CH_2SbMe_2)_2\}]^+$ and $[W(CO)_3\{1,3\text{-}C_6H_4(CH_2SbMe_2)_2\}]^+$. The failure to form the ditungsten complex is unexpected and given the ready formation of $[\{Fe(CO)_4\}_2\{1,3\text{-}C_6H_4(CH_2SbMe_2)_2\}]$ it seems unlikely to be due to steric reasons.

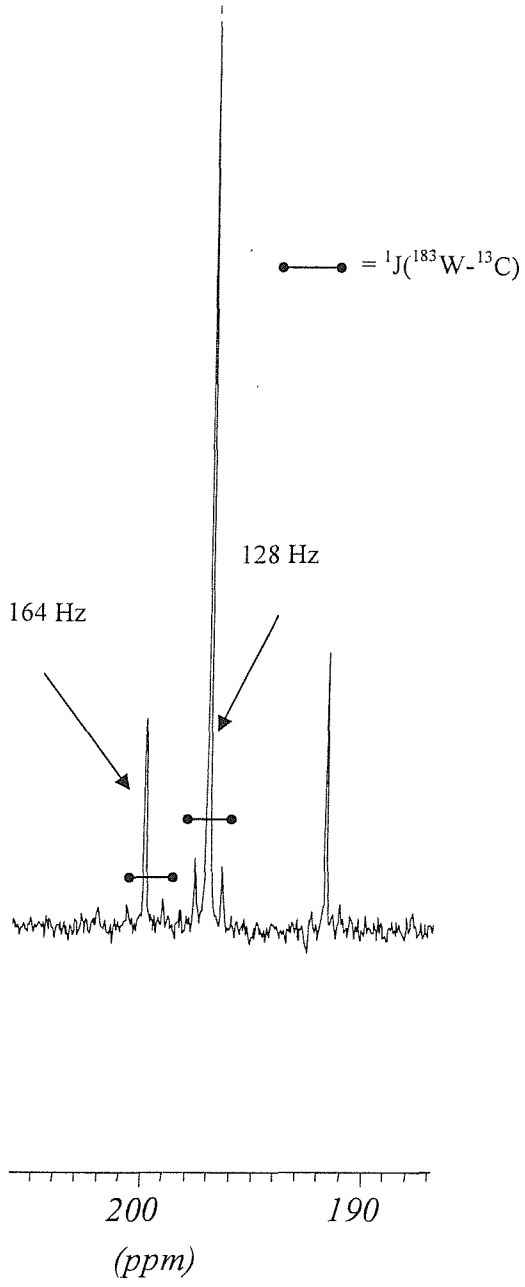

Figure 3.4 – CO region of the $^{13}C\{^{1}H\}$ NMR spectrum of $[\{W(CO)_5\}_2\{1,4\text{-}C_6H_4(CH_2SbMe_2)_2\}]$ in $CH_2Cl_2/CDCl_3$

Photolysis of $1,2\text{-}C_6H_4(CH_2SbMe_2)_2$ with $[W(CO)_6]$ in dry thf gives the monomeric complex $[W(CO)_4\{1,2\text{-}C_6H_4(CH_2SbMe_2)_2\}]$ with the distibine acting as a chelate ligand. The reaction mixture darkens significantly during the 2 hour photolysis and much black solid is generated indicative of substantial decomposition. The reaction mixture was filtered prior to work-up to remove any decomposition products but the complex was

isolated in very low yields (ca. 5 %). The same product can be made in higher yield by reaction of 1,2-$C_6H_4(CH_2SbMe_2)_2$ with $[W(CO)_4(piperidine)_2]$ in EtOH. The solution IR spectrum of the complex in CH_2Cl_2 shows four ν(CO) stretches consistent with the formation of a *cis*-tetracarbonyl complex (C_{2v}) (theory $2A_1 + B_1 + B_2$). The $^{13}C\{^1H\}$ NMR spectrum shows peaks corresponding to the ligand backbone and two carbonyl resonances in an approximate 1:1 ratio corresponding to CO *trans* CO and CO *trans* Sb and is again consistent with the formation of a *cis*-tetracarbonyl complex. The magnitude of the $^1J(^{183}W\text{-}^{13}C)$ coupling constant on the CO *trans* Sb provides a useful probe for the ligand electronic effects. Buchner and Schenk have reported such coupling constants for a wide range of related Group 15 tungsten carbonyl complexes.[20] The value of $^1J(^{183}W\text{-}^{13}C)$ on the carbonyl resonance CO *trans* Sb of 160 Hz is very similar to those observed in other tungsten stibine complexes, but comparison with other Group 15 ligands places the xylyl distibines low in the *trans* influence series (Table 3.3). This may be attributed to poor σ-donation by antimony.

The analogous Mo complex $[Mo(CO)_4\{1,2\text{-}C_6H_4(CH_2SbMe_2)_2\}]$ was prepared by reaction of 1,2-$C_6H_4(CH_2SbMe_2)_2$ with $[Mo(CO)_4(norbornadiene)]$ in CH_2Cl_2. The solution IR spectrum is very similar to that observed for the tungsten complex and is again consistent with a *cis*-tetracarbonyl complex. The ^{95}Mo NMR spectrum shows a relatively sharp peak at −1798 ppm which is comparable with that of the distibinomethane bridged dimer complex $[Mo_2(CO)_8\{Me_2SbCH_2SbMe_2\}_2]$ which shows a sharp resonance at −1830 ppm.[5]

	cis CO		*trans* CO	
Complex	δ	$^{1}J(^{183}W-^{13}C)$ Hz	δ	$^{1}J(^{183}W-^{13}C)$ Hz
[a][$W(CO)_5\{CN^-\}$][20]	197.6	124.3	200.2	139.0
[b][$W(CO)_5\{Ph_3P\}$][20]	197.2	125.7	199.0	140.0
[b][$W(CO)_5\{Me_3P\}$][20]	197.0	125.0	200.0	145.0
[c][$W(CO)_5\{C_5H_5N\}$][20]	199.2	131.6	202.7	150.0
[b][$W(CO)_5\{Ph_3As\}$][20]	196.7	125.7	199.0	155.0
[d][$W_2(CO)_{10}\{dpsm\}$][21]	196.5	123.0	198.2	156.0
[e][$W(CO)_4\{1,2\text{-}C_6H_4(CH_2SbMe_2)_2\}$]	201.7	126.0	206.1	160.0
[d][$W(CO)_5\{dpsm\}$][21]	196.7	126.0	199.0	162.0
[b][$W(CO)_5\{Ph_3Sb\}$][20]	196.1	124.3	198.2	162.0
[e][$W(CO)_5\{1,3\text{-}C_6H_4(CH_2SbMe_2)_2\}$]	197.0	128.0	199.7	163.0
[e][$\{W(CO)_5\}_2\{1,4\text{-}C_6H_4(CH_2SbMe_2)_2\}$]	197.0	128.0	199.7	164.0
[d][$W_2(CO)_{10}\{dmsm\}$][21]	197.1	127.0	199.0	164.0

[a] In $(CD_3)_2CO$, [b] In $CDCl_3$, [c] In C_6D_6, [d] In CH_2Cl_2/CD_2Cl_2, [e] In $CH_2Cl_2/CDCl_3$

(dmsm = $Me_2SbCH_2SbMe_2$, dpsm = $Ph_2SbCH_2SbPh_2$)

Table 3.3 – $^{13}C\{^{1}H\}$ NMR spectroscopy data of selected phosphine, arsine and stibine tungsten carbonyl complexes

Complex	ν(CO)/cm^{-1} (CH_2Cl_2)	$^{13}C\{^1H\}$ NMR[a] / ppm			
		δ (CH_3)	δ (CH_2)	δ (Ar-CH)	δ (CO)
[{$Fe(CO)_4$}$_2${1,4-$C_6H_4(CH_2SbMe_2)_2$}]	2040s, 1963m, 1931s	-1.5	25.0	129.0, 134.6	213.4
[{$Fe(CO)_4$}$_2${1,3-$C_6H_4(CH_2SbMe_2)_2$}]	2041s, 1964m, 1933s	-1.3	25.2	126.5, 128.0, 129.8, 137.5	213.3
[{$Fe(CO)_4$}$_2${1,2-$C_6H_4(CH_2SbMe_2)_2$}]	2041s, 1965m, 1932s	-1.1	23.5	127.6, 129.8, 134.0	213.3
[{$W(CO)_5$}$_2${1,4-$C_6H_4(CH_2SbMe_2)_2$}]	2068s, 1975vs, 1937vs	2.0	23.8	128.9, 134.4	197.0 $^1J(^{183}W\text{-}^{13}C)$ = 128 Hz 199.7 $^1J(^{183}W\text{-}^{13}C)$ = 164 Hz
[$W(CO)_5${1,3-$C_6H_4(CH_2SbMe_2)_2$}]	2069s, 1975vs, 1937vs	-1.6, 1.6	23.0, 24.2	126.0, 127.9, 129.8, 137.6, 138.6	197.0 $^1J(^{183}W\text{-}^{13}C)$ = 126 Hz 199.7 $^1J(^{183}W\text{-}^{13}C)$ = 163 Hz
[$W(CO)_4${1,2-$C_6H_4(CH_2SbMe_2)_2$}]	2012m, 1935sh, 1901vs, 1873sh	-1.1	24.6	123,4, 129.7, 140.0	201.7 $^1J(^{183}W\text{-}^{13}C)$ = 126 Hz 206.1 $^1J(^{183}W\text{-}^{13}C)$ = 160 Hz
[$Mo(CO)_4${1,2-$C_6H_4(CH_2SbMe_2)_2$}]		-0.2	24.4	126.3, 129.2, 137.0	210.9, 215.5
[$Ni(CO)_3${1,4-$C_6H_4(CH_2SbMe_2)_2$}]	2068s, 1993vs	-2.4, -0.8	23.6, 24.8	128.1, 128.3, 136.4, 138.3	197.1
[$Ni(CO)_3${1,3-$C_6H_4(CH_2SbMe_2)_2$}]	2068s, 1993bs	-2.1, -0.6	24.0, 25.2	124.9, 125.2, 126.3, 127.4, 128.9, 139.3, 139.6	197.0
[$Ni(CO)_2${1,2-$C_6H_4(CH_2SbMe_2)_2$}]	2002s, 1939s	-1.1	23.7	125.5, 129.5, 137.7	201.0

[a] In $CH_2Cl_2/CDCl_3$

Intensities: medium (m), strong (s), very strong (vs), strong and broad (bs), shoulder (sh).

Table 3.4 – IR and $^{13}C\{^1H\}$ NMR spectroscopy data

3.2.3 Nickel Carbonyl Complexes

CAUTION $Ni(CO)_4$ is extremely toxic and volatile; all reactions, including the preparation of spectroscopic samples, were carried out in a good fume cupboard. Syntheses were conducted using closed systems fitted with bromine-water scrubbers and all residues were destroyed using bromine. The nickel complexes were often obtained as oils, which even when stored under nitrogen, darkened within a few hours at room temperature, indicating decomposition. As a consequence conventional CH analyses could not be obtained. Instability of this type is not unusual for nickel carbonyl complexes. With the exception of $[Ni(CO)_2\{1,2\text{-}C_6H_4(CH_2SbMe_2)_2\}]$ attempts to obtain APCI mass spectra mostly gave low mass fragments, however the NMR and IR data obtained are able to unequivocally identify the complexes formed as described in subsequent sections.

Reaction of $Ni(CO)_4$ with $1,2\text{-}C_6H_4(CH_2SbMe_2)_2$ in a 2:1 ratio in CH_2Cl_2 at ambient temperature yields $[Ni(CO)_2\{1,2\text{-}C_6H_4(CH_2SbMe_2)_2\}]$ as an off-white solid. The reaction progress was monitored by recording solution IR spectra in the region 2200-1800 cm^{-1} at regular intervals. The T_2 mode of $Ni(CO)_4$ at 2043 cm^{-1} gradually reduced in intensity, to be replaced by two very strong bands at 2002 and 1939 cm^{-1}.The two ν(CO) bands are highly characteristic of a nickel dicarbonyl fragment (C_{2v} theory $A_1 + B_1$)[22], formed by chelation of the *ortho*-substituted ligand. The ^1H and $^{13}C\{^1H\}$ NMR spectra show single methyl and methylene resonances shifted to high frequency from the values of the free ligand and a single carbonyl resonance at δ 201.1 ppm consistent with the formulation $[Ni(CO)_2\{1,2\text{-}C_6H_4(CH_2SbMe_2)_2\}]$. The APCI mass spectrum showed a cluster of peaks at *m/z* 506 corresponding to $[^{58}Ni(CO)_2\{1,2\text{-}C_6H_4(CH_2{}^{121}SbMe_2)(CH_2{}^{121}SbMe)\}]+H$. The solution IR data can be compared with that of the related phosphine and arsine ligands $o\text{-}C_6H_4(PMe_2)_2$ and $o\text{-}C_6H_4(AsMe_2)_2$ (Table 3.4). The position of the A_1 ν(CO) stretch increases in frequency down Group 15 consistent with a decrease in σ-donor strength.

The reaction of $1,4\text{-}C_6H_4(CH_2SbMe_2)_2$ with $Ni(CO)_4$ was carried out as above using a 1 : 2.2 molar ratio of reagents to yield a colourless oil. The solution IR spectrum in CH_2Cl_2 shows two strong ν(CO) bands at 2068 and 1993 cm^{-1} indicative of a $Ni(CO)_3$ fragment (C_{3v} theory $A_1 + E$). However both the $^{13}C\{^1H\}$ and ^1H NMR spectra show two

methyl and two methylene resonances consistent with the formation of $[Ni(CO)_3\{\eta^1\text{-}1,4\text{-}C_6H_4(CH_2SbMe_2)_2\}]$ as the product rather than the expected ligand bridged dimer complex $[\{Ni(CO)_3\}_2\{\mu\text{-}1,4\text{-}C_6H_4(CH_2SbMe_2)_2\}]$. Attempts to achieve coordination at the second stibine group either by addition of excess $Ni(CO)_4$ or by prolonged reaction times failed. The NMR spectra remained unchanged but the solutions gradually darkened indicating decomposition. The failure to produce $[\{Ni(CO)_3\}_2\{\mu\text{-}1,4\text{-}C_6H_4(CH_2SbMe_2)_2\}]$ was unexpected since $[\{Ni(CO)_3\}_2\{Me_2SbCH_2SbMe_2\}]$ is readily produced under the same reaction conditions.[6] The methyl resonance corresponding to the uncoordinated stibine is slightly shifted to high frequency from that in the free ligand. This indicates that the second stibine may be deactivated as a result of inductive electronic effects.

The reaction of $1,3\text{-}C_6H_4(CH_2SbMe_2)_2$ with $Ni(CO)_4$ was conducted similarly to yield a colourless oil. The ^1H NMR spectrum shows two methyl resonances at δ 0.98 and 0.91 ppm and two methylene signals at δ 3.02 and 2.87 ppm each in a 1:1 ratio, indicative of the formation of $[Ni(CO)_3\{\eta^1\text{-}1,3\text{-}C_6H_4(CH_2SbMe_2)_2\}]$, as observed with $1,4\text{-}C_6H_4(CH_2SbMe_2)_2$. The $^{13}C\{^1H\}$ NMR spectrum is also consistent with the formation of the η^1-complex, but in addition shows a minor species with a methyl resonance at δ -0.3 ppm and a methylene resonance at δ 25.5 ppm. The $^{13}C\{^1H\}$ NMR spectrum also shows a large singlet at δ 197.0 ppm corresponding to a $Ni(CO)_3$ fragment with a second smaller carbonyl resonance at δ 201.1 ppm. This second carbonyl resonance clearly indicates that the second species present is a $Ni(CO)_2$ complex, formed either by chelation of the ligand to give $[Ni(CO)_2\{1,3\text{-}C_6H_4(CH_2SbMe_2)_2\}]$, as observed with the *ortho*-xylyl ligand or by the formation of the ligand bridged dimer complex $[\{Ni(CO)_2\{1,3\text{-}C_6H_4(CH_2SbMe_2)_2\}\}_2]$. This is confirmed by the solution IR spectrum (Figure 3.5) which shows two ν(CO) bands associated with the tricarbonyl complex at 2068s and 1993bs cm^{-1}, and a single ν(CO) stretch at 1938w cm^{-1}associated with the dicarbonyl complex, the second band of the dicarbonyl is most likely hidden below the broad band at 1993 cm^{-1}. Repeating the reaction in refluxing CH_2Cl_2 led to an increase in the ν(CO) band at 1938 cm^{-1} (Figure 3.6) but the reaction did not go to completion. Even

with addition of Me_3NO the reaction did not proceed further and extensive decomposition occurred with the production of much black solid.

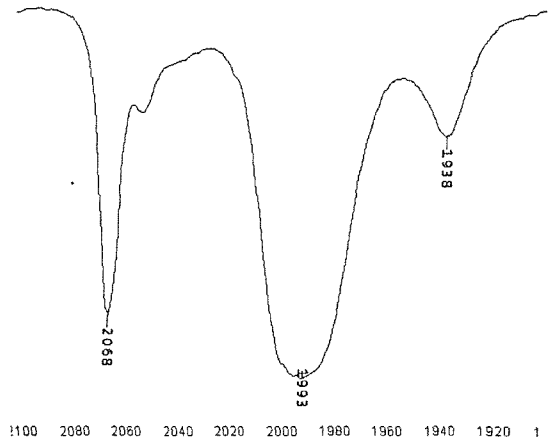

Figure 3.5 – IR spectrum of the $Ni(CO)_4$-1,3-$C_6H_4(CH_2SbMe_2)_2$ system (CH_2Cl_2)

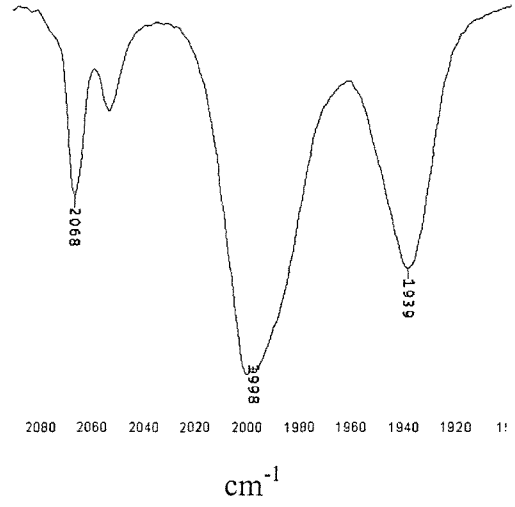

Figure 3.6 –IR spectrum of the $Ni(CO)_4$-1,3-$C_6H_4(CH_2SbMe_2)_2$ system after reflux (CH_2Cl_2)

Reaction of 1,3-$C_6H_4(SbMe_2)_2$ and 1,4-$C_6H_4(SbMe_2)_2$ with $[Ni(CO)_4]$ as above gives a mixture of products. The solution IR spectra in CH_2Cl_2 of both complexes show two ν(CO) bands at ca. 2070 and 2000 cm^{-1} associated with a $Ni(CO)_3$ fragment and an additional two ν(CO) bands at ca. 1996 and 1941 cm^{-1} indicating formation of a $Ni(CO)_2$ complex. The $^{13}C\{^1H\}$ NMR spectra (Figure 3.7) show four methyl resonances at ca.

δ 1.1, 0.5, -0.1 and –1.2 ppm and two carbonyl resonances at ca δ 197.0 and 201.0 ppm corrresponding to the tricarbonyl and dicarbonyl complexes respectively. From the relative intensities and shift patterns we have provisionally assigned the methyl resonances at –1.2 and 0.5 ppm to the free and coordinated $SbMe_2$ groups in $[Ni(CO)_3\{\eta^1\text{-}C_6H_4(SbMe_2)_2\}]$, the resonance at –0.1 ppm to the stibine groups in $[\{Ni(CO)_3\}_2\{C_6H_4(SbMe_2)_2\}]$ and the remaining methyl resonance at 1.1 ppm to the methyl groups in $[\{Ni(CO)_2\}_2\{C_6H_4(SbMe_2)_2\}_2]$.

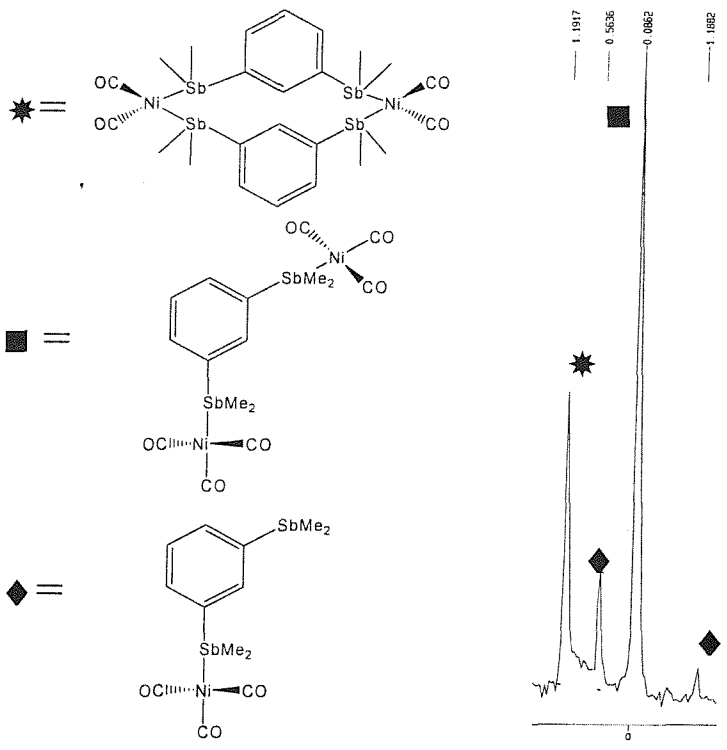

Figure 3.7 – Me region of the $^{13}C\{^1H\}$ NMR spectrum of $[\{Ni(CO)_3\}_2\{1,3\text{-}C_6H_4(SbMe_2)_2\}]$ in $CH_2Cl_2/CDCl_3$

The ^1H NMR spectra are also consistent with the formulations proposed above. The reactions were conducted in the presence of excess $Ni(CO)_4$ and the solution IR spectra prior to work-up show a strong ν(CO) stretch at 2043 cm^{-1} confirming the presence of remaining $Ni(CO)_4$ therefore the mixture of products does not arise as a result of insufficient $Ni(CO)_4$. It would appear therefore, that the phenylene ligands show no

preference for the type of complex formed. The dicarbonyl species formed with 1,4-$C_6H_4(SbMe_2)_2$ must be the ligand bridged dimer complex $[\{Ni(CO)_2\}_2\{1,4\text{-}C_6H_4(SbMe_2)_2\}_2]$, and although 1,3-$C_6H_4(SbMe_2)_2$ has the potential to chelate it is likely that it also forms a ligand bridged dimer complex to avoid ring strain.

3.3 Conclusions

The coordination studies described above have shown that the distibine ligands can exhibit a variety of coordination modes dependent on both the metal substrate used and also on the ligand architecture. These include monodentate, bridging bidentate and for 1,2-$C_6H_4(CH_2SbMe_2)_2$ and possibly for 1,3-$C_6H_4(CH_2SbMe_2)_2$ chelation is also possible.

Comparison of the carbonyl IR frequencies in related phosphine and arsine complexes (Table 3.5) show that the ν(CO) bands are slightly to higher frequency than those of the lighter Group 15 analogues, consistent with a decrease in σ-donation down Group 15. Comparison with available data on other distibine complexes has shown that the ligands have similar electronic properties to the distibinoalkane ligands and other trialkylstibines.

Complex	Solvent	ν(CO) / cm^{-1}
$[Ni(CO)_3\{Ph_2SbCH_2SbPh_2\}]$[6]	$CHCl_3$	2072, 2004
$[Ni_2(CO)_6\{Ph_2SbCH_2SbPh_2\}]$[6]	$CHCl_3$	2072, 1998
$[Ni_2(CO)_6\{Me_2SbCH_2SbMe_2\}]$[6]	$CHCl_3$	2067, 1994
$[Ni(CO)_3\{PPh_3\}_2]$[23]	$C_{16}H_{34}$	2070, 1997
$[Ni(CO)_3\{AsPh_3\}_2]$[23]	$C_{16}H_{34}$	2072, 1999
$[Ni(CO)_3\{SbPh_3\}_2]$[23]	$C_{16}H_{34}$	2074, 2004.5
$[Ni(CO)_2\{o\text{-}C_6H_4(PMe_2)_2\}]$[22]	CH_2ClCH_2Cl	1996, 1931
$[Ni(CO)_2\{o\text{-}C_6H_4(AsMe_2)_2\}]$[22]	CH_2ClCH_2Cl	1996, 1931
$[Ni(CO)_3\{m\text{-}C_6H_4(CH_2SbMe_2)_2\}]$	CH_2Cl_2	2068, 1993
$[Ni(CO)_3\{p\text{-}C_6H_4(CH_2SbMe_2)_2\}]$	CH_2Cl_2	2068, 1993
$[Ni(CO)_2\{o\text{-}C_6H_4(CH_2SbMe_2)_2\}]$	CH_2Cl_2	2002, 1939
$[\{Ni(CO)_3\}_2\{m\text{-}C_6H_4(SbMe_2)_2\}]$	CH_2Cl_2	2070, 2000
$[\{Ni(CO)_3\}_2\{p\text{-}C_6H_4(SbMe_2)_2\}]$	CH_2Cl_2	2070, 2000

Table 3.5 – IR spectroscopy data of selected phosphine, arsine and stibine nickel carbonyl complexes

3.4 Experimental

General Data. All preparations were conducted under a dry dinitrogen atmosphere. Tetrahydrofuran was distilled from sodium benzophenoneketyl before use. Other solvents were obtained commercially and used as supplied. $W(CO)_6$, $Fe_2(CO)_9$ and $Ni(CO)_4$ (Aldrich) were used as received. $[Mo(CO)_4(nbd)]$ and $[W(CO)_4(piperidine)_2]$ were made following the literature procedures.[24, 25] **Caution** $Ni(CO)_4$ is volatile and extremely toxic; all reactions (including the preparation of spectroscopic samples) were carried out in a good fume cupboard, and syntheses were conducted using closed systems fitted with bromine-water scrubbers. Residues were destroyed using bromine.

Synthesis of $[W(CO)_5\{1,3\text{-}C_6H_4(CH_2SbMe_2)_2\}]$: A solution of $1,3\text{-}C_6H_4(CH_2SbMe_2)_2$ (0.10 g, 0.24 mmol) in dry thf (10 mL) was added to a solution of $[W(CO)_5(thf)]$ generated *in situ* by the photolysis of $[W(CO)_6]$ (0.22 g, 0.62 mmol) in dry thf (50 mL). The reaction was stirred at RT for 2 h. The reaction mixture was filtered and the solvent removed *in vacuo* to give a brown residue. Trituration with ice-cold pentane gave a brown gum. Yield 0.078 g (44 %). Required for $[C_{17}H_{20}O_5Sb_2W].1/2C_5H_{12}$ C = 30.46, H = 3.38 %; found C = 30.92, H = 3.28 %. ^{1}H NMR ($CDCl_3$): δ 1.21 (s, 6H, C$\underline{H}_3$), 1.27 (s, 6H, C$\underline{H}_3$), 3.20 (s, 2H, C$\underline{H}_2$), 3.21 (s, 2H, C$\underline{H}_2$), 6.80-7.20 (m, 4H, Ar-C$\underline{H}$). APCI mass spectrum (MeCN): found *m/z* 704, 676. Calc. for $[^{184}W(CO)_4\{1,3\text{-}C_6H_4(CH_2{}^{121}SbMe_2)_2\}]$ = 702, $[^{184}W(CO)_3\{1,3\text{-}C_6H_4(CH_2{}^{121}SbMe_2)_2\}]$ = 674.

Synthesis of $[\{W(CO)_5\}_2\{1,4\text{-}C_6H_4(CH_2SbMe_2)_2\}]$: The reaction was carried out as above using $1,4\text{-}C_6H_4(CH_2SbMe_2)_2$ (0.10 g, 0.24 mmol) and $[W(CO)_6]$ (0.22 g, 0.62 mmol). The product was isolated as a brown solid. Yield 0.20 g (77 %). Required for $[C_{22}H_{20}O_{10}Sb_2W_2]$ C = 25.03, H = 1.91 %; found C = 25.49, H = 2.02 %.^{1}H NMR ($CDCl_3$): δ 1.19 (s, 12H, C$\underline{H}_3$), 3.22 (s, 4H, C$\underline{H}_2$), 7.05 (s, 4H, Ar-C$\underline{H}$). APCI mass spectrum (MeCN): found *m/z* 1055, 1028. Calc. for $[\{^{184}W(CO)_5\}_2\{1,4\text{-}C_6H_4(CH_2{}^{121}SbMe_2)_2\}]$ = 1054, $[^{184}W_2(CO)_9\{1,4\text{-}C_6H_4(CH_2{}^{121}SbMe_2)_2\}]$ = 1026.

Synthesis of $[W(CO)_4\{1,2\text{-}C_6H_4(CH_2SbMe_2)_2\}]$: To a solution of $[W(CO)_4(piperidine)_2]$ (0.11 g, 0.24 mmol) in EtOH was added a solution of $1,2\text{-}C_6H_4(CH_2SbMe_2)_2$ (0.10 g, 0.24 mmol) in EtOH (10 mL). Reaction was heated to reflux under N_2 for 2 h. The solvent was removed *in vacuo* and the resulting yellow residue triturated with ice-cold pentane to give a fawn coloured solid. Yield 75 mg (43 %). Required for $[C_{16}H_{20}O_4Sb_2W].1/2C_5H_{12}$: C = 30.00, H = 3.51 %; found C = 29.32, H = 3.54 %. ^{1}H NMR ($CDCl_3$): δ 1.31 (s, 12H, C<u>H</u>$_3$), 3.34 (s, 4H, C<u>H</u>$_2$), 7.00-7.28 (m, 4H, Ar-C<u>H</u>). APCI mass spectrum (MeCN): found *m/z* 704. Calc. for $[^{184}W(CO)_4\{1,2\text{-}C_6H_4(CH_2{}^{121}SbMe_2)_2\}] = 702$.

Synthesis of $[\{Fe(CO)_4\}_2\{1,3\text{-}C_6H_4(CH_2SbMe_2)_2\}]$: To a solution of $[Fe_2(CO)_9]$ (0.18 g, 0.49 mmol) in dry thf (30 mL) was added a solution of $1,3\text{-}C_6H_4(CH_2SbMe_2)_2$ (0.10 g, 0.24 mmol) in dry thf (10 mL). The reaction was stirred under N_2 for 15 h. The solvent was removed *in vacuo* and the resulting orange residue was taken up in CH_2Cl_2 (5 mL), and the solution filtered. The solvent was removed *in vacuo* and the residue triturated with ice-cold pentane to give the product as an orange/brown solid. Yield 88 mg (48 %). Required for $[C_{20}H_{20}O_8Fe_2Sb_2].1/2CH_2Cl_2$: C = 31.26, H = 2.73 %; found C = 30.97, H = 2.73 %. ^{1}H NMR ($CDCl_3$): δ 1.23 (s, 12H, C<u>H</u>$_3$), 3.30 (s, 4H, C<u>H</u>$_2$), 6.90-7.28 (m, 4H, Ar-C<u>H</u>). IR spectrum (ν(CO)/cm^{-1}, Nujol mull): 2033s, 1964m, 1935s. APCI mass spectrum (MeCN): found *m/z* 745, 577. Calc. for $[\{^{56}Fe(CO)_4\}_2\{1,3\text{-}C_6H_4(CH_2{}^{121}SbMe_2)_2\}]+H = 743$, $[^{56}Fe(CO)_4\{1,3\text{-}C_6H_4(CH_2{}^{121}SbMe_2)_2\}]+H = 575$.

Synthesis of $[\{Fe(CO)_4\}_2\{1,4\text{-}C_6H_4(CH_2SbMe_2)_2\}]$: The reaction was carried out as above using $1,4\text{-}C_6H_4(CH_2SbMe_2)_2$ (0.10 g, 0.24 mmol) and $[Fe_2(CO)_9]$ (0.18 g, 0.49 mmol) to give an orange/brown solid. Yield 54 mg (30 %). Required for $[C_{20}H_{20}O_8Fe_2Sb_2]$: C = 32.31, H = 2.70; found C = 32.19, H =2.99 %. ^{1}H NMR ($CDCl_3$): δ 1.19 (s, 12H, C<u>H</u>$_3$), 3.30 (s, 4H, C<u>H</u>$_2$), 7.09 (s, 4H, Ar-C<u>H</u>). IR spectrum (ν(CO)/cm^{-1}, Nujol mull): 2043s, 1959sh, 1938s. APCI mass spectrum (MeCN): found *m/z* 745, 577. Calc. for $[\{^{56}Fe(CO)_4\}_2\{1,4\text{-}C_6H_4(CH_2{}^{121}SbMe_2)_2\}]+H = 743$, $[^{56}Fe(CO)_4\{1,4\text{-}C_6H_4(CH_2{}^{121}SbMe_2)_2\}]+H = 575$.

Synthesis of [{Fe(CO)$_4$}$_2${1,2-C$_6$H$_4$(CH$_2$SbMe$_2$)$_2$}]: The reaction was carried out as above using 1,2-C$_6$H$_4$(CH$_2$SbMe$_2$)$_2$ (0.10 g, 0.24 mmol) and [Fe$_2$(CO)$_9$] (0.18g, 0.49 mmol) to give an orange oil. Yield 74 mg (40 %). ^{1}H NMR (CDCl$_3$): δ 1.20 (s, 12H, C<u>H</u>$_3$), 3.29 (s, 4H, C<u>H</u>$_2$), 7.15-7.20 (m, 4H, Ar-C<u>H</u>). IR spectrum (ν(CO)/cm^{-1}, thin film): 2038s, 1917s. APCI mass spectrum (MeCN): found *m/z* 744, 577. Calc. for [{^{56}Fe(CO)$_4$}$_2${1,4-C$_6$H$_4$(CH$_2$^{121}SbMe$_2$)$_2$}] = 742, [^{56}Fe (CO)$_4${1,2-C$_6$H$_4$(CH$_2$^{121}SbMe$_2$)$_2$}]+H = 575.

Synthesis of [{Fe(CO)$_4$}$_2${1,3-C$_6$H$_4$(SbMe$_2$)$_2$}]: The reaction was carried out as above using 1,3-C$_6$H$_4$(SbMe$_2$)$_2$ (0.10 g, 0.26 mmol) and [Fe$_2$(CO)$_9$] (0.19 g, 0.52 mmol), to give a yellow oil. Yield 62 mg (33 %). ^{1}H NMR (CDCl$_3$): δ 1.57 (s, 12H, C<u>H</u>$_3$), 7.31-7.72 (m, 4H, Ar-C<u>H</u>). ^{13}C{^{1}H} NMR (CH$_2$Cl$_2$/CDCl$_3$): δ 0.8 (<u>C</u>H$_3$), 130.5, 135.7, 138.9 (Ar-<u>C</u>H), 140.0 (*i*-<u>C</u>), 213.3 (<u>C</u>O). IR spectrum (ν(CO)/cm^{-1}, CH$_2$Cl$_2$): 2043s, 1966m, 1932s. IR spectrum (ν(CO)/cm^{-1}, thin film): 2041s, 1917vs. APCI mass spectrum (MeCN): found *m/z* 716, 548. Calc. for [{^{56}Fe(CO)$_4$}$_2${1,3-C$_6$H$_4$(^{121}SbMe$_2$)$_2$}] 714, [^{56}Fe(CO)$_4${1,3-C$_6$H$_4$(^{121}SbMe$_2$)$_2$}] 546.

Synthesis of [Fe(CO)$_4${η^1-1,4-C$_6$H$_4$(SbMe$_2$)$_2$}]: The reaction was carried out as above using 1,4-C$_6$H$_4$(SbMe$_2$) (0.10 g, 0.26 mmol) and [Fe$_2$(CO)$_9$] (0.19 g, 0.52 mmol) to give a yellow oil. Yield 73 mg (51 %). ^{1}H NMR (CDCl$_3$): δ 0.98 (s, 6H, C<u>H</u>$_3$), 1.52 (s, 6H, C<u>H</u>$_3$), 7.52-7.65 (m, 4H, Ar-C<u>H</u>). ^{13}C{^{1}H} NMR (CH$_2$Cl$_2$/CDCl$_3$): δ -1.4 (<u>C</u>H$_3$), 0.9 (<u>C</u>H$_3$), 133.3, 135.0 (Ar-<u>C</u>H), 135.9, 137.8 (*i*-<u>C</u>H), 213.3 (<u>C</u>O). IR spectrum (ν(CO)/cm^{-1}, CH$_2$Cl$_2$): 2043s, 1966 m, 1933s. IR spectrum (ν(CO)/cm^{-1}, thin film): 2040s, 1963sh, 1927vs. APCI mass spectrum (MeCN): found *m/z* 548, 397. Calc. for [^{56}Fe(CO)$_4${1,4-C$_6$H$_4$(^{121}SbMe$_2$)$_2$}] 546, [^{56}Fe(CO)$_4${PhSbMe$_2$}]+H 397.

Synthesis of [Ni(CO)$_3${1,3-C$_6$H$_4$(CH$_2$SbMe$_2$)$_2$}]: Ni(CO)$_4$ (0.10 g, 0.59 mmol) was injected into a solution of 1,3-C$_6$H$_4$(CH$_2$SbMe$_2$)$_2$ (0.10 g, 0.25 mmol) in CH$_2$Cl$_2$ (30 mL). The reaction was stirred at RT under N$_2$ for 3 h. The solvent was removed *in vacuo* to yield a brown oil. ^{1}H NMR (CDCl$_3$): δ 0.80 (s, 6H, C<u>H</u>$_3$), 0.98 (s, 6H, C<u>H</u>$_3$), 2.87 (s,

2H, C$\underline{H}_2$), 3.01 (s, 2H, C$\underline{H}_2$), 6.73-7.20 (m, 4H, Ar-C$\underline{H}$). IR spectrum (ν(CO)/cm^{-1}, thin film): 2067s 1987 vs.

Synthesis of [Ni(CO)$_3${1,4-C$_6$H$_4$(CH$_2$SbMe$_2$)$_2$}]: The reaction was carried out as above using 1,4-C$_6$H$_4$(CH$_2$SbMe$_2$)$_2$ (0.10 g, 0,25 mmol) and Ni(CO)$_4$ (0.10 g, 0.59 mmol). The product was isolated as a colourless oil. ^{1}H NMR (CDCl$_3$): δ 0.79 (s, 6H, C$\underline{H}_3$), 0.96 (s, 6H, C$\underline{H}_3$), 2.89 (s, 2H, C$\underline{H}_2$), 3.03 (s, 2H, C$\underline{H}_2$), 6.92 – 7.11 (m, 4H, Ar-C$\underline{H}$). IR spectrum (ν(CO)/cm^{-1}, thin film): 2067s, 1986vs.

Synthesis of [Ni(CO)$_2${1,2-C$_6$H$_4$(CH$_2$SbMe$_2$)$_2$}]: The reaction was carried out as above using 1,2-C$_6$H$_4$(CH$_2$SbMe$_2$)$_2$ (0.10 g, 0.25 mmol) and Ni(CO)$_4$ (0.10 g, 0.59 mmol). The product was isolated as a colourless oil. ^{1}H NMR (CDCl$_3$): δ 1.09 (s, 12H, C$\underline{H}_3$), 3.14 (s, 4H, C$\underline{H}_2$),, 6.96-7.02 (m, 4H, Ar-C$\underline{H}$). IR spectrum (ν(CO)/cm^{-1}, thin film): 1997s, 1922s. APCI mass spectrum (MeCN): found *m/z* 508, 451. Calc. for [^{58}Ni(CO)$_2${1,2-C$_6$H$_4$(CH$_2$^{121}SbMe$_2$)$_2$}]+H = 506, [^{58}Ni{1,2-C$_6$H$_4$(CH$_2$^{121}SbMe$_2$)(CH$_2$^{121}SbMe)}] = 449.

Synthesis of [{Ni(CO)$_3$}$_2${1,3-C$_6$H$_4$(SbMe$_2$)$_2$}]: The reaction was carried out as above using 1,3-C$_6$H$_4$(SbMe$_2$)$_2$ (0.18 g, 0.47 mmol) and Ni(CO)$_4$ (0.18 g, 1.03 mmol). The product was isolated as a brown oil. ^{1}H NMR (CDCl$_3$) (see text): δ 1.10 (s, C$\underline{H}_3$ of η^1-complex), 1.19 (s, C$\underline{H}_3$ of dicarbonyl complex), 1.28 (s, C$\underline{H}_3$ of η^1-complex), 1.31 (s, C$\underline{H}_3$ of tricarbonyl complex), 7.22-7.66 (m, Ar-C$\underline{H}$). ^{13}C{^{1}H} NMR (CH$_2$Cl$_2$/CDCl$_3$) (see text): δ -1.2 (C$\underline{H}_3$ of η^1-complex), -0.1 (C$\underline{H}_3$ of dicarbonyl complex), 0.6 (C$\underline{H}_3$ of η^1-complex), 1.19 (C$\underline{H}_3$ of tricarbonyl complex), 126.5, 126.7, 127.6, 127.9, 129.5, 129.7, 133.1, 133.5, 133.9, 134.2, 134.7, 134.9, 135.2, 136.3, 136.6, 137.1, 139.6, 139.8, 140.1 (Ar-C$\underline{H}$). IR spectrum (ν(CO)/cm^{-1}, CH$_2$Cl$_2$): 2070s, 2000vs, 1995vs, 1941m. IR spectrum (ν(CO)/cm^{-1}, thin film): 2070vs, 2007vs, 1985vs, 1943s.

Synthesis of [{Ni(CO)$_3$}$_2${1,4-C$_6$H$_4$(SbMe$_2$)$_2$}]: The reaction was carried out as above using 1,4-C$_6$H$_4$(SbMe$_2$)$_2$ (70 mg, 0.18 mmol) and Ni(CO)$_4$ (70 mg, 0.40 mmol). The product was isolated as a brown oil. ^{1}H NMR (CDCl$_3$) (see text): δ 1.00 (s, C$\underline{H}_3$ of

η^1-complex), 1.16 (s, C$\underline{H}_3$ of dicarbonyl complex), 1.21 (s, C$\underline{H}_3$ of η^1-complex), 1.27 (s, C$\underline{H}_3$ of tricarbonyl complex, 6.98-7.67 (m, Ar-C$\underline{H}$). $^{13}C\{^1H\}$ NMR ($CH_2Cl_2/CDCl_3$) (see text): δ -1.2 (C$\underline{H}_3$ of η^1-complex), -0.2 (C$\underline{H}_3$ of dicarbonyl complex), 0.5 (C$\underline{H}_3$ of η^1-complex), 1.1 (C$\underline{H}_3$ of tricarbonyl complex, 128.9, 129.2, 129.8, 133.6, 134.4, 134.6, 135.1, 135.2, 135.5 (Ar-C$\underline{H}$). IR spectrum (ν(CO)/cm^{-1}, CH_2Cl_2): 2070s, 2000vs, 1996vs, 1941m. IR spectrum (ν(CO)/cm^{-1}, thin film): 2069m, 1999vs, 1940s.

Synthesis of [Mo(CO)$_4${1,2-C$_6$H$_4$(CH$_2$SbMe$_2$)$_2$}]: To a solution on [Mo(CO)$_4$(nbd)] (0.10 g, 0.12 mmol) in CH_2Cl_2 (30 mL) was added a solution of 1,2-$C_6H_4(CH_2SbMe_2)_2$ (0.14 g, 0.12 mmol) in CH_2Cl_2 (5 mL). The reaction was stirred for 2 h under N_2 until solution IR studies showed the absence of bands associated with the starting material. The solvent volume was reduced *in vacuo* to ca. 5 mL and degassed hexane added to give a pale brown precipitate. The product was isolated by filtration and dried *in vacuo*. Yield 70 mg (33 %). Required for [$C_{16}H_{20}MoO_4Sb_2$]: C = 31.20, H = 3.30 %; found C = 31.60, H = 3.30 %. ^1H NMR ($CDCl_3$): δ 1.21 (s, 12H, C$\underline{H}_3$), 3.22 (s, 4H, C$\underline{H}_2$), 6.99 (m, 2H, Ar-C$\underline{H}$), 7.05 (m, 2H, C$\underline{H}$). ^{95}Mo NMR (CH_2Cl_2 / $CDCl_3$): δ -1798. IR spectrum (ν(CO)/cm^{-1}, CsI disc): 2017s, 1935bs, 1901s, 1867s.

3.5 References

1. N. R. Champness and W. Levason, *Coord. Chem. Rev.*, **133**, (1994), 115.
2. E. Shewchuk and S. B. Wild, *J. Organomet. Chem.*, **71**, (1974), C1.
3. E. Shewchuk and S. B. Wild, *J. Organomet. Chem.*, **128**, (1977), 115.
4. T. Fukumoto, Y. Matsumura and R. Okawara, *Inorg. Nucl. Chem. Let.*, **9**, (1973), 711.
5. A. M. Hill, N. J. Holmes, A. R. J. Genge, W. Levason, M. Webster and S. Rutschow, *J. Chem. Soc., Dalton Trans.*, (1998), 825.
6. A. M. Hill, W. Levason, M. Webster and I. Albers, *Organometallics*, **16**, (1997), 5641.
7. A. R. J. Genge, N. J. Holmes, W. Levason and M. Webster, *Polyhedron*, **18**, (1999), 2673.
8. T. Fukumoto, Y. Matsumura and R. Okawara, *J. Organomet. Chem.*, **37**, (1972), 113.
9. J. Chatt, G. J. Leigh and N. Thankarajan, *J. Organomet. Chem.*, **29**, (1971), 105.
10. M. O. Albers and N. J. Colville, *J. Organomet. Chem.*, **233**, (1982), 261.
11. T. Fukumoto, Y. Matsumura and R. Okawara, *J. Organomet. Chem.*, **69**, (1974), 437.
12. P. E. Garrou and G. E. Hartwell, *J. Organomet. Chem.*, **69**, (1974), 445.
13. F. A. Cotton and J. M. Troup, *J. Am. Chem. Soc.*, **96**, (1974), 3438.
14. L. R. Martin, F. W. B. Einstein and R. K. Pomeroy, *Inorg. Chem.*, **24**, (1985), 2777.
15. A. F. Clifford and A. K. Mukherjee, *Inorg. Chem.*, **2**, (1963), 151.
16. W. Levason and C. A. McAuliffe, 'Phosphine, Arsine and Stibine Complexes of the Transition Elements', Elsevier, New York, (1979).
17. P. A. Wegner, L. F. Evans and J. Haddock, *Inorg. Chem.*, **14**, (1975), 192.
18. N. J. Holmes, W. Levason and M. Webster, *J. Chem. Soc., Dalton Trans.*, (1997), 4223.
19. G. Becker, O. Mundt, M. Sachs, H. J. Breunig, E. Lork, J. Probst and A. Silvestru, *Z. Anorg. Allg. Chem.*, **627**, (2001), 699.
20. W. Buchner and W. A. Schenk, *Inorg. Chem.*, **23**, (1984), 132.
21. A. M. Hill, Ph.D. Thesis, University of Southampton, Southampton, (1997).
22. J. Chatt and F. A. Hart, *J. Chem. Soc.*, (1960), 1378.
23. L. S. Meriwether and M. L. Fiene, *J. Am. Chem. Soc.*, **81**, (1959), 4200.

24. J. J. Eisch and R. B. King, *Organomet. Synth.*, **1**, (1965), 123.

25. G. R. Dobson and G. C. Faber, *Inorg. Chim. Acta*, **4**, (1969), 87.

Chapter 4

Transition Metal Complexes of Distibine Ligands

4.1 Introduction

4.1.1 Cu(I) and Ag(I) complexes of distibine ligands

A number of Cu(I) and Ag(I) complexes with distibine ligands have been reported in the literature.[1-3] $[CuL_2][Y]$ (L = *o*-$C_6H_4(SbMe_2)_2$, $Me_2Sb(CH_2)_3SbMe_2$ or $Ph_2Sb(CH_2)_3SbPh_2$, Y = BF_4 or PF_6) have been prepared by reaction of $[Cu(MeCN)_4][Y]$ with the ligand in either MeCN or CH_2Cl_2.[2, 3] The alkyl substituted ligand complexes decompose slowly in air but complexes with $Ph_2Sb(CH_2)_3SbPh_2$ are air stable. ^{63}Cu NMR spectra have been obtained on all complexes suggesting that these complexes have close to tetrahedral symmetry and do not undergo ligand dissociation.

Reaction of $Me_2SbCH_2SbMe_2$ or $Ph_2SbCH_2SbPh_2$ with $[Cu(MeCN)_4][Y]$ (Y = BF_4 or PF_6) in CH_2Cl_2 gave $[CuL_2][Y]$ as white solids.[4] The analogous silver complexes were prepared similarly from $AgBF_4$ or $AgPF_6$ in CH_2Cl_2 and the gold analogues $[AuL_2][PF_6]$ have been prepared from [AuCl(tht)] (tht = tetrahydrothiophene), ligand and $TlPF_6$ in CH_2Cl_2.[4] $[Ag(Me_2SbCH_2SbMe_2)_2][BF_4]$ exhibits a weak $\delta(^{109}Ag)$ at 521 ppm indicative of silver coordinated to two Sb donor atoms. Neither copper complex showed ^{63}Cu resonances unless in the presence of excess ligand, suggesting the formation of $[Cu(\eta^1\text{-}L)_4]^+$ in the presence of excess ligand, and in its absence they most probably exists as a mixture of lower coordination number complexes.[4] Due to the strain in a four-membered chelate ring it is unlikely that any of the complexes contain chelated distibinomethane ligands and are instead more likely to be polymeric.

The Ag(I) complexes $[AgL_2][BF_4]$ (L = $Me_2Sb(CH_2)_3SbMe_2$ or $Ph_2Sb(CH_2)_3SbPh_2$) have been prepared by reaction of the ligand with anhydrous $AgBF_4$ in acetone or CH_2Cl_2.[1] The complexes are light sensitive, darkening slowly in the solid state and more quickly in solution when exposed to light.[1] The presence of $[Ag_2(Me_2Sb(CH_2)_3SbMe_2)_2BF_4]^+$ ions in the mass spectrum has led to suggestions that the distibinopropane complexes may be polymeric.[1]

4.1.2 Pt(II) and Pd(II) complexes with distibine ligands

Reaction of $Me_2SbCH_2SbMe_2$ with $[MCl_4]^{2-}$ in ethanol or $[MCl_2(MeCN)_2]$ (M = Pt ot Pd) gives the dimeric complexes $[M_2X_4(Me_2SbCH_2SbMe_2)_2]$[4] which were too insoluble in all solvents tried for spectroscopic studies. Monomeric $[MX_2(Ph_2SbCH_2SbPh_2)_2]$ and dimeric $[M_2X_4(Ph_2SbCH_2SbPh_2)_2]$ complexes are known (M = Pt or Pd, X = Cl, Br or I).[4, 5] Crystal structures show that $[Pt_2Cl_4(Ph_2SbCH_2SbPh_2)_2]$ and $[M_2Br_4(Ph_2SbCH_2SbPh_2)_2]$ (M = Pt or Pd) adopt the unusual structural type *cis,trans*-$[X_2M(\mu\text{-}Ph_2SbCH_2SbPh_2)_2MX_2]$ (Figure 4.1), where the two metal centres have identical donor groups but one has a *cis*- and the other a *trans*-geometry.[4] These are unprecedented in the chemistry of other C_1 backboned ligands.

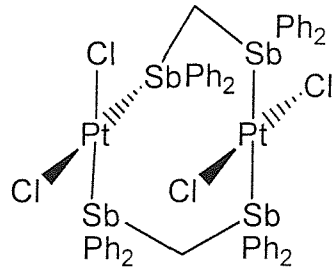

Figure 4.1 – Structure of $[Pt_2Cl_4(Ph_2SbCH_2SbPh_2)_2]$

The $[PdCl_2(Ph_2SbCH_2SbPh_2)_2]$ complex decomposes photochemically in solution with Ph-Sb cleavage to give *trans,trans*-$[Pd_2Cl_2Ph_2(Ph_2SbCH_2SbPh_2)_2]$ (Figure 4.2).[6]

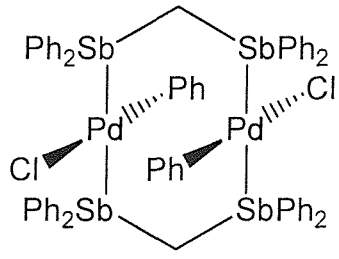

Figure 4.2 – Structure of *trans,trans*-$[Pd_2Cl_2Ph_2(Ph_2SbCH_2SbPh_2)_2]$

The corresponding bromo and iodo systems are less prone to Sb-C cleavage, although σ-Ph group fingerprints were observed as minor features in the NMR spectra of the crude products.[6]

A series of diaryl complexes $[Pt(Ph_2SbCH_2SbPh_2)(C_6H_4R)_2]$ (R = Me, CHMe, CMe_3, Br, F or CF_3) have been prepared from $[Pt(COD)(C_6H_4R)_2]$ and the ligand,[7] however it is unknown whether the complexes are monomeric with chelating distibines or dimeric with bridging ligands.

The ligands $Ph_2Sb(CH_2)_3SbPh_2$ and $Me_2Sb(CH_2)_3SbMe_2$ form planar $[MLX_2]$ complexes (M = Pd or Pt, X = Cl, Br, I or NCS) with the stibines acting as chelating ligands, even in the presence of excess ligand. The thiocyanate complexes have been shown to have S-bonded ligands.[8-10]

The *o*-$C_6H_4(SbPh_2)_2$ ligand reacts with Pt(II) and Pd(II) halides to give $[MLX_2]$,[11, 12] however reaction with Pd(II) nitrate or reaction of $[PdLX_2]$ with excess ligand in the presence of silver nitrate yields the bis ligand complex $[PdL_2][NO_3]_2$.[12]

The *o*-$C_6H_4(SbMe_2)_2$ also forms 1:1 complexes of the type $[MLX_2]$ (M = Pd or Pt, X = Cl, Br, I or SCN) with $[MCl_4]$[2,13, 14] whereas the analogous phosphine and arsine ligands *o*-$C_6H_4(EMe_2)_2$ (E = P or As) usually form 2:1 complexes in these reactions.

Platinum(IV) complexes $[PtLX_4]$ (L = *o*-$C_6H_4(SbPh_2)_2$, $Me_2Sb(CH_2)_3SbMe_2$ or $Ph_2Sb(CH_2)_3SbPh_2$, X = Cl or Br) have also been prepared by the addition of the appropriate halogen (X_2) to suspensions of the corresponding Pt(II) complexes in CCl_4.[11]

4.1.3 Ni(II) complexes with distibine ligands

The *o*-$C_6H_4(SbMe_2)_2$ reacts with nickel halides to give diamagnetic square pyramidal $[NiL_2X]X$ (X = Cl, Br or I),[10, 13, 14] the geometries have been determined by the interpretation of the electronic spectra and comparison with related phosphine and arsine complexes.

Reaction of $Me_2Sb(CH_2)_3SbMe_2$ with $Ni(ClO_4)_2$ and NiX_2 in butanol gives purple square pyramidal $[NiL_2X][ClO_4]$ (X = Cl, Br or I).[8] The direct reaction of $Ni(ClO)_4.6H_2O$ with $Me_2Sb(CH_2)_3SbMe_2$ does not give the expected square planar complex $[NiL_2]^{2+}$ but instead yields the purple five-coordinate complex $[NiL_2(H_2O)][ClO_4]_2$.[8] The analogous Ni(II) complexes with phenyl-substituted ligands have not been reported, however Ni(II)

complexes of both $Ph_2SbCH_2SbPh_2$ and $Ph_2Sb(CH_2)_3SbPh_2$ are known with $[(\eta^1\text{-Cp})Ni]^+$ moieties.[15] $Ph_2Sb(CH_2)_3SbPh_2$ chelates to give $[(\eta^5\text{-Cp})NiL]^+$ but $[(\eta^5\text{-Cp})NiLI]$ or $[(\eta^5\text{-Cp})NiL_2]^+$ are obtained with the distibinomethane ligand.[15]

4.1.3 Co(III) and Rh(III) complexes with distibine ligands

No Co(II) complexes with distibines have been reported, but the Co(III) complexes *trans*-$[Co\{o\text{-}C_6H_4(SbMe_2)_2\}_2X_2]X$ (X = Cl, Br or I) have been synthesised by the air-oxidation of a mixture of CoX_2 and ligand in n-propanol containing HX.[16] *trans*-$[Co\{Me_2Sb(CH_2)_3SbMe_2\}_2X_2]X$ (X = Br or I) have also been prepared but the chloro analogue could not be isolated.[16] *Trans*-$[Co\{o\text{-}C_6H_4(SbMe_2)_2\}_2Cl_2]_2[CoCl_4]$ has been structurally characterised and the structure shows the Co centre bound to two chelating ligands in an octahedral geometry with the two Cl atoms occupying the axial positions.[16]

The Rh(III) distibine complexes $[Rh\{o\text{-}C_6H_4(SbMe_2)_2\}_2X_2][BF_4]$ (X = Cl, Br or I) and $[Rh\{Ph_2Sb(CH_2)_3SbPh_2\}_2X_2]X$ (X = Cl, Br or I) can be prepared by reaction of the ligand with the appropriate rhodium(III) halide in ethanol [9, 17] and NMR studies have shown that all six complexes are the *trans*-isomers. Attempts to convert the complexes to the *cis*-isomers by sequential reaction with Li_2CO_3 and HX fail.[17] Addition of 70 % perchloric acid to $[Rh\{Ph_2Sb(CH_2)_3SbPh_2\}_2Cl_2]Cl$ yields the perchlorate complex which has been structually characterised.[17] The structure shows the *trans*-octahedral Rh geometry with the six-membered chelate ring in an 'unsymmetrical boat-configuration'. One tridentate stibine complex has also been described *fac*-$[Rh\{Me(CCH_2SbPh_2)_3\}Cl_3]$.[18]

4.1.4 Ru(II) and Ru(III) complexes with distibine ligands

Ruthenium(II) complexes of $Ph_2Sb(CH_2)_3SbPh_2$ have been prepared by the reaction of $[Ru(dmf)_6][CF_3SO_3]_2$ with the ligand in the presence of the appropriate lithium halide to give $[RuX_2L_2]$ (X = Cl, Br or I).[19] The complexes were identified as *trans*-isomers by diffuse reflectance UV/VIS spectrometry and $[RuBr_2L_2].2CH_2Cl_2$ has been structurally characterised.[19] Stirring the *trans*-$[RuX_2L_2]$ complexes in 40 % HBF_4 with concentrated HNO_3 oxidises the complexes to the Ru(III) species *trans*-$[RuX_2L_2][BF_4]$.[19]

Reaction of $Ph_2SbCH_2SbPh_2$ with $[Ru(dmf)_6][CF_3SO_3]_2$ under the reaction conditions outlined above yields $[RuX_2\{Ph_2SbCH_2SbPh_2\}_4]$ (X = Cl or Br).[4] The ^1H and $^{13}C\{^1H\}$ NMR spectra are consistent with equivalent η^1-ligands and the expected *trans*-geometry. In contrast reaction of $[Ru(dmf)_6][CF_3SO_3]_2$ and an excess of LiI with four equivalents of $Ph_2SbCH_2SbPh_2$ gives $[RuI_2\{Ph_2SbCH_2SbPh_2\}_3]$.[4] The crystal structure shows a distorted six-coordinate Ru centre with *trans*-iodines, two monodentate ligands and one chelating ligand to give *trans*-$[RuX_2\{\eta^1\text{-}Ph_2SbCH_2SbPh_2\}_2\{\eta^2\text{-}Ph_2SbCH_2SbPh_2\}]$.[4]

Reaction of *trans*-$[OsCl_2(dmso)_4]$ with four equivalents of $Ph_2SbCH_2SbPh_2$ gave *trans*-$[OsCl_2\{Ph_2SbCH_2SbPh_2\}_4]$[4] whilst reaction with *trans*-$[OsBr_2\{dmso\}_4]$ gives $[OsBr_2\{Ph_2SbCH_2SbPh_2\}_3]$.[4] No osmium iodo complex has been prepared.

4.1.5 Aims

The coordination chemistry of distibine ligands has been limited, and in general restricted to soft metals in low oxidation states such as low valent metal carbonyls which tend to give more stable complexes than those with transition metal halides. There are very few examples of distibine complexes with late 3d transition metals.[20]

The coordination chemistry of the distibinopropanes $R_2Sb(CH_2)_3SbR_2$ (R = Me or Ph) with a variety of metal halides has been investigated but spectroscopic data on the complexes are limited. In most cases the complexes have been characterised by C, H analysis, IR spectroscopy and in certain cases ^1H NMR spectroscopy.

In recent years the chemistry of the distibinomethanes $R_2SbCH_2SbR_2$ (R = Me or Ph) has been studied in some detail but their coordination chemistry is limited due to the fact that chelation is unfavourable, resulting in a highly strained four-membered chelate ring. As a consequence, most metal halide complexes of the distibinomethanes contain monodentate or bridging bidentate ligands.

Metal halide complexes of the *o*-phenylene distibine ligands *o*-$C_6H_4(SbR_2)_2$ (R = Me or Ph) are known, but as with the distibinopropanes spectroscopic data has been limited.

The aim of the work presented in this chapter was to study in detail the coordination chemistry of the novel xylyl-distibine 1,2-$C_6H_4(CH_2SbMe_2)_2$ with a wide

range of metal halide systems. The ligand can coordinate in one of two ways, it can function as a bridging bidentate ligand or it can act as a chelate. The latter will result in the formation of a seven-membered chelate ring which is usually regarded as an unfavourable process, and complexes containing seven membered chelate rings are often unstable. The complexes prepared have been characterised by a range of spectroscopic techniques including single crystal X-ray diffraction, to enable useful comparisons to be made with other Group 15 metal halide complexes both on the structures of the complexes formed, and also on their relative stability.

4.2 Results and Discussion

4.2.1 Cu(I) and Ag(I) Complexes

The complexes $[CuL_2][BF_4]$ (L = 1,2-$C_6H_4(CH_2SbMe_2)_2$ or 1,3-$C_6H_4(CH_2SbMe_2)_2$) were prepared by reaction of $[Cu(MeCN)_4][BF_4]$ with two equivalents of ligand in CH_2Cl_2. The products were isolated as white solids by precipitation with diethyl ether. The ^1H NMR spectra show peaks consistent with coordinated ligand, with δ(Me) and δ(CH_2) shifted by approximately +0.1 ppm from the corresponding resonances in the free ligand. The formulations as $[CuL_2][BF_4]$ were confirmed by elemental analysis and the solid state IR spectra show bands corresponding to the ligand backbone and uncoordinated BF_4 (ca. 1061 and 520 cm^{-1}).[21]

There are two NMR active copper isotopes ^{63}Cu (natural abundance = 69 %) and ^{65}Cu (natural abundance = 31 %) both of which have reasonable sensitivities, however both are quadrupolar (I = 3/2) and only in high symmetry environments are the resonances sharp enough to be observed.[22] Due to this fast relaxation and rapid ligand exchange in solution, very few copper NMR resonances have been reported for Group 15 complexes. Although both complexes are poorly soluble a ^{63}Cu NMR spectrum was obtained of $[Cu\{1,2\text{-}C_6H_4(CH_2SbMe_2)_2\}_2][BF_4]$ which shows a broad resonance at -171 ppm ($w_{1/2}$ = 1170 Hz), unfortunately no ^{63}Cu NMR spectrum could be obtained for the analogous *meta*-xylyl complex. The δ(^{63}Cu) for $[Cu\{1,2\text{-}C_6H_4(CH_2SbMe_2)_2\}_2][BF_4]$ of -171 is very similar to those observed for other related distibine copper complexes (Table 4.1).

Complex	Solvent	δ(^{63}Cu) / ppm	$W_{1/2}$ / Hz
$[Cu\{1,2\text{-}C_6H_4(CH_2SbMe_2)_2\}_2][BF_4]$	$DMF/CDCl_3$	-171	1170
$[Cu\{Me_2Sb(CH_2)_3SbMe_2\}_2][BF_4]$[3]	CH_2Cl_2/CD_2Cl_2	-167	390
$[Cu\{Ph_2Sb(CH_2)_3SbPh_2\}_2][BF_4]$[3]	CH_2Cl_2/CD_2Cl_2	-197	1250
$[Cu\{o\text{-}C_6H_4(SbMe_2)_2\}_2][PF_6]$[2]	CH_2Cl_2/CD_2Cl_2	-179	700

Table 4.1 – ^{63}Cu NMR data for selected distibine complexes

The failure to obtain a ^{63}Cu NMR spectrum of $[Cu\{1,3\text{-}C_6H_4(CH_2SbMe_2)_2\}_2][BF_4]$ may either be due to poor solubilty of the complex or may arise as a result of deviation from a regular tetrahedral environment at Cu(I). Although the meta-xylyl ligand is capable of chelation it would involve the formation of an eight-membered chelate ring resulting in a highly strained complex. It is more likely that a polymeric Cu(I) species is formed.

Reaction of $AgCF_3SO_3$ with two equivalents of $1,2\text{-}C_6H_4(CH_2SbMe_2)_2$ in CH_2Cl_2 gave $[Ag\{1,2\text{-}C_6H_4(CH_2SbMe_2)_2\}_2][CF_3SO_3]$ as a white solid in good yield. The reaction was carried out in a foil-wrapped flask to protect the solution from bright light. The complex darkens significantly when exposed to light and air and as a result conventional analytical data could not be obtained. However the electrospray mass spectrum provides clear evidence for the formation of $[Ag\{1,2\text{-}C_6H_4(CH_2SbMe_2)_2\}_2][CF_3SO_3]$ with peaks corresponding to *m/z* 919 $[^{107}Ag\{1,2\text{-}C_6H_4(CH_2SbMe_2)_2\}_2]^+$, *m/z* 554 $[^{107}Ag\{1,2\text{-}C_6H_4(CH_2SbMe_2)_2\}MeCN]^+$, *m/z* 513 $[^{107}Ag\{1,2\text{-}C_6H_4(CH_2SbMe_2)_2\}]^+$ and *m/z* 189 $[^{107}Ag(MeCN)_2]^+$. Acetonitrile was used as the solvent for the electrospray mass spectrometry and accounts for the presence of coordinated acetonitrile in some of the fragment ions. The mass spectrum obtained for the related distibine complex $[Ag\{Me_2Sb(CH_2)_3SbMe_2\}_2][BF_4]$ shows peaks corresponding to $[Ag_2\{Me_2Sb(CH_2)_3SbMe_2\}_2BF_4]$ which suggests that the distibine complex may be polymeric.[1] The absence of any higher mass ions in the electrospray mass spectrum of $[Ag\{1,2\text{-}C_6H_4(CH_2SbMe_2)_2\}_2][CF_3SO_3]$ suggests that the *ortho*-xylyl ligand is acting as a chelate ligand on Ag(I) as observed with the analogous Cu(I) complex. The ^1H NMR spectrum is also consistent with the proposed formulation, showing a single methyl and methylene resonance at δ 1.07 and 3.19 ppm respectively and a multiplet at 7.01-7.02 for the aromatic protons.

4.2.1.1. Crystallographic analysis of $[Cu\{1,2\text{-}C_6H_4(CH_2SbMe_2)_2\}_2][BF_4].Et_2O$

Crystals of $[Cu\{1,2\text{-}C_6H_4(CH_2SbMe_2)_2\}_2][BF_4]$ were grown by slow evaporation of an MeCN / Et_2O solution. The structure (Figure 4.3, Tables 4.2 and 4.3) consists of discrete cations containing the tetrahedrally coordinated Cu ion as well as the BF_4^- anion and solvate molecule. The structure represents the first structurally characterised copper complex of a distibine ligand. There are only two other structurally characterised copper

complexes containing antimony ligands, both of which contain monodentate stibines. After structure solution and refinement a large peak remains in the electron density map close to the disordered ether molecule. It most probably corresponds to a second solvate molecule of either CH_2Cl_2 or H_2O but successful modelling of the molecule could not be achieved.

The average Cu-Sb bond length of 2.5125(6) Å is slightly shorter than those reported in the two other known Cu(I) stibine complexes, $[CuCl(Ph_3Sb)_3].CHCl_3$ (d(Cu-Sb) = 2.554(5) Å (ave))[23] and $[Cu\{(p\text{-}FC_6H_4)_3Sb\}_4][BF_4]$ (d(Cu-Sb) = 2.552(1) Å (ave)).[24] The ∠Sb-Cu-Sb range from 103.21(2)-118.95(2)° and show a much greater distortion from a regular tetrahedral geometry than in $[CuCl\{Ph_3Sb\}_3].CHCl_3$ (∠Sb-Cu-Sb = 111.576°).[23] The ∠Sb-Cu-Sb bond angles between the two Sb atoms of the same ligand (103.21(2) and 103.94(2)°) are much smaller than the ideal 109.5° reflecting the strain involved in the chelation of the two distibines.

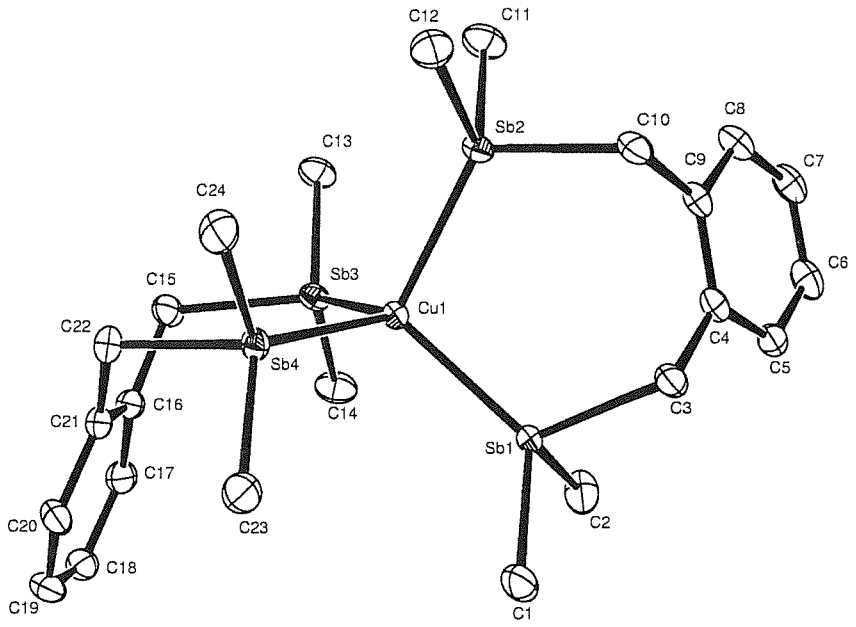

Figure 4.3 – View of the structure of the cation in $[Cu\{1,2\text{-}C_6H_4(CH_2SbMe_2)_2\}_2][BF_4]$ with numbering scheme adopted. Ellipsoids are drawn at 40 % probability. H atoms are omitted for clarity.

Bond Lengths (Å)		*Bond Angles* (°)	
Cu(1)-Sb(1)	2.5014(6)	C(1)-Sb(1)-Cu(1)	122.19(17)
Cu(1)-Sb(2)	2.5149(6)	C(2)-Sb(1)-Cu(1)	120.36(17)
Cu(1)-Sb(3)	2.5115(6)	C(3)-Sb(1)-Cu(1)	113.83(13)
Cu(1)-Sb(4)	2.5222(6)	C(10)-Sb(2)-Cu(1)	118.23(13)
Sb(1)-C(1)	2.124(5)	C(11)-Sb(2)-Cu(1)	119.85(16)
Sb(1)-C(2)	2.126(5)	C(12)-Sb(2)-Cu(1)	120.76(16)
Sb(1)-C(3)	2.163(4)	C(13)-Sb(3)-Cu(1)	122.86(15)
Sb(2)-C(10)	2.157(5)	C(14)-Sb(3)-Cu(1)	122.76(17)
Sb(2)-C(11)	2.122(5)	C(15)-Sb(3)-Cu(1)	114.02(14)
Sb(2)-C(12)	2.118(5)	C(22)-Sb(4)-Cu(1)	117.00(15)
Sb(3)-C(13)	2.128(5)	C(23)-Sb(4)-Cu(1)	120.02(15)
Sb(3)-C(14)	2.136(5)	C(24)-Sb(4)-Cu(1)	122.11(16)
Sb(3)-C(15)	2.168(5)	C(1)-Sb(1)-C(2)	98.0(3)
Sb(4)-C(22)	2.167(5)	C(1)-Sb(1)-C(3)	99.4(2)
Sb(4)-C(23)	2.132(5)	C(2)-Sb(1)-C(3)	98.7(2)
Sb(4)-C(24)	2.126(5)	C(10)-Sb(2)-C(11)	98.5(2)
		C(10)-Sb(2)-C(12)	95.4(2)
Bond Angles (°)		C(11)-Sb(2)-C(12)	99.0(2)
Sb(1)-Cu(1)-Sb(2)	103.21(2)	C(13)-Sb(3)-C(14)	97.7(2)
Sb(1)-Cu(1)-Sb(3)	118.95(2)	C(13)-Sb(3)-C(15)	96.1(2)
Sb(1)-Cu(1)-Sb(4)	114.27(2)	C(14)-Sb(3)-C(15)	97.7(2)
Sb(2)-Cu(1)-Sb(3)	109.10(2)	C(22)-Sb(4)-C(23)	98.0(2)
Sb(2)-Cu(1)-Sb(4)	106.84(2)	C(22)-Sb(4)-C(24)	95.7(2)
Sb(3)-Cu(1)-Sb(4)	103.94(2)	C(23)-Sb(4)-C(24)	98.8(2)

Table 4.2 - Selected bond lengths (Å) and angles (°) for $[Cu\{1,2\text{-}C_6H_4(CH_2SbMe_2)_2\}_2][BF_4].Et_2O$

Table 4.3 - Crystal Data and Structure Refinement Details for $[Cu\{1,2\text{-}C_6H_4(CH_2SbMe_2)_2\}_2][BF_4]$

compound	$[Cu\{1,2\text{-}C_6H_4(CH_2SbMe_2)_2\}_2][BF_4].Et_2O$
empirical formula	$C_{28}H_{50}BCuF_4OSb_4$
fw	1040.03
cryst. system	monoclinic
space group	$P2_1/c$ (No. 14)
a (Å)	14.6315(10)
b (Å)	18.5261(10)
c (Å)	14.2015(10)
β (°)	106.830(5)
volume ($Å^3$)	3684.6(4)
Z	4
density (calc.) (mg / m^3)	1.875
abs coef (mm^{-1})	3.502
F(000)	2000
total no. of obsns.	30492 (R_{int} = 0.045)
no. of unique obsns.	8391
min, max transmission	0.443, 0.506
no. of parameters, restraints	331, 4
goodness-of-fit on F^2	1.055
R1, wR2 ($I>2\sigma(I)$)[b]	0.037, 0.097
R1, wR2 (all data)	0.042, 0.100

Temperature = 120 K; wavelength (Mo-Kα) = 0.71073 Å; θ (max) = 27.5 deg.

[b] $R1 = \sum ||F_0| - |F_c|| / \sum |F_0|$ $wR_2 = [\sum w(F_0^2 - F_c^2)^2 / \sum wF_0^4]^{1/2}$

4.2.2 Pt(II) and Pd(II) Complexes

4.2.2.1 $[MX_2\{1,2\text{-}C_6H_4(CH_2SbMe_2)_2\}]$

Reaction of $1,2\text{-}C_6H_4(CH_2SbMe_2)_2$ with $[MCl_2(MeCN)_2]$ (M = Pd or Pt), generated *in situ* by refluxing MCl_2 in MeCN yields the complexes $[MCl_2\{1,2\text{-}C_6H_4(CH_2SbMe_2)_2\}]$ as yellow solids in modest yield. Both complexes are poorly soluble in chlorocarbons and alcohols but are moderately soluble in acetonitrile, allowing study by mass spectrometry. The electrospray mass spectrum of $[PtCl_2\{1,2\text{-}C_6H_4(CH_2SbMe_2)_2\}]$ shows a cluster of peaks near *m/z* 677 with the correct isotopic distribution for $[PtCl\{1,2\text{-}C_6H_4(CH_2SbMe_2)_2\}MeCN]^+$. Similarly the electrospray mass spectrum of $[PdCl_2\{1,2\text{-}C_6H_4(CH_2SbMe_2)_2\}]$ shows a cluster of peaks near *m/z* 588 with the correct isotopic distribution for $[PdCl\{1,2\text{-}C_6H_4(CH_2SbMe_2)_2\}MeCN]^+$. Due to poor solubility no ^{195}Pt NMR spectrum could be obtained for $[PtCl_2\{1,2\text{-}C_6H_4(CH_2SbMe_2)_2\}]$ and the ^1H NMR spectrum shows peaks corresponding to the ligand backbone, shifted upfield from free ligand, but no evidence of ^{195}Pt satellites. The microanalytical data is consistent with the formation of the monomeric M(II) complexes $[MCl_2\{1,2\text{-}C_6H_4(CH_2SbMe_2)_2\}]$ (M = Pt or Pd).

4.2.2.2 Crystallographic analysis of $[PtCl_2\{1,2\text{-}C_6H_4(CH_2SbMe_2)_2\}]$

Crystals of $[PtCl_2\{1,2\text{-}C_6H_4(CH_2SbMe_2)_2\}]$ suitable for single crystal X-ray diffraction were grown by slow evaporation of an MeCN solution of the complex. The structure (Figure 4.4, Tables 4.4 and 4.5) shows the *ortho*-xylyl ligand chelating to the Pt(II) centre to give an overall distorted square planar geometry at Pt. The structure represents the first structurally characterised platinum complex containing a chelating distibine ligand. There is only one other X-ray structure of a platinum distibine complex which is the distibine bridged dimer complex $[\{PtCl_2(Ph_2SbCH_2SbPh_2)\}_2].Me_2CO$.[4]

The Pt-Sb bond distances (2.4860(7) and 2.4931(7) Å) are comparable with those in the ligand bridged dimer complex $[\{PtCl_2(Ph_2SbCH_2SbPh_2)\}_2].Me_2CO$ (Pt-Sb = 2.479(1), 2.572(1), 2.494(1) and 2.554(1) Å).[4] The ∠Cl-Pt-Cl (92.27(8)°) is very similar to that observed in $[\{PtCl_2(Ph_2SbCH_2SbPh_2)\}_2].Me_2CO$ (∠Cl-Sb-Cl = 93.1(1)°) showing a slight distortion from a regular square planar geometry. The ∠Sb-Pt-Sb (97.5(2)°)

shows much greater distortion from the ideal square planar geometry (90°) due to the large bite angle of the seven membered chelate ring.

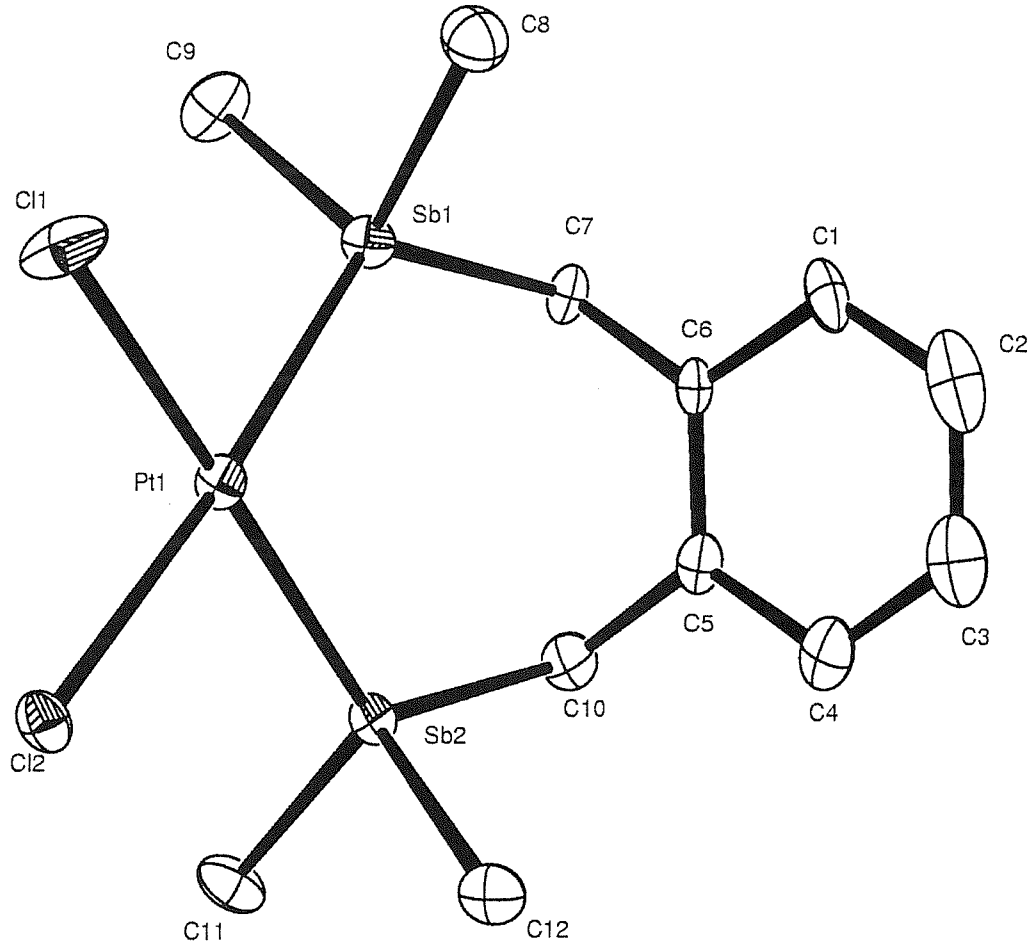

Figure 4.4 – View of the structure of $[PtCl_2\{1,2\text{-}C_6H_4(CH_2SbMe_2)_2\}]$ with numbering scheme adopted. Ellipsoids are drawn at 40 % probability. H atoms are omitted for clarity.

Bond Lengths (Å)		*Bond Angles* (°)	
Pt(1)-Cl(1)	2.369(3)	Cl(1)-Pt(1)-Cl(2)	92.27(8)
Pt(1)-Cl(2)	2.3746(19)	Cl(1)-Pt(1)-Sb(1)	85.35(6)
Pt(1)-Sb(1)	2.4860(7)	Cl(1)-Pt(1)-Sb(2)	175.95(7)
Pt(1)-Sb(2)	2.4931(7)	Cl(2)-Pt(1)-Sb(1)	175.41(6)
Sb(1)-C(7)	2.145(9)	Cl(2)-Pt(1)-Sb(2)	85.01(6)
Sb(1)-C(8)	2.117(10)	Sb(1)-Pt(1)-Sb(2)	97.57(2)
Sb(1)-C(9)	2.110(10)	C(7)-Sb(1)-Pt(1)	120.6(3)
Sb(2)-C(10)	2.148(8)	C(8)-Sb(1)-Pt(1)	113.5(3)
Sb(2)-C(11)	2.124(9)	C(9)-Sb(1)-Pt(1)	112.9(3)
Sb(2)-C(12)	2.110(10)	C(10)-Sb(1)-Pt(1)	121.1(3)
		C(11)-Sb(1)-Pt(1)	117.2(3)
		C(12)-Sb(1)-Pt(1)	109.2(3)
		C(7)-Sb(1)-C(8)	100.4(4)
		C(7)-Sb(1)-C(9)	105.5(4)
		C(8)-Sb(1)-C(9)	101.6(4)
		C(10)-Sb(2)-C(11)	104.2(4)
		C(10)-Sb(2)-C(12)	100.4(4)
		C(11)-Sb(2)-C(12)	101.9(4)

Table 4.4 – Selected bond lengths (Å) and angles (°) for $[PtCl_2\{1,2\text{-}C_6H_4(CH_2SbMe_2)_2\}]$

Table 4.5 - Crystal Data and Structure Refinement Details for $[PtCl_2\{1,2\text{-}C_6H_4(CH_2SbMe_2)_2\}]$

compound	$[PtCl_2\{1,2\text{-}C_6H_4(CH_2SbMe_2)_2\}]$
empirical formula	$C_{12}H_{20}Cl_2PtSb_2$
fw	673.77
cryst. system	orthorhombic
space group	Pbca (No. 61)
a (Å)	17.6538(4)
b (Å)	10.8090(3)
c (Å)	17.9084(5)
volume ($Å^3$)	3417.28(16)
Z	8
density (calc.) (mg / m^3)	2.619
abs coef (mm^{-1})	11.599
F(000)	2448
total no. of obsns.	6595 (R_{int} = 0.0514)
no. of unique obsns.	3866
min, max transmission	0.671, 1.784
no. of parameters, restraints	154, 0
goodness-of-fit on F^2	1.131
R1, wR2 ($I>2\sigma(I)$)[b]	0.0569, 0.1538
R1, wR2 (all data)	0.0675, 0.1650

Temperature = 120 K; wavelength (Mo-Kα) = 0.71073 Å; θ (max) = 27.5 deg.

[b] $R1 = \sum ||F_0| - |F_c|| / \sum |F_0|$ $wR_2 = [\sum w(F_0^2 - F_c^2)^2 / \sum wF_0^4]^{1/2}$

4.2.2.2 $[M\{1,2\text{-}C_6H_4(CH_2SbMe_2)_2\}_2][PF_6]_2$

Reaction of $[PtCl_2\{1,2\text{-}C_6H_4(CH_2SbMe_2)_2\}]$ with $TlPF_6$ in nitromethane, followed by addition of a second equivalent of ligand yields $[Pt\{1,2\text{-}C_6H_4(CH_2SbMe_2)_2\}_2][PF_6]_2$ as a yellow/orange solid in good yield. The electrospray mass spectrum provides evidence for the formation of the bis-ligand complex with peaks near *m/z* 1031 and 1131 with the correct isotopic distribution for $[Pt\{1,2\text{-}C_6H_4(CH_2SbMe_2)_2\}_2]^+$ and $[Pt\{1,2\text{-}C_6H_4(CH_2SbMe_2)_2\}\{1,2\text{-}C_6H_4(CH_2SbMe_2)(CH_2SbMe)PF_6]^+$. The ^1H NMR spectrum shows a single methyl resonance at δ 1.44 ppm, a single methylene resonance at δ 3.84 ppm and a multiplet at δ 7.07-7.10 ppm corresponding to the aromatic protons. The average shift upon coordination is higher than that observed for $[PtCl_2\{1,2\text{-}C_6H_4(CH_2SbMe_2)_2\}]$. The solid state IR spectrum shows peaks corresponding to the ligand backbone and uncoordinated $[PF_6]^-$.[25] The spectroscopic data together with C, H analysis confirms the formation of $[Pt\{1,2\text{-}C_6H_4(CH_2SbMe_2)_2\}_2][PF_6]_2$.

Attempts were made to prepare the analogous palladium complex using the procedure outlined above and a product was isolated as a dark red solid. The solid state IR spectrum is very similar to that observed for the platinum complex showing uncoordinated $[PF_6]^-$ [25] and bands corresponding to the ligand backbone. The ^1H NMR spectrum appears consistent with the formation of the bis-ligand complex, and shows a single methyl and methylene resonance at δ 1.56 and 4.15 ppm respectively with a multiplet for the aromatic protons at δ 7.14 – 7.30 ppm. However repeated attempts to obtain satisfactory microanalytical data failed. EDX of the product indicates the presence of both thallium and chlorine in the isolated solid, which could not be removed by washing or recrystallisation. A clean sample of $[Pd\{1,2\text{-}C_6H_4(CH_2SbMe_2)_2\}_2][PF_6]_2$ was obtained using a slightly modified procedure in which $[PdCl_2\{1,2\text{-}C_6H_4(CH_2SbMe_2)_2\}]$ was prepared *in situ* by reaction of $PdCl_2$ with one equivalent of ligand in refluxing MeCN. The chlorine was removed by the addition of $TlPF_6$ and the resulting solution filtered through celite to remove the TlCl, prior to the addition of a second equivalent of ligand. The complex was isolated as a yellow solid. ^1H NMR data and C,H analyses are consistent with the isolation of $[Pd\{1,2\text{-}C_6H_4(CH_2SbMe_2)_2\}_2][PF_6]_2$.

4.2.2.4 Crystallographic analysis of $[Pt\{1,2\text{-}C_6H_4(CH_2SbMe_2)_2\}_2][PF_6]_2.2MeCN$ and $[Pd\{1,2\text{-}C_6H_4(CH_2SbMe_2)_2\}_2][PF_6]_2$

Crystals of $[Pt\{1,2\text{-}C_6H_4(CH_2SbMe_2)_2\}_2][PF_6]_2.2MeCN$ were grown by layering a solution of the complex in MeCN with Et_2O. The structure (Figure 4.5, Tables 4.6, 4.7 and 4.8) shows discrete cations with two chelating ligands bound to the Pt centre resulting in a square planar geometry, as well as two PF_6 anions and two disordered acetonitile solvate molecules.

Crystals of $[Pd\{1,2\text{-}C_6H_4(CH_2SbMe_2)_2\}_2][PF_6]_2$ were grown by slow evaporation of an MeCN solution of the complex. The structure (Figure 4.6, Tables 4.9 and 4.10) is centrosymmetric, with a discrete square planar Pd(II) cation and two PF_6^- anions very similar to the Pt(II) analogue. There is very little difference between the M-Sb bond distances in the two structures (Pt-Sb = 2.575(8) Å ave., Pd-Sb = 2.572(4) Å ave.) and the angles around the metal centres are also very similar showing little deviation from a regular square-planar geometry (∠Sb-Pt-Sb = 87.66(2) – 92.24(2)°, ∠Sb-Pd-Sb = 88.503(12) – 91.497(12)°). The ∠Sb-M-Sb (M = Pt or Pd) between Sb atoms within the same ligand are on average slightly larger (∠Sb-Pt-Sb = 92.19(2)° and ∠Sb-Pd-Sb = 91.50(12)°) than the ∠Sb-M-Sb for Sb atoms on adjacent ligands (∠Sb-Pt-Sb = 87.82(2)° and ∠Sb-Pd-Sb = 88.503(12)) due to the bite angle of the chelating ligand.

The Pt-Sb bond distances (2.5746(8) Å ave.) are larger than those observed in $[PtCl_2\{1,2\text{-}C_6H_4(CH_2SbMe_2)_2\}]$ (2.4896(7) Å ave.), and the average ∠C-Sb-C are smaller (100.7(4)° ave.) than those in the 1:1 complex (102.4(4)° ave.). In particular the ∠C-Sb-C between one of the methyl groups on Sb and the CH_2 of the xylyl backbone is much more acute (97.3(4)° ave.) than the corresponding angle in $[PtCl_2\{1,2\text{-}C_6H_4(CH_2SbMe_2)_2\}]$ (100.4(4) ° ave.) which may indicate some steric hindrance between the methyl groups on the two adjacent ligands.

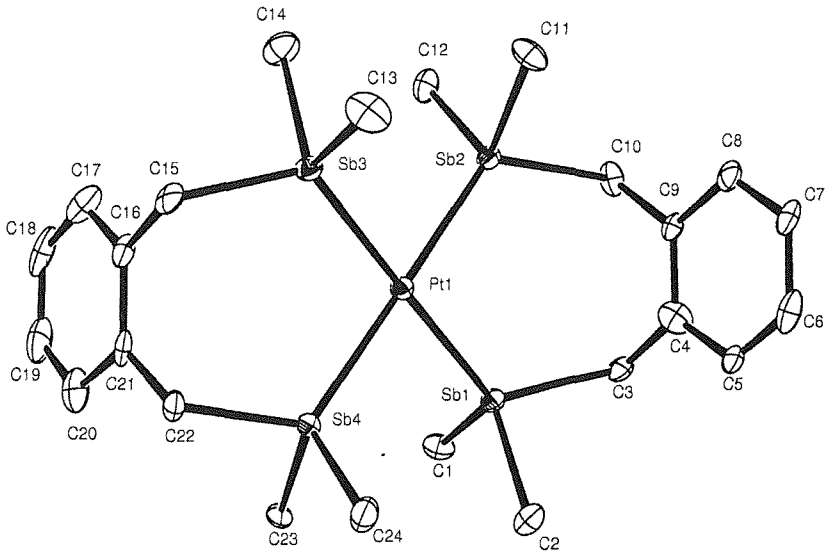

Figure 4.5 – View of the structure of the cation in $[Pt\{1,2\text{-}C_6H_4(CH_2SbMe_2)_2\}_2][PF_6]_2.2MeCN$ with numbering scheme adopted. Ellipsoids are drawn at 40 %. H atoms are omitted for clarity.

Bond Lengths (Å)			
Pt(1)-Sb(1)	2.5742(8)	Sb(2)-C(11)	2.147(9)
Pt(1)-Sb(2)	2.5748(8)	Sb(2)-C(12)	2.124(9)
Pt(1)-Sb(3)	2.5690(8)	Sb(3)-C(13)	2.119(4)
Pt(1)-Sb(4)	2.5802(8)	Sb(3)-C(14)	2.135(9)
Sb(1)-C(1)	2.122(9)	Sb(3)-C(15)	2.153(9)
Sb(1)-C(2)	2.132(9)	Sb(4)-C(22)	2.137(8)
Sb(1)-C(3)	2.148(9)	Sb(4)-C(23)	2.121(8)
Sb(2)-C(10)	2.151(8)	Sb(4)-C(24)	2.118(9)

Table 4.6 – Selected bond lengths (Å) for $[Pt\{1,2\text{-}C_6H_4(CH_2SbMe_2)_2\}_2][PF_6]_2.2MeCN$

Bond Angles (°)		*Bond Angles* (°)	
Sb(1)-Pt(1)-Sb(2)	92.24(2)	C(10)-Sb(2)-Pt(1)	121.6(3)
Sb(1)-Pt(1)-Sb(3)	178.39(3)	C(11)-Sb(2)-Pt(1)	112.2(3)
Sb(1)-Pt(1)-Sb(4)	87.98(2)	C(12)-Sb(2)-Pt(1)	117.4(3)
Sb(2)-Pt(1)-Sb(3)	87.66(2)	C(13)-Sb(3)-C(14)	103.8(3)
Sb(2)-Pt(1)-Sb(4)	178.82(3)	C(13)-Sb(3)-C(15)	102.1(3)
Sb(3)-Pt(1)-Sb(4)	92.14(2)	C(14)-Sb(3)-C(15)	96.8(4)
C(1)-Sb(1)-C(2)	103.6(4)	C(13)-Sb(3)-Pt(1)	113.91(12)
C(1)-Sb(1)-C(3)	100.8(4)	C(14)-Sb(3)-Pt(1)	116.2(3)
C(2)-Sb(1)-C(3)	96.2(4)	C(15)-Sb(3)-Pt(1)	121.3(2)
C(1)-Sb(1)-Pt(1)	116.4(3)	C(22)-Sb(4)-C(23)	98.5(3)
C(2)-Sb(1)-Pt(1)	115.0(3)	C(22)-Sb(4)-C(24)	100.6(4)
C(3)-Sb(1)-Pt(1)	121.5(2)	C(23)-Sb(4)-C(24)	103.4(4)
C(10)-Sb(2)-C(11)	97.6(4)	C(22)-Sb(4)-Pt(1)	120.5(3)
C(10)-Sb(2)-C(12)	102.0(3)	C(23)-Sb(4)-Pt(1)	112.9(3)
C(11)-Sb(2)-C(12)	102.8(4)	C(24)-Sb(4)-Pt(1)	117.9(3)

Table 4.7 – Selected bond angles (°) for $[Pt\{1,2\text{-}C_6H_4(CH_2SbMe_2)_2\}_2][PF_6]_2.2MeCN$

Table 4.8 - Crystal Data and Structure Refinement Details for $[Pt\{1,2\text{-}C_6H_4(CH_2SbMe_2)_2\}_2][PF_6]_2.2MeCN$

compound	$[Pt\{1,2\text{-}C_6H_4(CH_2SbMe_2)_2\}_2][PF_6]_2.2MeCN$
empirical formula	$C_{28}H_{46}F_{12}N_2P_2PtSb_4$
fw	1382.70
cryst. system	monoclinic
space group	$P2_1/n$ (no.14)
a (Å)	15.699(2)
b (Å)	15.344(2)
c (Å)	18.052(2)
β (°)	108.898(4)
volume ($Å^3$)	4114.2(9)
Z	4
density (calc.) (mg / m^3)	2.232
abs coef (mm^{-1})	6.136
F(000)	2592
total no. of obsns.	34100 (R_{int} = 0.085)
no. of unique obsns.	9344
min, max transmission	0.741, 0.862
no. of parameters, restraints	398, 4
goodness-of-fit on F^2	1.025
R1, wR2 ($I>2\sigma(I)$)[b]	0.053, 0.104
R1, wR2 (all data)	0.103, 0.120

Temperature = 120 K; wavelength (Mo-Kα) = 0.71073 Å; θ (max) = 27.5 deg.

[b] $R1 = \sum ||F_0| - |F_c|| / \sum |F_0|$ $wR_2 = [\sum w(F_0^2 - F_c^2)^2 / \sum wF_0^4]^{1/2}$

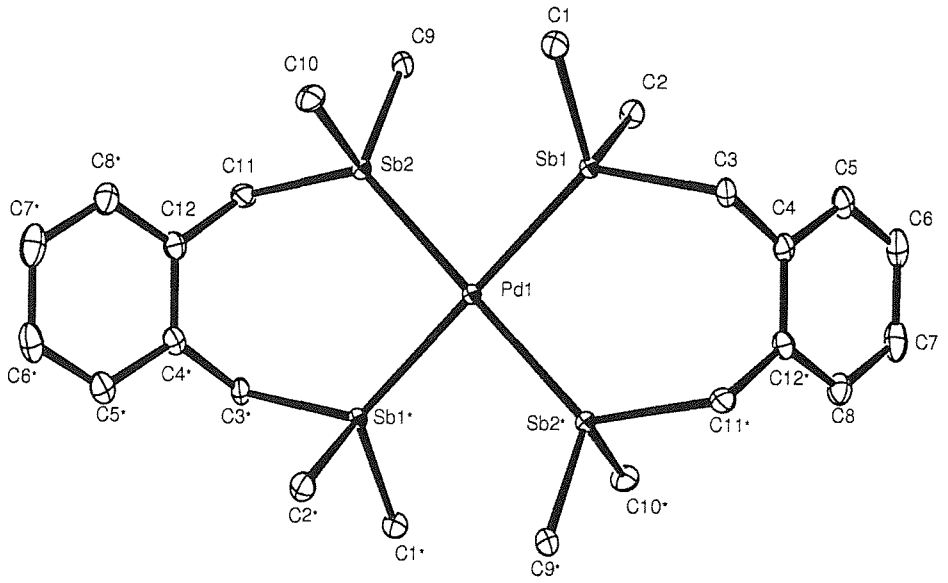

Figure 4.6 – View of the cation in the structure of $[Pd\{1,2\text{-}C_6H_4(CH_2SbMe_2)_2\}_2][PF_6]_2$ with numbering,scheme adopted. Ellipsoids are drawn at 40 % probabilty. H atoms are omitted for clarity.

Bond Lengths (Å)		Bond Angles (°)	
Pd(1)-Sb(1)	2.5745(4)	Sb(1)-Pd(1)-Sb(2)	88.503(12)
Pd(1)-Sb(2)	2.5694(4)	Sb(1)-Pd(1)-Sb(2*)	91.497(12)
Sb(1)-C(1)	2.128(7)	C(1)-Sb(1)-C(2)	103.9(2)
Sb(1)-C(2)	2.113(6)	C(1)-Sb(1)-C(3)	97.2(2)
Sb(1)-C(3)	2.152(6)	C(2)-Sb(1)-C(3)	98.3(2)
Sb(2)-C(9)	2.138(6)	C(1)-Sb(1)-Pd(1)	118.06(16)
Sb(2)-C(10)	2.123(6)	C(2)-Sb(1)-Pd(1)	112.90(17)
Sb(2)-C(11)	2.148(6)	C(3)-Sb(1)-Pd(1)	123.09(15)
		C(9)-Sb(2)-C(10)	104.3(3)
		C(9)-Sb(2)-C(11)	96.3(2)
		C(10)-Sb(2)-C(11)	99.0(3)
		C(9)-Sb(2)-Pd(1)	117.45(16)
		C(10)-Sb(2)-Pd(1)	113.13(18)
		C(11)-Sb(2)-Pd(1)	123.41(17)

Table 4.9 – Selected bond lengths (Å) and angles (°) for $[Pd\{1,2\text{-}C_6H_4(CH_2SbMe_2)_2\}_2][PF_6]_2$

Table 4.10 - Crystal Data and Structure Refinement Details for $[Pd\{1,2\text{-}C_6H_4(CH_2SbMe_2)_2\}_2][PF_6]_2$

compound	$[Pd\{1,2\text{-}C_6H_4(CH_2SbMe_2)_2\}_2][PF_6]_2$
empirical formula	$C_{24}H_{40}F_{12}P_2PdSb_4$
fw	1211.90
cryst. system	monoclinic
space group	$P2_1/n$ (No. 14)
a (Å)	10.6036(4)
b (Å)	15.2906(6)
c (Å)	11.6916(4)
β (°)	105.335(12)
volume ($Å^3$)	1828.13(12)
Z	2
density (calc.) (mg / m^3)	2.202
abs coef (mm^{-1})	3.564
F(000)	1144
total no. of obsns.	7560 (R_{int} = 0.058)
no. of unique obsns.	4160
min, max transmission	0.732, 0.812
no. of parameters, restraints	197, 0
goodness-of-fit on F^2	1.037
R1, wR2($I>2\sigma(I)$)[b]	0.041, 0.119
R1, wR2 (all data)	0.053, 0.119

Temperature = 120 K; wavelength (Mo-Kα) = 0.71073 Å; θ (max) = 27.5 deg.

[b] $R1 = \sum ||F_0| - |F_c|| / \sum |F_0|$ $wR_2 = [\sum w(F_0^2 - F_c^2)^2 / \sum wF_0^4]^{1/2}$

4.2.2 A Rh(III) Complex

Reaction of two equivalents of 1,2-$C_6H_4(CH_2SbMe_2)_2$ with one equivalent of $RhCl_3.3H_2O$ in ethanol in the presence of NH_4BF_4 yields $[RhCl_2\{1,2\text{-}C_6H_4(CH_2SbMe_2)_2\}_2][BF_4]$ as a yellow solid. Absorption bands in the IR spectrum are characteristic of the ligand and uncoordinated BF_4^- (1055, 540 cm^{-1}).[21] The electrospray mass spectrum shows one major species near *m/z* 988 with the correct isotopic distribution for $[RhCl_2\{1,2\text{-}C_6H_4(CH_2SbMe_2)_2\}_2]^+$ *m/z* 985. The ^1H NMR spectrum shows three methyl resonances at δ 1.46, 1.475 and 1.48 ppm, and curiously the $\delta(CH_2)$ resonances occur as two second order multiplets.

The kinetic inertness of low spin d^6 ions in pseudo-octahedral environments often allows the isolation of geometric isomers for Rh(III). Levason and co-workers have shown that under the same reaction conditions the ligands 1,2-$C_6H_4(PMe_2)_2$ and 1,2-$C_6H_4(AsMe_2)_2$ give almost exclusively (≥ 80 %) *trans*-$[RhCl_2L_2]^+$.[26] To isolate the *cis*-isomers the *trans*-isomers were heated with excess Li_2CO_3 in aqueous ethanol for 48 hours and treated subsequently with aqueous HX.[26] For the *trans*-isomers all methyl groups are equivalent resulting in a single methyl resonance in the ^1H NMR spectrum, whilst the *cis*-isomers exhibit four methyl resonances of equal intensity. A mixture of geometric isomers does not therefore account for the unusual ^1H NMR spectrum. It is possible that the ^1H NMR spectrum indicates the presence of different conformations of the xylyl backbone which cannot interconvert at the crowded Rh(III) centre. The previous work by Levason *et al* would suggest that the complex isolated is most probably *trans*-$[RhCl_2\{1,2\text{-}C_6H_4(CH_2SbMe_2)_2\}_2][BF_4]$.

The UV/VIS spectrum of $[RhCl_2\{1,2\text{-}C_6H_4(CH_2SbMe_2)_2\}_2][BF_4]$ shows a single band at 27,100 cm^{-1}. This value is comparable with the UV/VIS data on related *o*-$C_6H_4(PMe_2)_2$ and *o*-$C_6H_4(AsMe_2)_2$ systems (Table 4.11).[26]

Complex	E_{max} (10^3 cm^{-1}) ($\varepsilon_{mol}/cm^{-1}$ mol^{-1} dm^3)
trans-[Rh{*o*-$C_6H_4(PMe_2)_2$}$_2Cl_2$]Cl	33.1 (2520), 23.9 (270)
trans-[Rh{*o*-$C_6H_4(AsMe_2)_2$}$_2Cl_2$]Cl	32.9 (1780), 29.6 (1370), 24.4 (290)
cis-[Rh{*o*-$C_6H_4(PMe_2)_2$}$_2Cl_2$]Cl	30.3 (sh)
cis-[Rh{*o*-$C_6H_4(AsMe_2)_2$}$_2Cl_2$]Cl	33.1 (3940)

Table 4.11 – UV/VIS data for selected Rh(III) complexes[26]

4.2.4 A Co(III) Complex

[$CoBr_2${1,2-$C_6H_4(CH_2SbMe_2)_2$}$_2$][BPh_4] was prepared in low yield by reaction of 1,2-$C_6H_4(CH_2SbMe_2)_2$ with $CoBr_2$ and $NaBPh_4$ in dry nitromethane followed by air-oxidation, following the procedure used for the synthesis of [$CoBr_2(MeSeCH_2CH_2SeMe)_2$][$BPh_4$] by Levason and co-workers.[27] The brown solid is stable in dry air but decomposes in moist air or in solution in a matter of hours. Several attempts were made to obtain satisfactory microanalytical data on the complex but the results were repeatedly low in percentage C and H and this reflects the instability of the isolated complex. The electrospray mass spectrum shows only one major feature near *m/z* 1034 with the correct isotopic distribution for [$CoBr_2${1,2-$C_6H_4(CH_2SbMe_2)_2$}]$^+$.

The ^{1}H NMR spectrum shows a single broad methyl resonance at 1.45 ppm, a singlet at δ 3.3 ppm corresponding to the methylene protons and a multiplet at δ 6.9-7.7 ppm corresponding to the aromatic protons. One would expect to observe a single methyl resonance for the *trans*-isomer and four methyl resonances of equal intensity for the *cis*-isomer[28], therefore the isolated solid is clearly *trans*-[$CoBr_2${1,2-$C_6H_4(CH_2SbMe_2)_2$}$_2$][BPh_4]. Previous studies[28] have shown that the *trans*-isomers are generally more stable than the *cis*. *Cis*→*trans* isomerisation occurs relatively easily, probably via a Co(II) catalysed route. For the unstable Co(III) distibine system it is logical that it will adopt the more stable *trans*-configuration.

The sample develops new resonances in the ^{1}H NMR spectrum upon standing which are attributed to decomposition in solution. The broad resonances observed in freshly prepared samples could be due to the effect of the ^{59}Co quadrupole, the presence of different conformations of the xylyl backbone as discussed for the Rh(III) complex, or

to the onset of decomposition. The solution instability prevented more detailed studies to probe this further. The ability to obtain NMR spectra of the complex confirms that it is diamagnetic, consistent with T_2g^6 Co(III).

The electronic spectrum contains a weak band at 17,300 cm^{-1} and a second stronger band at 20,400 cm^{-1}. The UV/VIS spectra of *cis*-$[CoL_2X_2]^+$ (L = *o*-$C_6H_4(PMe_2)_2$, *o*-$C_6H_4(AsMe_2)_2$ or As(*o*-$C_6H_4AsMe_2)_3$, X = Cl, Br or I) exhibit one main band in the region ca. 27,000 – 23,000 cm^{-1} with a lower energy band and shoulder at ca. 23,000 – 20,000 cm^{-1} assigned to the $^1A_{1g} \rightarrow {}^1T_{2g}$ and $^1A_{1g} \rightarrow {}^1T_{1g}$ transitions respectively.[29] *Trans*-$[CoL_2X_2]^+$ (L = *o*-$C_6H_4(PMe_2)(SbMe_2)$, *o*-$C_6H_4(SbMe_2)_2$, $Me_2Sb(CH_2)_3SbMe_2$, *o*-$C_6H_4(PPh_2)(SMe)$ or *o*-$C_6H_4(PPh_2)(SeMe)$, X = Cl, Br or I) show a weak band at 14,000-16,000 cm^{-1} assigned as $^1A_{1g} \rightarrow {}^1E_g$ in D_{4h} symmetry with some higher energy absorptions in the range 18,000-22,000 cm^{-1} which have been attributed to the metal-centred $^1A_{1g} \rightarrow {}^1A_{2g}$ transition.[16] Comparisons with these data are again consistent with the presence of the *trans*-isomer in the present complex.

The ^{59}Co NMR spectrum shows a very broad resonance at 4550 ppm ($w_{1/2}$ = 22,000 Hz), the large line width is a consequence of the large quadrupole moment of ^{59}Co (Q = 0.42 x 10^{-28} m^2). The $\delta(^{59}Co)$ may be compared with those of related phosphine, arsine and stibine complexes (Table 4.12).

Complex	Solvent	$\delta(^{59}Co)$ / ppm ($w_{1/2}$ / Hz)
trans-$[Co\{o\text{-}C_6H_4(SbMe_2)_2\}_2Br_2]Br$ [16]	CH_2Cl_2	+ 4710
trans-$[Co\{o\text{-}C_6H_4(AsMe_2)_2\}_2Cl_2]Cl$ [30]	Me_2SO	+2830 (15,000)
cis-$[Co\{o\text{-}C_6H_4(AsMe_2)_2\}_2Cl_2]Cl$ [30]	Me_2SO	+2860 (12,000)
trans-$[Co\{o\text{-}C_6H_4(AsMe_2)_2\}_2]Br_2$ [30]	Me_2SO	+2880 (14,000)
trans-$[Co\{o\text{-}C_6H_4(PMe_2)_2\}_2Cl_2]Cl$ [30]	Me_2SO	+1710 (16,500)
$[Co\{1,2\text{-}C_6H_4(CH_2SbMe_2)_2\}_2Br_2][BPh_4]$	CH_2Cl_2	+4550 (22,000)

Table 4.12 - ^{59}Co NMR data for selected phosphine, arsine and stibine Co(III) complexes

The donor atom has a significant effect on the $\delta(^{59}Co)$ with a marked shift to high frequency as one moves down Group 15. The reported difference in $\delta(^{59}Co)$ between

cis-[Co{*o*-$C_6H_4(AsMe_2)_2$}$_2Cl_2$]Cl and *trans*-[Co{*o*-$C_6H_4(AsMe_2)_2$}$_2Cl_2$]Cl is only 30 ppm. It is doubtful that this represents a distinguishable difference as the very large linewidths of observed resonances in ^{59}Co NMR produces errors of the order +/- 50 ppm in $\delta(^{59}Co)$. Thus distinction of geometric isomers by ^{59}Co NMR in cases where the resonances are very broad is uncertain. This is true in the case of the distibine complex described here, although the chemical shift does confirm the presence of an Sb_4Br_2 donor set.[30]

4.2.5 Ni(II) Complexes

Reaction of one equivalent of 1,2-$C_6H_4(CH_2SbMe_2)_2$ with 0.25 equivalents of $NiX_2.6H_2O$ and 0.25 equivalents of $Ni(ClO_4)_2.6H_2O$ in warm n-butanol yields [NiX{1,2-$C_6H_4(CH_2SbMe_2)_2$}$_2$][ClO_4] (X = Br or I). [NiBr{1,2-$C_6H_4(CH_2SbMe_2)_2$}$_2$][ClO_4] is a dark purple solid and [NiI{1,2-$C_6H_4(CH_2SbMe_2)_2$}$_2$][ClO_4] is a dark green solid. Both complexes decompose quickly in coordinating solvents and even when stored under nitrogen slowly decolourise indicating decomposition, as a result mass spectra could not be obtained. C, H analysis of the iodo complex confirms the isolation of [NiI{1,2-$C_6H_4(CH_2SbMe_2)_2$}$_2$][ClO_4], however consistent analytical data on the bromo analogue could not be obtained. Instability of this type has also been observed for [$NiX_2(SbMe_3)_3$] (X = Br or I) which are decomposed by most donor solvents and by dioxygen.[31] Attempts were made to prepare the analogous chloro complex but no reaction was observed and the bromo complex appears less stable to decomposition than the iodo complex consistent with previous studies which have shown that the tendency for Ni(II) salts to complex with Group 15 ligands follows the order $I^- > Br^- > Cl^-$.[32] The softer the halide the more electron density it transfers to the metal softening the Ni(II) centre and increasing its ability to coordinate other soft donors.[32] The ^{1}H NMR spectra of both complexes show single methyl and methylene resonances with the iodo exhibiting slightly larger coordination shifts.

There are two possible coordination geometries for low spin five-coordinate Ni(II), square pyramidal or trigonal bipyramidal which can be differentiated by their electronic spectra.[33] Previous studies with Group 15 Ni(II) complexes have shown that square pyramidal cations exhibit absorptions in the range 18,000-21,000 cm^{-1} whilst the

trigonal bipyramidal cations show lower energy absorptions in the range 16,000-18,000 cm^{-1}.[8] Comparison of the electronic spectra of $[NiBr\{1,2\text{-}C_6H_4(CH_2SbMe_2)_2\}_2][ClO_4]$ and $[NiI\{1,2\text{-}C_6H_4(CH_2SbMe_2)_2\}_2][ClO_4]$ with related Ni(II) complexes (Table 4.13) suggests that both complexes adopt a trigonal bipyramidal geometry.

The factors which determine whether a five-coordinate Ni(II) complex will adopt a square-pyramidal or trigonal-bipyramidal geometry are widely disputed but previous studies have shown that the length of the carbon backbone has a major influence.[8] Ligands with a two carbon backbone produce square pyramidal complexes[32] whilst those with a three carbon backbone form complexes of both geometries dependent on the other ligand present. The *ortho*-xylyl distibine which has a four carbon backbone forms Ni(II) complexes with trigonal bipyramidal geometries, although the studies represented here are too limited to conclude that ligands with a four-carbon backbone will exclusively adopt this geometry.

Complex	Geometry	E_{max} / cm^{-1}
$[NiCl\{o\text{-}C_6H_4(AsMe_2)_2\}_2]Cl$ [33]	Square pyramidal	21,285, 25,895
$[NiCl\{o\text{-}C_6H_4(SbMe_2)_2\}_2]Cl$ [14]	Square pyramidal	18,300, 23,000
$[NiCl\{Me_2Sb(CH_2)_3SbMe_2\}_2][ClO_4]$ [8]	Square pyramidal	20,600
$[NiBr\{Me_2Sb(CH_2)_3SbMe_2\}_2][ClO_4]$ [8]	Square pyramidal	18,900
$[NiI\{Me_2Sb(CH_2)_3SbMe_2\}_2][ClO_4]$ [8]	Square pyramidal	18,100, 25,600
$[NiCl\{Me_2As(CH_2)_3AsMe_2\}_2][ClO_4]$ [8]	Trigonal bipyramidal	17,500
$[NiBr\{Me_2As(CH_2)_3AsMe_2\}_2][ClO_4]$ [8]	Trigonal bipyramidal	16,900, 27,700
$[NiI\{Me_2As(CH_2)_3AsMe_2\}_2][ClO_4]$ [8]	Trigonal bipyramidal	16,700, 26,500
$[NiBr\{1,2\text{-}C_6H_4(CH_2SbMe_2)_2\}_2][ClO_4]$	Trigonal bipyramidal	17,385, 22,935
$[NiI\{1,2\text{-}C_6H_4(CH_2SbMe_2)_2\}_2][ClO_4]$	Trigonal bipyramidal	17,337, 22,084

Table 4.13 – Selected UV/VIS data on Ni(II) diarsine and distibine complexes

4.2.5.1 Crystallographic analysis of $[NiI\{1,2\text{-}C_6H_4(CH_2SbMe_2)_2\}_2][ClO_4]$

Crystals of $[NiI\{1,2\text{-}C_6H_4(CH_2SbMe_2)_2\}_2][ClO_4]$ suitable for single crystal X-ray diffraction were grown by layering a solution of the complex in CH_2Cl_2 with Et_2O at

-20°C. The asymmetric unit contains two discrete Ni(II) cations and two perchlorate anions. Both cations are essentially identical and only one is shown (Figure 4.7, Tables 4.14 and 4.15). This structure represents the first nickel (II) complex of any stibine to be structurally characterised. The cation shows a pentacoordinate Ni(II) centre bonded to two xylyl ligands and one iodine in a distorted trigonal bipyramidal environment, consistent with the UV/VIS data. Sb(1), Sb(3) and I(1) lie in a plane with Sb(2) and Sb(4) occupying the axial positions of the trigonal bipyramid. The angles between the equitorial ligands are severely distorted from the ideal (117.98, 117.73 and 124.29°). Distortions from the ideal symmetry are also reflected in the displacements of Sb(2) and Sb(4) from the axial positions by ca. 9 degrees (∠Sb(2)-Ni(1)-Sb(4) = 171.28 °). These distortions from the idealised trigonal bipyramidal geometry reflect the strain in the two chelate rings.

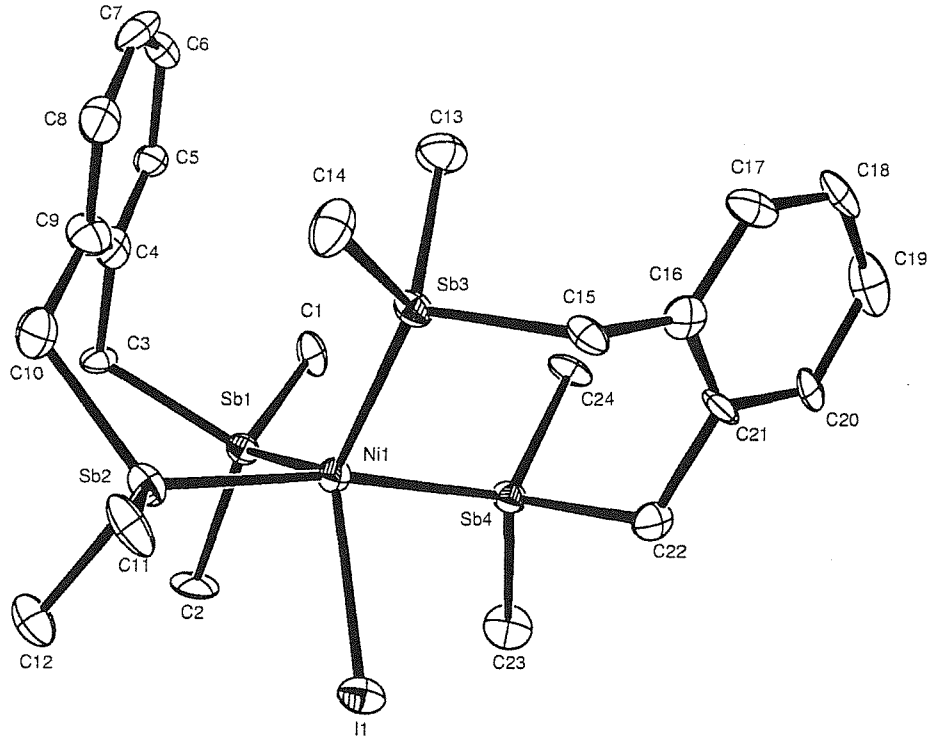

Figure 4.7 – View of the cation in the structure of $[NiI\{1,2\text{-}C_6H_4(CH_2SbMe_2)_2\}_2][ClO_4]$ with numbering scheme adopted. Ellipsoids are drawn at 40 % probability. H atoms are omitted for clarity.

Bond Lengths (Å)		*Bond Angles* (°)	
Ni(1)-Sb(1)	2.4590(19)	Sb(3)-Ni(1)-I(1)	117.73(7)
Ni(1)-Sb(2)	2.4367(19)	Sb(4)-Ni(1)-I(1)	85.75(6)
Ni(1)-Sb(3)	2.4678(19)	C(1)-Sb(1)-Ni(1)	120.4(4)
Ni(1)-Sb(4)	2.4424(19)	C(2)-Sb(1)-Ni(1)	119.2(5)
Ni(1)-I(1)	2.6194(19)	C(3)-Sb(1)-Ni(1)	114.6(4)
Sb(1)-C(1)	2.132(14)	C(10)-Sb(2)-Ni(1)	118.4(4)
Sb(1)-C(2)	2.141(14)	C(11)-Sb(2)-Ni(1)	118.5(5)
Sb(1)-C(3)	2.131(12)	C(12)-Sb(2)-Ni(1)	115.1(4)
Sb(2)-C(10)	2.135(16)	C(13)-Sb(3)-Ni(1)	115.9(4)
Sb(2)-C(11)	2.118(14)	C(14)-Sb(3)-Ni(1)	124.0(5)
Sb(2)-C(12)	2.157(15)	C(15)-Sb(3)-Ni(1)	116.5(4)
Sb(3)-C(13)	2.131(15)	C(22)-Sb(4)-Ni(1)	113.6(4)
Sb(3)-C(14)	2.134(14)	C(23)-Sb(4)-Ni(1)	113.3(5)
Sb(3)-C(15)	2.170(14)	C(24)-Sb(4)-Ni(1)	121.5(4)
Sb(4)-C(22)	2.140(14)	C(1)-Sb(1)-C(2)	101.9(6)
Sb(4)-C(23)	2.101(14)	C(1)-Sb(1)-C(3)	96.1(5)
Sb(4)-C(24)	2.150(13)	C(2)-Sb(1)-C(3)	100.7(6)
		C(10)-Sb(2)-C(11)	102.0(7)
Bond Angles (°)		C(10)-Sb(2)-C(12)	98.8(7)
Sb(1)-Ni(1)-Sb(2)	89.36(6)	C(11)-Sb(2)-C(12)	100.8(6)
Sb(1)-Ni(1)-Sb(3)	124.29(7)	C(13)-Sb(3)-C(14)	100.1(7)
Sb(1)-Ni(1)-Sb(4)	93.20(6)	C(13)-Sb(3)-C(15)	100.2(6)
Sb(1)-Ni(1)-I(1)	117.98(7)	C(14)-Sb(3)-C(15)	95.8(6)
Sb(2)-Ni(1)-Sb(3)	95.19(6)	C(22)-Sb(4)-C(23)	106.4(6)
Sb(2)-Ni(1)-Sb(4)	171.31(8)	C(22)-Sb(4)-C(24)	100.0(6)
Sb(2)-Ni(1)-I(1)	85.72(6)	C(23)-Sb(4)-C(24)	100.0(6)
Sb(3)-Ni(1)-Sb(4)	90.23(6)		

Table 4.14 - Selected Bond Lengths (Å) and angles (°) for $[NiI\{1,2\text{-}C_6H_4(CH_2SbMe_2)_2\}_2][ClO_4]$

Table 4.15 - Crystal Data and Structure Refinement Details for $[NiI\{1,2\text{-}C_6H_4(CH_2SbMe_2)_2\}_2][ClO_4]$

compound	$[NiI\{1,2\text{-}C_6H_4(CH_2SbMe_2)_2\}_2][ClO_4]$
empirical formula	$C_{24}H_{40}ClINiO_4Sb_4$
fw	1100.62
cryst. system	triclinic
space group	P-1 (No. 2)
a (Å)	9.4620(3)
b (Å)	13.6084(5)
c (Å)	27.1456(7)
α	95.815(2)
β	95.742(2)
γ (°)	107.789(2)
volume ($Å^3$)	3279.28(18)
Z	4
density (calc.) (mg / m^3)	2.229
abs coef (mm^{-1})	4.866
F(000)	2072
total no. of obsns.	44483 (R_{int} = 0.1082)
no. of unique obsns.	7933
min, max transmission	0.789, 0.883
no. of parameters, restraints	622, 0
goodness-of-fit on F^2	0.968
R1, wR2 ($I>2\sigma(I)$)[b]	0.066, 0.146
R1, wR2 (all data)	0.148, 0.174

Temperature = 120 K; wavelength (Mo-Kα) = 0.71073 Å; θ (max) = 27.5 deg.

[b] $R1 = \sum ||F_0| - |F_c|| / \sum |F_0|$ $wR_2 = [\sum w(F_0^2 - F_c^2)^2 / \sum wF_0^4]^{1/2}$

4.3 Conclusions

The coordination chemistry of the novel ligand 1,2-$C_6H_4(CH_2SbMe_2)_2$ has been investigated with a wide range of transition metal halides. The results demonstrate that 1,2-$C_6H_4(CH_2SbMe_2)_2$ is an extremely versatile ligand and can coordinate to a wide range of transition metals, forming stable seven membered chelate rings. Although the formation of seven membered chelate rings is unfavourable all of the complexes isolated are reasonably stable and show no signs of ligand decomposition via Sb-C bond cleavage.

Although antimony is a soft donor atom the results have shown that 1,2-$C_6H_4(CH_2SbMe_2)_2$ can form complexes with a range of both soft and hard metal centres in medium oxidation states, including Pt(II), Pd(II), Ni(II) and Co(III).

Several of the complexes have been characterised by single crystal X-ray diffraction. There are very few structurally characterised distibine complexes and those containing chelating ligands are extremely rare. The crystal structure of [NiI{1,2-$C_6H_4(CH_2SbMe_2)_2$}$_2$][ClO_4] represents the first structurally characterised nickel (II) complex of any antimony ligand. In all cases the structures are distorted from the regular geometries by varying degrees, reflecting the strain involved in the formation of the chelate ring.

4.4 Experimental

General Data. All preparations were conducted under a dinitrogen atmosphere, and the Ag(I) complex was stored in a sealed container wrapped in aluminium foil. $PtCl_2$, $PdCl_2$ and hydrated $RhCl_3$ were obtained from Johnson Matthey and used as received. $[Cu(MeCN)_4][BF_4]$ was prepared following the literature procedure.[3]

Synthesis of $[Cu\{1,2\text{-}C_6H_4(CH_2SbMe_2)_2\}_2][BF_4]$: $[Cu(MeCN)_4][BF_4]$ (77 mg, 0.25 mmol) was added to a solution of $1,2\text{-}C_6H_4(CH_2SbMe_2)_2$ (0.20 g, 0.49 mmol) in CH_2Cl_2 (30 mL). The reaction was stirred at RT overnight. The solvent volume was reduced *in vacuo* to ca. 5 mL and diethyl ether added to give a white precipiate which was isolated by filtration and dried *in vacuo*. Yield = 43 mg (18 %). Required for $[C_{24}H_{40}BCuF_4Sb_4].CH_2Cl_2$ C = 28.58, H = 4.03 %; found C = 28.58, H = 4.12. ^{1}H NMR ($CDCl_3$): δ 1.07 (s, 24H, C<u>H</u>$_3$), 3.16 (s, 8H, C<u>H</u>$_2$), 6.97-7.02 (m, 8H, Ar-C<u>H</u>). ^{63}Cu NMR (DMF /$CDCl_3$): δ -171. IR (CsI disc / cm^{-1}): 2919 w, 2355 w, 1684 w, 1649 w, 1596 w, 1567 w, 1484 m, 1408 m, 1361 m, 1296 w, 1214 w, 1190 w, 1061 vs br, 832 s, 808 s, 756 s, 615 w, 521 s.

Synthesis of $[Cu\{1,3\text{-}C_6H_4(CH_2SbMe_2)_2\}_2][BF_4]$: The reaction was carried out as above using $1,3\text{-}C_6H_4(CH_2SbMe_2)_2$ (0.20 g, 0.49 mmol) and $[Cu(MeCN)_4][BF_4]$ (77 mg, 0.25 mmol). Yield 72 mg (30 %). Required for $[C_{24}H_{40}BCuF_4Sb_4].1/2Et_2O$ C = 31.13, H = 4.52 %; found C = 30.98, H = 4.36 %. ^{1}H NMR (d_6-DMSO): δ 0.80 (s, 24H, C<u>H</u>$_3$), 2.95 (s, 8H, C<u>H</u>$_2$), 6.81-7.26 (m, 8H, Ar-C<u>H</u>).

Synthesis of $[Ag\{1,2\text{-}C_6H_4(CH_2SbMe_2)_2\}_2][CF_3SO_3]$: $AgCF_3SO_3$ (63 mg, 0.25 mmol) was added to a solution of $1,2\text{-}C_6H_4(CH_2SbMe_2)_2$ (0.20 g, 0.49 mmol) in CH_2Cl_2 (30 mL). The reaction was stirred under nitrogen overnight in a foil-wrapped flask to protect the solution from bright light. The resulting white precipitate was isolated by filtration and dried *in vacuo*. Yield 0.12 g (46 %). The sample decomposed within 12 h so analytical data could not be obtained. ^{1}H NMR (d_6-DMSO): δ 1.07 (s, 24H, C<u>H</u>$_3$), 3.18 (s, 8H, C<u>H</u>$_2$), 7.01-7.02 (m, 8H, Ar-C<u>H</u>).

ES^+ mass spectrum (MeCN): found *m/z* 922, 556, 515, 189. Calc. for $[^{107}Ag\{1,2\text{-}C_6H_4(CH_2{}^{121}SbMe_2)_2\}_2]^+$ 919, $[^{107}Ag\{1,2\text{-}C_6H_4(CH_2{}^{121}SbMe_2)_2\}MeCN]^+$ 554, $[^{107}Ag\{1,2\text{-}C_6H_4(CH_2{}^{121}SbMe_2)_2\}]^+$ 513, $[^{107}Ag(MeCN)_2]^+$ 189. IR spectrum (Nujol mull / cm^{-1}): 2725 w, 2677w, 2359 w, 2333 w, 2295 w, 1695 w, 1595 w, 1564 w, 1275vs, 1247 vs, 1224 m, 1160 vs, 1102 m, 1027 vs, 973 w, 880 w, 819 m, 762 s, 723 m, 637 vs, 573 m, 535 m, 515 m, 469 w, 441 w, 413 w, 395 w, 335 w, 321 w, 273 w, 243 w, 215 w.

Synthesis of $[PtCl_2\{1,2\text{-}C_6H_4(CH_2SbMe_2)_2\}]$: $PtCl_2$ (0.13 g, 0.49 mmol) was refluxed in MeCN (40 mL) under nitrogen for 3 h and allowed to cool. A solution of 1,2-$C_6H_4(CH_2SbMe_2)_2$ (0.20 g, 0.49 mmol) in MeCN (10 mL) was added and the reaction stirred at RT overnight. The resulting yellow precipitate was collected by filtration and dried *in vacuo*. Yield 0.12 g (36 %). Required for $[C_{12}H_{20}Cl_2PtSb_2]$ C = 21.39, H =2.99 %; found C = 21.59, H = 2.81 %. ^1H NMR (d_6-DMSO): δ 1.27 (s, 12H, $C\underline{H}_3$), 3.70 (s, 4H $C\underline{H}_2$), 7.12-7.34 (m, 4H, Ar-C<u>H</u>). ES^+ mass spectrum (MeCN): found *m/z* 678. Calc. for $[^{195}Pt^{35}Cl\{1,2\text{-}C_6H_4(CH_2{}^{121}SbMe_2)\}MeCN]^+$ 677. IR spectrum (CsI disc / cm^{-1}): 3002 w, 2908 w, 2390 w, 2249 w, 1655 w, 1631 w, 1559 w, 1487 s, 1449 m, 1430 w, 1405 w, 1358 m, 1296 w, 1258 w, 1214 m, 1129 s, 1117 m, 1091 w, 1038 m, 991 w, 950 w, 847 vs, 829 vs, 782 w, 756 vs, 726 w, 709 m, 685 w, 544 vs.

Synthesis of $[PdCl_2\{1,2\text{-}C_6H_4(CH_2SbMe_2)_2\}]$: $[PdCl_2(MeCN)_2]$ (0.13 g, 0.49 mmol) was added to a solution of 1,2-$C_6H_4(CH_2SbMe_2)_2$ (0.20 g, 0.49 mmol) in CH_2Cl_2 (30 mL). The reaction was stirred at RT for 2 h and the resulting yellow precipiate was collected by filtration and dried *in vacuo*. Yield 0.11 g (38 %). Required for $[C_{12}H_{20}Cl_2PdSb_2]$ C =24.63, H = 3.45 %; found C = 25.49, H = 3.73 %. ^1H NMR (d_6-DMSO): δ 1.41 (s, 12H, $C\underline{H}_3$), 3.52 (s, 4H, $C\underline{H}_2$), 6.9-7.3 (m, 4H, Ar-C<u>H</u>). ES^+ mass spectrum (MeCN): found *m/z* 590. Calc. for $[^{106}Pd^{35}Cl\{1,2\text{-}C_6H_4(CH_2{}^{121}SbMe_2)_2\}MeCN]^+$ 588. IR spectrum (CsI disc / cm^{-1}): 3025 w, 2908 w, 2390 w, 1637 m, 1490 s, 1485 m, 1408 w, 1355 m, 1267 m, 1208 m, 1120 s, 1084 w, 1043 m, 1035 m, 848 vs, 872 vs, 774 s, 753 w, 728 s, 698 m, 548 s, 539 s.

Synthesis of $[Pt\{1,2\text{-}C_6H_4(CH_2SbMe_2)_2\}_2][PF_6]_2$: $TlPF_6$ (54 mg, 0.15 mmol) was added to a solution of $[PtCl_2\{1,2\text{-}C_6H_4(CH_2SbMe_2)_2\}]$ (50 mg, 0.074 mmol) in nitromethane (30 mL) and the reaction stirred overnight. The reaction was filtered through Celite to remove TlCl and a solution of $1,2\text{-}C_6H_4(CH_2SbMe_2)_2$ (30 mg, 0.074 mmol) in nitromethane (10 mL) was added. The resulting orange solution was stirred at RT for 4 h. The solvent volume was reduced *in vacuo* to ca. 5 mL and diethyl ether added to yield a yellow/orange solid which was collected by filtration and dried *in vacuo*. Yield 70 mg (73 %). Required for $[C_{24}H_{40}F_{12}P_2PtSb_4].2CH_2Cl_2$ C = 21.23, H = 3.02 %; found C = 21.10, H = 2.90 %. ^1H NMR (d_6-DMSO): δ 1.44 (s, 24H, C<u>H</u>$_3$), 3.84 (s, 8H, C<u>H</u>$_2$), 7.07-7.10 (m, 8H, Ar-C<u>H</u>). ES^+ mass spectrum (MeCN): found *m/z* 1136, 1012. Calc. for $[^{195}Pt\{1,2\text{-}C_6H_4(CH_2{}^{121}SbMe_2)_2\}\{1,2\text{-}C_6H_4(CH_2{}^{121}SbMe_2)(CH_2{}^{121}SbMe)P^{18}F_6]^+$ 1131, $[^{195}Pt\{1,2\text{-}C_6H_4(CH_2{}^{121}SbMe_2)_2\}_2]^+$ 1007. IR spectrum (Nujol mull / cm^{-1}): 2356 w, 2036 w, 1749 w, 1602 w, 1304 w, 1259 w, 1153 w, 1078 w, 969 w, 841 s, 733 w, 720 s, 555 m, 491 w, 389 w, 310 w.

Synthesis of $[Pd\{1,2\text{-}C_6H_4(CH_2SbMe_2)_2\}_2][PF_6]_2$: $PdCl_2$ (43 mg, 0.24 mmol) was refluxed in MeCN (30 mL) for 1.5 h. A solution of $1,2\text{-}C_6H_4(CH_2SbMe_2)_2$ (0.10 g, 0.24 mmol) in MeCN (5 mL) was added and the reaction stirred at RT for 2 h. More MeCN (30 mL) was added to dissolve the yellow precipitate which had formed. $TlPF_6$ (0.18 g, 51 mmol) was added and the reaction stirred overnight. The reaction was filtered through Celite to remove TlCl and a solution of $1,2\text{-}C_6H_4(CH_2SbMe_2)_2$ (0.10 g, 0.24 mmol) in MeCN (10 mL) was added. The resulting solution was stirred at RT for 2 h before removing the solvent *in vacuo*. The residue was taken up in CH_2Cl_2 (ca. 25 mL), filtered and concentrated to ca. 5 mL. The yellow solid was filtered off, rinsed with diethyl ether and dried *in vacuo*. Yield 0.25 g (76 %). Required for $[C_{24}H_{40}F_{12}P_2PdSb_4]$ C = 23.79, H = 3.33 %; found C = 24.11, H = 3.59 %. ^1H NMR (d_6-acetone): δ 1.56 (s, 24H, C<u>H</u>$_3$), δ 4.14 (s, 8H, C<u>H</u>$_2$), 7.10-7.25 (m, 8H, Ar-C<u>H</u>). IR spectrum (Nujol mull / cm^{-1}): 2727 w, 2672 w, 1601 w, 1562 m, 1301 w, 1154 w, 1110 w, 1054 w, 1040 w, 971 w, 843 vs, 755 m, 738 m, 722 s, 556 s, 528 sh, 435 w, 394 w, 325 w, 312 w, 273 w.

Synthesis of $[RhCl_2\{1,2\text{-}C_6H_4(CH_2SbMe_2)_2\}_2][BF_4]$: A solution of $RhCl_3.3H_2O$ (49 mg, 0.19 mmol) in H_2O (ca. 2 mL) was added to a solution of $1,2\text{-}C_6H_4(CH_2SbMe_2)_2$ (0.15 g, 0.37 mmol) in EtOH (30 mL). The reaction was stirred for 2 h at RT. The solvent volume was reduced *in vacuo* to ca. 10 mL and a solution of NH_4BF_4 (29 mg, 0.28 mmol) in EtOH (5mL) was added. The reaction was stirred at RT for 1 h and the solvent removed *in vacuo*. The yellow residue was taken up in CH_2Cl_2 (ca. 3 mL) and diethyl ether added to yield a yellow solid. Yield 81 mg (41 %). Required for $[C_{24}H_{40}BCl_2F_4RhSb_4]$ C = 26.79, H = 3.75 %; found C = 26.03, H = 3.70 %. ^1H NMR ($CDCl_3$): δ 1.02 (s, 6H, C<u>H</u>$_3$), 1.47 (m, 18H, C<u>H</u>$_3$), 3.62-3.67 (4H, dd, C<u>H</u>$_2$), 4.07-4.14 (m, 4H, C<u>H</u>$_2$), 7.15-7.31 (m, 8H, Ar-C<u>H</u>). ES^+ mass spectrum (MeCN): found *m/z* 989. Calc. for $[^{103}Rh^{35}Cl_2\{1,2\text{-}C_6H_4(CH_2{}^{121}SbMe_2)_2\}_2]^+$ 985. UV spectrum (E_{max} / cm^{-1}, (ε_{mol} / dm^3 mol^{-1} cm^{-1}, CH_2Cl_2)): 27,100 (1400). IR spectrum (Nujol mull / cm^{-1}): 2733 w, 2667 w, 1303 w, 1261 w, 1169 w, 1151 w, 1055 s, 973 w, 851 m, 814 m, 768 w, 722 s, 547 w, 432 w, 394 w, 311 w, 300 w, 274 w, 242 w.

Synthesis of $[CoBr_2\{1,2\text{-}C_6H_4(CH_2SbMe_2)_2\}_2][BPh_4]$: A solution of $1,2\text{-}C_6H_4(CH_2SbMe_2)_2$ (0.10 g, 0.25 mmol) in dry nitromethane (10 mL) was added to a solution of anhydrous $CoBr_2$ (27 mg, 0.12 mmol) in dry nitromethane (20 mL). The reaction was stirred for 30 mins under nitrogen before replacing the nitrogen inlet with a drying tube packed with calcium chloride to allow entry of dry air. $NaBPh_4$ (43 mg, 0.13 mmol) was added and the reaction stirred for 1.5 h. The reaction was filtered and the solvent removed *in vacuo*. The brown residue was dissolved in dry CH_2Cl_2 (5 mL) and filtered to removed NaBr. Dry hexane was added to yield a dark brown solid. Yield 37 mg (22 %). ^1H NMR ($CDCl_3$): δ 1.03 (s, C<u>H</u>$_3$), 1.12 (s, C<u>H</u>$_3$), 1.22 (s, C<u>H</u>$_3$), 1.53 (s, C<u>H</u>$_3$), 1.57 (s, C<u>H</u>$_3$), 3.49 (s, C<u>H</u>$_2$), 6.76-7.62 (m, Ar-C<u>H</u>). ^{59}Co NMR (CH_2Cl_2 / $CDCl_3$): δ 4550 ($w_{1/2}$ = 22,000 Hz). Electrospray mass spectrum (MeCN): found *m/z* 1034. Calc. for $[^{59}Co^{79}Br_2\{1,2\text{-}C_6H_4(CH_2{}^{121}SbMe_2)_2\}_2]^+$ 1029. UV spectrum (E_{max} /cm^{-1} (ε_{mol} / dm^3 mol^{-1} cm^{-1}, CH_2Cl_2)): 17,300 sh, 20,400 (2440).

Synthesis of [NiBr{1,2-$C_6H_4(CH_2SbMe_2)_2$}$_2$][ClO_4]: As solution of 1,2-$C_6H_4(CH_2SbMe_2)_2$ (0.13 g, 0.32 mmol) in dry BuOH (10 mL) was added to a warm solution of $NiBr_2.6H_2O$ (26 mg, 0.08 mmol) and $[Ni(ClO_4)_2].6H_2O$ (29 mg, 0.08 mmol) in BuOH (10 mL). The purple solution was stirred under nitrogen for 10 mins. The resulting dark blue solid was isolated by filtration and dried *in vacuo*. Yield 81 mg (48 %). ^{1}H NMR ($CDCl_3$): δ 1.21 (s, 24H, C<u>H</u>$_3$), 3.53 (s, 8H, C<u>H</u>$_2$), 7.01-7.05 (m, 8H, Ar-C<u>H</u>). UV spectrum (E_{max} / cm^{-1} (ε_{mol} / dm^3 mol^{-1} cm^{-1}, CH_2Cl_2)): 22,900 (1450), 17,400 (1100). IR spectrum (Nujol mull / cm^{-1}): 2732 w, 2659 w, 1212w, 1060 s, 977 w, 830 w, 812 m, 799 m, 752 m, 741 w, 723 w, 620 s, 539 sh, 523 s, 462 w, 437 m, 303 w, 271 w, 207 m.

Synthesis of [NiI{1,2-$C_6H_4(CH_2SbMe_2)_2$}$_2$][ClO_4]: Reaction was carried out as above using 1,2-$C_6H_4(CH_2{}^{121}SbMe_2)_2$ (89 mg, 0.22 mmol), $NiI_2.6H_2O$ (23 mg, 0.05 mmol) and $[Ni(ClO_4)_2].6H_2O$ (20 mg, 0.05 mmol) to give the product as a dark green solid. Yield 36 mg (30 %). Required for [$C_{24}H_{40}ClINiO_4Sb_4$] C = 26.20, H = 3.70 %; found C = 26.15, H = 3.70 %. ^{1}H NMR ($CDCl_3$): δ 1.30 (s, 24H, C<u>H</u>$_3$), 3.67 (s, 8H, C<u>H</u>$_2$), 7.01-7.04 (m, 8H, Ar-C<u>H</u>). UV spectrum (E_{max} / cm^{-1} (ε_{mol} / dm^3 mol^{-1} cm^{-1}, CH_2Cl_2)): 22,100 (248), 17,300 (244). IR spectrum (Nujol mull / cm^{-1}): 2727 w, 2667 w, 1303 w, 1261 w, 1212 w, 1169 w, 1073 s, 976 w, 892 w, 831 s, 814 s, 803 s, 752 s, 723 s, 666 w, 620 s, 522 m, 465 w, 439 m, 417 w, 395 w, 372 w, 349 w, 322 w, 300 w, 274 m, 244 m.

4.5 References

1. A. M. Hill, W. Levason and M. Webster, *Inorg. Chem.*, **35**, (1996), 3428.
2. J. R. Black, W. Levason, M. D. Spicer and M. Webster, *J. Chem. Soc., Dalton Trans.*, (1993), 3129.
3. A. Hetherington, W. Levason and M. D. Spicer, *Polyhedron*, **9**, (1990), 1609.
4. T. Even, A. R. J. Genge, A. M. Hill, N. J. Holmes, W. Levason and M. Webster, *J. Chem. Soc., Dalton Trans.*, (2000), 655.
5. W. Levason and C. A. McAuliffe, *J. Coord. Chem*, **4**, (1974), 47.
6. A. F. Chiffey, J. Evans, W. Levason and M. Webster, *Organometallics*, **14**, (1995), 1522.
7. H. A. Brune, R. Klotzbuecher and G. Schmidtberg, *J. Organomet. Chem.*, **371**, (1989), 113.
8. R. J. Dickinson, W. Levason, C. A. McAuliffe and R. V. Parish, *J. Chem. Soc., Dalton Trans.*, (1978), 177.
9. W. Levason and C. A. McAuliffe, *Inorg. Chem.*, **13**, (1974), 2765.
10. R. J. Dickinson, W. Levason, C. A. McAuliffe and R. V. Parish, *J. Chem. Soc., Chem. Commun.*, (1975), 272.
11. D. J. Gulliver, W. Levason and K. G. Smith, *J. Chem. Soc., Dalton Trans.*, (1981), 2153.
12. W. Levason and C. A. McAuliffe, *Inorg. Nucl. Chem. Letters*, **12**, (1976), 849.
13. E. Shewchuk and S. B. Wild, *J. Organomet. Chem.*, **71**, (1974), C1.
14. E. Shewchuk and S. B. Wild, *J. Organomet. Chem.*, **128**, (1977), 115.
15. R. G. Goel and R. G. Montemayor, *J. Coord. Chem.*, **8**, (1978), 1.
16. H. C. Jewiss, W. Levason, M. D. Spicer and M. Webster, *Inorg. Chem.*, **26**, (1987), 2102.
17. A. M. Hill, W. Levason and M. Webster, *Inorg. Chim. Acta*, **271**, (1998), 203.
18. A. F. Chiffey, J. Evans, W. Levason and M. Webster, *Organometallics*, **15**, (1996), 1280.
19. N. J. Holmes, W. Levason and M. Webster, *J. Chem. Soc., Dalton Trans.*, (1998), 3457.

20. N. R. Champness and W. Levason, *Coord. Chem. Rev.*, **133**, (1994), 115.

21. N. N. Greenwood, *J. Chem. Soc.*, (1959), 3811.

22. J. Mason, 'Multinuclear NMR', Plenum Press, New York, (1987).

23. A. L. Rheingold and M. E. Fountain, *J. Crystallogr. Spectrosc. Res.*, **14**, (1984), 549.

24. A. Baiada, F. H. Jardine, R. D. Willett and K. Emerson, *Inorg. Chem.*, **30**, (1991), 1365.

25. R. Schmutzler, 'Advance in Fluorine Chemistry, Series 5', Butterworths, London, (1965).

26. A. M. Hill, W. Levason, S. R. Preece and M. Webster, *Polyhedron*, **16**, (1997), 1307.

27. J. M. Brown, T. Kemmitt and W. Levason, *J. Chem. Soc., Dalton Trans.*, (1990), 1513.

28. B. K. Baylis and J. C. Bailar, *Inorg. Chem.*, **13**, (1974), 1133.

29. W. Levason, S. R. Preece and C. Frampton, *Polyhedron*, **15**, (1996), 2719.

30. H. C. Jewiss, W. Levason and M. Webster, *Inorg. Chem.*, **25**, (1986), 1997.

31. M. F. Ludmann-Obier, M. Dartiguenave and Y. Dartiguenave, *Inorg. Nucl. Chem. Lett.*, **10**, (1974), 149.

32. W. Levason and C. A. McAuliffe, *Inorg. Chim. Acta*, **11**, (1974), 33.

33. J. R. Preer and H. B. Gray, *J. Am. Chem. Soc.*, **92**, (1970), 7306.

Chapter 5

Ag(I) and Group 6 and 7 Metal Carbonyl Complexes with Acyclic Mixed Donor P/O and P/S Ligands

5.1 Introduction

5.1.1 Coordination Chemistry of Mixed P/O Donor Ligands

A wide range of transition metal complexes with mixed P/O donor ligands have been reported in the literature,[1] and almost all form *trans*-metal complexes with the ligand coordinating via the phosphine functions alone.

Kapoor and co-workers have investigated the coordination chemistry of the P_2O donor ligand $Ph_2PCH_2(o\text{-}C_6H_4)O(o\text{-}C_6H_4)CH_2PPh_2$ (pop) and have shown it to form monomeric, *trans*-spanning square planar complexes of the type *trans*-$[M(pop)X_2]$ (where M = Ni, Pd, Pt or Rh and X = Cl, Br, I, N_3, NCS, CN or NO_3].[2] The related ligand $Ph_2PCH_2(m\text{-}C_6HF_3)O(m\text{-}C_6HF_3)CH_2PPh_2$ (*m*-CF_3) also forms monomeric square planar complexes of the type $[M(m\text{-}CF_3)X_2]$ (where M = Ni, Pd or Pt and X = Cl).[3]

Trans-spanning complexes have also been obtained with the mixed P/O donor ligands $Ph_2P(CH_2CH_2O)_nCH_2CH_2PPh_2$ (where n = 1-3). Reaction of these ligands with dichlorotetracarbonyl di-rhodium gives complexes of the form [Rh(L)(CO)Cl].[4] These complexes can in turn be treated with $AgPF_6$ to yield $[Rh(L)(CO)]PF_6$ which exhibit unusual coordination properties, the crystal structures dependent on the value of n.[5] When n = 1 the ligand is tridentate, coordinating strongly to rhodium via both the phosphine functions and the oxygen atom. When n = 2 the ligand binds through the terminal phosphines to from a large chelate ring. Encapsulated within the ring is an ethanol molecule interacting weakly with the rhodium centre and hydrogen bonded to one oxygen atom in the chain. When n = 3 the ligand again binds solely through the phosphine functions with a tightly bound water molecule within the chelate ring hydrogen bonded to the two terminal ether functions of the ligand.

Similar results have been obtained with Rh(I) complexes of the related P/O containing ligands $Ph_2P(o\text{-}C_6H_4((CH_2)_nO)_2\text{-}o\text{-}C_6H_4)PPh_2$ (n = 2 or 3) and $Me(Ph)P\text{-}(o\text{-}C_6H_4O((CH_2)_2O)_2\text{-}o\text{-}C_6H_4)P(Ph)Me$. IR and NMR studies indicate formation of the *trans*-complexes by binding of the ligand through the terminal phosphines and ether functions.[6]

Ether interactions with soft metal centres are unusual and thus these examples illustrate the importance of chelation in stabilising weak metal-ligand interactions.

Edwards *et al* have prepared a series of early transition metal complexes with the mixed P/O-donor ligand $Ph_2PCH_2P(CH_2CH_2OEt)_2$.[7] Reaction with $[Mo(CO)_3\{2,4,6\text{-}(C_6H_3Me_3)\}]$ affords the distorted octahedral complex $[Mo(CO)_3L_2]$ with one ligand acting as a P/O chelate and the other bound solely through the P atom.

Varshney and Gray have prepared a series of metallacrown ether complexes with the longer chain mixed donor ligands $Ph_2P(CH_2CH_2O)_nCH_2CH_2PPh_2$ (where n = 3-5).[8, 9] The ligands *cis*-coordinate to Mo and Pt via the phosphines resulting in the formation of large ring metallocyclic species which are capable of binding alkali metal cations. Photolysis of the *cis*-$[Mo(CO)_4(L)]$ complexes or reaction with catalytic amounts of $HgCl_2$ results in isomerisation to the corresponding *trans*-species.[10] Reaction of $[PtCl_2(Ph_2P(CH_2CH_2O)_nCH_2CH_2PPh_2)]$ where n = 4 with $AgBF_4$ yields the cationic $[Pt(L)(H_2O)]BF_4$ complex which shows an unusual structure in the solid state. The platinum centre coordinates to both phosphine groups, an ether oxygen and a water molecule resulting in a distorted *cis*-square planar geometry. It is surprising that H_2O coordination is favoured as the chelate effect should favour coordination to a second ether function. The preferential coordination to water appears to be due to hydrogen bonding between the two ether oxygens and the two protons on water.[9]

5.1.2 Coordination Chemistry of $Ph_2P(CH_2)_2O(CH_2)_2O(CH_2)_2PPh_2$ (L^1)

The chemistry of L^1 was first investigated by Dapporto and Sacconi who synthesised the diamagnetic complex $[Ni(L^1)I_2]$. X-ray crystallographic analysis shows the ligand to coordinate via a P_2 donor set to give a coordination geometry intermediate between square planar and tetrahedral.[11] Although the Ni-O bond distances are large (3.20(7) and 3.16(6) Å) it was thought that this unusual geometry was stabilised by Ni---O interactions.

Further studies into the coordination chemistry of L^1 with Ni(II) have been carried out by Hill and Taylor[12] who have prepared the complexes $[Ni(L^1)X_2]$ (where X = Cl, Br, I or NCS). Structural characterisation of $[Ni(L^1)(NCS)_2]$ reveals a *trans*-square planar coordination at Ni(II), with the ligand coordinated through the P atoms and the thiocyanate anions coordinated through the N donor atoms.

The same authors have also reported studies of L^1 with Pt(II) and Pd(II). Both *cis* and *trans* Pd complexes have been prepared with the ligand. Both complexes adopt slightly distorted square planar geometries and show coordination via the P donor atoms only.[13]

More recently our research group has prepared Cu(I), Ag(I) and Au(I) complexes with L^1 which all show coordination through the P atoms alone.[14] Crystallographic analysis of the $[Ag(L^1)]BF_4$ complex shows L^1 acting as a *trans*-chelate to give an approximately linear coordination at Ag. The analogous $[Au(L^1)]PF_6$ complex adopts a similar structure.[14]

5.1.3 Coordination Chemistry of Mixed Donor P/S Ligands

The mixed P/S donor ligand $Ph_2P(CH_2)_3S(CH_2)_3S(CH_2)_3PPh_2$ forms four-coordinate square planar complexes of the type $[M(L)]ClO_4$ (where M = Ni, Pd or Pt) with all four donor atoms of the ligand coordinated.[15] Five coordinate trigonal bipyramidal complexes $[M(L)X]ClO_4$ (where M = Ni and X = Cl, Br I, M = Pd or Pt and X = I, M = Co and X = Cl) have also been synthesised and again show coordination of the ligand through a P_2S_2 donor set.[15]

The related ligands $Ph_2PCH_2CH_2SEt$ and $Ph_2P(CH_2)_2S(CH_2)_3S(CH_2)PPh_2$ also form square planar complexes with Ni(II).[16] Both ligands coordinate via both the phosphines and thioether functions with the S atoms in a *trans*-arrangement.

Our research group has studied the P_2S_2 donor ligand $Ph_2P(CH_2)_2S(CH_2)_3S(CH_2)_2PPh_2$ and its coordination with Cu(I), Ag(I) and Au(I).[17, 18] Crystallographic analysis of $[Au(L)]^+$ reveals primary coordination via the terminal phosphines with long range Au-thioether interactions (Au---S = 3.097(5), 3.101(6) Å). The structure appears to be a compromise between linear coordination favoured by Au(I) and 4-coordination favoured by the ligand.[18]

The related P_2S_2 donor ligand $Ph_2P(CH_2)_2S(o\text{-}C_6H_4)S(CH_2)_2PPh_2$ reacts with $[Cu(MeCN)_4]PF_6$ to form the complex $[Cu(L)]PF_6$.[18] The structure shows Cu(I) coordinated to a distorted tetrahedral arrangement of four ligand donor atoms. Co(III) and Cr(III) complexes with the ligand have also been reported [19], and in each case the ligand

coordinates via both the phosphine and thioether functions to give *cis*-dihalo distorted octahedral species.

5.1.4 Coordination Chemistry of $Ph_2P(CH_2)_2S(CH_2)_2S(CH_2)_2PPh_2$ (L^2)

The research group has previously reported several transition metal complexes with this ligand.[17, 20] Reaction of $[Cu(MeCN)_4]PF_6$ with one molar equivalent of the ligand affords the complex $[Cu(L^2)]PF_6$. Crystallographic analysis of this compound shows the Cu(I) ion tetraligated to L^2 via all four donor atoms, resulting in a severely distorted and flattened tetrahedral geometry. The analogous Au complex shows coordination via both the phosphine functions with additional long range weak thioether interactions.[20] A much more unusual structure is adopted by $[Au_2(L^2)_2]Cl_2$ formed by the 1:1 reaction of L^2 with [AuCl(tht)]. The crystal structure shows a linear P_2 donor set at each Au giving a helical metallocyclic cavity which contains a Cl^- anion.[17]

The coordination chemistry of L^2 has also been investigated with Rh(III) and Ir(III) to form complexes with the general formula $[MCl_2(L^2)]^+$, and with Ru(II) to form $[RuCl_2(L^2)]$.[21] Both Ru and Rh form distorted octahedral complexes with the metal coordinated to all four donor atoms of the ligand and to two mutally *cis*-chloride ligands.

Complexes with Pt(II) and Pd(II) have also been reported.[22] In both cases solution ^{31}P NMR studies show a large positive chemical shift indicative of the formation of a five membered chelate ring, resulting from P_2S_2 coordination. Single crystal X-ray diffraction studies confirm the retention of this geometry in the solid state. L^2 also supports Pt(IV) in *cis*-$[PtCl_2(L^2)]^{2+}$ which is assigned a distorted octahedral geometry.[22]

5.2 Results and Discussion

5.2.1 Ag(I) complexes of $Ph_2P(CH_2)_2O(CH_2)_2O(CH_2)_2PPh_2$ (L^1)

Addition of one molar equivalent of L^1 to AgX ($X^- = ClO_4^-$, $CF_3SO_3^-$, NO_3^-, Cl^-, I^-) in degassed CH_2Cl_2 at 0°C (or at reflux for the Cl and I derivatives) gave colourless solutions. Concentration of the solutions followed by addition of Et_2O gave the products as white solids with formula $[Ag(L^1)][X]$. The reaction of $AgCF_3SO_3$ with 2 molar equivalents of L^1 repeatedly yielded the 2:3 Ag:L^1 complex $[Ag_2(L^1)_3][CF_3SO_3]_2$ with no evidence of a 2:1 Ag:L^1 complex. However reaction of L^1 with 2 molar equivalents of AgI yielded the dinuclear species $[(AgI)_2(L^1)]$. The electrospray mass spectra (ES^+) of the 1:1 Ag:L^1 complexes each show peaks with the correct isotopic distribution for $[Ag(L^1)]^+$ (*m/z* = 593, 595) (Figure 5.1), in addition the spectrum of $[Ag(L^1)I]$ shows peaks with the correct isotopic distribution for $[Ag_2(L^1)_2I]^+$ (*m/z* = 1313, 1315).

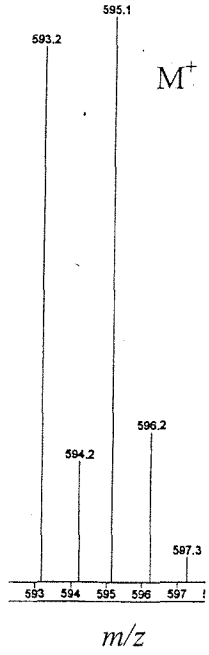

Figure 5.1 – ES^+ Mass Spectrum of $[Ag(L^1)]ClO_4$ (MeCN)

The ES^+ mass spectrum of $[Ag_2(L^1)_3][CF_3SO_3]_2$ shows peaks consistent with $[Ag(L^1)_2]^+$ (*m/z* = 1079, 1081) and $[Ag(L^1)]^+$ (*m/z* = 593, 595). These data together with ^1H NMR

spectroscopy and microanalyses confirm the stoichiometries as $Ag(L^1)X$ (X = ClO_4, CF_3SO_3, NO_3, Cl, I), $[Ag_2(L^1)_3][CF_3SO_3]_2$ and $[(AgI)_2(L^1)]$.

It is known that the magnitude of ^1J(Ag-P) coupling constants in silver phosphine complexes varies with the coordination number at Ag. As the coordination number increases the coupling constants become smaller.[23, 24] Therefore the solution coordination environment at Ag(I) in the range of complexes has been probed using $^{31}P\{^1H\}$ NMR spectroscopy. For all complexes the $^{31}P\{^1H\}$ NMR spectra show a single phosphorus environment with a resonance to high frequency of free L^1 (δ = -21.4 ppm), with the exception of $[(AgI)_2(L^1)]$ which shows a resonance to low frequency of free ligand. Upon cooling of the solutions two doublets were observed consistent with coupling to $^{107/109}Ag$ (both I = 1/2, 49% 51% abundant respectively). In all cases the ratio of the ^{107}Ag-P /^{109}Ag-P coupling constants is close to 0.87 which is consistent with the relative magnetogyric ratios $^{107}\gamma$ / $^{109}\gamma$ = 0.87 (10^7 rad.T^{-1}.s^{-1}).[25]

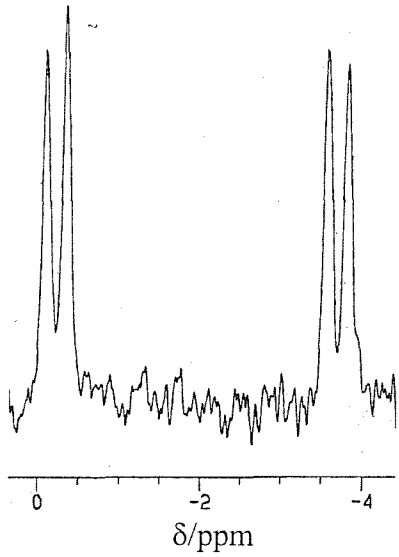

Figure 5.2 – $^{31}P\{^1H\}$ (145.8 MHz, $CH_2Cl_2/CDCl_3$) NMR spectrum of $[Ag(L^1)][ClO_4]$

The research group has shown previously that $^1J(^{107}$Ag-P) and $^1J(^{109}$Ag-P) for $[Ag(L^1)][BF_4]$ are 523 and 601 Hz respectively and a crystallographic analysis of the complex revealed two-coordinate Ag(I).[14] By comparison with this data it has been possible to deduce the coordination environment at Ag(I) for each of the complexes prepared. Chemical shifts and coupling constants for all the complexes discussed are given in Table 5.1.

Compound	δ ^{31}P (ppm)	^{1}J($^{107/109}$Ag-P) (Hz)
$Ag(L^1)BF_4$	-3.4	523, 601
$Ag(L^1)CF_3SO_3$	-1.4	511, 582
$Ag(L^1)ClO_4$	-0.7	522, 604
$Ag(L^1)NO_3$	-1.9	497, 568
$Ag(L^1)Cl$	-5.5	438, 505
$Ag(L^1)I$	-5.4	410, 473
$(AgI)_2(L^1)$	-22.9	458, 536
$Ag_2(L^1)_3(CF_3SO_3)_2$	-5.4	332, 380

Table 5.1 – $^{31}P\{^1H\}$ NMR data [a]

[a] Spectra recorded in $CH_2Cl_2/CDCl_3$ at 193 K

The significant reduction in the coupling constants observed for the Cl, I and NO_3 complexes (cf.the BF_4^- salt) is consistent with an increase in coordination number at Ag(I) which suggests some interaction with the relatively strongly coordinating anions. This is confirmed by electrical conductivity measurements which indicate neutral species.

In contrast the coupling constants for the 1:1 CF_3SO_3 and ClO_4 complexes show little deviation from the values observed for the BF_4 salt, suggesting retention of a linear P_2 donor set.

In order to unequivocally determine the coordination mode of L^1 in these complexes single crystal X-ray analyses were undertaken on $[Ag(L^1)][CF_3SO_3]$ and $[Ag(L^1)][ClO_4]$. Crystals of both complexes were grown by vapour diffusion of diethyl ether into CH_2Cl_2 solutions of the complex at -15°C. A crystal structure of $[Ag(L^1)(NO_3)]$ was obtained by a project student prior to the start of this research.[26]

The structure of $[Ag(L^1)][ClO_4]$ is isostructural with $[Ag(L^1)][BF_4]$ with crystallographic two-fold symmetry and linear Ag(I) coordinated to the two P-donor atoms of L^1, d(Ag-P) = 2.405(1) Å and $\angle$P(1)-Ag(1)-P(1*) = 165.16(7)°. The crystal structure of $[Ag(L^1)][CF_3SO_3]$ (Figure 5.3, Table 5.2) shows a very similar geometry at

Ag(I) with coordination via the two phosphine functions to give an approximately linear arrangement at Ag(I). In both cases there is no evidence of anion interaction.

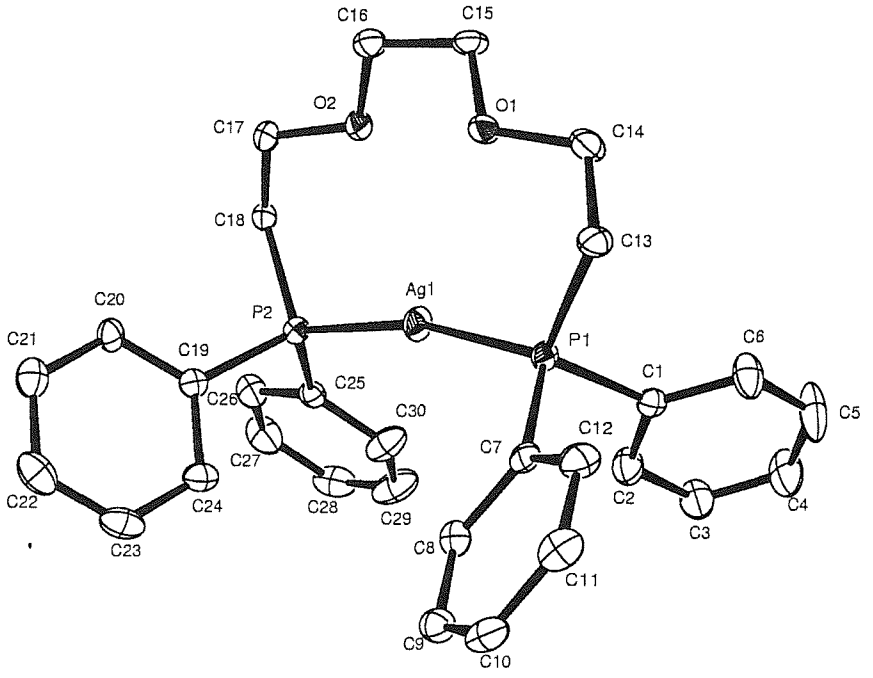

Figure 5.3 – View of the Ag-containing species in $[Ag(L^1)][CF_3SO_3].CH_2Cl_2$ with numbering scheme adopted. Ellipsoids are drawn at 40% probability. H atoms are omitted for clarity.

Bond Lengths (Å)	
Ag(1)-P(1)	2.4070(9)
Ag(1)-P(2)	2.4172(9)
Bond Angles (°)	
P(1)-Ag(1)-P(2)	167.55(3)

Table 5.2– Selected bond lengths (Å) and bond angles (°) for $[Ag(L^1)][CF_3SO_3].CH_2Cl_2$

Table 5.3 – Crystal Data and Structure Refinement Details for $[Ag(L^1)][CF_3SO_3].CH_2Cl_2$

compound	$[Ag(L^1)][CF_3SO_3].CH_2Cl_2$
empirical formula	$C_{32}H_{34}AgCl_2F_3O_5P_2S$
fw	828.39
crystal system	triclinic
space group	P-1
a (Å)	10.0928(1)
b (Å)	10.4575(1)
c (Å)	16.5622(2)
α (°)	90.5877(5)
β (°)	90.8655(5)
γ (°)	100.5412(3)
volume ($Å^3$)	1718.22(3)
Z	2
abs coef (cm^{-1})	9.49
unique observed reflections	7022
reflections observed [$I_0 > n\sigma(I_0)$]	5031, n = 3
no. of parameters	415,
R	0.039
R_w	0.048

Temperature = 150 K; wavelength (Mo-Kα) = 0.71073 Å; θ (max) = 27.5 deg.

[b] $R = \sum||F_0| - |F_c||/\sum|F_0|$ $\quad R_w = [\sum w(F_0^2 - F_c^2)^2/\sum wF_0^4]^{1/2}$

In contrast the crystal structure of $[Ag(L^1)(NO_3)]$ (Figure 5.4, Table 5.3) shows Ag(I) coordinated to the two P atoms of L^1, with additional weak interactions to two O atoms from an asymmetrically bound bidentate NO_3^- ligand, resulting in a severely distorted tetrahedral geometry.

Addition of a second molar equivalent of L^1 to $[Ag(L^1)][CF_3SO_3]$ leads to the formation of a complex with much lower coupling constants than those observed for the 1:1 complex, suggesting an increase in the coordination number at Ag(I). The coupling constants of 322 and 380 Hz are intermediate between those seen for P_2 coordination in $[Ag(L^1)][BF_4]$ ($^1J(^{107}Ag\text{-}P)$ = 523 Hz and $^1J(^{109}Ag\text{-}P)$ = 601 Hz) and those observed for P_4 coordination in $[Ag(dppe)_2]^+$ ($^1J(^{107}Ag\text{-}P)$ = 231 Hz, $^1J(^{109}Ag\text{-}P)$ = 266 Hz)[27] , suggesting coordination via a P_3 donor set, which has been confirmed by crystallographic analysis of the salt. Crystals were grown by vapour diffusion of diethyl ether into a CH_2Cl_2 solution of the complex at -15°C. The crystal structure (Figure 5.5, Table 5.4) shows each of the two Ag(I) centres coordinated to one chelating L^1 through the terminal phosphines, and to one P donor atom of a bridging L^1, resulting in an overall distorted trigonal planar environment at Ag(I).

In conclusion these results have shown L^1 to coordinate to Ag(I) via the terminal phosphines alone. Although anion interaction has been observed in the NO_3 complex there is no evidence to support any interaction between the ether oxygen atoms in the ligand and Ag(I). The solid-state structures determined are consistent with the conclusions drawn from the $^{31}P\{^1H\}$ solution NMR studies. The $^{107}Ag\text{-}P$ and $^{109}Ag\text{-}P$ coupling constants change in a predictable way with changes in coordination number at Ag(I) and thus provide a useful tool for predicting the overall coordination environment.

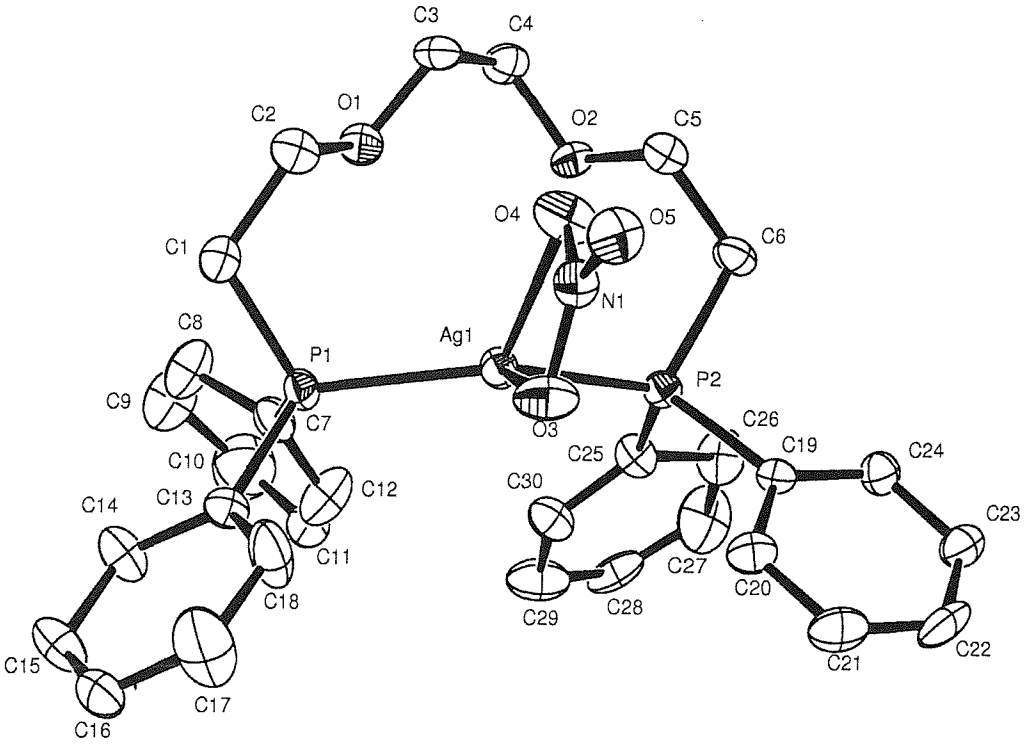

Figure 5.4 – View of the structure of $[Ag(L^1)(NO_3)]$ with numbering scheme adopted. Ellipsoids are drawn at 40% probability. H atoms are omitted for clarity.

Bond Lengths (Å)	
Ag(1)-P(1)	2.412(2)
Ag(1)-P(2)	2.616(2)
Ag(1)-O(3)	2.675(7)
Ag(1)-O(4)	2.496(9)
Bond Angles (°)	
P(1)-Ag(1)-P(2)	139.2(1)
P(1)-Ag(1)-O(3)	106.9(2)
P(1)-Ag(1)-O(4)	115.9(2)
P(2)-Ag(1)-O(3)	110.2(1)
P(2)-Ag(1)-O(4)	101.2(1)
O(3)-Ag(1)-O(4)	49.2(2)

Table 5.4 – Selected bond lengths (Å) and angles (°) for $[Ag(L^1)(NO_3)]$

Table 5.5 – Crystal Data and Structure Refinement Details for $[Ag(L^1)(NO_3)]$

compound	$[Ag(L^1)(NO_3)]$
empirical formula	$C_{30}H_{32}AgNO_5P_2$
fw	656.40
crystal system	monoclinic
space group	C2/c
a (Å)	25.87(7)
b (Å)	9.20(2)
c (Å)	24.74(4)
β (°)	101.1(2)
volume ($Å^3$)	5777.8(2)
Z	8
abs coef (cm^{-1})	8.46
unique observed reflections	5427
reflections observed $[I_0>n\sigma(I_0)]$	3725, n = 2
no. of parameters	437,
R	0.050
R_w	0.070

Temperature = 150 K; wavelength (Mo-Kα) = 0.71073 Å; θ (max) = 27.5 deg.

[b] $R = \sum||F_0|-|F_c||/\sum|F_0|$ $\quad R_w = [\sum w(F_0^2-F_c^2)^2/\sum wF_0^4]^{1/2}$

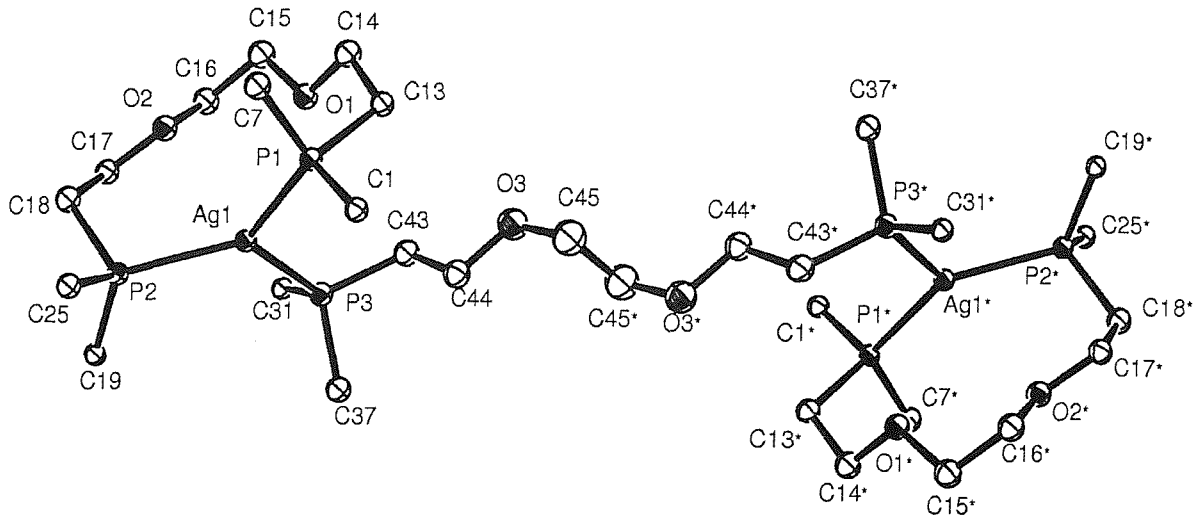

Figure 5.5 – View of the structure of the Ag-containing species in $[Ag_2(L^1)_3][CF_3SO_3]_2$ with numbering scheme adopted. Ellipsoids are drawn at 40% probability. H atoms and phenyl rings are omitted for clarity. Atoms marked * are related by a crystallographic inversion centre.

Bond lengths (Å)	
Ag(1)-P(1)	2.4551(12)
Ag(1)-P(2)	2.4494(12)
Ag(1)-P(3)	2.4729(12)
Bond angles (°)	
P(1)-Ag(1)-P(2)	125.84(4)
P(1)-Ag(1)-P(3)	119.93(4)
P(2)-Ag(1)-P(3)	114.10(4)

Table 5.6 - Selected bond lengths (Å) and bond angles (°) for $[Ag_2(L^1)_3](CF_3SO_3)_2$

Table 5.7– Crystal Data and Structure Refinement Details for $[Ag_2(L^1)_3][CF_3SO_3]_2$

compound	$[Ag_2(L^1)_3][CF_3SO_3]_2$
empirical formula	$C_{92}H_{96}Ag_2F_6O_{12}P_6S_2$
fw	1973.45
crystal system	triclinic
space group	P-1
a (Å)	11.0275(1)
b (Å)	12.5004(2)
c (Å)	16.9448(2)
α (°)	80.7110(8)
β (°)	81.7090(8)
γ (°)	76.0320(5)
volume ($Å^3$)	2223.47
Z	1
abs coef (cm^{-1})	6.67
unique observed reflections	10186
reflections observed $[I_0>n\sigma(I_0)]$	7028, n = 3
no. of parameters	541
R	0.058
R_w	0.067

Temperature = 150 K; wavelength (Mo-Kα) = 0.71073 Å; θ (max) = 27.5 deg.

[b] $R1 = \Sigma||F_0| - |F_c||/\Sigma|F_0|$ $\quad R_w = [\Sigma w(F_0^2-F_c^2)^2/\Sigma wF_0^4]^{1/2}$

5.2.2 Ag(I) Complexes of $Ph_2P(CH_2)_2S(CH_2)_2S(CH_2)_2PPh_2$ (L^2)

Having observed anion coordination in $[Ag(L^1)(NO_3)]$ and the adoption of an unusual trigonal planar geometry at Ag(I) in $[Ag_2(L^1)_3][CF_3SO_3]_2$ attempts were made to prepare the L^2 analogues. It was thought that the replacement of the ether functions in L^1 with the much softer thioether functions in L^2 may result in some unusual coordination chemistry at Ag(I).

The complexes were prepared in the same way as the L^1 complexes described previously to yield the products as white solids.

Electrospray mass spectrometry of the $[Ag(L^2)][NO_3]$ complex shows peaks with the correct isotopic distribution for $[Ag(L^2)]^+$ (*m/z* = 625, 627) and ^1H NMR spectroscopy and microanalysis confirm the stoichiometry as $Ag(L^2)NO_3$. $^{31}P\{^1H\}$ NMR spectroscopy of solutions at 193 K reveals two doublets at δ 2.5 ppm with $^1J(^{107}Ag\text{-}P)$ = 442 Hz and $^1J(^{109}Ag\text{-}P)$ = 502 Hz. This reduction in the coupling constants (cf. $[Ag(L^1)][BF_4]$) indicates an increase in the coordination number at Ag(I) either by interaction with the NO_3^- anion or by coordination of the thioether functions of L^2. Electrical conductivity measurements on the salt confirm that the NO_3 anion is non-coordinating and thus the increase in coordination at Ag(I) arises from coordination of L^2 via a P_2S_2 donor set. This is consistent with the higher affinity of Ag(I) for soft donor atoms such as S over the hard NO_3 anion.

Electrospray mass spectrometry of $[Ag(L^2)][CF_3SO_3]$ complex shows peaks with the correct isotopic distribution for $[Ag(L^2)]^+$ (*m/z* = 625, 627). However $^{31}P\{^1H\}$ NMR spectroscopy shows a mixture of species. The $^{31}P\{^1H\}$ NMR spectrum shows a single resonance at δ -1.4 ppm which upon cooling resolves into 2 doublets with $^1J(^{107}Ag\text{-}P)$ = 435 Hz and $^1J(^{109}Ag\text{-}P)$ = 522 Hz which is consistent with the formation of $[Ag(L^2)][CF_3SO_3]$ with coordination of L^2 via a P_2S_2 donor set. However a second set of doublets is observed at δ -5 ppm with $^1J(^{107}Ag\text{-}P)$ = 251 Hz and $^1J(^{109}Ag\text{-}P)$ = 383 Hz. This significant reduction in the coupling constants suggests an increase in the coordination number at Ag(I) either by formation of a 2:1 L^2:Ag complex or by formation of a 2:3 Ag:L^2 complex as formed with L^1. Attempts were made to prepare this second species by reaction of 2 molar equivalents of ligand with $AgCF_3SO_3$. $^{31}P\{^1H\}$ NMR spectroscopy repeatedly showed a mixture of the product and free ligand. Attempts to

purify the product through recrystallisation failed and no further investigation was possible.

5.2.3 Metal Carbonyl complexes of L^1

Few studies have been carried out on transition metal carbonyl chemistry with mixed phospha-oxa and phospha-thia ligands. Varshney and Gray have investigated the coordination of the larger P_2O_x-donor ligands (x = 3-5) with molybdenum carbonyl.[8] The resulting metallocyclic species have been shown to act as hosts for alkali metal ions. A summary of the products obtained from the reaction of L^1 with various Group 6 and 7 carbonyl species is given in Scheme 5.1.

The solution IR spectrum (CH_2Cl_2) of $[Mo(CO)_4(L^1)]$ shows four bands in the carbonyl region at 2022, 1924, 1903 and 1885 cm^{-1} consistent with the retention of the *cis*-tetracarbonyl arrangement (C_{2v}, theory $2a_1 + b_1 + b_2$). These values are comparable with those of the related compound *cis*-$[Mo(CO)_4(Ph_2P(CH_2)_2O)_3(CH_2)_2PPh_2]$ which shows ν(CO) at 2022, 1920, 1905 and 1885 cm^{-1}.[8]

The solution IR spectrum (CH_2Cl_2) of $[W(CO)_4(L^1)]$ shows only three bands at 2017, 1916 and 1883 cm^{-1} probably due to accidental coincidence of two peaks at 1883 cm^{-1}.

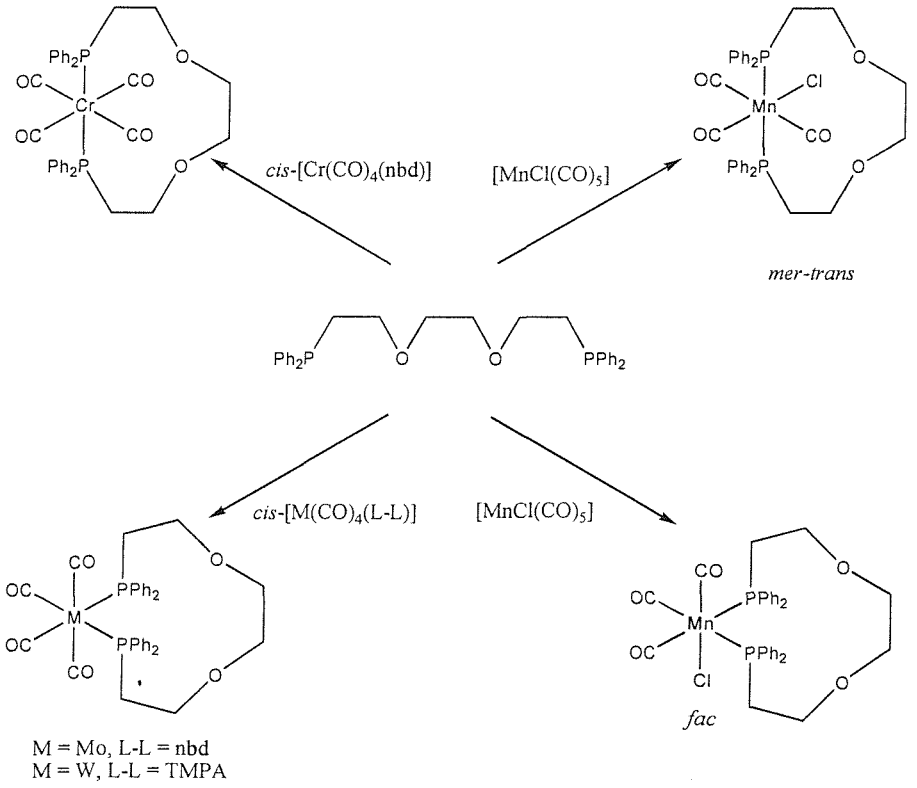

Scheme 5.1 – Complexes of L^1 with group 6 and 7 metal carbonyls

The $^{31}P\{^1H\}$ NMR spectra of $[Mo(CO)_4(L^1)]$ and $[W(CO)_4(L^1)]$ each show a single resonance to high frequency of L^1 at δ 17.8 and δ 3.9 ppm respectively, with ^{183}W satellites on the latter ($^1J(^{183}W\text{-}^{31}P)$ = 225 Hz). These data together with ^1H NMR spectroscopy and microanalyses are consistent with the formulation $[M(CO)_4(L^1)]$ for the products.

$^{13}C\{^1H\}$ NMR spectroscopy shows resonances associated with coordinated L^1 together with a poorly resolved triplet and doublet of doublets in the carbonyl region due to CO *trans* CO and CO *trans* P. Thus confirming L^1 to act as a *cis* chelate ligand to Mo(0) and W(0) to give *cis*-$[Mo(CO)_4(L^1)]$ and *cis*-$[W(CO)_4(L^1)]$ as the products.

A crystal structure of *cis*-$[Mo(CO)_4(L^1)]$ (Figure 5.6, Table 5.4)was obtained within the group prior to my research and shows L^1 to act as a *cis*-chelate coordinating via the terminal phosphines with four CO ligands completing the distorted octahedral coordination at Mo(0)

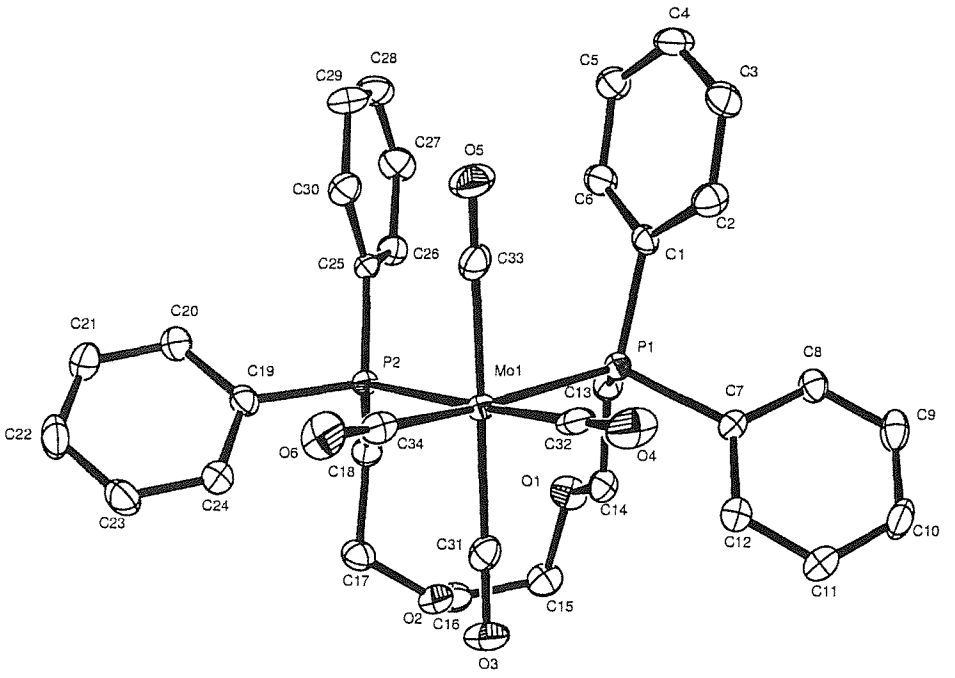

Figure 5.6 – View of the structure of *cis*-[$Mo(CO)_4(L^1)$] with numbering scheme adopted. Ellipsoids are drawn at 40 % probability. H atoms are omitted for clarity.

Bond Lengths (Å)		*Bond Angles* (°)	
Mo(1)-P(1)	2.539(1)	P(1)-Mo(1)-C(34)	169.7(1)
Mo(1)-P(2)	2.573(1)	P(2)-Mo(1)-C(31)	91.9(9)
Mo(1)-C(31)	2.041(5)	P(2)-Mo(1)-C(32)	176.7(1)
Mo(1)-C(32)	1.982(5)	P(2)-Mo(1)-C(33)	91.5(1)
Mo(1)-C(33)	2.033(5)	P(2)-Mo(1)-C(34)	92.6(1)
Mo(1)-C(34)	2.004(5)	C(31)-Mo(1)-C(32)	90.5(2)
		C(31)-Mo(1)-C(33)	174.5(2)
Bond Angles (°)		C(31)-Mo(1)-C(34)	90.7(2)
P(1)-Mo(1)-P(2)	95.41(4)	C(32)-Mo(1)-C(33)	85.9(2)
P(1)-Mo(1)-C(31)	95.6(1)	C(32)-Mo(1)-C(34)	85.1(2)
P(1)-Mo(1)-C(32)	86.7(1)	C(33)-Mo(1)-C(34)	84.9(2)
P(1)-Mo(1)-C(33)	88.4(1)		

Table 5.8 – Selected bond lengths (Å) and angles (°) for *cis*-[$Mo(CO_4)(L^1)$]

Table 5.9 – Crystal data and structure refinement details for *cis*-$[Mo(CO)_4(L^1)]$

compound	*cis*-$[Mo(CO)_4(L^1)]$
empirical formula	$C_{34}H_{32}O_6MoP_2$
fw	694.51
crystal system	monoclinic
space group	$P2_1/n$
a (Å)	15.776(4)
b (Å)	12.543(3)
c (Å)	16.296(3)
β (°)	102.28(2)
volume ($Å^3$)	3150(1)
Z	4
abs coef (cm^{-1})	5.47
unique observed reflections	5833
reflections observed [$I_0 > n\sigma(I_0)$]	3885, n = 2
R	0.038
R_w	0.047

Temperature = 150 K; wavelength (Mo-Kα) = 0.71073 Å; θ (max) = 27.5 deg.

[b] $R = \Sigma||F_0| - |F_c||/\Sigma|F_0|$ $\quad R_w = [\Sigma w(F_0^2 - F_c^2)^2/\Sigma wF_0^4]^{1/2}$

The solution IR spectrum (CH_2Cl_2) of $[Cr(CO)_4(L^1)]$ shows a single ν(CO) absorption at 1877 cm^{-1}, which is in sharp contrast to the spectra observed for $[Mo(CO)_4(L^1)]$ and $[W(CO)_4(L^1)]$. The $^{13}C\{^1H\}$ NMR spectrum shows resonances associated with coordinated L^1 and a single, poorly resolved, triplet in the CO region. This data strongly suggests the formation of *trans*-$[Cr(CO)_4(L^1)]$.The $^{31}P\{^1H\}$ NMR spectrum of the isolated compound shows a single resonance at 56.5 ppm. However a $^{31}P\{^1H\}$ NMR spectrum of the reaction mixture at an earlier stage in the reaction shows three separate resonances. A resonance at δ 56.5 ppm corresponding to the *trans*-isomer, a peak for free ligand at δ -21 ppm and a third singlet at δ 28.8 ppm which can tentatively be assigned as an intermediate *cis*-isomer. The ease with which the Cr(0) complex undergoes isomerisation is in contrast with reports from Gray and co-workers who have shown that UV irradiation or $HgCl_2$ catalysis are required to convert $[Mo(CO)_4\{Ph_2P(CH_2CH_2O)_nCH_2CH_2PPh_2\}]$ (n = 3,5) to the corresponding *trans* species.[10]

Reaction of L^1 with one molar equivalent of $[MnCl(CO)_5]$ in $CHCl_3$ followed by work-up as detailed previously yielded a yellow solid. Solution IR spectroscopy (CH_2Cl_2) showed several ν(CO) absorptions in the range 2095 - 1908 cm^{-1}. If L^1 coordinates via the phosphines alone (ether coordination is unlikely with soft d^6 metals) there are three possible products from the reaction; *fac*, *mer-cis*, and *mer-trans* isomers. All three products should give three CO stretching vibrations in the IR spectrum, although the exact frequencies and intensities will vary. Thus the IR spectrum of the isolated solid suggests the presence of more than one geometric isomer. This is confirmed by $^{31}P\{^1H\}$ NMR spectroscopy which shows two resonances at δ 44.0 and δ 29.9 ppm.

Repeating the reaction with prolonged reflux gave a yellow solid. The solution IR spectrum (CH_2Cl_2) shows three ν(CO) bands at 2045, 1949 and 1909 cm^{-1}. The $^{31}P\{^1H\}$ NMR spectrum shows a single peak at δ 44.0 ppm. The absence of a second phosphorus resonance excludes the possibilty of *mer-cis* and thus suggests the isolation of the thermodynamic *mer-trans* isomer. Further evidence is provided by the $^{13}C\{^1H\}$ NMR spectrum which shows a single CO resonance at δ 212 ppm, although couplings can not be resolved due to broadening by the ^{55}Mn quadrupole.

Repeating the reaction at room-temperature with stirring for only 2 hours resulted in incomplete consumption of the $[MnCl(CO)_5]$ starting material however solution IR spectroscopy (CH_2Cl_2) shows three CO stretching vibrations at 2027, 1957 and 1910 cm^{-1}, suggesting that the major product is fac-$[MnCl(CO)_3(L^1)]$. This is confirmed by $^{31}P\{^1H\}$ NMR spectroscopy which shows a single resonance at δ 29.9 ppm.

Reaction of $[ReBr(CO)_5]$ with one molar equivalent of L^1 in refluxing $CHCl_3$ also leads to a mixture of isomers even after 24 h reflux. This is consistent with Re(I) being much more inert to substitution than Mn(I). The solid-state IR spectrum (CsI) shows four carbonyl absorptions at 2108, 2036, 1950 and 1910 cm^{-1} and the $^{31}P\{^1H\}$ NMR spectrum shows 2 resonances of unequal intensity at δ -12.9 and δ-13.5 ppm . This data suggests that as with the Mn(I) complex the two isomers present are likely to be *fac* and *mer-trans.* Attempts to isolate a single species either by prolonged reflux or by the use of shorter reaction times resulted in changes in the relative quantities of the two species but also showed evidence of decomposition or unreacted $[ReBr(CO)_5]$.

5.2.4 Metal Carbonyl Complexes of L^2

A summary of the products obtained from the reaction of L^2 with Mn(I) and Mo(0) metal carbonyls is given in Scheme 5.2.

Reaction of one molar equivalent of L^2 with $[Mo(CO)_4(nbd)]$ in CH_2Cl_2 followed by concentration *in vacuo* and precipitation with hexane yields a pale brown solid. Solution IR spectroscopy indicates a mixture of species which is confirmed by $^{31}P\{^1H\}$ and $^{13}C\{^1H\}$ NMR spectroscopy. The $^{31}P\{^1H\}$ NMR spectrum shows three singlets, a 1:1 pair at δ 52.9 and δ –16.6 ppm, and a third resonance at δ 26.1 ppm. The low frequency resonance is very close to that of free L^2 (-16.5 ppm) suggesting that this corresponds to an uncoordinated phosphine, whilst the large coordination shift accompanying the resonance at δ 52.9 ppm (δ_{coord} = +68 ppm) is indicative of the formation of a 5-membered chelate ring.[28] Therefore this pair of resonances can be attributed to the formation of a single Mo species involving L^2 coordination via a P/S-donor set to form a 5-membered chelate ring with the remaining terminal phosphine non-bonded. The third resonance at δ 26.1 ppm shows a similar coordination shift to that observed for $[Mo(CO)_4(L^1)]$ and thus suggests formation of a second Mo species involving

P_2-coordination only. The $^{13}C\{^1H\}$ NMR spectrum is consistent with the conclusions drawn above.

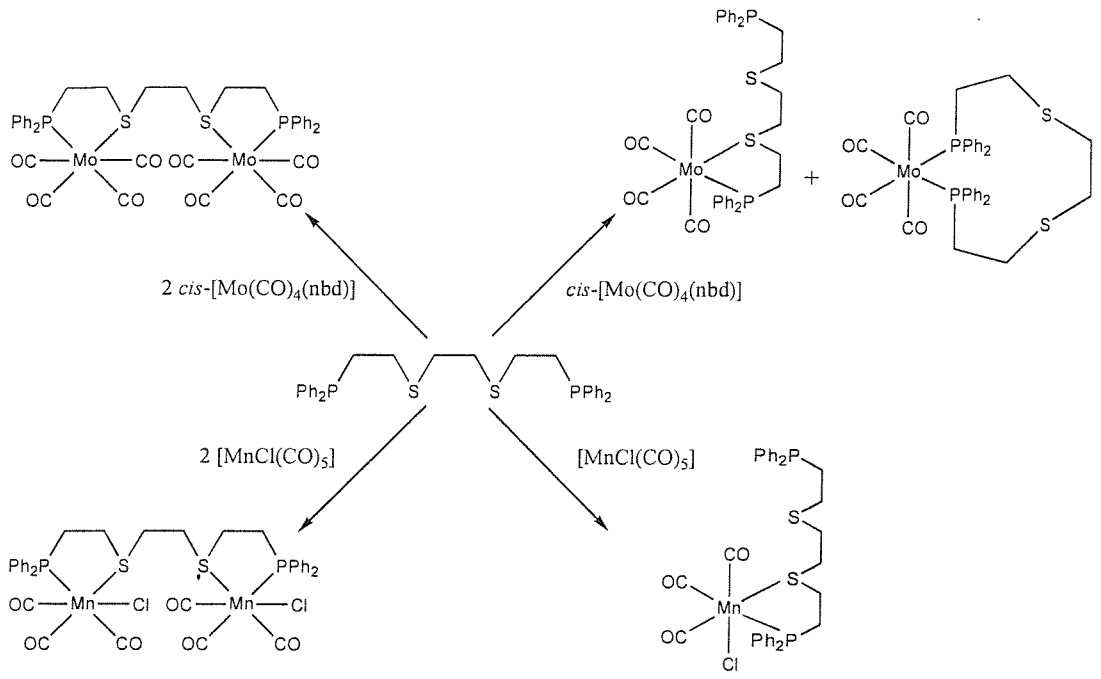

Scheme 5.2 – Group 6 and 7 metal carbonyl complexes of L^2

Reaction of L^2 with two molar equivalents of $[Mo(CO)_4(nbd)]$ yields a pale brown solid. Solution IR spectroscopy (CH_2Cl_2) shows four bands associated with ν(CO) at 2024, 1919, 1910 and 1872 cm^{-1} consistent with the retention of a *cis*-tetracarbonyl arrangement. The $^{31}P\{^1H\}$ NMR spectrum shows a single resonance at δ 53.0 ppm. The large shift upon coordination, similar to that observed for the 1:1 reaction, suggests formation of a 5-membered chelate ring via coordination of L^2 via a P/S-donor set.[28] The absence of a second resonance corresponding to a non-coordinating phosphine indicates the formation of a dinuclear species involving coordination of L^2 to two separate *cis*-$Mo(CO)_4$ units by P/S-chelation to give $[\{Mo(CO)_4\}_2(\mu^2\text{-}L^2)]$. The $^{13}C\{^1H\}$ NMR spectrum is consistent with the formation of the dinuclear species, showing three doublet CO resonances for CO *trans* CO, CO *trans* P and CO *trans* S.

Reaction of L^2 with one molar equivalent of $[MnCl(CO)_5]$ in CH_2Cl_2 yields a yellow solid. The solution IR spectrum (CH_2Cl_2) shows three strong ν(CO) absorptions consistent with retention of a *fac*-tricarbonyl arrangement (C_s) The $^{31}P\{^1H\}$ NMR

spectrum of the complex shows two resonances of equal intensity at δ 70.0 ppm and δ -16.6 ppm, suggesting coordination of L^2 to Mn(I) via a P/S-donor set to form a 5-membered chelate ring, with the remaining P/S functions remaining non-coordinated. The ^{55}Mn NMR spectrum shows a single resonance at ca. δ -700 ppm, broadened significantly as a consequence of fast relaxation. The chemical shift is intermediate between those observed for *fac*-$[MnCl(CO)_3\{MeS(CH_2)_2SMe\}]$ ($\delta(^{55}Mn)$ = -168, -228 and -279 ppm), and *fac*-$[MnCl(CO)_3\{Ph_2P(CH_2)_2PPh_2\}]$ (δ (^{55}Mn) = -1141 ppm) which is consistent with P/S-chelation by L^2 at Mn(I).[29, 30]

Reaction of L^2 with two molar equivalents of $[MnCl(CO)_5]$ results in the formation of the dinuclear complex *fac*-$[\{MnCl(CO)_3\}_2(\mu^2\text{-}L^2)]$. The $^{31}P\{^1H\}$ NMR spectrum shows a single resonance at δ 70.6 ppm, the large coordination shift is again indicative of the formation of a 5-membered chelate ring.[28] The $^{13}C\{^1H\}$ NMR, IR spectroscopic data and microanalysis are all consistent with the formation of the dinuclear species.

5.3 Conclusions

These results show that L^1 and L^2 are very versatile ligands for a range of transition metals, readily altering their mode of coordination to accommodate changes at the metal centre.

L^1 coordinates to Ag(I) via the terminal phosphines alone. Although anion interaction has been observed in the NO_3 complex there is no evidence to support any interaction between the ether oxygen atoms in the ligand and Ag(I). In contrast L^2 coordinates to Ag(I) via both the phosphine and thioether functions which is consistent with the higher affinity of Ag(I) for soft donor-atoms The solid state structures determined are consistent with the conclusions drawn from the ^{31}P solution NMR studies. The ^{107}Ag-P and ^{109}Ag-P coupling constants change in a predictable way with changes in coordination number at Ag(I) and thus provide a useful tool for predicting the overall coordination environment.

L^1 reacts with a range of Group 6 and 7 metal carbonyls to give a new series of mononuclear products. As expected the hard ether functions remain non-bonded with L^1 functioning as a long-chain diphosphine ligand coordinating to the metal centre via a

P_2-donor set. With Mo(0) and W(0) the products isolated involve *cis*-coordination of L^1 to form 11-membered ring metallocyclic species. With Mn(I) and Cr(0) the thermodynamic products are the *mer*-trans and *trans*-isomers respectively, which demonstrate the ability of L^1 to function as a *trans*-chelate. These observations are consistent with earlier work which has been carried out on a variety of other transition metal complexes with L^1, including Ni(II), Ag(I) and Au(I).[11, 14, 17]

Reaction of L^2 with Mo(0) and Mn(I) gives rise to both mono- and dinuclear products. The presence of the soft thioether functions in the ligand backbone allows coordination via both the phosphine and thioether functions, resulting in the formation of favourable 5-membered P/S-chelate rings. In the 1:1 Mn:L^2 complex L^2 coordinates through a P/S donor set to form a 5-membered chelate ring, easily identifiable through the characteristic $^{31}P\{^1H\}$ chemical shift, with the remaining thioether and phosphine functions non-bonded. A similar species is isolated from the 1:1 Mo:L^2 reaction along with the 11-membered ring metallocyclic species involving P_2 coordination. Addition of a second molar equivalent of the metal precursor gives rise to the dinuclear complexes *cis*-$[\{Mo(CO)_4\}_2(L^2)]$ and *fac*-$[\{MnCl(CO)_3\}_2(L^2)]$ which involve μ^2-coordination of L^2 to form two five-membered chelate rings.

5.4 Experimental

$[Cr(CO)_4(nbd)]$,[31] $[Mo(CO)_4(nbd)]$,[31] $[W(CO)_4(tmpa)]$,[32] $[MnCl(CO)_5]$[33] and $[ReBr(CO)_5]$[34] were prepared according to the literature procedures. L^1 and L^2 were prepared following modifications of the literature procedures.

Synthesis of $[Ag(L^1)](CF_3SO_3)$: To a degassed solution of L^1 (0.100 g, 0.206 mmol) in CH_2Cl_2 (20 mL) at 0°C was added $Ag(CF_3SO_3)$ (0.053 g, 0.206 mmol). The resulting solution was stirred for approximately 3 hr in a foil-wrapped flask. The solution was then concentrated *in vacuo* to approximately 5 mL and hexane (ca. 30 mL) was added to afford a white solid, which was filtered, washed with diethyl ether and dried *in vacuo*. Yield 0.110 g (72%). Required for $[C_{31}H_{32}AgF_3O_5P_2S]$ C = 50.1, H = 4.3 %; found C = 50.1, H = 4.3 %. Electrospray mass spectrum (MeCN): found *m/z* = 595, 593. Calc. for $[^{109}Ag(L^1)]^+$ 595, $[^{107}Ag(L^1)]^+$ 593. ^1H NMR ($CDCl_3$): δ 7.3-7.6 (m, Ph, 20H), 3.6-3.8 (m, CH_2O, 8H), 2.7 (m, CH_2P, 4H). IR spectrum (CsI disc / cm^{-1}): 3059 w, 2961 w, 2925 w, 2866 w, 1560 w, 1484 w, 1439 w, 1349 m, 1271 s, 1221 m, 1147 m, 1122 m, 1097 m, 1023 s, 904 w, 795 m, 750 m, 691 s, 667 m, 513 s, 463 w, 433 w, 349 w.

Synthesis of $[Ag(L^1)](ClO_4)$: Method as above giving a white solid. Yield 0.06 g (42%). Required for $[C_{30}H_{32}AgClO_4P_2.1/2CH_2Cl_2]$ C = 49.8, H = 4.5%; found: C, 50.6; H 4.7. Electrospray mass spectrum (MeCN): found *m/z* = 595, 593. Calc. for $[^{109}Ag(L^1)]^+$ 595, $[^{107}Ag(L^1)]^+$ 593. ^1H NMR ($CDCl_3$): δ 7.4-8.0 (m, Ph, 20H), 3.7-4.0 (m, CH_2O, 4H), 3.5 (m, CH_2O, 2H), 2.8 (m, CH_2O, 2H), 2.6 (m, CH_2P, 4H). IR spectrum (CsI disc / cm^{-1}): 3046 w, 2956 w, 2907 w, 2862 w, 1560 w, 1473 m, 1463 w, 1438 s, 1406 w, 1367 m, 1346 m, 1306 w, 1285 m, 1237 w, 1221 m, 1185 w, 1164 m, 1097 vs br, 995 s, 909 m, 884 m, 792 m, 759 s, 748 s, 710 m, 694 s, 623 s, 548 w, 510 m, 463 m, 419 w, 362 w.

Synthesis of $[Ag(L^1)Cl]$: Method as above except the CH_2Cl_2 solution was refluxed. Yield 0.07 g (54%). Required for $[C_{30}H_{32}AgClP_2.1/2CH_2Cl_2]$ C = 54.5, H = 4.9 %; found: C, 55.2; H 5.5 %. Electrospray mass spectrum (MeCN): found *m/z* = 595, 593. Calc. for $[^{109}Ag(L^1)]^+$ 595, $[^{107}Ag(L^1)]^+$ 593. ^1H NMR ($CDCl_3$): δ 7.4-7.7 (m, Ph, 20H), 3.8 (m, CH_2O, 4H), 3.7 (s, CH_2O, 4H), 2.6 (m, CH_2P, 4H). IR spectrum(CsI disc / cm^{-1}):

3061 w, 2970 w, 2864 w, 1540 w, 1489 m, 1441 m, 1359 m, 1262 m, 1190 w, 1103 s, 1036 m, 809 m, 751 m, 698 m, 621 w, 545 w, 515 m, 486 w, 445 w, 410 w. Λ_m (CH_2Cl_2, 10^{-3} mol dm^{-3}) = 1.7 ohm^{-1} cm^2 mol^{-1}.

Synthesis of [Ag(L^1)I]: Method as above, with refluxing CH_2Cl_2. Yield 0.125 g (84%). Required for [$C_{30}H_{32}AgIO_2P_2$] C = 50.3; H = 4.6%; found: C = 50.0; H = 4.5. Electrospray mass spectrum (MeCN): found *m/z* = 1315, 595, 593. Calc. for $[^{109}Ag_2(L^1)_2I]^+$ 1317, $[^{109}Ag(L^1)]^+$ 595, $[^{107}Ag(L^1)]^+$ 593. ^1H NMR ($CDCl_3$): δ 7.3-7.7 (m, Ph, 20H), 3.8 (m, CH_2O, 4H), 3.6 (s, CH_2O, 4H), 2.6 (m, CH_2P, 4H). IR spectrum (CsI disc / cm^{-1}): 3069 w, 2960 w, 2935 w, 2870 w, 1590 w, 1484 m, 1431 m, 1359 m, 1312 w, 1187 w, 1100 s, 1036 w, 989 m, 890 m, 850 w, 744 m, 692 m, 619 w, 540 w, 507 m. Λ_m (CH_2Cl_2, 10^{-3} mol dm^{-3}) = 1.9 ohm^{-1} cm^2 mol^{-1}.

Synthesis of [Ag(L^1)(NO_3)]: Method as above giving a white solid. Yield 0.0580 g (43 %).Required for [$C_{30}H_{32}AgNO_3P_2$] C =54.9, H = 4.9 %; found C = 54.9, H = 4.7%. Electrospray mass spectrum (MeCN): found *m/z* = 595, 593. Calc. for $[^{109}Ag(L^1)]^+$ 595, $[^{107}Ag(L^1)]^+$ 593. ^1H NMR ($CDCl_3$): δ 7.3 – 7.7 (m, Ph, 20H), 3.5 – 3.8 (m, CH_2O, 8H), 2.6 (m, CH_2P, 4H). IR spectrum (KBr disc/ cm^{-1}): 3051 w, 2959 w, 2955 w, 1484 m, 1435 m, 1384 s, 1297 s, 1187 w, 1130 m, 1100 s, 1034 w, 998 m, 894 w, 821 w, 741 m, 694 m, 517 m, 473 w, 438 w.

Synthesis of [$(AgI)_2(L^1)$]: Method as above, with refluxing CH_2Cl_2 and using two molar equivalents of AgI. Yield 0.081 g (41 %). Required for [$C_{30}H_{32}Ag_2I_2O_2P_2$] C = 37.7; H = 3.4 %;. found: C = 38.0; H = 3.5 %. Electrospray mass spectrum (MeCN): found *m/z* = 595, 593. Calc. for $[^{109}Ag(L^1)]^+$ 595, $[^{107}Ag(L^1)]^+$ 593. ^1H NMR ($CDCl_3$): δ 7.3-7.7 (m, Ph, 20H), 3.8 (m, CH_2O, 4H), 3.6 (s, CH_2O, 4H), 2.6 (m, CH_2P, 4H). IR (CsI disc / cm^{-1}):3069 w, 2945 w, 2859 w, 1572 w, 1482 m, 1435 m, 1357 m, 1308 w, 1260 m, 1185 w, 1158 w, 1096 s, 1025 w, 996 m, 975 w, 788 m, 741 m, 694 m, 618 w, 512 m, 482 w. Λ_m (CH_2Cl_2, 10^{-3} mol dm^{-3}) = 1.6 ohm^{-1} cm^2 mol^{-1}

Synthesis of $[Ag(L^2)](NO_3)$: Method as above. Yield 0.10 g (71 %). Required for $[C_{30}H_{32}AgNO_3P_2S_2].1.5CH_2Cl_2$ C = 47.3, H = 4.6 %; found C = 46.96, H = 5.08 %. Electrospray mass spectrum (MeCN): found *m/z* = 627, 625. Calc. for $[^{109}Ag(L^2)]^+$ 627, $[^{107}Ag(L^2)]^+$ 625. ^1H NMR ($CDCl_3$): δ 7.3-7.6 (m, Ph, 20H), 3.1 (m, CH_2S, 4H), 2.9 (m, CH_2S, 4H), 2.6 (m, CH_2P, 4H). $^{31}P\{^1H\}$ NMR (CH_2Cl_2 / $CDCl_3$): δ 2.5 (d, $^1J(^{107}Ag\text{-}P)$ = 442 Hz, $^1J(^{109}Ag\text{-}P)$ = 502 Hz). IR spectrum (CsI disc / cm^{-1}): 3071 w, 2975 w, 2914 w, 2361 w, 1960 w, 1899 w, 1838 w, 1590 w, 1574 w, 1483 w, 1440 w, 1413 w, 1280 w, 1224 w, 1153 m, 1100 m, 1075 w, 1031 m, 1000 w, 916 w, 827 m, 774 s, 697 s, 638 s, 573 s, 517 s, 483 s, 447 w, 416 w, 391 w. Λ_m (CH_2Cl_2, 10^{-3} mol dm^{-3}) = 31.05 ohm^{-1} cm^2 mol^{-1}

Synthesis of $[Ag_2(L^1)_3](CF_3SO_3)_2$: Method as above but using two molar equivalents of L^1. Yield 0.093 g (23%). Required for $[C_{92}H_{96}Ag_2F_6O_{12}P_6S]$ C = 56.0; H = 4.9 %; found: C = 56.7; H = 5.1. Calc. Electrospray mass spectrum (MeCN): found *m/z* = 1081, 1079, 595, 593. Calc. for $[^{109}Ag(L^1)_2]^+$ 1081, $[^{107}Ag(L^1)_2]^+$ 1079, $[^{109}Ag(L^1)]^+$ 595, $[^{107}Ag(L^1)]^+$ 593. ^1H NMR ($CDCl_3$): δ 7.3-7.6 (m, Ph, 20H), 3.5-3.7 (m, CH_2O, 8H), 2.6 (br m, CH_2P, 4H). IR spectrum(CsI disc / cm^{-1}): 3062 w, 2950 w, 2930 w, 2874 w, 1484 m, 1437 m, 1403 m, 1364 m, 1266 s, 1224 m, 1148 m, 1100 s, 1033 m, 999 m, 911 w, 750 s, 697 s, 638 s, 518 s, 524 w, 486 w.

Synthesis of *trans*-$[Cr(CO)_4(L^1)]$: To a degassed solution of L^1 (0.100 g, 0.206 mmol) in toluene (30 mL) was added $[Cr(CO)_4(nbd)]$ (0.057 g, 0.206 mmol). The resulting solution was stirred at 40°C for 48 hr. The solution was then concentrated *in vacuo* to approximately 5 mL and hexane (ca. 30 mL) was added to afford a green solid, which was filtered and dried *in vacuo*. Yield 0.053 g (40%). $^{31}P\{^1H\}$ NMR: δ 56.5 (s, L^1).
^1H NMR ($CDCl_3$): δ 7.1-7.7 (m, 20H, Ph), 3.3- 3.5 (m, 8H, CH_2O), 2.7-2.9 (m, 4H, CH_2P). $^{13}C\{^1H\}$ NMR (CH_2Cl_2 / $CDCl_3$): δ 222.7 (poorly resolved t, CO), 128.7-141.2 (Ph), 70.8 (CH_2O), 67.1(CH_2O), 33.8 (CH_2P). IR (CsI disc ν (CO)/ cm^{-1}): 1877 s.

Synthesis of *cis*-[Mo(CO)$_4$(L^1)]: To a degassed solution of L^1 (0.100 g, 0.206 mmol) in CH_2Cl_3 (30 mL) was added [Mo(CO)$_4$(nbd)] (0.062 g, 0.206 mmol). The resulting solution stirred at RT for ca. 18h. Solvent was removed *in vacuo* and the residue was redissolved in CH_2Cl_2 (ca. 5mL) and hexane (ca. 30 mL) was added to afford a yellow solid which was filtered, washed with hexane and dried *in vacuo*. Yield 0.076 g (53 %). Required for $[C_{34}H_{32}MoO_6P_2].1/2CH_2Cl_2$: C = 56.2, H = 4.7 %; found C = 56.7, H = 4.8 %. Electrospray mass spectrum (MeCN): Found *m/z* = 641, 613, 487; Calc. for $[^{98}Mo(CO)_2(L^1)]^+$ *m/z* = 640, $[^{98}Mo(CO)(L^1)]^+$ *m/z* = 612, $[L^1]^+$ *m/z* = 486. ^{1}H NMR ($CDCl_3$): δ 7.3-7.6 (m, 20H, Ar-C<u>H</u>), 3.7 (m, 4H, C<u>H</u>$_2$O), 3.5 (s, 4H, C<u>H</u>$_2$O), 2.6 (m, 4H, C<u>H</u>$_2$P). $^{31}P\{^1H\}$ NMR: δ 17.8 (s, L^1). $^{13}C\{^1H\}$ NMR (CH_2Cl_2 / $CDCl_3$): δ 215.8 (t, <u>C</u>O *trans* CO), 210.1 (dd, <u>C</u>O *trans* P), 128.7-136.7 (Ar-<u>C</u>H), 70.1 (<u>C</u>H$_2$O), 67.2 (<u>C</u>H$_2$O), 33.1 (<u>C</u>H$_2$P). IR spectrum (CsI disc, ν(CO) / cm^{-1}): 2020s, 1918s, 1903s, 1885 sh.

Synthesis of *cis*-[W(CO)$_4$(L^1)]: Method as above using [W(CO)$_4$(tmpa)] (0.089 g, 0.206 mmol) in refluxing $CHCl_3$. Yield 0.117g (73%). Required for $[C_{34}H_{32}O_6P_2W].2CH_2Cl_2$ C = 45.4, H = 3.8 %; found C = 45.7, H = 5.1 %. APCI mass spectrum (MeCN): Found *m/z* =726, 669; Calc. for $[^{183}W(CO)_2(L^1)]^+$ *m/z* = 725, $[^{183}W(L^1)]^+$ *m/z* = 669. $^{31}P\{^1H\}$ NMR: δ 3.9 (s, L^1, $^1J(^{183}W\text{-}P)$ = 232 Hz). ^{1}H NMR ($CDCl_3$): δ 7.3-7.7 (m, 20H, Ph), 3.6 (m, 4H, CH_2O), 3.4 (s, 4H, CH_2O), 2.6 (m, 4H, CH_2P). $^{13}C\{^1H\}$ NMR (CH_2Cl_2 / $CDCl_3$): δ 205.7 (t, CO *trans* CO), 203.5 (dd, CO *trans* P), 127.7-139.4 (Ph), 71.1 (CH_2O), 67.5(CH_2O), 32.8 (CH_2O). IR (CsI disc ν(CO) / cm^{-1}): 2013 m, 1883 br s.

Synthesis of *fac*-[MnCl(CO)$_3$(L^1)]: To a solution of L^1 (0.320 g, 0.65 mmol) in degassed $CHCl_2$ (50 cm^3) in a foil-wrapped flask was added [MnCl(CO)$_5$]. The reaction mixture was stirred under N_2 for 2 h. The solvent was then concentrated *in vacuo* and then added to ice-cold hexane to give a bright yellow solid. Yield 0.22 g (51 %). Required for $[C_{33}H_{32}ClMnO_5P_2].1/3CH_2Cl_2$: C = 58.1, H = 4.8 %; found C = 58.0, H = 4.7 %.^{1}H NMR ($CDCl_3$): δ 7.3 –7.7 (br m, Ph, 20H), 3.5 (br m, CH_2O, 4H), 3.4 (br s, CH_2O, 4H), 2.5 (br m, CH_2P, 4H). $^{31}P\{^1H\}$ NMR: δ 29.9 (s, L^1, *fac* isomer, major), 44 (s, L^1, *mer-trans* isomer, minor). IR spectrum (CH_2Cl_2, ν(CO) /cm^{-1}): 2027s, 1957s, 1910s.

Synthesis of *mer-trans*-[MnCl(CO)$_3$(L^1)]: Method as above, except that the reaction was refluxed under N_2 for 49 h. Yield 0.27g (63%). Required for [$C_{33}H_{32}ClMnO_5P_2$]: C = 60.0, H = 4.9 %; found C = 60.3, H = 4.7 %. Electrospray mass spectrum (MeCN): Found *m/z* = 625, 597, 569, 541, 487; Calc. for [Mn(CO)$_3$(L^1)]$^+$ *m/z* = 625, [Mn(CO)$_2$(L^1)]$^+$ *m/z* = 597, [Mn(CO)(L^1)]$^+$ *m/z* = 569, [Mn(L^1)]$^+$ *m/z* = 541, [L^1]$^+$ *m/z* = 486. ^{1}H NMR ($CDCl_3$): δ 7.2-7.9 (br m, Ph, 20H), 3.4 (br m, CH_2O, 4H), 3.3 (br s, CH_2O, 4H), 2.9 (br m, CH_2P, 4H). ^{31}P{^{1}H} NMR: δ 44 (s, L^1, *mer-trans* isomer). ^{55}Mn NMR: δ -1300 (br, $w_{1/2}$ ca. 19,000 Hz). ^{13}C{^{1}H} NMR: 211.7 (br, CO), 127.5-137.4 (Ph), 70.2 (CH_2O), 66.4 (CH_2O), 27.9 (CH_2P). IR spectrum (CH_2Cl_2, ν(CO) / cm^{-1}): 2045m, 1949s, 1909m.

Synthesis of [ReBr(CO)$_3$(L^1)]: To a degassed solution of L^1 (0.100g, 0.206 mmol) in $CHCl_3$ was added [ReBr(CO)$_5$] (0.08g, 0.206 mmol). The resulting solution was refluxed for 24 hr. The solution was then reduced to approximately 5 cm^3 and added to ice-cold hexane (30 cm^3) to afford a pale brown solid, which was filtered and dried *in vacuo*. Yield 23%. *Anal.* Found C, 44.0; H, 4.0. Calc. for $C_{33}H_{32}BrO_5P_2Re.1/2CHCl_3$: C, 44.9; H, 3.7%. Maldi-Toff mass spectrum: m/z = 729, 727. Calc. for [^{187}Re(CO)$_2$(L^1)] 729, [^{185}Re(CO)$_2$(L^1)] 727. ^{31}P{^{1}H} NMR: δ -12.8 (s, L^1, *fac*-isomer), -13.4 (s, L^1, *mer*-isomer). IR (CsI disc ν(CO/cm^{-1}): 2108 w, 2036 s, 1950 s, 1910 s

Synthesis of [{MnCl(CO)}$_2$(L^2)]: To a degassed solution of L^2 (0.200g, 0.39 mmol) in CH_2Cl_2 was added [MnCl(CO)$_5$] (0.18g, 0.77 mmol). The resulting solution was stirred, in a foil wrapped flask to protect the solution from bright light, at RT for 4 hr. The solution was then concentrated *in vacuo* to approximately 5 cm^3 and hexane (30 cm^3) was added to afford a bright yellow solid, which was filtered and dried *in vacuo*. Yield 61%. Required for [$C_{36}H_{32}Cl_2Mn_2O_6P_2$].1/2$CH_2Cl_2$: C, 48.8; H, 3.8 %; found C = 48.2, H = 4.0 %. ^{31}P{^{1}H} NMR: δ 70.6 (br s, L^2). ^{55}Mn NMR: δ -955 (s). ^{1}H NMR: 7.0-7.8 (m, 20H, Ph), 2.5-3.2 (br s, 8H, S-CH_2), 1.5-1.8 (br s, 4H, CH_2P). ^{13}C{^{1}H} NMR: δ 221.4 (CO), 218.6 (CO), 216.4 (CO), 128.9-133.4 (Ph), 34.7 (CH_2O), 31.9 (CH_2O), 30.7 (CH_2P).

Synthesis of $[MnCl(CO)_3(L^2)]$: As above but using a 1:1 ratio of $MnCl(CO)_5$: L^2. Yield 59 %. Required for $[C_{33}H_{32}ClMnO_3P_2S_2].1/2CH_2Cl_2$ C = 54.7, H = 4.5 %; found C = 55.2, H = 4.7 %. Electrospray mass spectrum (MeCN): found *m/z* 693, 657, 629: Calc. for $[Mn^{35}Cl(CO)_3(L^2)]^+$ 692, $[Mn(CO)_3(L^2)]^+$ 657, $[Mn(CO)_2(L^2)]^+$ 629. ^1H NMR ($CDCl_3$): δ 7.1-7.8 (m, Ph, 20H), 2.5-3.4 (m, CH_2, 12H). $^{31}P\{^1H\}$ NMR ($CH_2Cl_2/CDCl_3$): δ 70.9 (s, coord. PPh_2 on L_2), -16.6 (s, uncoord. PPh_2 on L^2). $^{13}C\{^1H\}$ NMR (CH_2Cl_2 / $CDCl_3$): δ 222, 218, 216 (br, CO), 129.2-138.4 (Ph), 38.5-23.0 (CH_2). ^{55}Mn NMR ($CH_2Cl_2/CDCl_3$): δ -700 ($w_{1/2}$ = ca. 15,000 Hz). IR spectrum (CsI disc, cm^{-1}): 2032, 1957, 1919.

Synthesis of $[\{Mo(CO)_4\}_2(L^2)]$: To a degassed solution of L^2 (0.200g, 0.39 mmol) in CH_2Cl_2 was added $[Mo(CO)_4(pip)_2]$ (0.29g, 0.77 mmol). The resulting solution was stirred at RT for 12 hr. The solution was then concentrated *in vacuo* to approximately 5 cm^3 and hexane (30 cm^3) was added to afford a brown/yellow solid, which was filtered and dried *in vacuo*. Yield 52%. Required for $[C_{38}H_{32}Mo_2O_8P_2S_2]$ C = 48.8, H = 3.5 %; found C = 49.6, H = 3.6 %. ^1H NMR ($CDCl_3$): δ 7.3-7.7 (m, Ph, 20H), 3.1 (s, CH_2S, 4H), 2.9 (m, CH_2S, 4H), 2.5 (m, CH_2P, 4H). $^{31}P\{^1H\}$ NMR ($CH_2Cl_2/CDCl_3$): δ 53.0 (s, L^2). $^{13}C\{^1H\}$ NMR ($CH_2Cl_2/CDCl_3$): δ 217.3 (d, 7 Hz, CO *trans* S), 215.1 (d, 28 Hz, CO *trans* P), 206.9 (d, 9 Hz, CO *trans* CO), 134.8-128.0 (Ph), 39.2 ($S\underline{C}H_2\underline{C}H_2S$), 34.7 (d, 15 Hz, $S\underline{C}H_2CH_2P$), 26.2 (d, 23 Hz, CH_2P). IR spectrum (CsI disc, cm^{-1}):2033, 1950, 1921.

Synthesis of $[Mo(CO)_4(L^2)]$: As above but using a 1:1 ratio of $[Mo(CO)_4(nbd)]$:L^2. Yield 57 %. Required for $[C_{34}H_{32}MoO_4P_2S_2].1/4CH_2Cl_2$ C = 55.0, H = 4.4 %; found C = 54.9, H = 4.6 %. ^1H NMR ($CDCl_3$): δ 7.3-7.7 (m, Ph, 20H), 2.1-2.7 (m, CH_2, 12H). $^{31}P\{^1H\}$NMR ($CH_2Cl_2/CDCl_3$): δ 52.9 (coord. PPh_2 on L^2), 26.2 (coord. PPh_2 on L^2), -16.6 (uncoord. PPh_2 on L^2). $^{13}C\{^1H\}$ NMR ($CH_2Cl_2/CDCl_3$): δ 217.5 (d, 7Hz, CO *trans* S in P/S chelate), 215.0 (d, 28 Hz, CO *trans* P in P/S chelate), 214.8 (poorly resolved dd, CO *trans* P in P_2 chelate), 209.0 (poorly resolved t, CO *trans* CO in P_2 chelate), 136.2-128.9 (Ph), 41.9-26.7 (CH_2). IR spectrum (CH_2Cl_2, cm^{-1}): 2022 s, 1918 sh, 1908 s, 1881 s.

5.5 References

1. C. A. Bessel, P. Aggarwal, A. C. Marschilol and K. J. Takeuchi, *Chem. Rev.*, **101**, (2001), 1031.

2. W. Marty, P. N. Kapoor, H.-B. Buergi and E. Fischer, *Helv. Chim. Acta*, **70**, (1987), 158.

3. P. N. Kapoor, *J. Organomet. Chem.*, **341**, (1988), 363.

4. N. W. Alcock, J. M. Brown and J. C. Jeffery, *J. Chem. Soc., Chem. Commun.*, (1974), 829.

5. N. W. Alcock, J. M. Brown and J. C. Jeffery, *J. Chem. Soc., Dalton Trans.*, (1977), 888.

6. K. Timmer and D. H. M. W. Thewissen, *Inorg. Chem.*, **100**, (1985), 235.

7. S. J. Chadwell, S. J. Coles, P. G. Edwards and M. J. Hursthouse, *J. Chem. Soc., Dalton Trans.*, (1996), 1105.

8. A. Varshney and G. M. Gray, *Inorg. Chem.*, **30**, (1991), 1748.

9. A. Varshney, M. L. Webster and G. M. Gray, *Inorg. Chem.*, **31**, (1992), 2580.

10. C. H. Duffey, C. H. Lake and G. M. Gray, *Inorg. Chim. Acta*, **317**, (2001), 199.

11. P. Dapporto and L. Sacconi, *J. Chem. Soc.*, **A**, (1971), 1914.

12. W. E. Hill, J. G. Taylor, C. A. McAuliffe, K. W. Muir and L. Manojlovic-Muir, *J. Chem. Soc., Dalton Trans.*, (1982), 833.

13. W. E. Hill, J. G. Taylor, C. P. Falshaw, T. J. King, B. Beagley, D. M. Tonge, R. G. Pritchard and C. A. McAuliffe, *J. Chem. Soc., Dalton Trans.*, (1986), 2289.

14. B. Heuer, S. J. A. Pope and G. Reid, *Polyhedron*, **19**, (2000), 743.

15. T. D. Dubois and D. W. Meek, *Inorg. Chem.*, **8**, (1969), 146.

16. Y. M. Hsiao, S. S. Chojnacki, P. Hinton, J. H. Reibenspies and M. Y. Darensbourg, *Organometallics*, **12**, (1993), 870.

17. A. M. Gibson and G. Reid, *J. Chem. Soc., Dalton Trans.*, (1996), 1267.

18. A. R. J. Genge, A. M. Gibson, N. K. Guymer and G. Reid, *J. Chem. Soc., Dalton Trans.*, (1996), 4099.

19. J. Connolly, R. J. Forder, G. W. Goodban, S. J. A. Pope, M. Predel and G. Reid, *Polyhedron*, **18**, (1999), 3553.

20. C. L. Doel, A. M. Gibson, G. Reid and C. Frampton, *Polyhedron*, **14**, (1995), 3139.

21. N. R. Champness, R. J. Forder, C. S. Frampton and G. Reid, *J. Chem. Soc., Dalton Trans.*, (1996), 1261.

22. J. Connolly, R. J. Forder and G. Reid, *Inorg. Chim. Acta*, **264**, (1997), 137.

23. P. F. Barron, J. C. Dyason, P. C. Healy, L. M. Engelhardt, B. W. Skelton and A. H. White, *J. Chem. Soc., Dalton Trans.*, (1986), 1965.

24. R. Stein and C. Knobler, *Inorg. Chem.*, **16**, (1977), 242.

25. J. A. Iggo, 'NMR Spectroscopy in Inorganic Chemistry', Oxford University Press, Oxford, (1999).

26. F. Harrington, Project Report, Southampton University, (2000).

27. S. J. B. Price, C. Brevard, A. Pagelot and P. J. Sadler, *Inorg. Chem.*, **24**, (1985), 4278.

28. P. E. Garrou, *Chem. Rev.*, **81**, (1981), 229.

29. S. J. A. Pope and G. Reid, *J. Chem. Soc., Dalton Trans.*, (1999), 1615.

30. J. Connolly, G. W. Goodban, G. Reid and A. M. Z. Slawin, *J. Chem. Soc., Dalton Trans.*, (1998), 2225.

31. R. B. King, 'Organometallic Syntheses', Academic Press, New York, (1965).

32. G. R. Dobson and G. C. Faber, *Inorg. Chim. Acta*, **4**, (1969), 87.

33. K. J. Reimer and A. Shaver, *Inorg. Synth.*, **19**, (1979), 159.

34. S. A. Moya, R. Pastene, R. Schmidt, J. Guerrero and R. Sartori, *Polyhedron*, **11**, (1992), 1665.

Chapter 6

Template Synthesis of a P_2S-Donor Macrocycle

6.1 Introduction

6.1.1 Phosphine Macrocycles

In recent years there has been much interest in the preparation and properties of phosphine macrocycles.[1] Acyclic phosphines represent an important class of ligands for a wide range of transition metals and the resulting complexes have wide ranging applications. The incorporation of phosphine functions within a macrocycle will affect their ligating behaviour as a result of the macrocyclic effect.

The synthesis of phosphine macrocycles however is not straightforward. Many phosphines and phosphine macrocycle precursors are highly air-sensitive and difficult to handle, particularly over the duration of a high dilution synthesis. As with other macrocyclic syntheses, ring closure uses either a template assisted cyclisation or high dilution cyclisation. Both methods offer benefits and disadvantages which are discussed in chapter 1.

6.1.2 Template Syntheses of Phosphine Macrocycles

Norman and co-workers have prepared the P_3-donor macrocycle [12]aneP_3 using a Mo(0) template. Reaction of [{mesitylene}$Mo(CO)_3$] with three equivalents of allylphopshine yields the macrocycle precursor *fac*-[$Mo(CO)_3${$H_2PCH_2CH{=}CH_2$}$_3$] which upon heating in the presence of a free-radical initiator to facilitate the addition of the P-H bonds across the C=C double bonds cyclises to give *fac*-[$Mo(CO)_3${[12]aneP_3}] (Scheme 6.1).[2, 3] The crystal structure shows the macrocycle [12]aneP_3 facially coordinated to the $Mo(CO)_3$ moiety.[2, 3]

The larger ring P_3-donor macrocycle [15]aneP_3 can also be prepared using the same template procedure by reaction of $PH_2CH_2CH_2CH{=}CH_2$ with [{mesitylene}$Mo(CO)_3$].[3] Interestingly the small ring macrocycle [9]aneP_3 cannot be prepared from $H_2PCH{=}CH_2$.

The use of the *fac*-$Mo(CO)_3$ moiety as a template is important as it orientates the coordinated phosphines in a suitable geometry for cyclisation. The low spin d^6 Mo(0) centre exhibits a strong propensity for octahedral coordination, however the complexes have proved extremely difficult to demetallate.

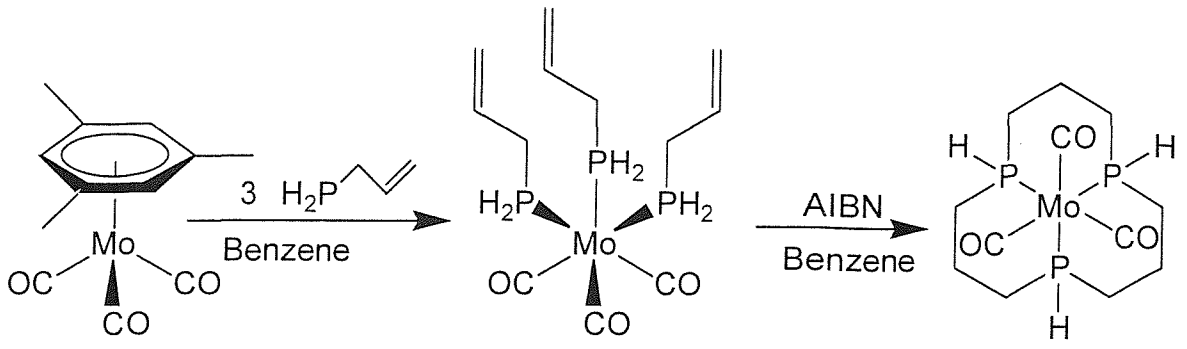

Scheme 6.1 – Template synthesis of [12]aneP_3

Subsequently Edwards and co-workers have functionalised *fac*-[Mo(CO)$_3${[12]aneP_3}] at phosphorus by deprotonation and alkylation with alkyl halide to give *fac*-[Mo(CO)$_3${R_3[12]aneP_3}] where R = Me, CH_2CHCH_2, ^iPr or CH_2SiMe_3, or by the radical induced coupling of allylamine with the secondary PH functions to give *fac*-[Mo(CO)$_3${R_3[12]aneP_3}] where R = $CH_2CH_2CH_2NH_2$ derivative.[4] They have also prepared the analogous W(0) and Cr(0) macrocycle complexes *fac*-[M(CO)$_3${[12]aneP_3}] from [{mesitylene}W(CO)$_3$] and [{mesitylene}Cr(CO)$_3$] using the route developed by Norman *et al.*[4, 5] Both the tungsten and chromium complexes can be derivatised at phosphorus in the same way as the molybdenum analogue.[4, 5]

Oxidative addition of halogen X_2 (X = Cl, Br or I) to *fac*-[Mo(CO)$_3${R_3[12]aneP_3}] (R = ^iPr, Me_3SiCH_2 or H) and *fac*-[W(CO)$_3${R_3[12]aneP_3}] (R = H) give seven coordinate salts containing a [M(CO)$_3$X{R_3[12]aneP_3}]$^+$ cation with a halide anion. The anion may be exchanged for BPh_4 by reaction with $NaBPh_4$ in $EtOH/CH_2Cl_2$.[6] These halogenohalide complexes are slowly converted over time to the dihalogendicarbonyls [M(CO)$_2$X$_2${R_3[12]aneP_3}].[6]

The chromium and molybdenum macrocyclic complexes can be reacted with an excess of alkene in the presence of a free-radical initiator to give the derivatised complexes *fac*-[M(CO)$_3${R_3[12]aneP_3}] (R = Et, $EtOCH_2CH_2$, $MeO(CH_2)_3$, $NH_2(CH_2)_3$, $MeS(CH_2)_3$ or $Ph_2P(CH_2)_3$) which contain alkyl functions or alkyl arms containing pendant donor functions attached to phosphorus.[5] It has been proposed that the complexes containing pendant donor groups may be used in the formation of bimetallic systems or may act as multidentate ligands with denticities up to hexadentate.[5]

The same research group has stereoselectively liberated the free tritertiary triphospha-macrocycle [12]aneP_3 from the Mo(0) metal template by halogen oxidation of *fac*-[Mo(CO)$_3${[12]aneP_3}] to the much more labile seven-coordinate Mo(II) species followed by hydrolysis with NaOH in alcoholic solution (Scheme 6.2).[7] The same method can be used to liberate the derivatised tritertiary phosphine macrocycles R_3[12]aneP_3 (R = Me_3CH, ^{i}Pr, Me_3SiCH_2, Et and ^{i}Bu) from the Mo(0) template.[7] Similarly the free trisecondary phosphine macrocycle can be liberated from Cr(0) by heating [Cr(CO)$_2$X{[12]aneP_3}]$^+$ with a large excess of NaOH (Scheme 6.2).[8]

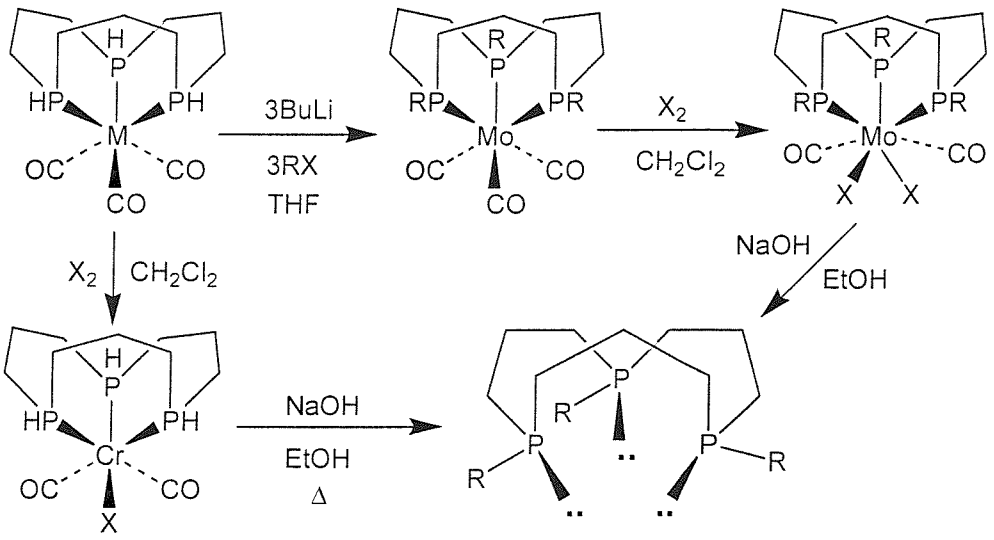

Scheme 6.2 – Liberation of stereopure R_3[12]aneP_3 from Mo(0) and Cr(0)

The liberation of the free P_3-donor macrocycles represents a major advance which has allowed more detailed studies of their coordination chemistry with other transition metals.

The reaction of ^{i}Pr$_3$[12]aneP_3 with $RhCl_3.3H_2O$ in ethanol gives [$RhCl_3${^{i}Pr$_3$[12]aneP_3}] in which the macrocycle is facially coordinated to the octahedral Rh(III) centre to give a half-sandwich structure.[9] Reaction of the Rh macrocyclic complex with $NaBH_4$ in ethanol or with NaI in ethanol yields [RhH_3{^{i}Pr$_3$[12]aneP_3}] and [RhI_3{^{i}Pr[12]aneP_3}] respectively.[9]

The mixed sandwich complex [FeCp{^{i}Pr$_3$[12]aneP_3}] has been made by reaction of ^{i}Pr$_3$[12]aneP_3 with [FeCp(η^6-C_6H_5)][PF_6] (Cp = η^5-C_5H_5) under UV irradiation.[9]

Reaction of $^{i}Pr_3[12]aneP_3$ with $[RuCl_2(dmso)_4]$ yields $[RuCl_2(dmso)\{^{i}Pr_3[12]aneP_3\}]$ whilst reaction with 0.5 equivalents of $[RuCl_2\{\eta^6\text{-}C_{10}H_{14}\}]_2$ ($\eta^6\text{-}C_{10}H_{14}$ = η^6-1-isopropyl-4-methylbenzene) results in the displacement of the arene to give $[Ru_2(\mu\text{-}Cl)_3\{^{i}Pr_3[12]aneP_3\}_2]Cl$ (Scheme 6.3).[9] The rhodium and ruthenium complexes are of particular interest as rhodium-phosphine and ruthenium-phosphine complexes are known to catalyse a number of homogeneous reactions.[9]

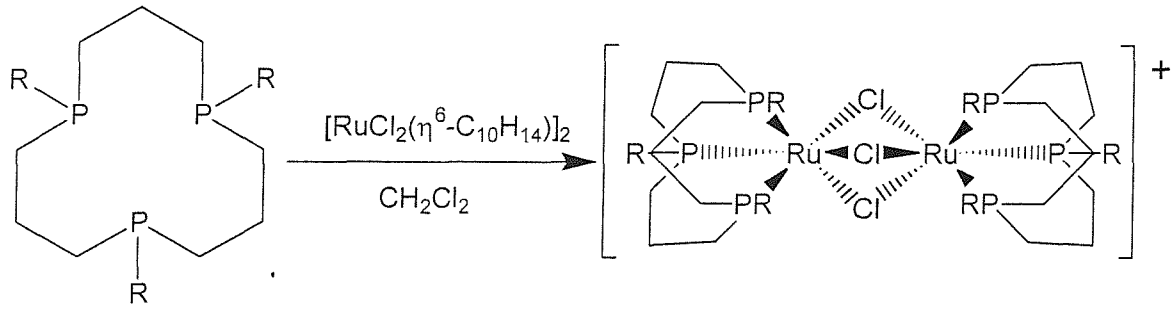

Scheme 6.3 – Synthesis of $[Ru_2(\mu\text{-}Cl)_3\{R_3[12]aneP_3\}_2]Cl$ ($R = {}^{i}Pr$)[9]

More recently Re(III), Re(I) and Mn(I) complexes of $R_3[12]aneP_3$ (R = Et or ^{i}Bu) have been reported.[10] Reaction of $R_3[12]aneP_3$ with $[ReCl_3(PPh_3)_2\{MeCN\}]$ or $[ReCl_3(PPhMe_2)_3]$ gives octahedral d^4 complexes of the type $[ReCl_3\{R_3[12]aneP_3\}]$.[10] Reduction of $[ReCl_3\{R_3[12]aneP_3\}]$ with Na/Hg under a CO atmosphere gives the Re(I) complex $[Re(CO)_2Cl\{R_3[12]aneP_3\}]$. The Re(I) complex reacts with $LiAlH_4$ to give the hydride complex $[Re(CO)_2H\{R_3[12]aneP_3\}]$.[10] Alternatively abstraction of the halide from $[Re(CO)_2Cl\{R_3[12]aneP_3\}]$ using silver triflate and reaction with a terminal acetylene or with $HC{\equiv}CC(OH)Ph_2$ gives the vinylidene or cumulene complexes respectively.[10] $Et_3[12]aneP_3$ reacts with $[Mn(CO)_5Br]$ to give the octahedral d^6 complex $[Mn(CO)_2Br\{Et_3[12]aneP_3\}]$.[10]

Free triphenyl substituted 1,5,9-triphosphacyclododecane has been prepared via the templated reaction of 1,5,9-trichloro-1,5,9-triphosphacyclododecane on molybdenum with phenylcopper or lithium-diphenylcuprate (Scheme 6.4).[11] The chloro precursor *fac*-$[Mo(CO)_3\{ClPC_3H_6\}_3]$ is prepared by reaction of *fac*-$[Mo(CO)_3\{[12]aneP_3\}]$ with CCl_4 in the presence of triethylamine. Subsequent reaction with PhCu or Ph_2CuLi in thf gives

the phenyl-substituted macrocyclic complex $[Mo(CO)_3\{Ph_3[12]aneP_3\}]$. The free macrocycle is liberated by oxidation with I_2 and demetallation in ethanolic NaOH.[11]

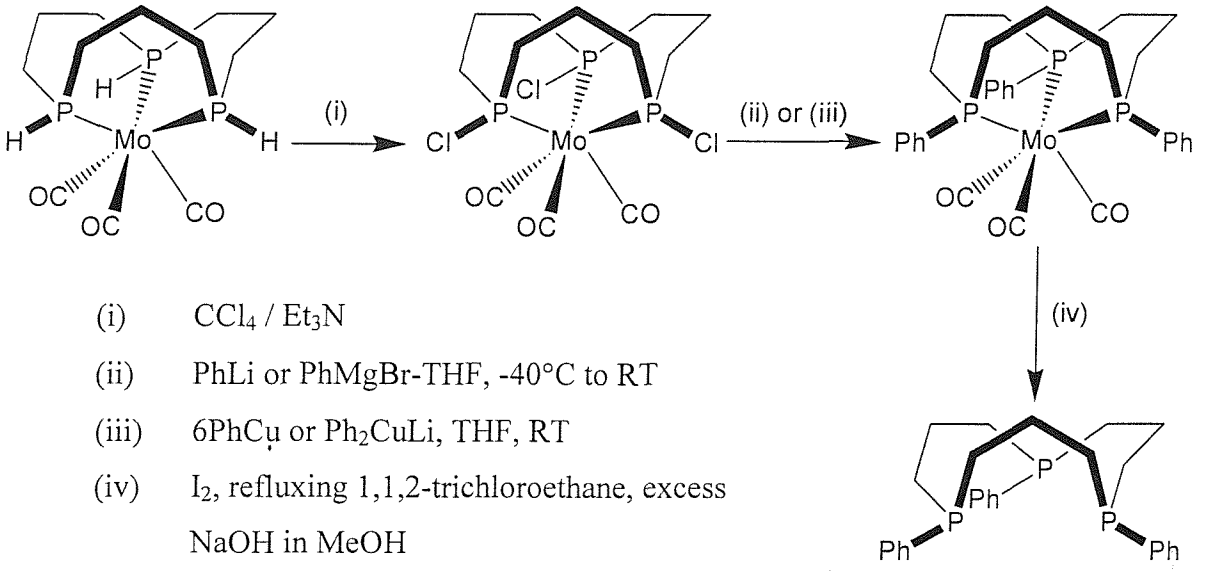

Scheme 6.4 – Template synthesis and liberation of triphenyl substituted 1,5,9-triphosphacyclododecane

Edwards and co-workers have also used an Fe(II) template to synthesise macrocycles based on the [12]aneP_3 framework by intramolecular hydrophosphination reactions.[12] UV photolysis of $[(\eta^5\text{-}C_5H_5)Fe(\eta^6\text{-}C_6H_6)][PF_6]$ in the presence of allylphosphine yields $[(\eta^5\text{-}C_5H_5)Fe\{H_2PCH_2CHCH_2\}_3][PF_6]$. Cyclisation is carried out in chlorobenzene using a 1-2 % mol. equivalent of the free-radical initiator AIBN, to induce an intramolecular hydrophosphination.[12] Hydrophosphination of ethene by the macrocyclic complex yields $[(\eta^5\text{-}C_5H_5)Fe\{Et_3[12]aneP_3\}]^+$. The analogous phenyl substituted macrocyclic complex is prepared similarly using phenylallylphosphine.[12] Free $Et_3[12]aneP_3$ can be liberated stereospecifically as the syn-syn isomer by reduction in Na/liquid ammonia.[12]

Attempts to prepare smaller ring macrocycles using Group 6 metal templates are unsuccessful however 9- and 10-membered P_3-donor macrocycles have been synthesised

using an $[Fe(\eta^5\text{-}C_5Me_5)]^+$ fragment.[13, 14] The first [10]aneP_3 macrocycle has been prepared using the route outlined in Scheme 6.5. Reaction of $H_2P(CH_2)_2PH_2$ with $[(\eta^5\text{-}C_5Me_5)Fe(CO)_2MeCN][BF_4]$ yields $[(\eta^5\text{-}C_5Me_5)Fe\{H_2P(CH_2)_2PH_2\}MeCN][BF_4]$.[13] The coordinated acetonitrile molecule is substituted with diallylphenylphosphine which can then be cyclised via a radical initiated intramolecular hydrophosphination reaction to give the macrocyclic Fe(II) complex.[13] To date there have been no reports of successful demetallations of these Fe(II) complexes.

The first triphosphacyclononane, [9]aneP_3, derivatives have been synthesised by an Fe(II) mediated intramolecular cyclisation of $H_2P(CH_2)_2PH_2$ and trivinylphosphine.[14] $[(\eta^5\text{-}C_5Me_5)Fe\{H_2P(CH_2)_2PH_2\}MeCN][BF_4]$ is prepared as above and is cyclised by heating with trivinylphosphine.[14] Subsequent hydrogenation and reaction with potassium tert-butoxide gives $[(\eta^5\text{-}C_5Me_5)Fe\{Et_3[9]aneP_3\}]^+$.[14]

The Fe(II) template approach has also allowed the introduction of an *o*-phenylene (*o*-C_6H_4) unit into the macrocycle backbone.[15]

The iron template is of particular interest as the substituents on the Cp ring may be varied which may in turn allow manipulation of steric influences upon the *trans*-coordinated phosphines, however the small ring P_3-donor macrocycles have not yet been liberated from the Fe(II) template.

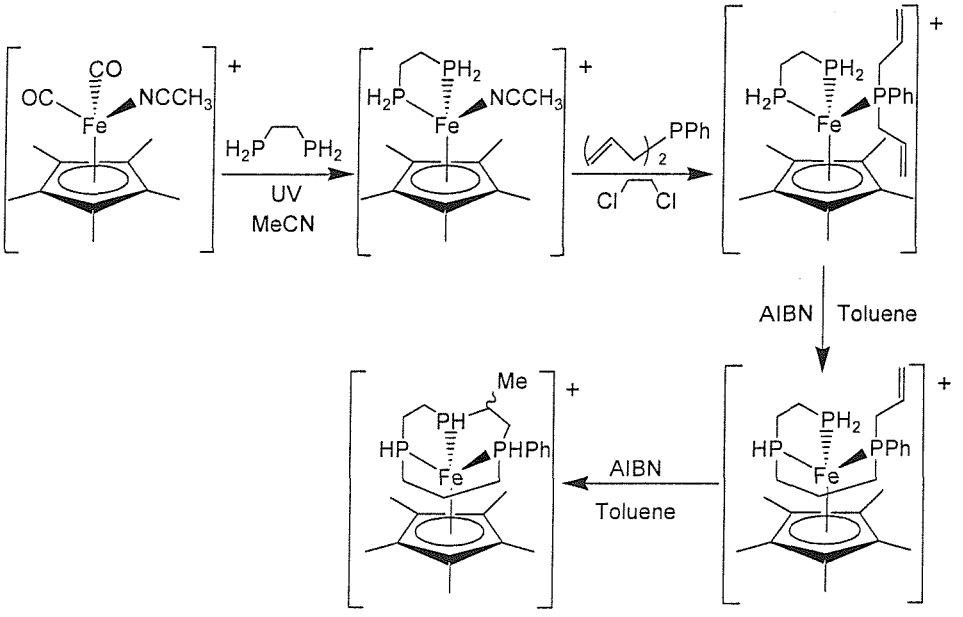

Scheme 6.5 – Synthesis of a P_3-donor macrocycle using an Fe(II) template[13]

Stelzer *et al* have prepared Ni(II) and Pd(II) complexes containing 14-membered macrocyclic tetradentate phosphine ligands.[16] Reaction of $MeHP(CH_2)_nPHMe$ (n = 2 or 3) with $NiBr_2.3H_2O$ or K_2PdCl_4 gives the disubstituted Ni(II) and Pd(II) complexes $[M\{MeHP(CH_2)_nPHMe\}_2]X_2$ (M = Ni, X = Br, n = 2 or M = Pd, X = Cl, n = 2 or 3).[16] The complexes contain stable five- or six-membered chelate rings and reactive P-H functions. Cyclisation was achieved by reaction with 2 molar equivalents of an α-β-dicarbonyl compound to give the macrocyclic complex with OH groups in the α-position relative to each P atom (Scheme 6.6).[16]

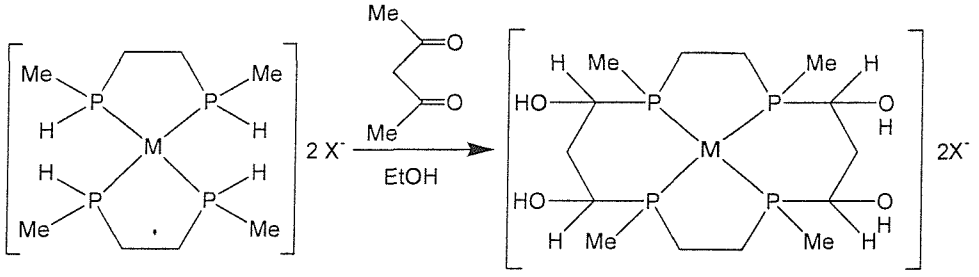

Scheme 6.6 – Template synthesis of a P_4-donor macrocycle [16]

The same research group have incorporated *o*-xylyl interdonor linkages by reaction of $MeHP(CH_2)_2PHMe$, *o*-$C_6H_4(CH_2Cl)_2$ and K_2CO_3 as base using Pd(II) as a template. The reaction proceeds in good yield and the Pd(II) template can be removed by cyanolysis to give the free P_4-donor macrocycle.[17]

The related macrocycle Me_4[14]aneP_4 has been prepared using a Pt(II) and Pd(II) template using the macrocycle precursor prepared by Stelzer $[Pd\{MeHP(CH_2)_2PHMe\}_2]Cl_2$. Cyclisation is achieved using 1,3-dibromopropane in the presence of K_2HPO_4.[18]

Blower and co-workers have prepared the small ring PS_2-donor macrocycle Ph[9]anePS_2 using a Mo(0) template.[19, 20] The same macrocycle can also be prepared using a high dilution synthesis (see section 6.1.3) from $HS(CH_2)_2PPh(CH_2)_2SH$ and 1,2-dibromoethane in dmf solution with Cs_2CO_3. The template reaction is a modification of the method used to synthesise [9]aneS_3.[21] Reaction of $[Me_4N]_2[PhP(CH_2CH_2S)_2]$ with $[Mo(CO)_3\{MeCN\}_3]$ gives $[Me_4N]_2[Mo(CO)_3\{PhP(CH_2CH_2S)_2\}]$. This molybdenum phosphine precursor reacts with $Cl(CH_2)_2Cl$ to produce *fac*-$[Mo(CO)_3\{Ph[9ane]PS_2\}]$.[19,

[20] A variety of other dichloroalkanes have been used to prepare larger ring phosphadithia macrocycles.[19] Treatment of *fac*-[$Mo(CO)_3${Ph[9]anePS_2}] with sulfur results in loss of the $Mo(CO)_3$ fragment and isolation of the macrocycle as the phosphine-sulfide derivative Ph[9]aneS_2P=S.[19]

6.1.1 High Dilution Syntheses of Phopshine Macrocycles

Kyba and co-workers have prepared a wide variety of tridentate 11-membered and tetradentate 14-membered macrocycles by cyclo-condensation of diphosphine lithium salts with bis-electrophiles under high dilution conditions. The general synthetic strategy is shown in Scheme 6.7.[22, 23]

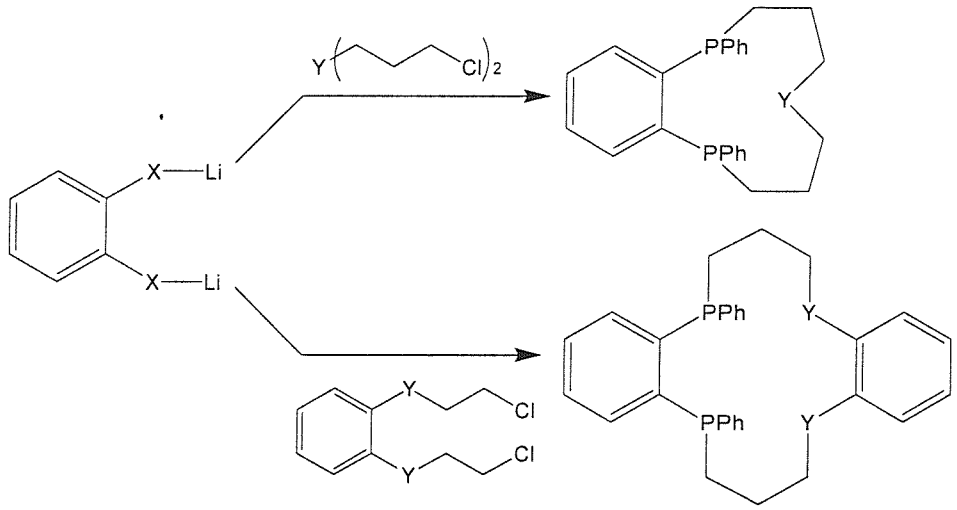

Scheme 6.7 – Kyba high dilution syntheses of phosphine macrocycles (X = PPh, Y = PPh, S, O, NMe, NPh, CH_2 or AsPh).

The 11-membered macrocycles were isolated in yields of ca. 30-60 %,[22] whilst the 14-membered macrocycles gave lower yields of ca. 18-45 %.[23] The larger ring macrocycles are of interest as they are capable of ligating a transition metal in a square planar fashion whilst the ll-membered ring macrocycles are too small to host a metal within the macrocyclic cavity and thus allow only pyramidal coordination.[23] Coordination studies with the 11-membered ring macrocycles have shown that the ligands can function in a bidentate or tridentate fashion dependent on a variety of factors.[24-26] When Y is relatively soft e.g. PPh, S, AsPh or NMe tridentate facial complexes are obtained with Group 6

metal hexacarbonyls. However if Y is hard only bidentate complexes were formed.[24] When Y = PPh or AsPh the configuration was shown to be important with only the *meso-cis*-ligands giving tridentate complexes unless temperatures sufficiently high enough for pyramidal inversion at phosphorus or arsenic were used.[24] The 14-membered macrocycles show only coordination through the phosphine functions to give transition metal complexes of the type $[ML_2]^{n+}$ where four phosphorus atoms are bound to the metal centre from two separate ligands.

Kyba *et al* have also prepared the more complex macrocycles shown in Figure 6.1 which contain an *o*-C_6H_4(PPh)S moiety with the aim to encouraging coordination of sulfur.[27, 28]

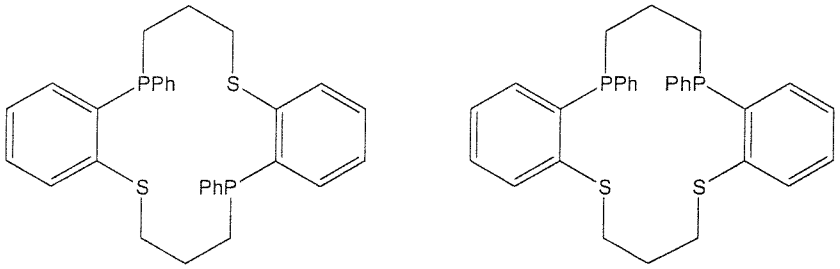

Figure 6.1 – Kyba's P_2S_2 donor macrocycles containing an *o*-C_6H_4(PPh)S moiety

Each macrocycle exists as a pair of diastereoisomers where the phenyl substituents on phosphorus are either *cis* or *trans*. A series of Ni(II) complexes with the macrocycles have been prepared and several examples have been structurally characterised.[28] The results show that the type of complex formed is dependent on the stereoisomer used. When the phenyl groups on P are *cis*, square planar complexes are obtained whilst the *trans*-isomers give pentacoordinate complexes with the metal bound to a P_2S_2-donor set from the macrocycle with the fifth coordination site occupied by a halide atom or in its absence by an acetonitrile molecule.[28]

Kyba *et al* have prepared a novel P_3-donor macrocycle by high dilution synthesis which incorporates an *o*-$C_6H_4(PPh)_2$ moiety and a secondary phosphine function within the ring.[29] To protect the P-H group a 1-naphthylmethyl protecting group has been developed which can be removed quantitatively with potassium naphthalenide.[29] The secondary phosphine can be deprotonated and should therefore allow further

functionalisation and tuning of the macrocycle. The macrocycle readily complexes to Rh(I) and Mo(0) with all three donor atoms coordinated to the metal centre.[29]

Ciampolini and co-workers have prepared a series of larger ring 18-membered mixed donor macrocycles [18]aneP_4E_2 (E = N, O or S).[30-33] The macrocycles are prepared by reaction of the lithium salt of 1,2-bis(phenylphosphino)ethane with 2,2-dichlorodiethylether or 2,2-dichlorodiethylsulfide or by reaction of the potassium salt of 1,2-bis(phenylphosphino)ethane with 2,2-dichlorodiethylpropylamine. Each of the macrocycles has five possible stereoisomers shown in Figure 6.2.

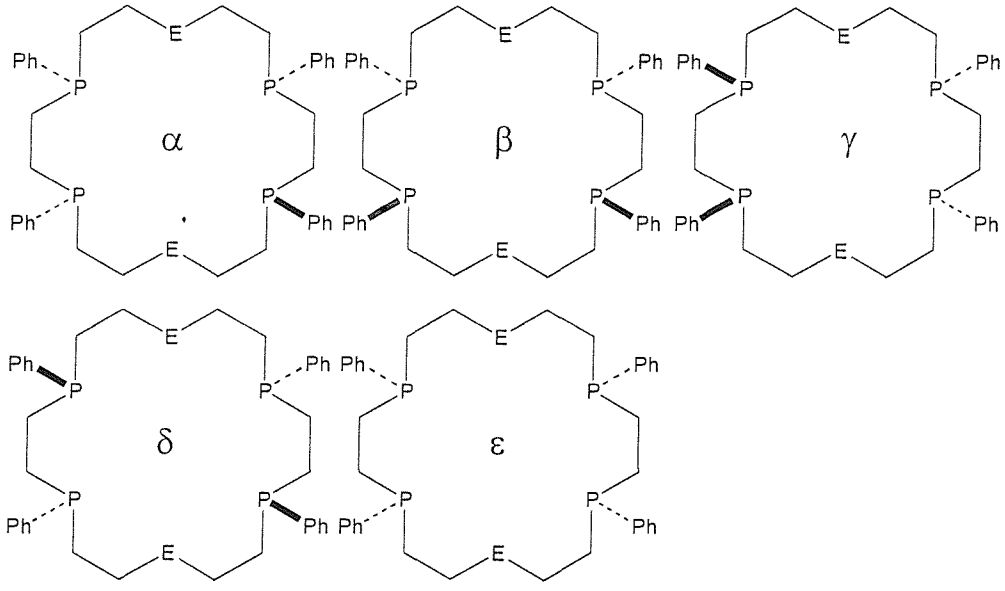

Figure 6.2 – The five possible stereoisomers of [18]aneP_4E_2 (E = N, O, S)

Extensive coordination studies have been carried out on the coordination of the 18-membered macrocycles [18]aneP_4E_2 (E = S, O and N) with Co(II), Ni(II) and Fe(II). These studies have shown that the complexes formed are highly dependent on the stereochemistry at phosphorus.[30, 32-37] For example [18]aneP_4O_2 behaves towards Co(II) as a hexadentate (β and δ), pentadentate (α and ε) and tetradentate ligand (γ).[30, 36]

Ciampolini and co-workers have also prepared Ph_4[22]aneP_4S_2 by reaction of bis(3-chloropropyl)sulphide and the dilithium salt of 1,2-bis(phenylphosphino)ethane.[38] The diastereoisomers can be separated by fractional crystallisation and ion-exchange chromatography of their nickel salts.[38] The β-isomer forms 1:1 metal:ligand complexes

with Ni(II) with non-coordinating anions and 2:1 complexes in the presence of coordinating halide anions. The crystal structure of $[Ni_2Br_2(\beta\text{-}Ph_4[22]aneP_4S_2)]$ contains two Ni atoms in a slightly distorted square planar environment coordinated to two P atoms, one S atom and one halide.[38] The δ-isomer coordinates to Co(II) via all six donor atoms to give an overall octahedral geometry.[39]

Our research group has prepared the novel mixed donor macrocycle $Ph_2[14]aneP_2S_2$.[40] The fully saturated backbone should allow greater flexibility and a number of possible coordination modes. The macrocycle is synthesised using a modification of the method employed by Blower *et al* in the synthesis of $Ph[9]anePS_2$.[41] Reaction of $PhLiP(CH_2)_3PLiPh$ with two equivalents of episulfide gives the macrocycle precursor $HS(CH_2)_2PPh(CH_2)_3PPh(CH_2)_2SH$. Cyclisation is achieved by reaction with 1,3-dibromopropane under high dilution conditions in dmf-Cs_2CO_3 at 65°C. The macrocycle coordinates readily to Pt(II), Pd(II), Co(III) and Rh(III) in an endocyclic arrangement bonding to the metal through a P_2S_2 donor set.[40]

Reaction of the $LiS(CH_2)_2PPh(CH_2)_2SLi$ with bis(3-chloropropyl)phenylphosphine yields $Ph_2[12]aneP_2S_2$ as a mixture of *cis*- and *trans*-isomers. The two isomers are readily separated by crystallisation. The *trans*-isomer reacts with hydrated $Ni(ClO_4)_2$ in CH_2Cl_2/MeCN to give $[Ni\{trans\text{-}Ph_2[14]aneP_2S_2\}MeCN]^{2+}$ which has been structurally characterised. The crystal structure shows a pentacoordinate Ni(II) centre bound to all four donor atoms of the macrocycle and to one acetonitrile molecule.[42]

The smaller mixed P/S-donor macrocycle $Ph[9]anePS_2$ has been prepared by Blower *et al* by the reaction of $PhP(CH_2CH_2SH)_2$ with 1,2-dichloroethane and Cs_2CO_3 under high dilution conditions.[20, 41] $Ph[9]anePS_2$ reacts with $[Cu(MeCN)_4][PF_6]$ to give the tetrahedral complex $[Cu\{\eta^1\text{-}Ph[9]anePS_2\}\{\eta^3\text{-}Ph[9]anePS_2\}][PF_6]$ with one ligand facially bound to the Cu centre via all three donor atoms and a second macrocycle bound via the phosphine function alone.[20] Reaction with $Hg(ClO_4)_2$ affords $[Hg\{Ph[9]anePS_2\}_2][ClO_4]_2$ in which the macrocycle coordinates through a PS_2 donor set resulting in a very distorted octahedral geometry.[41]

6.2 Results and Discussion

Kyba *et al* have prepared a number of phosphorus containing macrocycles via high dilution syntheses. These macrocycles are often isolated as mixtures of stereoisomers which are not easily interconverted due to the high energy barrier to inversion at phosphorus. High dilution syntheses are lengthy procedures and relatively low yielding. The aim of the work described in this chapter was to investigate new routes for the synthesis of mixed donor phosphorus containing macrocycles using a metal template approach that would overcome many of the problems associated with these high dilution syntheses.

For this investigation an eleven-membered P_2S-donor macrocycle (P_2S) was chosen as the target molecule (Figure 6.3). The choice of this particular macrocycle offers a number of advantages. Firstly the macrocycle precursors are easily obtainable. The diprimary phosphine 1,2-$C_6H_4(PH_2)_2$ is readily prepared by the reduction of the corresponding phosphonite 1,2-$C_6H_4\{PO(OMe)_2\}_2$ with $LiAlH_4$ and the thioether function is introduced as diallylsulfide which is commercially available.

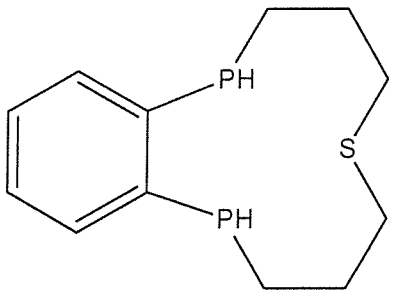

Figure 6.3 – Target P_2S-donor macrocycle (P_2S)

The use of a diprimary phosphine prevents the formation of stereoisomers and also allows further tuning of the macrocycle by variation of the substituents at phosphorus. This can easily be achieved by deprotonation and reaction with an alkylhalide derivative of choice.

The study of mixed donor tridentate macrocycles and their coordination chemistry is of interest since they can act as face-capping six electron donor ligands. They may be considered as neutral analogues of the cyclopentadienyl ligand, complexes of which are important catalyst precursors.

6.2.1 Mn(I) as a Template

The approach adopted here for the synthesis of a P_2S donor macrocycle was to use a metal ion as a template. Mn(I), a low spin d^6 and relatively inert metal ion has been employed to provide a stable octahedral environment. The synthetic strategy is outlined below in Scheme 6.8.

For this chemistry $[MnCl(CO)_5]$ has been used as the starting material. The formation of *fac*-$[MnCl(CO)_3\{1,2\text{-}C_6H_4(PH_2)_2\}]$ specifically is crucial to this work as it orientates the precursors in a suitable geometry for cyclisation. Following addition of the primary phosphine to the Mn(I) ion, the halide can be removed under mild reaction conditions using $AgCF_3SO_3$ or $AgClO_4$.[2] The $CF_3SO_3^-$ and ClO_4^- ligands bind weakly to the soft Mn(I) centre and thus can be easily displaced by a second precursor, in this case diallylsulfide. This sequential introduction of reagents to the metal centre allows much more control than the method originally employed by Norman and co-workers [2, 3] for the preparation of [12]aneP_3 and [15]aneP_3 in which the precursors are introduced to the $Mo(CO)_3$ fragment in a single step.

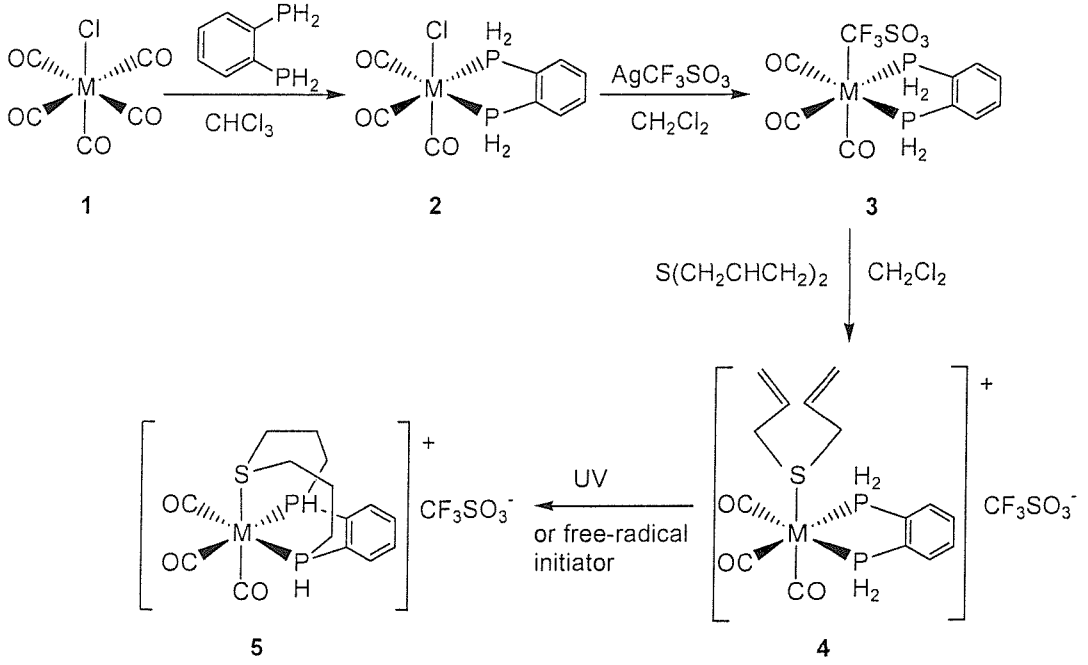

Scheme 6.8 – Synthesis of P_2S using a M(I) template (M = Mn or Re)

The use of Mn(I) as a template should allow easier demetallation of the macrocyclic complex than with Mo(0) as the macrocycle should be more labile on a 3d metal ion. Possible methods for demetallation include oxidation of the Mn(I) ion to the more labile Mn(II) and extraction of the liberated macrocycle. An alternative approach would be to reduce the metal centre to M(0) and remove the metal by electrolysis. Both methods would require a thorough investigation of the electrochemistry of the metal involved.

6.2.1.1 Synthesis of Precursor 2

Precursor 2 was prepared following a slight modification of the literature procedure.[43] Reaction of $[MnCl(CO)_5]$ with one molar equivalent of 1,2-$C_6H_4(PH_2)_2$ in gently refluxing $CHCl_3$ followed by concentration *in vacuo* and precipitation with hexane yields the neutral species *fac*-$[MnCl(CO)_3\{1,2\text{-}C_6H_4(PH_2)_2\}]$ as a bright yellow solid in ca. 60 % yield. The reaction progress was monitored by *in situ* solution IR spectroscopy and was considered complete when ν(CO) associated with the starting material (2058, 2011, 1978 cm^{-1}) were replaced by three new strong bands at 2045, 1983 and 1932 cm^{-1}. The solution IR data are consistent with the formation of *fac*-$[MnCl(CO)_3\{1,2\text{-}C_6H_4(PH_2)_2\}]$ (theory C_s 2A' + A'').[43] The ^{31}P NMR spectrum shows a triplet at 1.6 ppm with $^1J(^{31}P\text{-}^1H)$ = 340 Hz, consistent with the formation of the *fac*-isomer and with retention of two protons on each phosphorus. The ^{55}Mn NMR spectrum shows a broad resonance at −1261 ppm ($w_{1/2}$ = 2975 Hz), the broadness a consequence of the quadrupole moment on ^{55}Mn. The value is identical to that reported in the literature.[43] Although P-H bonds are weakened by coordination to a metal centre the complex shows no evidence of either oxidation or decomposition and remains stable for a period of months if stored under nitrogen in the freezer.

6.2.1.2 Synthesis of Precursor 3

The intermediate species *fac*-$[Mn(CO)_3\{1,2\text{-}C_6H_4(PH_2)_2\}CF_3SO_3]$ was prepared by reaction of precursor 2 with one equivalent of $AgCF_3SO_3$ in CH_2Cl_2. The reaction was carried out in a foil-wrapped flask to protect the solution from bright light. After ca. 30 minutes a AgCl precipitate was formed which was removed from the reaction by

filtration. Concentration of the filtrate and addition of hexane gives precursor 3 as a pale yellow solid in ca. 70% yield. As with all of the carbonyl work in this chapter, the reaction was conveniently monitored by *in situ* solution IR spectroscopy. The solution IR spectrum of *fac*-$[Mn(CO)_3\{1,2\text{-}C_6H_4(PH_2)_2\}CF_3SO_3]$ (Figure 6.4) shows three strong bands at 2057, 1993 and 1942 cm^{-1} which are in close agreement with those reported by Carriedo and co-workers for a series of other Mn(I) carbonyl diphosphine complexes.[44] The ^{31}P NMR spectrum shows a triplet at –3.5 with $^{1}J(^{31}P\text{-}^{1}H)$ =350 Hz consistent with retention of a *fac*-tricarbonyl unit and of the diprimary phosphine. The only significant species in the electrospray mass spectrum is a cluster of peaks at *m/z* 322 with the correct isotopic distribution for $[Mn(CO)_3\{1,2\text{-}C_6H_4(PH_2)_2\}MeCN]^+$. The fragment ion shows loss of $CF_3SO_3^-$ to give the monocation which is consistent with the group being only weakly bound to the soft Mn(I) centre. The mass spectrum is run in MeCN and this accounts for the coordinated MeCN molecule in the fragment ion.

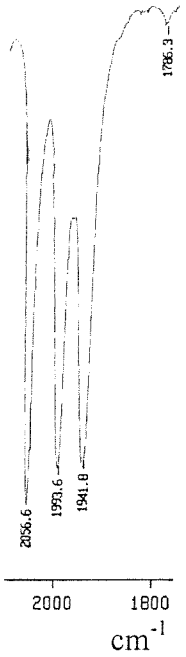

Figure 6.4 – Solution IR spectrum of *fac*-$[Mn(CO)_3\{1,2\text{-}C_6H_4(PH_2)_2\}CF_3SO_3]$ in CH_2Cl_2

6.2.1.3 Synthesis of Precursor 4

The next stage in the attempted macrocycle formation involves substitution of the weakly coordinated triflate to allow introduction of the thioether unit.

One equivalent of diallylsulfide was added to a solution of precursor 3 in CH_2Cl_2. The reaction was stirred at room temperature under nitrogen for approximately 48 hours. Concentration of the reaction *in vacuo* and addition of hexane yields precursor 4 as a yellow gum in ca. 70 % yield.

The ^{31}P NMR spectrum shows two triplets in an approximate 1:10 ratio. The minor species at δ -3.6 ppm corresponds to residual precursor 3 *fac*-$[Mn(CO)_3\{1,2\text{-}C_6H_4(PH_2)_2\}CF_3SO_3]$. The major species at δ -6.0 ppm corresponds to a new species and and is consistent with the formation of precursor 4 in which the weakly bound triflate group has been displaced by the diallylsulfide. The ^1H NMR spectrum also provides clear evidence for incomplete consumption of diallylsulfide with two multiplets at δ 5.74-5.79 and 5.38-5.44 and a doublet at δ 3.47 ppm corresponding to the CH, CH_2 and $S(CH_2)$ protons respectively on coordinated diallylsulfide. The ^1H NMR spectrum shows an additional two multiplets of much weaker intensity at δ 5.60-5.64 and 5.13-5.24 ppm corresponding to the CH and CH_2 protons respectively on free diallylsulfide with a doublet corresponding to the $S(CH_2)$ protons at δ 3.10 ppm. The ^1H NMR spectrum also shows a multiplet at δ 7.73-8.14 ppm corresponding to the aromatic backbone of the coordinated phosphine and PH resonances at δ 6.84 and 6.75 ppm. The remaining two PH resonances are hidden beneath the large diallylsulfide multiplets.

The electrospray mass spectrum shows two major species at *m/z* 395 and 322 corresponding to the desired $[^{55}Mn(CO)_3\{1,2\text{-}C_6H_4(PH_2)_2\{S(CH_2CHCH_2)_2\}\}]^+$ and $[^{55}Mn(CO)_3\{1,2\text{-}C_6H_4(PH_2)_2\}MeCN]^+$ respectively

Various attempts were made to push the reaction to completion. The reaction was repeated using an excess of diallylsulfide. It was important to remove any unreacted diallylsulfide prior to any cyclisation attempts to prevent the possibility of intermolecular reaction. This was achieved by precipitation of precursor 4 from a CH_2Cl_2 solution by addition of hexane with thorough washing of the isolated solid. Diallylsulfide is highly soluble in organic solvents and therefore any excess is removed in the washings. Although the ^{31}P NMR spectrum shows an improvement in the ratio of product to residual precursor 3 there remains a triplet at δ -3.5 ppm corresponding to residual *fac*-$[Mn(CO)_3\{1,2\text{-}C_6H_4(PH_2)_2\}CF_3SO_3]$.

An attempt to drive the reaction to completion by heating a solution of precursor 3 with one equivalent of diallylsulfide in CH_2Cl_2 to gentle reflux also failed. The ^{31}P NMR spectrum shows an increase in the ratio of residual precursor 3 to product suggesting increased dissociation of diallylsulfide at high temperatures. This was confirmed by recording a $^{31}P\{^1H\}$ NMR spectrum of the original sample containing a 1:10 ratio of residual precursor 3 to product at 60°C. The spectrum shows a single resonance at δ -3.7 ppm indicating complete conversion back to *fac*-$[Mn(CO)_3\{1,2\text{-}C_6H_4(PH_2)_2\}CF_3SO_3]$ and suggesting that diallylsulfide is highly labile on Mn(I). Previous studies in our laboratory have shown that the complex $[MnCl(CO)_3\{Me_2S\}_2]$ readily loses methylsulfide *in vacuo* providing further support for the lability of sulfide ligands on Mn(I).[45]

6.2.1.4 Attempted Cyclisation of Precursor 4

Cyclisation was attempted via the route devised by Norman and co-workers which involves the addition of P-H bonds across the C=C double bonds induced by the presence of a free radical initiator.

Cyclisation was attempted on a sample of precursor 4 containing ca. 10 % *fac*-$[Mn(CO)_3\{1,2\text{-}C_6H_4(PH_2)_2\}CF_3SO_3]$. It was hoped that the presence of residual precursor 3 would not have an adverse affect on the cyclisation attempt and that it could be removed after successful cyclisation. The sample of precursor 4 was dissolved in toluene containing 1 mol % of the free radical initiator AIBN. The reaction was heated at 70°C to avoid dissociation of the diallylsulfide for four hours, after which time a sample was removed for $^{31}P\{^1H\}$ NMR spectroscopy. The $^{31}P\{^1H\}$ NMR spectrum shows no change from that of the starting sample showing that no reaction had occurred. This is most probably due to insufficient temperatures for activation of the free radical initiator.

6.2.2 Re(I) as a template

Due to the difficulties encountered with Mn(I) with respect to the lability of the diallylsulfide ligand a new template was required. Re(I) maintains a d^6 configuration but as a 5d metal ion is much more inert to substitution. Although reactions with rhenium are significantly slower than those with Mn(I), once coordinated the diallylsulfide ligand

should not easily be displaced. Otherwise the chemistry of Re(I) should parallel that of Mn(I). For this chemistry *fac*-[ReBr(CO)$_5$] has been used as the starting material and a similar strategy to that of the Mn(I) template has been employed (Scheme 6.1).

6.2.2.1 Synthesis of Precursor 2

The treatment of [ReBr(CO)$_5$] with one molar equivalent of 1,2-$C_6H_4(PH_2)_2$ in refluxing $CHCl_3$ followed by concentration *in vacuo* and precipitation with hexane affords the neutral species *fac*-[ReBr(CO)$_3${1,2-$C_6H_4(PH_2)_2$}] as a white solid in ca. 50 % yield. The solution IR spectrum shows three strong ν(CO) bands at 2046, 1972 and 1920 cm^{-1} consistent with the isolation of a *fac*-tricarbonyl species. The ^{31}P NMR spectrum shows a triplet at δ -50.9 ppm with $^1J(^{31}P\text{-}^1H)$ = 370 Hz again consistent with the formation of the novel complex *fac*-[ReBr(CO)$_3${1,2-$C_6H_4(PH_2)_2$}]. The ^{1}H NMR spectrum shows two multiplets at δ 7.58-7.65 and 7.95-8.09 ppm corresponding to the aromatic protons of the coordinated diprimary phosphine and four broad resonances at δ 5.43, 5.80, 6.69 and 6.85 ppm corresponding to the the four PH protons, although couplings to ^{31}P are unresolved.

6.2.2.2 Structural Characterisation of *fac*-[ReBr(CO)$_3${1,2-$C_6H_4(PH_2)_2$}]

Crystals of *fac*-[ReBr(CO)$_3${1,2-$C_6H_4(PH_2)_2$}] suitable for single crystal X-ray diffraction were grown by layering a solution of the complex in CH_2Cl_2 with hexane. The structure (Figure 6.5, Tables 6.1 and 6.2) shows the Re centre bound to the two P atoms of the diprimary phosphine, three carbonyl groups and Br in a distorted octahedral geometry. The structure confirms the isolation of the *fac*-isomer. The P(1)-Re(1)-P(2) bond angle of 80.69(6)° arising through chelation of the diprimary phosphine is much smaller than the 90° expected for a regular octahedron and is slightly smaller than ∠P-Mn-P (81.97(6) in the related complex *fac*-[MnCl(CO)$_3${1,2-$C_6H_4(PH_2)_2$}].[43] The Re-C bond length *trans* to Br is significantly shorter than the Re-C bond distances *trans* to P and the Re-P distances (2.4233(18), 2.4111(18)) are comparable with those in [([12]ane$P_3{}^t Bu_3$)$ReCl_3$] (Re-P = 2.389(2), 2.381(3)).[10]

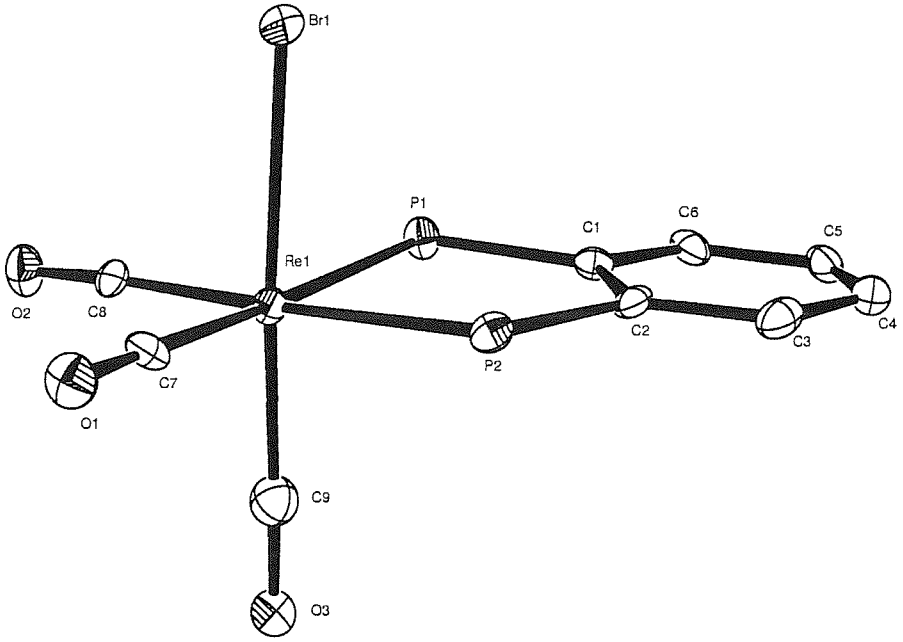

Figure 6.5 – View of the structure of *fac*-[$ReBr(CO)_3\{1,2\text{-}C_6H_4(PH_2)_2\}$] with numbering scheme adopted. Ellipsoids are drawn at 40 % probability. H atoms are omitted for clarity.

Bond Lengths (Å)		*Bond Angles (°)*	
Re(1)-Br(1)	2.6446(7)	P(1)-Re(1)-P(2)	80.69(6)
Re(1)-P(1)	2.4233(18)	P(1)-Re(1)-C(7)	170.95(19)
Re(1)-P(2)	2.4111(18)	P(1)-Re(1)-C(8)	93.54(19)
Re(1)-C(7)	1.963(7)	P(1)-Re(1)-C(9)	92.93(19)
Re(1)-C(8)	1.961(7)	P(2)-Re(1)-C(7)	92.2(2)
Re(1)-C(9)	1.920(8)	P(2)-Re(1)-C(8)	174.2(2)
Bond Angles (Å)		P(2)-Re(1)-C(9)	90.4(2)
Br(1)-Re(1)-P(1)	85.51(5)	C(7)-Re(1)-C(8)	93.5(3)
Br(1)-Re(1)-P(2)	85.27(5)	C(7)-Re(1)-C(9)	92.7(3)
Br(1)-Re(1)-C(7)	88.35(19)	C(8)-Re(1)-C(9)	90.3(3)
Br(1)-Re(1)-C(8)	93.8(2)	Re(1)-P(1)-C(1)	110.9(2)
Br(1)-Re(1)-C(9)	175.63(19)	Re(1)-P(2)-C(2)	111.2(2)

Table 6.1 – Selected bond lengths (Å) and angles (°) for *fac*-[$ReBr(CO)_3\{1,2\text{-}C_6H_4(PH_2)_2\}$]

Table 6.2 – Crystal data and structure refinement details for *fac*-[$ReBr(CO)_3\{1,2\text{-}C_6H_4(PH_2)_2\}$]

compound	[$ReBr(CO)_3\{1,2\text{-}C_6H_4(PH_2)_2\}$]
empirical formula	$C_9H_8BrO_3P_2Re$
fw	492.20
cryst. system	orthorhombic
space group	Pbca
a (Å)	11.7291(3)
b (Å)	9.5852(4)
c (Å)	22.4772(8)
volume (Å)	2527.02(15)
Z	8
density (calc) (mg/m^3)	2.587
abs coef (mm^{-1})	13.020
F(000)	1808
total no. of obsns	8899 (R_{int} = 0.0795)
no. of unique obsns	2564
min, max transmission	0.256, 0.555
no. of parameters, restraints	146, 0
goodness-of-fit on F^2	1.015
R1, wR2 ($I > 2\sigma(I)$)[b]	0.0390, 0.0839
R1, wR2 (all data)	0.0550, 0.0901

Temperature = 120 K; wavelength (Mo-Kα) = 0.71073 Å; θ (max) = 27.5 deg.

[b] $R1 = \sum || F_0| - |F_c|| / \sum |F_0|$ $\quad wR2 = [\sum w(F_0^2 - F_c^2)^2 / \sum wF_0^4]^{1/2}$

6.2.2.3 Synthesis of Precursor 3

The intermediate species *fac*-$[Re(CO)_3\{1,2\text{-}C_6H_4(PH_2)_2\}CF_3SO_3]$ was prepared by reaction of precursor 2 with one molar equivalent of $AgCF_3SO_3$ in CH_2Cl_2. The reaction was carried out in a foil-wrapped flask to protect the solution from bright light. After approximately one hour the resulting AgBr precipitate was removed from the reaction by filtration and the filtrate was concentrated *in vacuo*. Addition of hexane yields $[Re(CO)_3\{1,2\text{-}C_6H_4(PH_2)_2\}CF_3SO_3]$ as a white solid in 70 % yield.

The solution IR spectrum shows three strong ν(CO) bands at 2061, 1992 and 1936 cm^{-1} shifted significantly from the bands in precursor 2. The ^{31}P NMR spectrum (Figure 6.6) shows a triplet at δ -44.4 ppm with $^1J(^{31}P\text{-}^1H)$ = 370 Hz consistent with retention of the diprimary phosphine and also with a *fac*-tricarbonyl geometry. The electrospray mass spectrum in acetonitrile is also consistent with the isolation of precursor 3, showing a cluster of peaks at *m/z* 454 with the correct isotopic distribution for $[Re(CO)_3\{1,2\text{-}C_6H_4(PH_2)_2\}MeCN]^+$. As with the analogous Mn(I) complex the fragment ion observed corresponds to loss of the weakly coordinating triflate group and coordination of an acetonitrile molecule from solution.

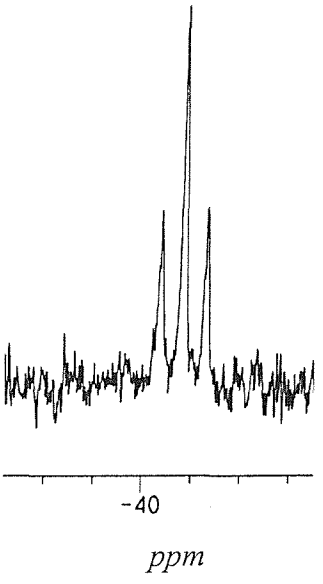

Figure 6.6 – ^{31}P NMR spectrum of *fac*-$[Re(CO)_3\{1,2\text{-}C_6H_4(PH_2)_2\}CF_3SO_3]$ in $CH_2Cl_2/CDCl_3$

6.2.2.4 Synthesis of Precursor 4

Precursor 4, *fac*-$[Re(CO)_3\{1,2\text{-}C_6H_4(PH_2)_2\}\{S(CH_2CHCH_2)_2\}]CF_3SO_3$, was prepared by reaction of precursor 3 with one equivalent of diallylsulfide in gently refluxing $CHCl_3$. Concentration of the reaction and addition of hexane yields precursor 4 as a yellow gum in ca 75% yield.

The solution IR spectrum shows three ν(CO) bands at 2055, 2020 and 1985 cm^{-1} only slightly shifted from those observed for precursor 3. The ^{31}P NMR spectrum shows a triplet at δ-55.1 ppm with $^1J(^{31}P\text{-}^1H)$ = 389 Hz, consistent with the retention of a *fac*-tricarbonyl unit and also of the diprimary phosphine. Unlike the Mn(I) analogue the ^{31}P NMR spectrum shows no signs of diallylsulfide dissociation. The ^1H NMR confirms the presence of coordinated diallylsulfide alone, showing a doublet at δ 3.62 ppm corresponding to the CH_2S protons and a large multiplet at δ 5.30-5.85 ppm due to the CH and CH_2 protons of coordinated diallylsulfide. The ^1H NMR spectrum also shows two multiplets at δ 7.61-7.76 and 7.98-8.30 corresponding to the aromatic protons of the diprimary phosphine and two broad singlets at δ 6.86 and 6.92 corresponding to PH resonances. The remaining two PH resonances are hidden beneath the large multiplet at δ 5.30-5.83 ppm. Importantly the ^1H NMR spectrum shows no signs of free diallylsulfide, confirming that as expected the Re(I) complex shows higher stability than the analogous Mn(I) complex.

The electrospray mass spectrum (Figure 6.7) shows peaks consistent with *m/z* 567 $[^{187}Re(CO)_3\{1,2\text{-}C_6H_4(PH_2)_2\}\{S(CH_2CHCH_2)_2\}MeCN]^+$, *m/z* 527 $[^{187}Re(CO)_3\{1,2\text{-}C_6H_4(PH_2)_2\}\{S(CH_2CHCH_2)_2\}]^+$, *m/z* 494 $[^{187}Re(CO)_3\{1,2\text{-}C_6H_4(PH_2)(PH)\}\{MeCN\}_2]^+$, *m/z* 454 $[^{187}Re(CO)_3\{1,2\text{-}C_6H_4(PH_2)_2\}]^+$.

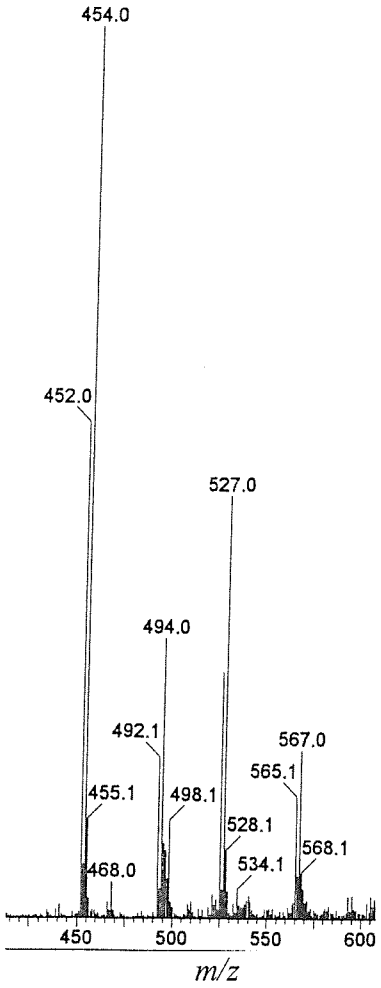

Figure 6.7 - Electrospray mass spectrum (MeCN) of *fac*-[Re(CO)$_3${1,2-C$_6$H$_4$(PH$_2$)$_2$}{S(CH$_2$CHCH$_2$)$_2$}][CF$_3$SO$_3$]

6.2.2.5 Attempted Cyclisations of Precursor 4

Several attempts at cyclisation were made using the free radical initiator 1,1-azobis(cyclohexane-carbonitrile) to facilitate the addition of the P-H bonds across the C=C double bonds.

Precursor 4 was dissolved in *o*-dichlorobenzene and ca. 0.1 mol % of 1,1-azobis(cyclohexane-carbonitrile) was added. The reaction was stirred at 45°C for 1.5 hours after which time a sample was removed for $^{31}P\{^1H\}$ NMR spectroscopy. However the $^{31}P\{^1H\}$ NMR spectrum shows only a single resonance at δ -55.3 ppm corresponding to unreacted precursor 4. The reaction was continued at 45°C for a further 8 hours. The $^{31}P\{^1H\}$ NMR spectrum of the crude reaction mixture shows mainly unreacted *fac*-[Re(CO)$_3${1,2-C$_6$H$_4$(PH$_2$)$_2$}{S(CH$_2$CHCH$_2$)$_2$}]CF$_3$SO$_3$ with a number of smaller

unassignable resonances in the region δ 2.7 to –45 ppm. The reaction was carried out at 45°C to prevent possible decomposition, however these results indicate that the temperature is insufficient for cyclisation to proceed.

Two further cyclisation attempts were made using a 1 mol % of the free radical initiator 1,1-azobis(cyclohexane-carbonitrile) in *o*-dichlorobenzene at 80°C and 100°C respectively. After 8 hours both reactions contained small amounts of insoluble black solid indicating some decomposition. The reactions were filtered and the solvent removed by vacuum distillation to give dark brown gums. The $^{31}P\{^{1}H\}$ NMR spectrum of the reaction carried out at 80°C shows evidence of unreacted precursor 4 as well as a number of unassignable peaks. The $^{31}P\{^{1}H\}$ NMR spectrum of the reaction carried out at 100°C shows a very noisy broad multiplet at δ -15.8 ppm. The breadth of the resonance prevented the observation of any P-H couplings in the ^{1}H coupled spectrum and thus this peak could not be assigned. Due to the evidence of some decomposition no further work was carried out using 1,1-azobis(cyclohexane-carbonitrile).

A further cyclisation attempt was made using the alternative free radical initiator AIBN. A 1 mol % of AIBN was added to a solution of precursor 4 in toluene and the reaction was heated at 80°C for 4 hours. Over the course of the reaction the solution darkened significantly and small amounts of black solid precipitated out of solution indicating decomposition. The toluene was removed *in vacuo* to give a poorly soluble brown gum. The $^{31}P\{^{1}H\}$ NMR spectrum shows two noisy weak resonances at δ -15 and 24 ppm. Due to poor solubility no ^{31}P-^{1}H couplings could be obtained and thus the reaction was abandonned.

An alternative cyclisation attempt was made by photolysing a solution of precursor 4 in dry thf for 2 hours, after which time a sample was removed for $^{31}P\{^{1}H\}$ NMR spectroscopy. The spectrum shows a decrease in the intensity of the resonance associated with precursor 4 at δ -55.1 ppm and the appearance of a new resonance at δ -25.7 ppm. The large positive shift in the $^{31}P\{^{1}H\}$ NMR spectrum may be indicative of P-C bond formation to give a coordinated secondary diphosphine. The value may be compared with the data on the related phosphorus containing macrocycle complex $[ReCl(CO)_2\{^{t}Bu_3[12]aneP_3\}]$ which shows a triplet at δ -8.72 and a doublet at δ -26.4

ppm in the $^{31}P\{^{1}H\}$ NMR spectrum corresponding to P *trans* Cl and P *trans* CO respectively.[10] Attempts were made to push the reaction to completion by photolysing the reaction for a further 7 hours. Unfortunately, the solution darkened significantly and the $^{31}P\{^{1}H\}$ NMR spectrum of the crude reaction mixture shows a large number of peaks in the range δ -55.3 to +12.6 ppm indicating significant decomposition.

6.2.2.6 Cyclisation of Precursor 4

A further cyclisation attempt was made in which a solution of *fac*-$[Re(CO)_3\{1,2\text{-}C_6H_4(PH_2)_2\}CF_3SO_3]$ was stirred with one equivalent of diallylsulfide in CH_2Cl_2 at room temperature for 48 hours. Although any reaction on Re(I) would be very slow at room temperature, it was hoped that under the mild reaction conditions used the decomposition observed during previous cyclisation attempts would be avoided. It was important that only one equivalent of diallylsulfide was used to promote intramolecular cyclisation and prevent the occurrence of any intermolecular reactions.

The $^{31}P\{^{1}H\}$NMR spectrum shows four resonances at δ -54.9, -47.6, -25.8 and -23.9 ppm. The major peak at δ -54.9 ppm corresponds to *fac*-$[Re(CO)_3\{1,2\text{-}C_6H_4(PH_2)_2\}\{S(CH_2CHCH_2)_2\}][CF_3SO_3]$. The minor species at δ –25.8 ppm shows a shift to high frequency from precursor 4 which may be indicative of P-C bond formation to give a secondary phosphine. A similar resonance was observed in the previous cyclisation attempt and therefore this resonance may indicate macrocycle formation. The two remaining resonances at δ-52.5 and -23.9 ppm are of equal intensity and therefore are indicative of a partially cyclised product in which one end of the diallylsulfide ligand has formed a P-C bond and the other allyl function remains uncoordinated (Scheme 6.9). Further support for these assignments is observed in the ^{31}P NMR spectrum which shows a triplet at δ -54.9 ppm corresponding to residual precursor 4, a doublet at δ -25.9 ppm which is believed to be the fully cyclised macrocyclic complex, a triplet at δ -52.5 and a doublet at δ -23.9 ppm corresponding to the primary and secondary phosphine functions respectively of the partially cyclised macrocylic species.

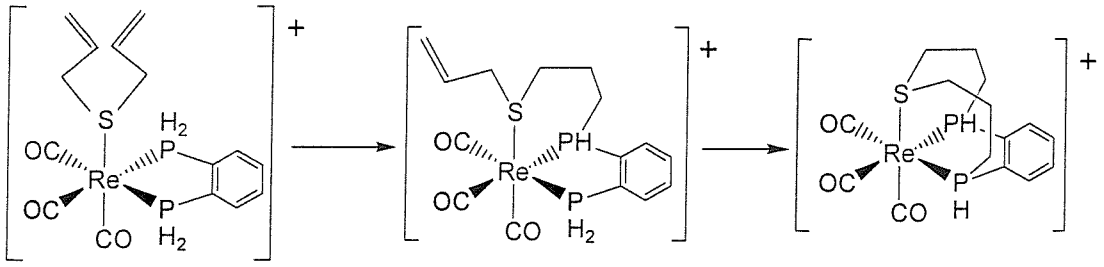

Scheme 6.9 – Cyclisation of *fac*-$[Re(CO)_3\{1,2\text{-}C_6H_4(PH_2)_2\}\{S(CH_2CHCH_2)_2\}][CF_3SO_3]$

The reaction was stirred at room temperature and monitored at regular intervals by $^{31}P\{^1H\}$ NMR spectroscopy. After 12 days the $^{31}P\{^1H\}$ NMR spectrum shows peaks corresponding to the macrocycle, the partially cyclised product and the diallylsulfide complex but also shows an additional two resonances at δ -53.5 and –17.8 ppm of approximately equal intensity. The ^{31}P NMR spectrum is complex as many of the couplings overlap but the new resonance at δ -17.8 is clearly a doublet with $^1J(^{31}P\text{-}^1H)$ = 401 Hz indicating formation of a secondary phosphine. The two new resonances are clearly related and therefore must correspond to a second partially cyclised product. The slower formation of this second partially cyclised species is consistent with isomerisation to give the thermodynamic *mer*-isomer. The $^{31}P\{^1H\}$ NMR spectrum still shows large amounts of *fac*-$[Re(CO)_3\{1,2\text{-}C_6H_4(PH_2)_2\}\{S(CH_2CHCH_2)_2\}][CF_3SO_3]$ and therefore the reaction was allowed to continue and closely monitored by $^{31}P\{^1H\}$ NMR spectroscopy.

After 40 days the $^{31}P\{^1H\}$ NMR spectrum (Figure 6.8) shows only minor amounts of the diallylsulfide complex and also shows several low intensity resonances in the range –9 to +34 ppm indicating some slight decomposition therefore the reaction was worked up. The $^{31}P\{^1H\}$ NMR spectrum of the isolated solid clearly shows three different species. The resonances at δ -53.5 and –17.7 ppm correspond to the *mer*-partially cyclised product, the resonances at δ -52.4 and –23.7 ppm correspond to the *fac*-partially cyclised product and the remaining resonance at δ -25.6 ppm corresponds to the fully cyclised macrocycle complex. The $^{31}P\{^1H\}$ NMR spectrum shows no evidence of residual precursor 4 or of *fac*-$[Re(CO)_3\{1,2\text{-}C_6H_4(PH_2)_2\}CF_3SO_3]$.

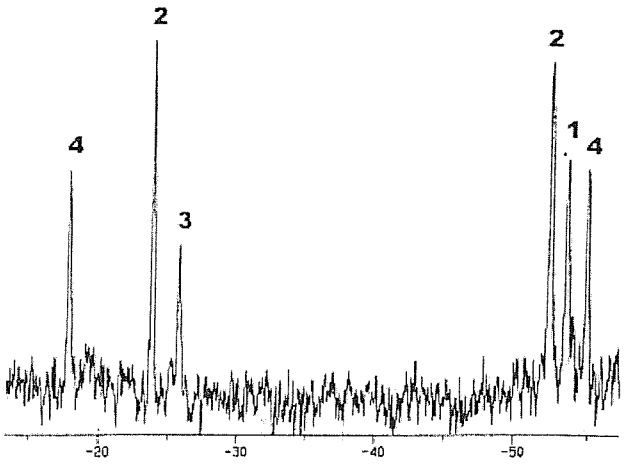

Figure 6.8 – $^{31}P\{^{1}H\}$ NMR spectrum of cyclisation reaction mixture prior to work-up

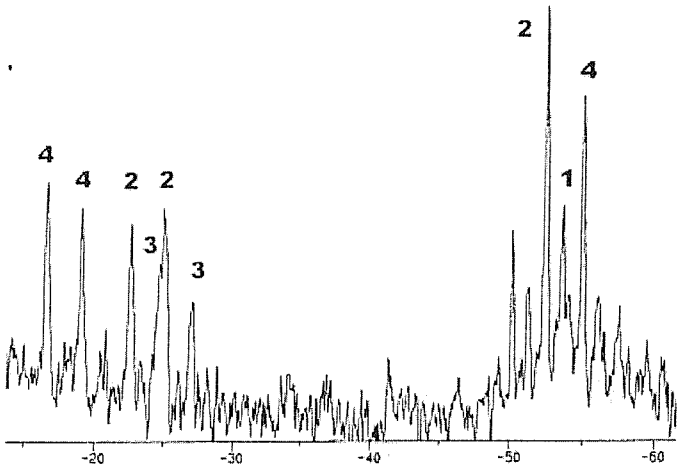

Figure 6.9 – ^{31}P NMR spectrum of cyclisation reaction mixture prior to work-up

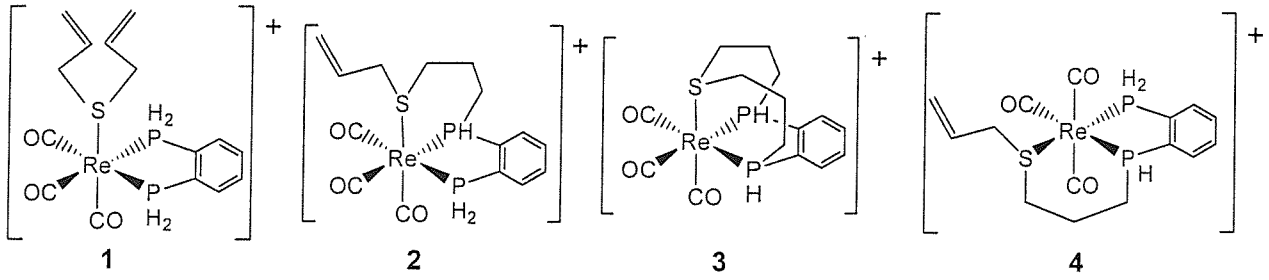

The solution IR spectrum in CH_2Cl_2 shows ν(CO) bands at 2117, 2054, 2017 and 1967 cm^{-1}, consistent with a mixture of *fac*- and *mer*-isomers, the ν(CO) bands at 2054, 2017 and 1967 cm^{-1} correspond to the *fac*-isomer whilst the band at 2117 cm^{-1} corresponds to the *mer*-isomer. The macrocyclic complex and both partially cyclised products have the same chemical composition as the precursor *fac*-$[Re(CO)_3\{1,2\text{-}C_6H_4(PH_2)_2\}\{S(CH_2CHCH_2)\}][CF_3SO_3]$ therefore definitive characterisation by mass spectrometry or elemental analysis is difficult. The electrospray mass spectrum (Figure 6.10) however shows one major ion at *m/z* 567 consistent with the proposed formulations. In contrast to the spectrum observed for the diallylsulfide precursor no lower mass ions are observed corresponding to the loss of diallylsulfide. The change in fragmentation suggests that the diallylsulfide precursor has been consumed during the cyclisation by P-C bond formation, confirming the formation of *fac*-$[Re(CO)_3\{P_2S\}]^+$ and the *mer*- and *fac*-partially cyclised products.

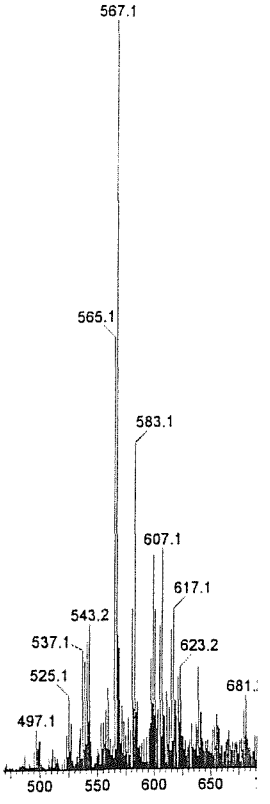

Figure 6.10 - Electropray mass spectrum (MeCN) of the solid isolated from the cyclisation reaction

Attempts were made to obtain a $^{13}C\{^1H\}$ NMR spectrum as consumption of the diallylsulfide should lead to significant shifts in the NMR spectrum. However no spectrum was observed even after an 18 hour acquisition. This suggests the presence of a small amount of paramagnetic Re(II) formed through decomposition.

Attempts were made to separate the macrocycle complex from the partially cyclised products by recrystallisation, however unfortunately all three species appear to have very similar solubilities and a mixture of all three species was always isolated.

6.3 Conclusions

A new strategy for the preparation of a P_2S donor macrocycle has been investigated and a number of different synthesis attempts have been performed via a metal template mediated ring closure using *fac*-$[Mn(CO)_3]^+$ and *fac*-$[Re(CO)_3]^+$ fragments.

The precursors *fac*-$[M(CO)_3\{1,2\text{-}C_6H_4(PH_2)_2\}\{S(CH_2CHCH_2)_2\}][CF_3SO_3]$ have been successfully isolated for both manganese and rhenium by the sequential introduction of reagents to the metal centre. The reactions proceed in high yield to give stable metal complexes which show no evidence of P-H bond cleavage or decomposition.

Ring closure has been attempted for the Mn(I) species via the addition of the P-H bonds across the C=C double bonds induced by a free-radical initiator. However the diallysulfide ligand proved suprisingly labile on Mn(I) and dissociated readily upon heating, as a consequence ring closure was unsuccessful.

A number of cyclisation attempts have been made with the Re(I) species using free-radical initiated intramolecular hydrophosphination reactions, however these largely resulted in decomposition. UV photolysis proved much more successful, giving a high-frequency shift in the $^{31}P\{^1H\}$ NMR spectrum indicative of ring-closure. However as with the previous cyclisation attempts, decomposition was evident during the reaction.

A much more successful cyclisation reaction was achieved by reaction of *fac*-$[Re(CO)_3\{1,2\text{-}C_6H_4(PH_2)_2\}CF_3SO_3]$ with one molar equivalent of diallysulfide in CH_2Cl_2 at room temperature over a period of forty days. Due to the long reaction time required for cyclisation to occur on Re(I) at room-temperature the complex also undergoes isomerisation to give a partially cyclised *mer*-isomer. This species cannot

undergo cyclisation due to the *mer*-geometry and therefore acts as a competing reaction to ring closure.

Although the final macrocyclic complex could not be isolated cleanly, these results have clearly demonstrated that mixed-donor phosphine macrocycles can be prepared using a metal-templated approach, which avoids the problems of stereoisomers obtained in high-dilution procedures. This work has successfully demonstrated that the necessary organic precursors can be introduced sequentially to the metal centre whilst retaining the *fac*-geometry necessary for cyclisation to occur. With a few modifications to the final cyclisation step (see section 6.4) it should be possible to successfully isolate the Re(I) macrocyclic complex.

6.4 Further Work

The work described in this chapter has shown that a template method can be used successfully for the synthesis of phosphine containing macrocycles. The macrocycle precursors can be introduced sequentially to the metal centre using facile reactions to give stable metal complexes in high yield. Further work should focus on improving the cyclisation procedure to avoid, if possible, both decomposition and isomerisation, both of which will decrease the overall yield of the fully cyclised macrocyclic complex.

The work so far has shown that the isomerisation proceeds at a much slower rate than cyclisation. Therefore the key to preventing the formation of the partially cyclised *mer*-isomer is to speed up the final cyclisation procedure. This may be achieved by the use of elevated temperatures or with the addition of a free-radical initiator to induce intramolecular hydrophosphination. However previous cyclisation attempts have shown evidence of significant decomposition at temperatures greater than 80°C. A possible solution would be to investigate the use of alternative free-radical initiators which can be activated at lower temperatures, for example BEt_3/O_2 which is an active free radical initiator at 0°C.[46]

A second possible cyclisation route would involve photolysing a solution of *fac*-$[Re(CO)_3\{1,2\text{-}C_6H_4(PH_2)_2\}\{S(CH_2CHCH_2)_2\}][CF_3SO_3]$ in the presence of a free-radical initiator, which should increase the rate of cyclisation whilst minimising decomposition.

Once isolated it is unlikely that traditional demetallation techniques such as the use of CN^- will liberate the free macrocycle from the 5d Re centre, therefore further work would involve a study of the electochemistry of the Re macrocyclic complex with the aim of liberating the macrocycle by either oxidation of the metal centre to Re(II) or reduction to Re(0).

If successful, the route could in principle allow the preparation of P_2S donor macrocycles with different ring sizes or alternative backbones, by altering the precursors used. It may also be possible to produce the analogous P_2N donor macrocycle by substituting diallylamine for diallylsulfide.

6.5 Experimental

General Data. All preparations were carried out under a dinitrogen atmosphere, and the Mn(I) complexes were stored in sealed containers, wrapped in aluminium foil. $[MnCl(CO)_5]$[47], $[ReBr(CO)_5]$[48] and $[MnCl(CO)_3\{1,2\text{-}C_6H_4(PH_2)_2\}]$[43] were prepared following the literature procedures.

Synthesis of $1,2\text{-}C_6H_4(PH_2)_2$[49]: Me_3SiCl (22.30 g, 0.21 mol) was added to a suspension of $LiAlH_4$ (7.8 g, 0.21 mol) in dry thf (100 mL) at -78°C. The reaction mixture was allowed to warm to RT and stirred for 2 h. The reaction mixture was cooled to -30°C and a solution of $1,2\text{-}C_6H_4\{PO(OMe)_2\}_2$ (10.00 g, 0.034 mol) in dry thf (100 mL) was added dropwise. The reaction mixture was allowed to warm to RT and stirred under N_2 for 36 h. The reaction mixture was hydrolysed with water (100 mL) followed by NaOH (1M, 100 mL). The organic layer was separated and the aqueous washed with diethyl ether (2 x 100 mL), and the combined organics were dried over anhydrous $MgSO_4$. The $MgSO_4$ was removed by filtration and the diethyl ether removed by distillation at atmospheric pressure. $1,2\text{-}C_6H_4(PH_2)_2$ was collected as a colourless oil at 90°C, 6mm Hg. Yield 2.50 g (52 %). $^{31}P\{^1H\}$ NMR (Neat): δ -123.8.

Synthesis of *fac*-$[MnCl(CO)_3\{1,2\text{-}C_6H_4(PH_2)_2\}]$: A solution of $1,2\text{-}C_6H_4(PH_2)_2$ (0.10 g, 0.7 mmol) in $CHCl_3$ (10 mL) was added to a solution of $[MnCl(CO)_5]$ (0.16 g, 0.7 mmol) in $CHCl_3$ (30 mL). The reaction was stirred, in a foil-wrapped flask to protect the solution from bright light, for 4 h. The solution was concentrated *in vacuo* to ca. 5 mL and degassed hexane added to yield a yellow solid which was isolated by filtration and dried *in vacuo*. Yield 0.14 g (63 %). ^{31}P NMR ($CH_2Cl_2/CDCl_3$): δ 1.6, t, $^1J(^{31}P\text{-}^1H)$ = 340 Hz. ^{55}Mn NMR ($CH_2Cl_2/CDCl_3$): δ -1261 ($w_{1/2}$ = 2975 Hz). IR spectrum (ν(CO) / cm^{-1}, CH_2Cl_2): 2045s, 1983s, 1932s.

Synthesis of *fac*-$[Mn(CO)_3\{1,2\text{-}C_6H_4(PH_2)_2\}CF_3SO_3]$: $AgCF_3SO_3$ (0.12 g, 0.48 mmol) was added to a solution of *fac*-$[MnCl(CO)_3\{1,2\text{-}C_6H_4(PH_2)_2\}]$ (0.15 g, 0.48 mmol) in CH_2Cl_2 (30 mL). The reaction was stirred, in a foil-wrapped flask to protect the solution

from bright light, for 30 mins. AgCl was removed by filtration and the filtrate concentrated *in vacuo* to ca. 5 mL. Degassed hexane was added to yield a pale yellow solid which was isolated by filtration and dried *in vacuo*. Yield 0.14 g (68 %). ^{31}P NMR ($CH_2Cl_2/CDCl_3$): δ -3.5, t, $^1J(^{31}P\text{-}^1H)$ = 350 Hz. Electrospray mass spectrum (MeCN): found *m/z* 322. Calc. for $[^{55}Mn(CO)_3\{1,2\text{-}C_6H_4(PH_2)_2\}MeCN]^+$ 322. IR spectrum (ν(CO/cm^{-1}, CH_2Cl_2): 2057s, 1993s, 1942s.

Synthesis of *fac*-[Mn(CO)$_3${1,2-C$_6$H$_4$(PH$_2$)$_2$}{S(CH$_2$CHCH$_2$)$_2$}][CF$_3$SO$_3$]: Diallylsulfide (40 mg, 0.35 mmol) was added to a solution of *fac*-[Mn(CO)$_3${1,2-$C_6H_4(PH_2)_2$}CF_3SO_3] (0.15 g, 0.35 mmol) in CH_2Cl_2 (30 cm^3). The reaction was stirred, in a foil-wrapped flask to protect the solution from bright light, for 48 h. The solution was concentrated *in vacuo* to ca. 5 mL and degassed hexane was added to give a yellow gum. Yield = 0.14 g (73 %). ^{1}H NMR ($CDCl_3$): δ 3.10 (d, C<u>H</u>$_2$ free allysulfide), 3.47 (d, C<u>H</u>$_2$), 5.13-5.24 (m, C<u>H</u>$_2$ free allylsulfide), 5.38-5.44 (m, C<u>H</u>$_2$), 5.60-5.64 (m, C<u>H</u> free allylsulfide), 5.74-5.79 (m, C<u>H</u> + P<u>H</u>), 6.75-6.83 (m, P<u>H</u>). 7.69-7.81 (m, Ar-C<u>H</u>), 8.02 – 8.23 (m, Ar-C<u>H</u>). ^{31}P NMR ($CH_2Cl_2/CDCl_3$): δ -3.5, t, $^1J(^{31}P\text{-}^1H)$ = 369 Hz, *fac*-[Mn(CO)$_3${1,2-$C_6H_4(PH_2)_2$}CF_3SO_3]), -6.0, t, $^1J(^{31}P\text{-}^1H)$ = 383 Hz, *fac*-[Mn(CO)$_3${1,2-$C_6H_4(PH_2)_2$}{S(CH$_2$CHCH$_2$)$_2$}][CF$_3$SO$_3$]. ^{55}Mn NMR spectrum ($CH_2Cl_2/CDCl_3$): δ -1489 ($w_{1/2}$ = 11,300 Hz). Electrospray mass spectrum (MeCN): found *m/z* 395, 322. Calc. for $[^{55}Mn(CO)_3\{1,2\text{-}C_6H_4(PH_2)_2\}\{S(CH_2CHCH_2)_2\}]^+$ 395, $[^{55}Mn(CO)_3\{1,2\text{-}C_6H_4(PH_2)_2\}MeCN]^+$ 322. IR spectrum (ν(CO) / cm^{-1}, CH_2Cl_2): 2053s, 1990s, 1972s.

Synthesis of *fac*-[ReBr(CO)$_3${1,2-C$_6$H$_4$(PH$_2$)$_2$}]: A solution of 1,2-$C_6H_4(PH_2)_2$ (0.20 g, 1.4 mmol) in $CHCl_3$ (10 mL) was added to a solution of $[ReBr(CO)_5]$ (0.57 g, 1.4 mmol) in $CHCl_3$ (50 mL). The reaction was refluxed under nitrogen for 24 h. The solution was concentrated *in vacuo* to ca. 5 mL and ice-cold degassed hexane was added to give a white solid which was isolated by filtration and dried *in vacuo*. Yield 0.36 g (52 %). Calc. for $[C_9H_8O_3BrP_2Re]$ C = 21.96, H = 1.64 %; found C = 23.54, H = 1.84 %. ^{1}H NMR ($CDCl_3$): δ 5.7 (m, 1H, P<u>H</u>), 5.8 (m, 1H, P<u>H</u>), 6.7 (m, 1H, P<u>H</u>), 7.0 (m, 1H, P<u>H</u>), 7.6 (m,

2H, Ar-CH), 8.0 (m, 2H, Ar-CH). ^{31}P NMR ($CH_2Cl_2/CDCl_3$): δ -50.9, t, $^1J(^{31}P-^1H)$ = 373 Hz. IR spectrum (ν(CO) / cm^{-1}, CH_2Cl_2): 2047s, 1981s, 1925s.

Synthesis of *fac*-[Re(CO)$_3${1,2-C$_6$H$_4$(PH$_2$)$_2$}CF$_3$SO$_3$]: $AgCF_3SO_3$ (0.10 g, 0.41 mmol) was added to a solution of *fac*-[ReBr(CO)$_3${1,2-C$_6$H$_4$(PH$_2$)$_2$}] (0.20 g, 0.41 mmol) in $CHCl_3$ (30 mL). The reaction was stirred, in a foil-wrapped flask to protect the solution from bright light, for 1 h. AgCl was removed by filtration and the filtrate reduced *in vacuo* to ca. 5 mL. Degassed hexane was added to give a white solid which was filtered and dried *in vacuo*. Yield 0.16 g (70 %). ^{31}P NMR ($CH_2Cl_2/CDCl_3$): δ -44.4, t, $^1J(^{31}P-^1H)$ = 370 Hz. Electrospray mass spectrum (MeCN): found 454. Calc. for [^{187}Re(CO)$_3${1,2-C$_6$H$_4$(PH$_2$)$_2$}MeCN]$^+$ 454. IR spectrum (ν(CO) / cm^{-1}, CH_2Cl_2): 2061s, 1992s, 1936s.

Synthesis of *fac*-[Re(CO)$_3${1,2-C$_6$H$_4$(PH$_2$)$_2$}{S(CH$_2$CHCH$_2$)$_2$}][CF$_3$SO$_3$]: Diallylsulfide (70 mg, 0.64 mmol) was added to a solution of *fac*-[Re(CO)$_3${1,2-C$_6$H$_4$(PH$_2$)$_2$}CF$_3$SO$_3$] (0.36 g, 0.64 mmol) in $CHCl_3$ (30 mL). The reaction was refluxed for 3 hours and the volume reduced *in vacuo* to ca 5 mL. Degassed hexane was added to give a yellow gum. Yield 0.30g (77 %). ^1H NMR ($CDCl_3$): δ 3.62 (d, 4H, CH$_2$S), 5.30-5.83 (m, 8H, CH + CH$_2$ + PH), 6.86 (m, 1H, PH), 6.92 (m, 1H, PH), 7.61-7.76 (m, 2H, Ar-CH), 7.98-8.30 (m, 2H, Ar-CH). ^{31}P NMR (CH_2Cl_2//$CDCl_3$): δ -55.1, t, $^1J(^{31}P-^1H)$ = 389 Hz. Electrospray mass spectrum (MeCN): found 567, 527, 494, 454. Calc. for [^{187}Re(CO)$_3${1,2-C$_6$H$_4$(PH$_2$)(PH)}{S(CH$_2$CHCH$_2$)$_2$}MeCN]$^+$ 567, [^{187}Re(CO)$_3${1,2-C$_6$H$_4$(PH$_2$)$_2$}{S(CH$_2$CHCH$_2$)$_2$}]$^+$ 527, [^{187}Re(CO)$_3${1,2-C$_6$H$_4$(PH$_2$)(PH)}{MeCN}$_2$]$^+$, 494, [^{187}Re(CO)$_3${1,2-C$_6$H$_4$(PH$_2$)$_2$}MeCN]$^+$ 454. IR spectrum (ν(CO) / cm^{-1}, CH_2Cl_2): 2055s, 1986s, 1962sh.

Cyclisation of *fac*-[Re(CO)$_3${1,2-C$_6$H$_4$(PH$_2$)$_2$}{S(CH$_2$CHCH$_2$)$_2$}][CF$_3$SO$_3$]: $AgCF_3SO_3$ (0.20 g, 0.78 mmol) was added to a solution of *fac*-[ReBr(CO)$_3${1,2-C$_6$H$_4$(PH$_2$)$_2$}] (0.25 g, 0.51 mmol) and the reaction was stirred, in a foil-wrapped flask to protect the solution from bright light, for 2 h. AgCl was removed by filtration and diallylsulfide (58 mg, 0.51 mmol) was added. The reaction was stirred at RT and monitored by ^{31}P NMR for 40 days. The reaction was filtered through Celite and the filtrate concentrated *in vacuo* to ca.

5 mL. Addition of degassed diethyl ether gave an-off white solid which was collected by filtration and dried *in vacuo*. Yield 0.10 g (29 %). Calc. for $[C_{16}H_{18}F_3O_6P_2ReS_2]$ C = 28.53, 2.39 %; found C = 29.33, H = 2.96 %. $^{31}P\{^1H\}$ NMR ($CH_2Cl_2/CDCl_3$) (see text): δ -53.5 and –17.7 (*mer*-partially cyclised), -52.4 and –23.7 (*fac*-partially cyclised), -25.5 (macrocycle). Electrospray mass spectrum (MeCN): found *m/z* 567. Calc. for $[^{187}Re(CO)_3\{1,2\text{-}C_6H_4(PH_2)(PH)\{S(CH_2CHCH_2)_2\}MeCN]^+$ 567. IR spectrum (ν(CO) / cm^{-1}, CH_2Cl_2): 2054s, 1968s br.

6.6 References

1. C. A. McAuliffe, 'Phosphorus, Arsenic, Antimony and Bismuth Ligands', Chapter 14, Vol. 2, 'Comprehensive Coordination Chemistry I', G. Wilkinson, R. D. Gillard and J. A. McCleverty, Pergamon, (1987).

2. B. N. Diel, R. C. Haltiwanger and A. D. Norman, *J. Am. Chem. Soc.*, **104**, (1982), 4700.

3. B. N. Diel, P. F. Brandt, R. C. Haltiwanger, M. L. J. Hackney and A. D. Norman, *Inorg. Chem.*, **28**, (1989), 2811.

4. S. J. Coles, P. G. Edwards, J. S. Fleming and M. B. Hursthouse, *J. Chem. Soc., Dalton Trans.*, (1995), 1139.

5. P. G. Edwards, J. S. Fleming and S. S. Liyanage, *J. Chem. Soc., Dalton Trans.*, (1997), 193.

6. S. J. Coles, P. G. Edwards, J. S. Fleming and M. B. Hursthouse, *J. Chem. Soc., Dalton Trans.*, (1995), 4091.

7. P. G. Edwards, J. S. Fleming and S. S. Liyanage, *Inorg. Chem.*, **35**, (1996), 4563.

8. S. J. Coles, P. G. Edwards, J. S. Fleming, M. B. Hursthouse and S. S. Liyanage, *Chem. Commun.*, (1996), 293.

9. P. G. Edwards, J. S. Fleming, S. J. Coles and M. B. Hursthouse, *J. Chem. Soc., Dalton Trans.*, (1997), 3201.

10. R. J. Baker, P. G. Edwards, J. Gracia-Mora, F. Ingold and K. M. A. Malik, *J. Chem. Soc., Dalton Trans.*, (2002), 3985.

11. D. J. Jones, P. G. Edwards, R. P. Tooze and T. Albers, *J. Chem. Soc., Dalton Trans.*, (1999), 1045.

12. A. J. Price and P. G. Edwards, *Chem. Commun.*, (2000), 899.

13. P. G. Edwards, P. D. Newman and D. E. Hibbs, *Angew. Chem., Int. Ed.*, **39**, (2000), 2722.

14. P. G. Edwards, P. D. Newman and K. M. A. Malik, *Angew. Chem., Int. Ed.*, **39**, (2000), 2922.

15. P. G. Edwards, M. L. Whatton and R. Haigh, *Organometallics*, **19**, (2000), 2652.

16. R. Bartsch, S. Hietkamp, S. Morton, H. Peters and O. Stelzer, *Inorg. Chem.*, **22**, (1983), 3624.

17. D. J. Brauer, F. Gol, S. Hietkamp, H. Peters, H. Sommer, O. Stelzer and W. S. Sheldrick, *Chem. Ber.*, **119**, (1986), 349.

18. T. Mizuta, A. Okano, T. Sasaki, H. Nakazana and K. Miyoshi, *Inorg. Chem.*, **2**, (1997), 200.

19. P. J. Blower, J. C. Jeffery, J. R. Miller, S. N. Salek, S. N. Schmaljohann, R. J. Smith and M. J. Went, *Inorg. Chem.*, **36**, (1997), 1578.

20. R. J. Smith, A. K. Powell, N. Barnard, J. R. Dilworth and P. J. Blower, *Chem. Commun.*, (1993), 54.

21. D. Seilmann and L. Zapf, *Angew. Chem.*, **96**, (1984), 799.

22. E. P. Kyba, A. M. John, S. B. Brown, C. W. Hudson, M. J. McPhaul, A. Harding, K. Larsen, S. Niedzwiecki and R. E. Davis, *J. Am. Chem. Soc.*, **102**, (1980), 139.

23. E. P. Kyba, R. E. Davis, C. W. Hudson, A. M. John, S. B. Brown, M. J. McPhaul, L.-K. Liu and A. C. Glover, *J. Am. Chem. Soc.*, **103**, (1981), 3868.

24. E. P. Kyba and S. B. Brown, *Inorg. Chem.*, **19**, (1980), 2159.

25. E. P. Kyba and S.-S. P. Chou, *J. Am. Chem. Soc.*, **102**, (1980), 7012.

26. E. P. Kyba, R. E. Davis, S. T. Liu, K. A. Hassett and S. B. Larson, *Inorg. Chem.*, **24**, (1985), 4629.

27. E. P. Kyba, C. N. Clubb, S. B. Larson, V. J. Schueler and R. E. Davis, *J. Am. Chem. Soc.*, **107**, (1985), 2141.

28. E. P. Kyba, R. E. Davis, M. A. Fox, C. N. Clubb, S. T. Liu, G. A. Reitz, V. J. Scheuler and R. P. Kashyap, *Inorg. Chem.*, **26**, (1987), 1647.

29. E. P. Kyba and S. T. Liu, *Inorg. Chem.*, **24**, (1985), 1613.

30. M. Ciampolini, P. Dapporto, N. Nardi and F. Zanobini, *Chem. Commun.*, (1980), 177.

31. M. Ciampolini, P. Dapporto, N. Nardi and F. Zanobini, *Inorg. Chim. Acta*, **45**, (1980), L239.

32. M. Ciampolini, N. Nardi, F. Zanobini, R. Cini and P. L. Orioli, *Inorg. Chim. Acta*, **76**, (1983), L17.

33. M. Ciampolini, N. Nardi, P. Dapporto, P. Innocenti and F. Zanobini, *J. Chem. Soc., Dalton Trans.*, (1984), 575.

34. M. Ciampolini, N. Nardi, P. Dapporto and F. Zanobini, *J. Chem. Soc., Dalton Trans.*, (1984), 995.

35. M. Ciampolini, N. Nardi, P. L. Orioli, S. Mangani and F. Zanobini, *J. Chem. Soc., Dalton Trans.*, (1985), 1425.

36. M. Ciampolini, P. Dapporto, N. Nardki and F. Zanobini, *Inorg. Chem.*, **22**, (1983), 13.

37. C. Mealli, M. Sabat, F. Zanobini, M. Ciampolini and N. Nardi, *J. Chem. Soc., Dalton Trans.*, (1985), 479.

38. M. Ciampolini, N. Nardi, P. L. Orioli, S. Mangani and F. Zanobini, *J. Chem. Soc., Dalton Trans.*, (1984), 2265.

39. M. Ciampolini, N. Nardi, P. L. Orioli, S. Mangani and F. Zanobini, *J. Chem. Soc., Dalton Trans.*, (1985), 1179.

40. N. R. Champness, C. S. Frampton, G. Reid and D. A. Tocher, *J. Chem. Soc., Dalton Trans.*, (1994), 3031.

41. P. J. Blower, A. V. Chadwick, J. C. Jeffery, G. E. D. Mullen, A. K. Powell, S. N. Salek, R. S. Smith and M. J. Went, *Inorg. Chim. Acta*, **294**, (1999), 170.

42. J. A. Muñoz, L. Escriche, J. Casabó, C. Pérez-Jiménez, R. Kivekäs and R. Sillanpää, *Inorg. Chem.*, **36**, (1997), 947.

43. S. J. A. Pope and G. Reid, *J. Chem. Soc., Dalton Trans.*, (1999), 1615.

44. G. A. Carriedo and V. Riera, *J. Organomet. Chem.*, **205**, (1981), 371.

45. W. Levason, S. D. Orchard and G. Reid, *Organometallics*, **18**, (1999), 1275.

46. K. Nozaki and K. Utimoto, *J. Am. Chem. Soc.*, **109**, (1987), 2547.

47. K. J. Reimer and A. Shaver, *Inorg. Synth.*, **19**, (1979), 158.

48. R. H. Reimann and E. Singleton, *J. Organomet. Chem.*, **59**, (1973), 309.

49. E. P. Kyba, S. T. Liu and R. L. Harris, *Organometallics*, **2**, (1983), 1877.

Appendix

Experimental Techniques and Instrumentation

Experimental techniques

Unless otherwise stated, experiments were performed under dry dinitrogen using standard Schlenk line techniques. The distibine ligands were stored and handled in an inert dry box containing dinitrogen. Glassware was pre-dried prior to use. Unless otherwise stated, commercial reagents and solvents were used as received from Acros, Aldrich, Avocado, and BDH. Deuterated solvents were used as received from Apollo Scientific. Where stated, solvents were dried and then distilled from sodium benzophenone (thf, diethylether, toluene and hexane), calcium hydride (dichloromethane, acetonitrile) or magnesium/diiodine (ethanol).

Instrumentation

^{1}H NMR spectra (300 MHz) were recorded on a Bruker AM300, and were referenced to the residual ^{1}H solvent resonance.

$^{13}C\{^{1}H\}$ NMR spectra (100.6 MHz) and ^{31}P NMR spectra (162.0 MHz) were recorded in CH_2Cl_2 containing 10-15% $CDCl_3$ using a Bruker DPX400 spectrometer and were referenced to the residual ^{13}C solvent resonance and 85% H_3PO_4 ($\delta = 0$) respectively. For the tungsten carbonyl complexes reported in chapter 3 and the carbonyl complexes in chapter 5, $[Cr(acac)_3]$ was added to the NMR solutions prior to recording the $^{13}C\{^{1}H\}$ NMR spectra and a pulse delay of 2 s was employed to take account of the long relaxation times.

^{63}Cu NMR (106.1 MHz) and ^{59}Co NMR (95.4 MHz) were recorded in DMF or CH_2Cl_2 containing 10-15% $CDCl_3$ using a Bruker DPX400 spectrometer and were referenced to a solution of $[Cu(MeCN)_4][BF_4]$ in MeCN ($\delta = 0$) or to external aqueous $K_3[Co(CN)_6]$ ($\delta = 0$) respectively.

^{95}Mo (63.7 MHz) and ^{55}Mn NMR (99.2 MHz) were recorded in CH_2Cl_2 containing 10-15% $CDCl_3$ using a Bruker DPX400 spectrometer and were referenced to aqueous $Na_2[MoO_4]$ ($\delta = 0$) or to aqueous $K[MnO_4]$ ($\delta = 0$) respectively.

Infrared spectra were recorded using a Perkin-Elmer PE 983G spectrometer. Microanalyses were undertaken by the University of Strathclyde microanalytical service. UV-vis spectra were recorded on a Perkin Elmer PE Lambda 19 spectrometer in CH_2Cl_2 solutions or by diffuse reflectance.

Electrospray (ES^+), and atmospheric pressure chemical ionisation (APCl) mass spectra were recorded in MeCN solution using a VG Biotech platform an electron ionisation mass spectra were recorded similarly in CH_2Cl_2 solution.

Electrical conductivity measurements were recorded in 10^{-3} mol dm^{-3} $MeNO_2$ or CH_2Cl_2 solution using a Pye Conductivity Bridge and platinised platinum electrodes, calibrated with standard KCl solutions.

X-ray crystallography

Data collections for the structures reported in Chapter 5 were carried out using a Rigaku AFC7S four-circle diffractometer or an Enraf-Nonius Kappa CCD diffractometer with graphite monochromated Mo-Kα radiation (λ = 0.71073 Å) with the crystals held at 150 K in a gas stream. Structure solution and refinement were routine with H-atoms normally introduced in calculated positions.[1-3]

Data collections for the structures reported in Chapters 2,3,4 and 6 were carried out using an Enraf-Nonius Kappa CCD diffractometer with graphite monochromated Mo-Kα radiation (λ = 0.71073 Å) with the crystals held at 120 K in a gas stream. Structure solution and refinement were routine with H-atoms normally introduced in calculated positions.[4-8]

References

1. P. T. Beurskens, G. Admiraal, G. Beurskens, W. P. Bosman, S. Garcia-Granda, R. O. Gould, J. M. M. Smits and C. Smykalla, PATTY, The DIRDIF Program System, Technical Report of the Crystallography Laboratory, University of Nijmegan, The Netherlands, (1992).

2. TEXSAN: Crystal Structure Analysis Package, Molecular Structure Corporation, Texas, (1995).

3. R. H. Blessing, *Acta Crystallogr., Sect. A*, **51**, (1995), 33.

4. G. M. Sheldrick, SHELXL-97, Program for Crystal Structure Refinement, University of Gottingen, Germany, (1997).

5. G. M. Sheldrick, SHELXS-97, Program for Crystal Structure Solution, University of Gottingen, Germany, (1997).

6. R. H. Blessing, *J. Appl. Crystallogr.*, **30**, (1997), 421.

7. L. J. Farrugia, *J. Appl. Cryst.*, **32**, (1999), 837.

8. L. J. Farrugia, WinGX-Version 1.64.05, An Intergrated System of Windows Programs for the Solution, Refinement and Analysis of Single Crystal X-Ray Diffraction Data, Department of Chemistry, University of Glasgow, (2003).